FLEXURAL STIFFNESS OF RECTANGULAR COMPOSITE STEEL-CONCRETE COLUMNS

BY

TIMO K. TIKKA

A Thesis
Submitted to the Faculty of Graduate Studies
in Partial Fulfillment of the Requirements
for the Degree of

MASTER OF SCIENCE

Department of Civil Engineering
University of Manitoba
Winnipeg, Manitoba

October, 1991

ISBN 0-315-78017-7

FLEXURAL STIFFNESS OF RECTANGULAR COMPOSITE STEEL-CONCRETE COLUMNS

BY

TIMO K. TIKKA

A thesis submitted to the Faculty of Graduate Studies of the University of Manitoba in partial fulfillment of the requirements of the degree of

MASTER OF SCIENCE

ACKNOWLEDGEMENTS

The author would like to acknowledge the financial assistance of the Natural Sciences and Engineering Research Council of Canada through Dr. S.A. Mirza's operating grant. The guidance provided by Dr. S.A. Mirza throughout the work of the study was greatly appreciated.

This thesis is dedicated to my wife Camilla and my sons Villiam and Aleksandar for their support, love and sacrifice which sustained me through the two years of this study.

ABSTRACT

The ACI Building Code and the CSA Code A23.3 for the design of concrete structures permit a moment magnifier approach for design of slender composite beam-columns in which a structural steel shape is encased in concrete. The AISC LRFD Specifications for the design of Structural Steel Buildings utilize the interaction equations for steel beam-columns by converting the slender composite beam-column cross-section into an equivalent steel column with modified cross-section properties.

Both ACI and CSA approaches are strongly influenced by the effective flexural stiffness (*EI*) of the column which varies due to cracking, creep, and nonlinearity of the concrete stress-strain curve. A procedure was developed to obtain an effective flexural stiffness from the AISC interaction equations that is comparable to the ACI and CSA *EI*. However, the *EI* expressions given by the ACI and CSA Building Codes and the comparable AISC *EI* are quite approximate when compared with values of *EI* obtained from moment, curvature, and axial load relationships. This study was undertaken to determine the influence of a full range of variables on *EI* of slender composite beam-columns subjected to single axis bending about the major axis or minor axis of an encased structural steel shape. To study the full range of variables, 11880 composite beam-columns bending about the major axis and 11880 composite beam-columns bending about the minor axis, each with a different combination of variables, were used to generate the stiffness data. The *EI* expressions were then statistically developed for use in slender composite column design. Two design equations are proposed in this report.

TABLE OF CONTENTS

		Page
1.0	INTRODUCTION	1
2.0	THEORETICAL BEAM-COLUMN STIFFNESS AND STRENGTH	6
2.1	Determining the Theoretical Flexural Stiffness	8
2.1.1	Development of Theoretical Stiffness Equation	10
2.2	Determining the Cross-Section and Column Strength	13
2.3	Cross-Section Discretization	15
2.3.1	Discretization for Major Axis Bending	17
2.3.2	Discretization for Minor Axis Bending	20
2.4	Cross-Section Strength	23
2.5	Slender Beam-Column Strength	30
2.6	Material Stress-Strain Curves	36
2.6.1	Stress-Strain Curves for Concrete	37
2.6.2	Stress-Strain Curves for Steel	41
2.7	Residual Stresses in Structural Steel	43
3.0	COMPARISON OF THEORETICAL MODEL TO EXPERIMENTAL RESULTS	48
3.1	Comparison of Theoretical Strength of Columns Subjected to Major axis Bending to Experimental Results	51
3.2	Comparison of Theoretical Strength of Columns Subjected to Minor Axis Bending to Experimental Results	65

4.0 ACI AND AISC FLEXURAL STIFFNESSES 89

4.1 ACI Code Effective Flexural Stiffness 89

4.2 AISC-LRFD Code Effective Flexural Stiffness 89

4.2.1 AISC Axial Load-Bending Moment Relationship 90

4.2.2 Computation of AISC Effective Flexural Stiffness 99

5.0 EVALUATION OF EFFECTIVE STIFFNESS FOR BEAM-COLUMS SUBJECTED TO MAJOR AXIS BENDING 103

5.1 Description of Beam-Columns Studied 103

5.2 Examination of ACI and AISC Stiffnesses 110

5.3 Development of Proposed Design Equations for Short-Term EI 114

5.3.1 Variables Used for Regression Analysis 114

5.3.2 Regression Analysis 119

5.3.3 Proposed Design Equations 126

5.4 Analysis of Stiffness Data 127

5.4.1 Overview of Stiffness Ratio Statistics 127

5.4.2 Effect of Variables on Stiffness Ratios 135

5.4.3 Stiffness Ratios Produced by Proposed Design Equations for Usual Columns 165

5.5 Theoretically Calculated Critical Buckling Load 176

5.6 Another Look at the AISC Effective Stiffness 180

6.0 EVALUATION OF EFFECTIVE STIFFNESS FOR BEAM-COLUMNS SUBJECTED TO MINOR AXIS BENDING 185

6.1 Description of Beam-Columns Studied 185

6.2 Examination of ACI and AISC Stiffnesses 192

6.3 Development of Proposed Design Equations for Short-Term EI 196

6.3.1 Variables Used for Regression Analysis 197

6.3.2 Regression Analysis 202

6.3.3 Proposed Design Equations 209

6.4 Analysis of Stiffness Data 210

6.4.1 Overview of Stiffness Ratio Statistics 210

6.4.2 Effect of Variables on Stiffness Ratios 220

6.4.3 Stiffness Ratios Produced by Proposed Design Equations for Usual Columns 249

6.5 Theoretically Calculated Critical Buckling Load 260

6.6 Another Look at the AISC Effective Stiffness 263

7.0 SUMMARY, CONCLUSIONS AND RECOMMENDATIONS 270

7.1 Summary 270

7.2 Conclusions Related to Composite Beam-Columns Bending About the Major Axis 271

7.3 Conclusions Related to Composite Beam-Columns Bending About the Minor Axis 272

7.4 Recommendations 274

LIST OF SYMBOLS 275

LIST OF REFERENCES 279

APPENDIX A 283

1 - INTRODUCTION

The ACI Building Code (1989) and the CSA Code A23.3 for the Design of Concrete Structures for Buildings (1984) permit a moment magnifier approach for design of slender composite beam-columns in which a structural steel shape is encased in concrete. The AISC-LRFD Specifications (AISC Code 1986) for the design of Structural Steel Buildings utilize the interaction equations for steel beam-columns by converting the slender composite beam-column cross-section into an equivalent steel column with modified cross-section properties.

The ACI and CSA approach uses the axial load obtained from a first-order elastic analysis and a magnified moment that includes the second-order effect caused by the lateral displacement of the column. The ACI and CSA methods are strongly influenced by the effective stiffness (EI) of the column which varies due to cracking, creep, and the nonlinearity of the concrete stress-strain curve. The EI expressions given by the ACI Building Code (ACI 318-89 Equation 10-14) and the CSA Code (CSA CAN3-A23.3-M84 Equation 10-16) are identical and are reproduced here as Equation 1.1.

$$EI = \frac{(E_c I_g / 5)}{1 + \beta_d} + E_s I_{ss} \qquad (1.1)$$

in which E_c equals the elastic modulus for concrete; I_g equals the moment of inertia for the gross concrete cross-section; E_s equals the elastic modulus of steel; I_{ss} equals the moment of inertia of the structural steel section taken about the axis of bending; and β_d equals the ratio of maximum factored dead (or sustained load) to maximum total factored load and is always taken as positive. For short term loads, β_d equals zero and Equation 1.1 becomes:

$$EI = \frac{E_c I_g}{5} + E_{ss} I_{ss} \tag{1.2}$$

The ACI Building Code also utilizes the expression for reinforced concrete columns for determining EI (ACI 318-89 Equation 10-9) shown here as Equation 1.3.

$$EI = \frac{0.4 E_c I_g}{(1 + \beta_d)} \tag{1.3}$$

Again, β_d is equal to zero for short term loads and Equation 1.3 becomes Equation 1.4.

$$EI = 0.4 E_c I_g \tag{1.4}$$

Equation 1.4 was not included as part of this study because it neglects the flexural stiffness of the encased structural steel shape ($E_s I_{ss}$) that will in many instances exceed the flexural stiffness calculated from Equation 1.4.

The expression given by the ACI Building Code and CSA Code (Equation 1.2) does not include the effective stiffness contributed by longitudinal reinforcing steel. The Commentary on the ACI Building Code states that complete interaction between the steel core, the concrete, and any longitudinal reinforcing steel should not be assumed. The Commentary on the ACI Building Code also says that "because of probable separation at high strains between the steel core and the concrete, longitudinal bars will be ineffective in stiffening cross sections even though they would be useful in sustaining compression forces." An examination of test results collected and analyzed as part of this study showed that this assumption is not valid. This is especially a very conservative assumption for cases where the *EI* of the properly confined longitudinal reinforcing steel exceeds that of the encased steel section.

The AISC-LRFD Specifications (AISC Code 1986) for the design of Structural Steel Buildings does not compute the effective flexural stiffness (*EI*) of a composite beam-column as do the ACI Code and CSA Code. A procedure, described in detail in Chapter 4, was developed to obtain effective flexural stiffness from the AISC interaction equations. The AISC *EI* so computed is comparable to the ACI *EI*.

The understanding of slender column behaviour has expanded during the past 15 to 20 years and analytical procedures have become available to accurately model slender composite beam-column stiffness and strength. However, no studies have been completed to critically examine the effective flexural stiffness of composite beam-columns. Mirza (1990) conducted a study on the effective flexural stiffness of reinforced concrete beam-columns.

This study was undertaken to determine the influence of a full range of variables on the effective flexural stiffness of slender composite beam-columns bending about the major axis and bending about the minor axis. In this study 11880 rectangular beam-columns were analyzed for bending about each axis, each with a different combination of specified values of variables. These beam-columns were used to generate the stiffness data. *EI* expressions were then statistically developed for use in slender composite column designs. The composite columns studied were bent in symmetrical single curvature in braced frames subjected to short term loads. The moment magnifier approach specified in the ACI Building Code was developed for this type of column. The effects of different end restraints, loading conditions and lateral supports are accounted for in the ACI Code through the use of effective length factor (k), equivalent uniform moment diagram factor (C_m), and sustained load factor (β_d).

The columns studied are graphically represented in Figure 1.1, and are similar to those investigated by Mirza (1990) for slender reinforced concrete columns. These columns were chosen because the errors in k, C_m, and β_d would not affect the accuracy of the *EI* expressions derived in the later part of this report.

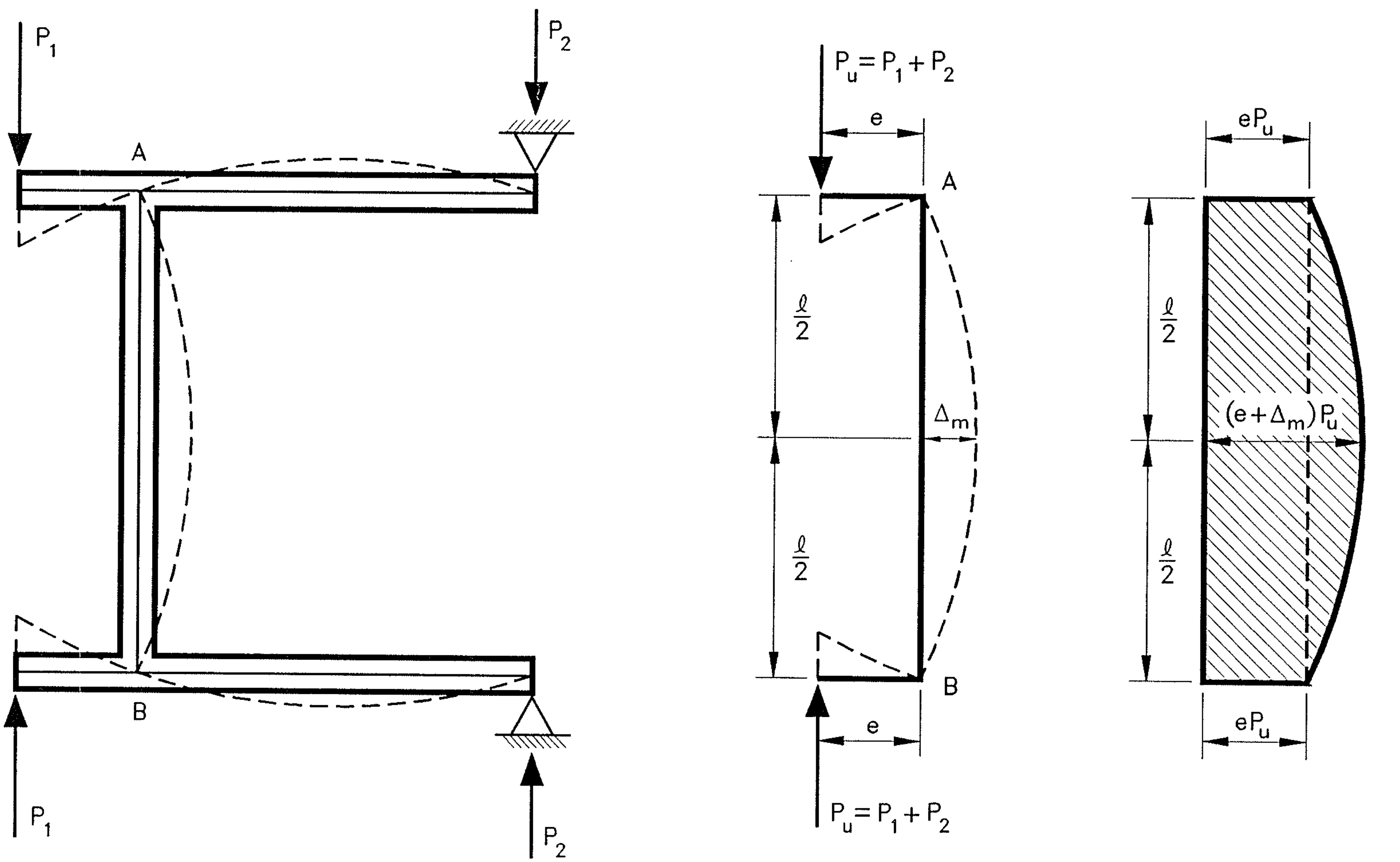

(a) MODEL OF COLUMN IN SYMMETRICAL SINGLE CURVATURE

(b) FORCES ON COLUMN

(c) BENDING MOMENT DIAGRAM

Figure 1.1 - Type of columns studied (Mirza 1990).

2 - THEORETICAL BEAM-COLUMN STIFFNESS AND STRENGTH

Two computer programs were used to analyze the theoretical strength and stiffness of composite beam-columns. One program for analyzing beam-columns bending about the major axis, the other for bending about the minor axis. A computer program previously developed at Lakehead University by Mirza (1989) and revised by Skrabek and Mirza (1990) was further revised and then tested for use in this study. The changes implemented into the program for use in this study were: a) ability to analyze theoretical beam-column strength for bending about the minor axis (the original program was developed for major axis bending only); b) computation of the theoretical effective stiffness *EI* of a beam-column, from the theoretically calculated strength, by applying the secant-modulus approach (the approach was similar to the one used by Mirza(1990) for reinforced concrete beam-columns). A brief flow chart of the computation procedure employed is show in Figure 2.1.

The entire program consists of a main driver program, a theoretical strength subroutine and a stiffness subroutine. The main driver reads input, initiates the parametric study of input data, calls the theoretical strength subroutine and the stiffness subroutine, and saves the required output data for later use. The theoretical strength subroutine computes the theoretical strength of the composite cross section and slender column with the help of 20 other subroutines. Using

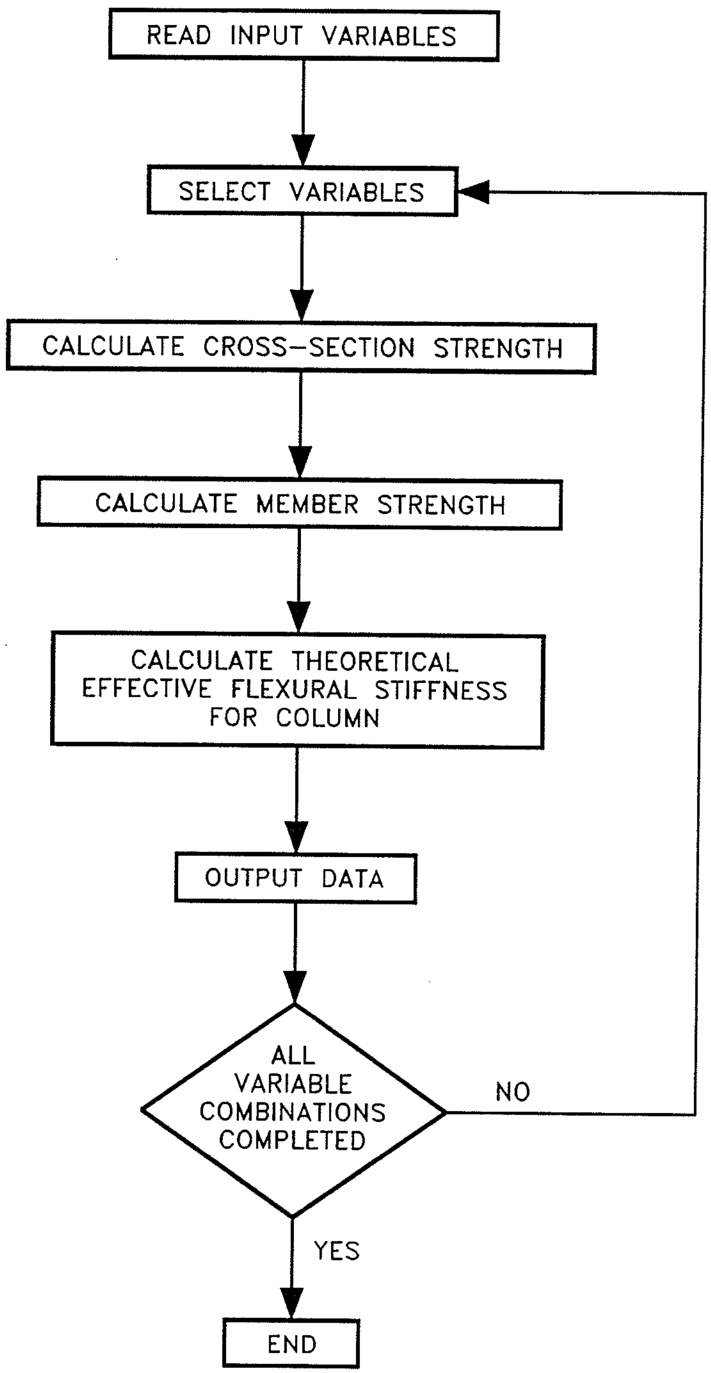

Figure 2.1 - Flow chart of computation procedure.

the secant-modulus approach, the stiffness subroutine calculates the theoretical effective stiffness from the cross section and slender column interaction diagrams developed by the theoretical strength subroutine.

The theoretical strength subroutine (theoretical model) and related subroutines are discussed in this chapter along with the subroutine which was developed for determining the theoretical effective stiffness.

2.1 DETERMINING THE THEORETICAL FLEXURAL STIFFNESS

In reviewing previous work no references were found that presented a method for evaluating the theoretical flexural stiffness of composite beam-columns.

Mirza (1990) presented a method for evaluating the theoretical flexural stiffness of rectangular reinforced concrete columns. Using the bending moment relationship (secant formula) for a pin-ended slender column subjected to equal and opposite end moments, given by Timoshenko and Gere (1961), and the equation for Euler's buckling strength, Mirza was then able to establish theoretical flexural stiffness, EI.

A method identical to that developed by Mirza (1990) for determining the effective flexural stiffness of slender reinforced concrete columns subjected to short term loads is applied in this study for determining the effective flexural stiffness of slender composite columns. Equation 2.1 is specified by the ACI and CSA codes to establish the effective flexural stiffness of slender composite columns subjected to short term loading.

$$EI = 0.2E_cI_g + E_sI_{ss} \tag{2.1}$$

In the above equation, E_c is the modulus of elasticity for concrete, I_g is the moment of inertia for the gross concrete cross section, E_s is the modulus of elasticity for steel, and I_{ss} is the moment of inertia of the structural steel shape about the centroidal axis of the composite cross-section. The equation does not directly account for any stiffness contributed by the reinforcing steel. This plus the use of a constant value of the coefficient 0.2 to compute the column EI introduce inaccuracies into the equation. Consequently, Equation 2.1 neglects the effects of cracking of the concrete, nonlinearity of the concrete stress-strain curve and other factors. Therefore, a modified version of this expression is proposed.

$$EI = \alpha_cE_c(I_g - I_{ss}) + \alpha_{ss}E_sI_{ss} + \alpha_{rs}E_sI_{rs} \tag{2.2}$$

in which α_c, α_{ss} and α_{rs} are dimensionless reduction factors (effective stiffness factors) for concrete, structural steel and reinforcing steel, and I_{rs} is the moment of inertia of reinforcement about the centroidal axis of the cross-section. The effective flexural stiffness EI is equated to the theoretically computed stiffness using the procedure described in Section 2.1.1. The effective stiffness factors α_c, α_{ss} and α_{rs} are then determined using multiple linear regression, which is explained fully in Chapter 5 and 6. Note the effective stiffness factor for concrete α_c is dependent on a number of variables which are also described in Chapter 5 and 6.

2.1.1 Development of Theoretical Stiffness Equation

The secant formula given by Timoshenko and Gere (1961) describes the bending moment relationship for a pin-ended slender column subjected to equal and opposite end moments.

$$M_c = M_2 \sec\left(\frac{\pi}{2}\sqrt{\frac{P_u}{P_c}}\right) \tag{2.3}$$

where M_c is the design bending moment including second-order effects, M_2 is the applied end moment calculated from elastic analysis, P_u is the axial load acting on the column, and P_c is Euler's buckling strength described by Equation 2.4.

$$P_c = \frac{\pi^2 EI}{\ell^2} \tag{2.4}$$

in which EI is the effective stiffness and ℓ is the unsupported height of the column. Rearranging Equation 2.3, solving for P_c, and simplifying yields:

$$P_c = \frac{\pi^2 P_u}{4\left[arcsec\left(\frac{M_c}{M_2}\right)\right]^2} \tag{2.5}$$

Equating Equations 2.4 and 2.5 and solving for EI gives the following expression:

$$EI = \frac{P_u \ell^2}{4\left[\operatorname{arcsec}\left(\frac{M_c}{M_2}\right)\right]^2} \tag{2.6}$$

Then for the purpose of analysis, M_c is replaced by the cross-section bending moment capacity M_{cs}, and M_2 is replaced by the overall column bending moment capacity M_{col}, so that Equation 2.6 becomes:

$$EI = \frac{P_u \ell^2}{4\left[\operatorname{arcsec}\left(\frac{M_{cs}}{M_{col}}\right)\right]^2} \tag{2.7}$$

This expression gives the theoretical effective flexural stiffness of a pin-ended slender column subjected to equal end moments causing single curvature bending. The terms P_u, M_{col} and M_{cs} used in the equation were obtained from the column axial load-bending moment interaction diagram (Figure 2.2) computed by the program described in Section 2.4 and 2.5. The stored value of M_{col} and P_u, for each desired eccentricity ratio e/h, were used directly in the equation. The value of P_u was then used, using Lagrangian interpolation, to determine a value of M_{cs} from the stored cross-sectional axial load-bending moment interaction diagram and corresponded to the desired axial load P_u. The procedure is documented in the literature (Mirza 1990).

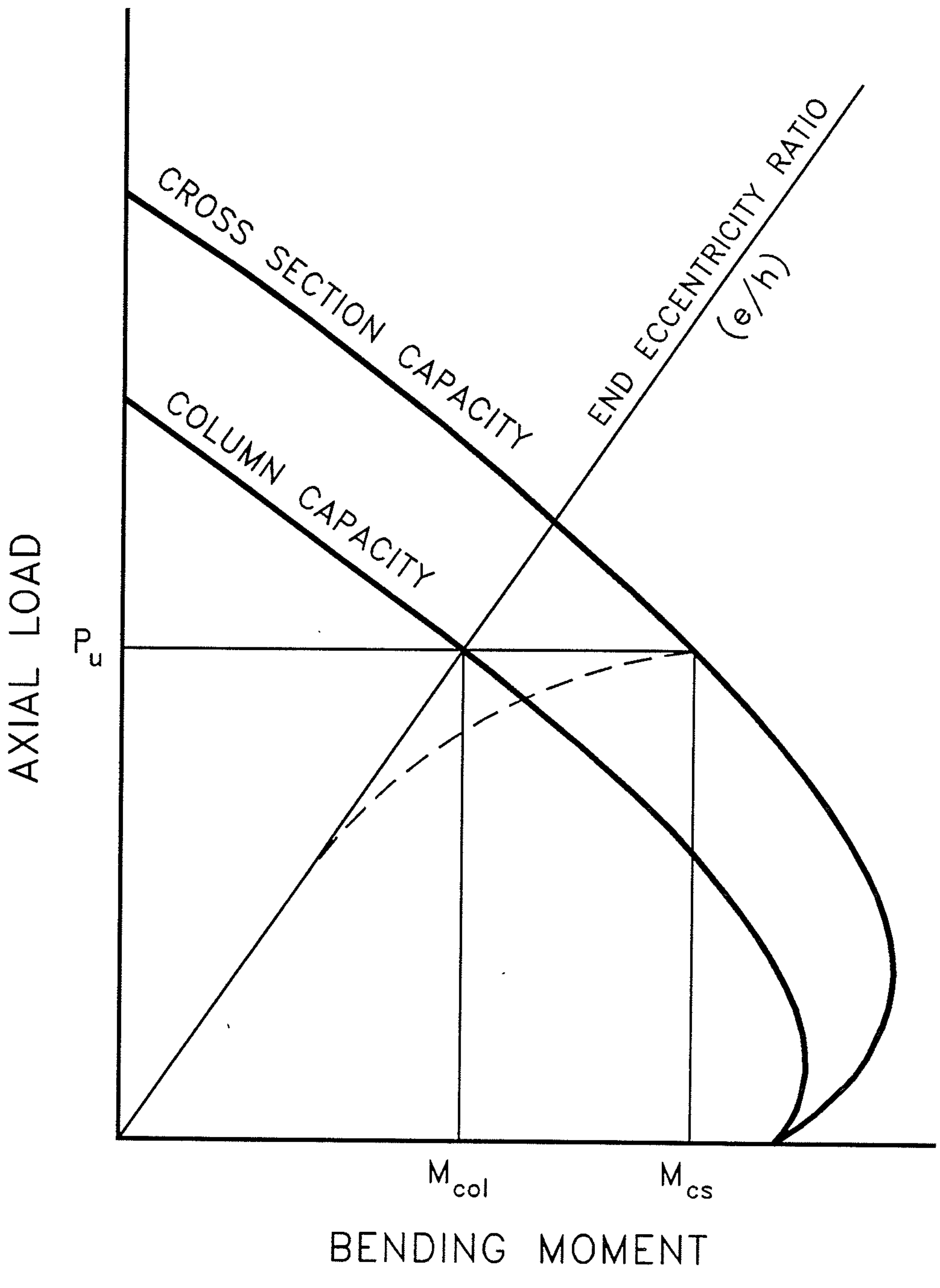

Figure 2.2 - Schematic cross-section and column axial load-bending moment interaction diagrams.

2.2 DETERMINING THE CROSS-SECTION AND COLUMN STRENGTH

The theoretical model used in the study for determining the cross section and slender column strength is the same as that used by Skrabek and Mirza (1990). Skrabek and Mirza give a detailed review of the techniques and assumptions that have been used by Basu (1967) and others in previous studies of composite beam-columns.

A summary of the description presented by Skrabek and Mirza for the theoretical strength model was adopted for use in this study and portions of their work are included unaltered in this Section plus in Sections 2.3.1, 2.4, 2.5, 2.6, and 2.7. A detailed description of the theoretical strength subroutine is given by Skrabek and Mirza (1990).

The theoretical strength program computes the moment, curvature, axial load (M-ϕ-P) relationship for the cross-section using a strain compatibility solution, discussed in Section 2.4. The capacity of the member (beam-column) was calculated by solving for the maximum eccentricity for which equilibrium could be maintained between the ends and mid-height of the beam-column. The procedure used to calculate the beam-column strength is discussed in Section 2.5.

The assumptions regarding the loading and the end conditions of the beam-columns are given in Figure 1.1. The assumptions used in determining the theoretical strength are as follows:

(a) strains between concrete and steel are compatible and no slip occurs;

(b) strain is linearly proportional to the distance from the neutral axis;

(c) deflections are small such that curvatures can be calculated as the second derivative of the deflection;

(d) shear stresses are small and their effect on the strength can be neglected;

(e) effects of axial shorting are negligible;

(f) residual stresses in the rolled steel section exist;

(g) the column is perfectly straight before loading;

(h) the column cross-section is symmetric about the major and minor axis; and

(i) failure does not take place by local or torsional buckling.

Assumptions (a) and (b) were required for the strain compatibility solution of the cross-section M-ϕ-P relationship. Assumption (c) was needed for the calculation of length effect due to the secondary moments. Assumptions (d) and (e) were used to simplify the calculations. Assumption (f) acknowledges the existence of residual stresses in the rolled steel section and is discussed in Section 2.7. Assumption (g) was based on Wakabayashi's (1976) observation that the encasement of the steel section in the concrete will negate any detrimental effects of initial camber of the steel section. Assumption (h) simplified the cross-section M-ϕ-P calculations since discretization of only one-quarter of the cross-section was required to model the entire cross-section. Assumption (i) was valid since a review of test data in the literature did not indicate any failure by local or torsional buckling. This assumption was also made by Bondale (1966 a,b,c) and would seem to be particularly valid where rectangular hoops along with surrounding concrete stiffen the compression flange of the steel section. Further assumptions directly related to the stress-strain curve for individual materials are discussed in Sections 2.6 and 2.7.

2.3 CROSS-SECTION DISCRETIZATION

The cross-section of a composite column consists of three materials (concrete, structural steel and reinforcing steel), each possessing a unique stress-strain relationship. The concrete was subdivided into three distinct types: unconfined, partially confined and highly confined, with each of these concrete types having different stress-strain characteristics. The rolled steel section was separated into the web and the flanges to account for the differences in their stress-strain characteristics. Therefore, six different stress-strain curves are used to represent the materials in the cross-section shown in Figure 2.3.

Skrabek and Mirza (1990) point out that discretizing between the three areas of concrete realizes the beneficial effects that increased confinement has on concrete strength and ductility.

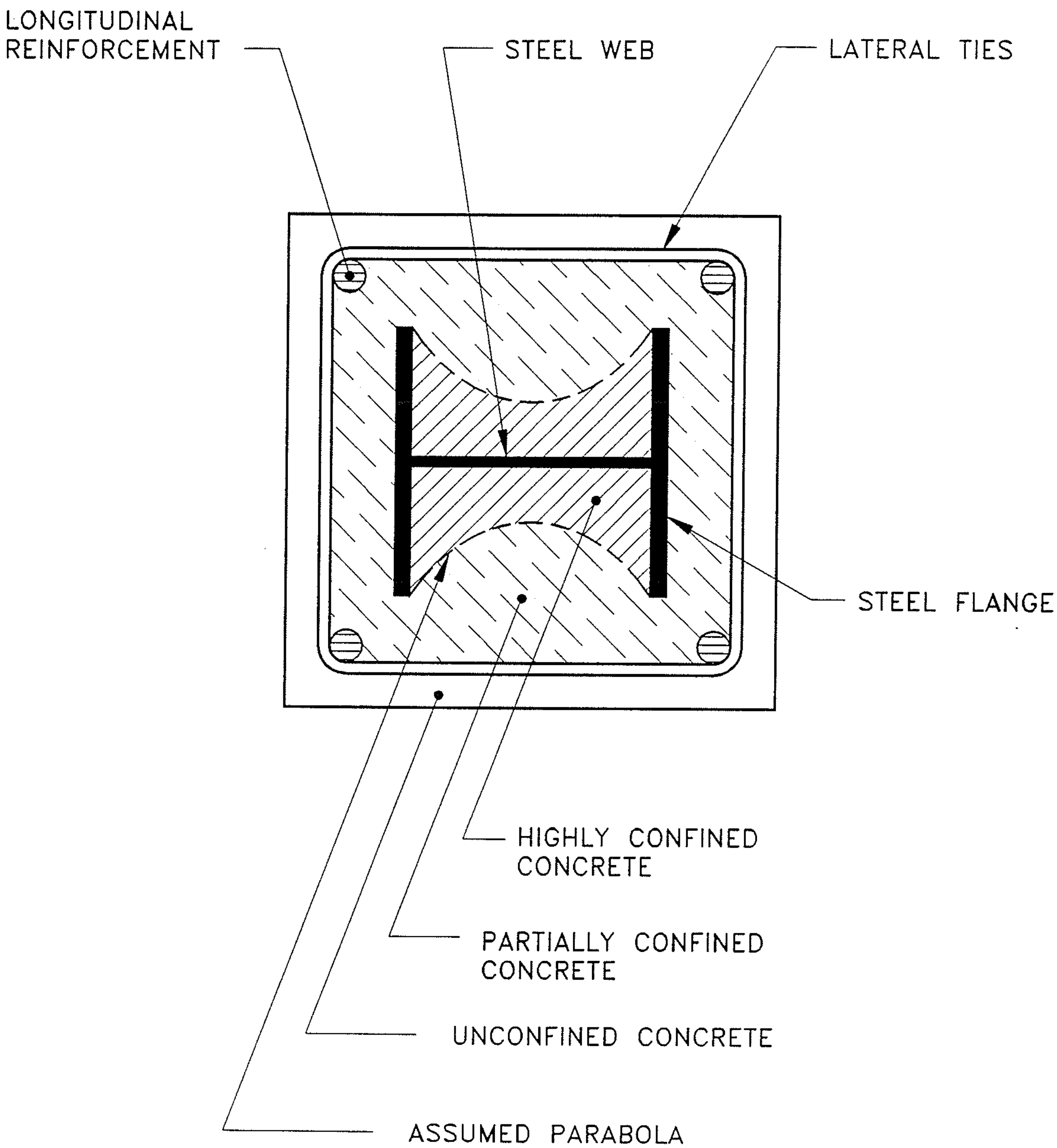

Figure 2.3 - Material types in composite cross-section.

2.3.1 Discretization for Major Axis Bending

The cover concrete outside the lateral ties was considered to be unconfined. The concrete inside the periphery of the ties but outside the flanges of the steel section was assumed to be partially confined. The concrete within an assumed parabola and between the web and flanges of the steel section was assumed to be highly confined. This is indicated in Figure 2.3. The assumed parabola had a vertex intersecting the edge of the web at the mid-depth of the steel section when the flange overhang was less than one-quarter of the steel section depth between the flanges. The vertex of the parabola at the mid-height of the steel section was, otherwise, taken at a distance from the web d_{vert}. The term d_{vert} depended on the flange width b, flange thickness t, depth of steel section d, and web thickness w as indicated by Equation 2.8.

$$\begin{aligned} d_{vert} &= \frac{b-w}{2} - \frac{d-2t}{4} \\ d_{vert} &\geq 0.0 \end{aligned} \tag{2.8}$$

The distance, parallel to the major axis, from the edge of the web to parabola w_{hc-1} (Figure 2.4) for an elemental slice was computed by Equation 2.9.

$$w_{hc-1} = d_{vert} + \left[\frac{\left(\frac{b - w}{2} - d_{vert} \right) d_{pc-1}^2}{\left(\frac{d - 2t}{2} \right)^2} \right] \tag{2.9}$$

in which d_{pc-1} is measured perpendicular to the major axis from

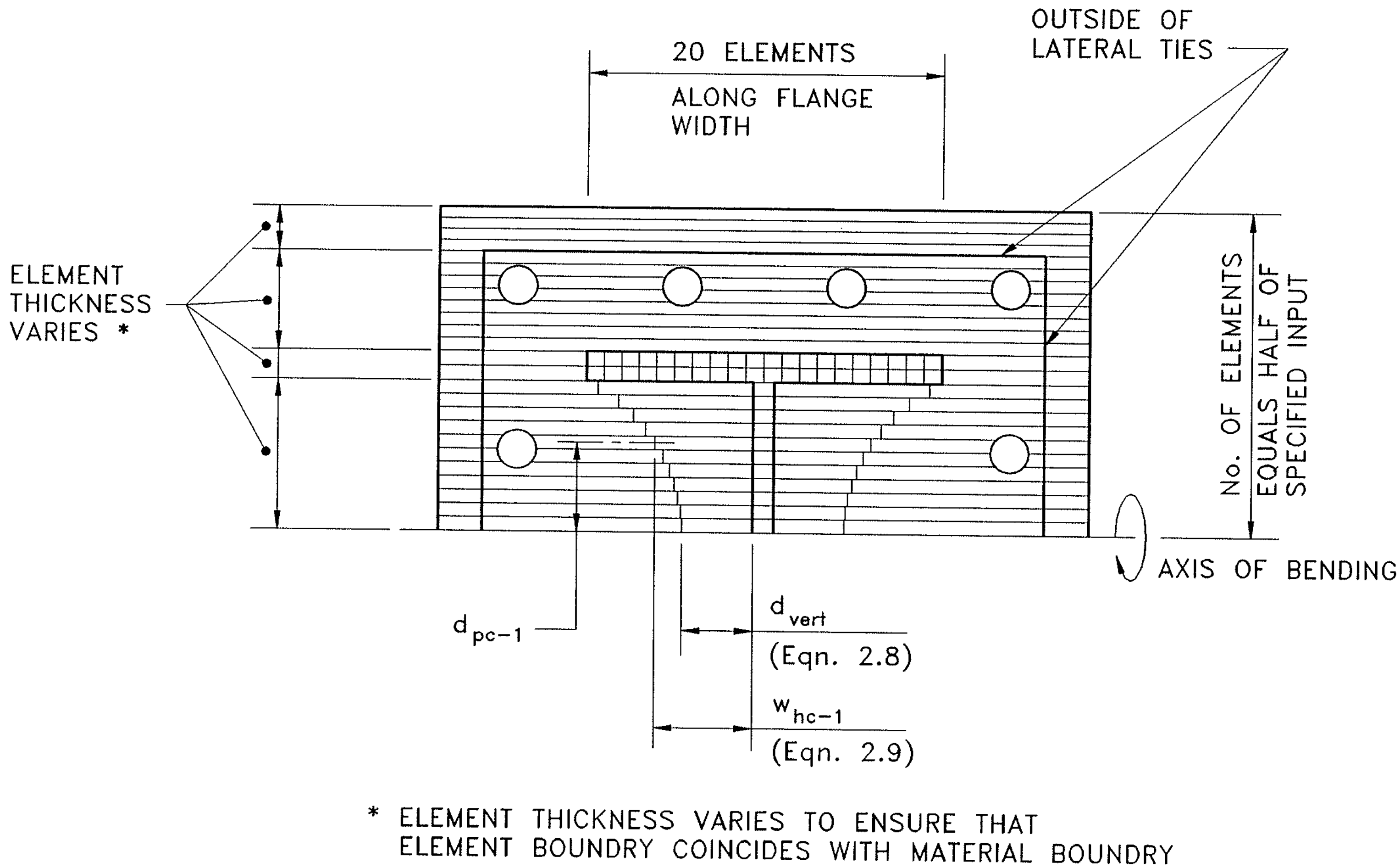

Figure 2.4 - Discretization of composite one-half cross-section used for theoretical strength subroutine for beam-columns subjected to bending about the major axis of the steel section.

the plastic centroid of the composite cross-section to the centroid of the element.

The steel section was subdivided into two areas, the web and the flanges, to account for the differences in yield strengths of the two elements reported by Galambos and Ravindra (1978), and Kennedy and Gad Aly (1980).

To calculate the M-ϕ-P relationship the computer numerically integrates the forces throughout the cross-section. To accomplish this the program discretizes the cross-section into a finite number of strips parallel to the major axis. Each strip, if required, is then further discretized to account for the various material properties contained within the strip. The thickness of the strip perpendicular to the major axis is determined by the number of strips requested, an input to the program. The width of each material within a given strip is automatically calculated. Fifty elemental strips for the entire cross-section were used for the computer simulations described in Chapter 5.

To account for varying stresses due to residual stresses along the width of the flange, the flange is discretized into 20 equal width elements perpendicular to the major axis. The initial strain in each element due to residual stresses is calculated with subsequent strains being added algebraically to each element. The discretization for a typical 1/2-section for major axis bending of a composite cross-section is shown in Figure 2.4.

2.3.2 Discretization for Minor Axis Bending

The procedure for discretization for minor axis bending is similar to that of the major axis bending with some differences.

As was in the case of major axis bending, the cover concrete, outside the lateral ties, was considered to be unconfined. The concrete inside the periphery of the ties but outside the flanges of the steel section was assumed to be partially confined. The concrete within an assumed parabola and between the web and flanges of the steel section was assumed to be highly confined. This is shown in Figure 2.3. The assumed parabola had a vertex intersecting the edge of the web at the mid-depth of the steel section when the flange overhang was less than one-quarter of the steel section depth between the flanges. The vertex of the parabola at the mid-height of the steel section was, otherwise, taken at a distance from the web d_{vert} which depended on the flange width b, flange tip thickness t_1, depth of steel section d, and web thickness w as indicated by Equation 2.10.

$$d_{vert} = \frac{b-w}{2} - \frac{d-2t_1}{4} \qquad (2.10)$$
$$d_{vert} \geq 0.0$$

The distance, parallel to the minor axis, from the edge of the flange at the tapered end to the parabola w_{hc-2} (Figure 2.5) for an elemental slice was computed by Equation 2.11.

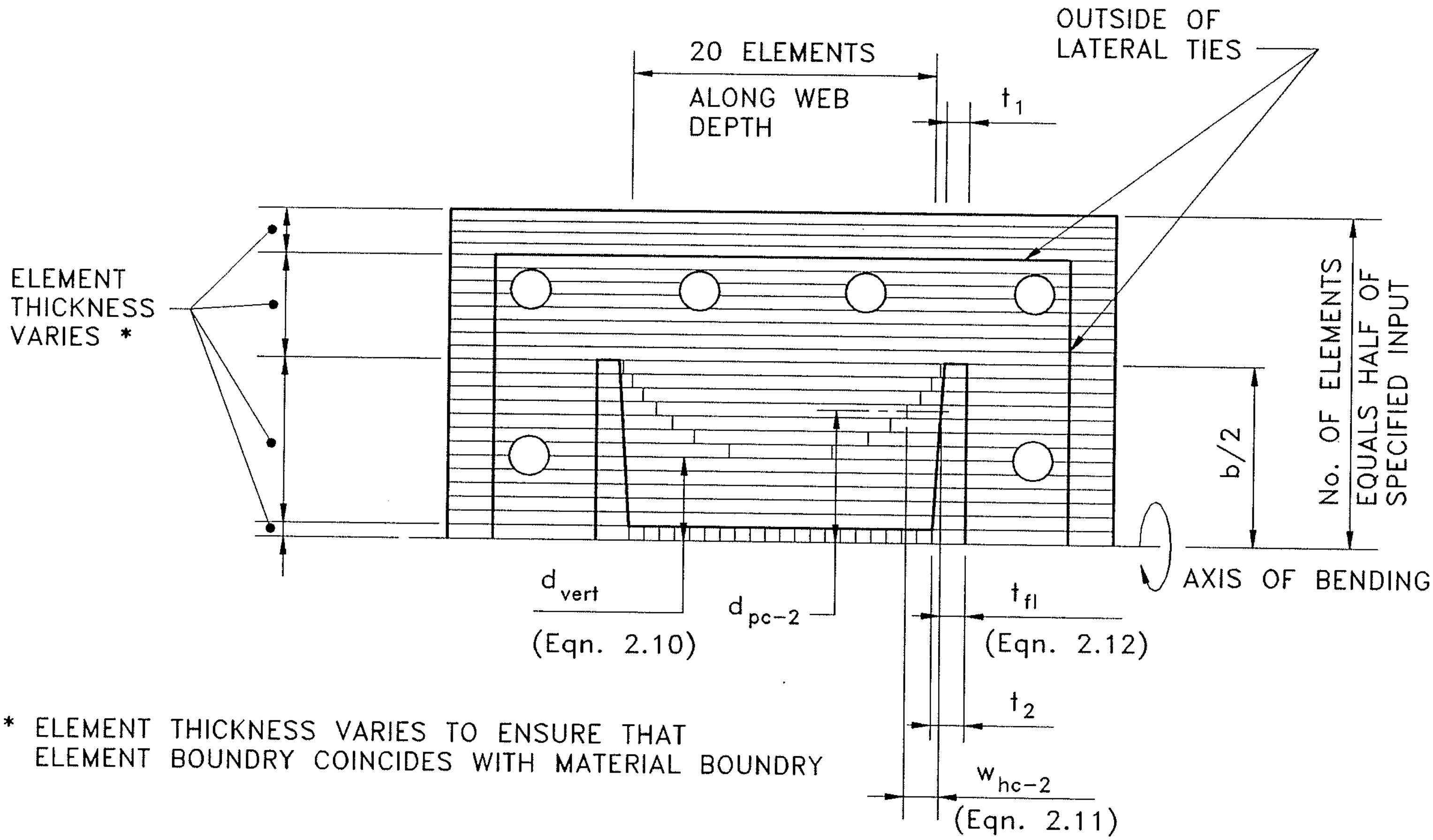

* ELEMENT THICKNESS VARIES TO ENSURE THAT ELEMENT BOUNDRY COINCIDES WITH MATERIAL BOUNDRY

Figure 2.5 - Discretization of composite one-half cross-section used for theoretical strength subroutine for beam-columns subjected to bending about the minor axis of the steel section.

$$w_{hc-2} = \frac{d}{2} - t_{f1} - \sqrt{\frac{\left(d_{pc-2} - d_{vert} - \frac{w}{2}\right)\left(\frac{d}{2} - t_1\right)^2}{\left(\frac{b - w}{2} - d_{vert}\right)}} \tag{2.11}$$

in which d_{pc-2} is measured perpendicular to the minor axis from the plastic centroid of the composite cross-section to the centroid of the element. The flange thickness t_{f1} at centroid of the desired element varies to take account for tapered flanges and is determined by Equation 2.12.

$$t_{f1} = t_2 - \left(d_{pc-2} - \frac{w}{2}\right)\left(\frac{t_2 - t_1}{\frac{b - w}{2}}\right) \tag{2.12}$$

in which t_2 is the thickness of the flange at the web-flange juncture.

Tapered flanges were not included as part of the study of effective flexural stiffness described in Chapter 6. It was necessary, however, to include the effect of tapered flanges for the calibration of the computer model because the majority of physical tests gathered from available literature were for tapered flanges.

The steel section was subdivided into two areas, the web and the flanges, to account for the differences in yield strengths of the two elements reported by Galambos and Ravindra (1978), and Kennedy and Gad Aly (1980).

To calculate the M-ϕ-P relationship the computer numerically integrates the forces throughout the cross-section. To accomplish this the program discretizes the cross-section into a finite number of strips parallel to the minor axis. Each strip, if required, is then further discretized to account for the various material properties contained within the strip. The thickness of the strip perpendicular to the minor axis is determined by the number of strips requested, an input to the program. The width of each material within a given strip is automatically calculated. Fifty elemental strips for the entire cross-section were used for the computer simulations described in Chapter 6.

To account for varying stresses due to residual stresses along the width of the web, the web is discretized into 20 equal width elements perpendicular to the minor axis. The initial strain in each element due to residual stresses is calculated with subsequent strains being added algebraically to each element. The discretization for a typical 1/2-section for minor axis bending of a composite cross-section is shown in Figure 2.5.

2.4 CROSS-SECTION STRENGTH

To determine cross-section strength, which is represented by an axial load-bending moment (P-M) interaction diagram, the relationship between bending moment, curvature and axial load (M-ϕ-P), similar to the one shown in Figure 2.6, was established. The maximum moment from the moment-curvature relationship (Figure 2.6) for a given axial load level represents one point on the cross-section P-M interaction

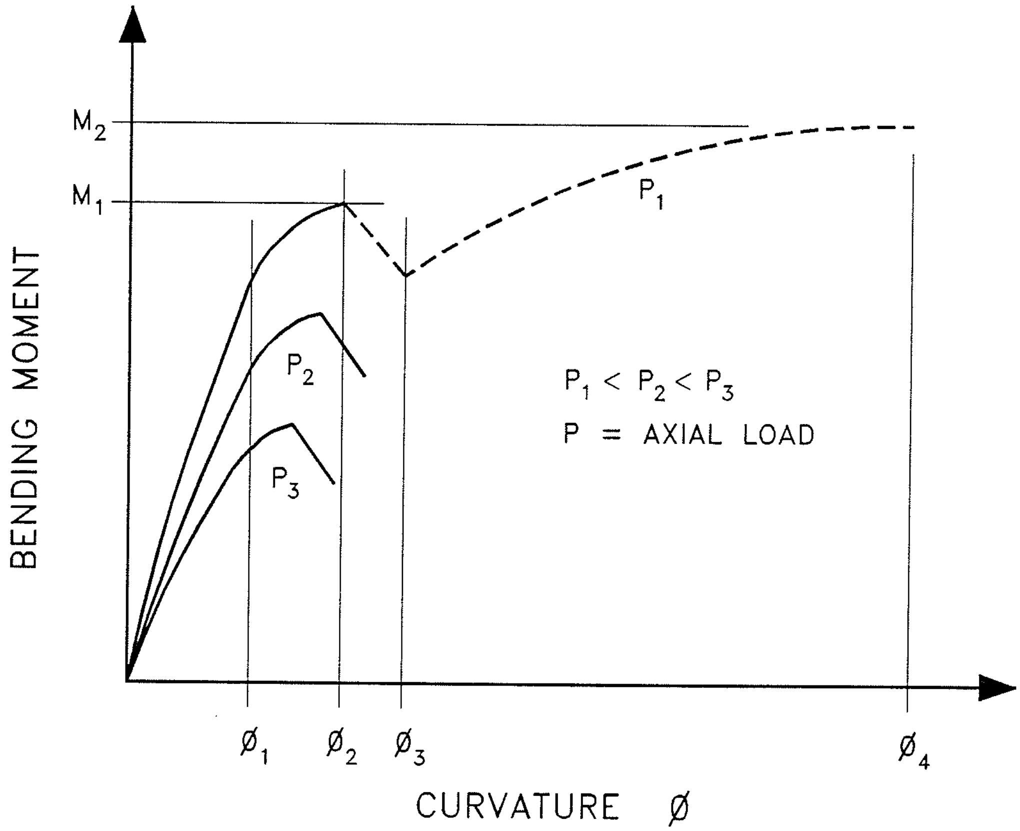

<u>For Axial Load P_1 :</u>

$\emptyset_1$ – yielding of flange in tension zone

$\emptyset_2$ – spalling of concrete cover begins

$\emptyset_3$ – concrete cover spalled off.
– strain-hardening initiated in tension region of flange

$\emptyset_4$ – rupture of tension flange

M_1 – maximum bending moment (strain-hardening neglected)

M_2 – maximum bending moment (strain-hardening considered)

Figure 2.6 - Schematic M-ϕ-P relationships for composite cross-section.

diagram. To accurately define the interaction diagram (Figure 2.7), approximately 48 points (48 axial load levels) were needed for both the major axis bending (Figure 2.7(a)) and the minor axis bending (Figure 2.7(b)). To determine the M-ϕ-P relationship, the maximum axial load level which can be applied to a cross-section at its plastic centroid (pure compression capacity) was first established. This defined the range of axial load to be examined. An iterative technique was employed to determine the pure axial load capacity by incrementing the strain from the lowest strain at peak stress, obtained from the stress-strain relationships for the six material types, to the highest strain at peak stress and calculating the load at each strain level. The maximum axial load calculated during the iterative process was taken as the cross-section concentric axial load capacity, thus establishing the point on the P-M interaction diagram that corresponds to zero bending moment.

The distance *DNA* between the neutral axis and the plastic centroid, shown in Figure 2.8, must be known to determine the M-ϕ-P relationship. By using a strain compatibility solution for a given curvature ϕ and depth of neutral axis *DNA*, the equilibrium forces of axial load P and bending moment M can be calculated.

An iterative procedure was used to create a matrix of P versus *DNA* values. By assuming a starting curvature, and holding this value constant, the depth of the neutral axis *DNA*

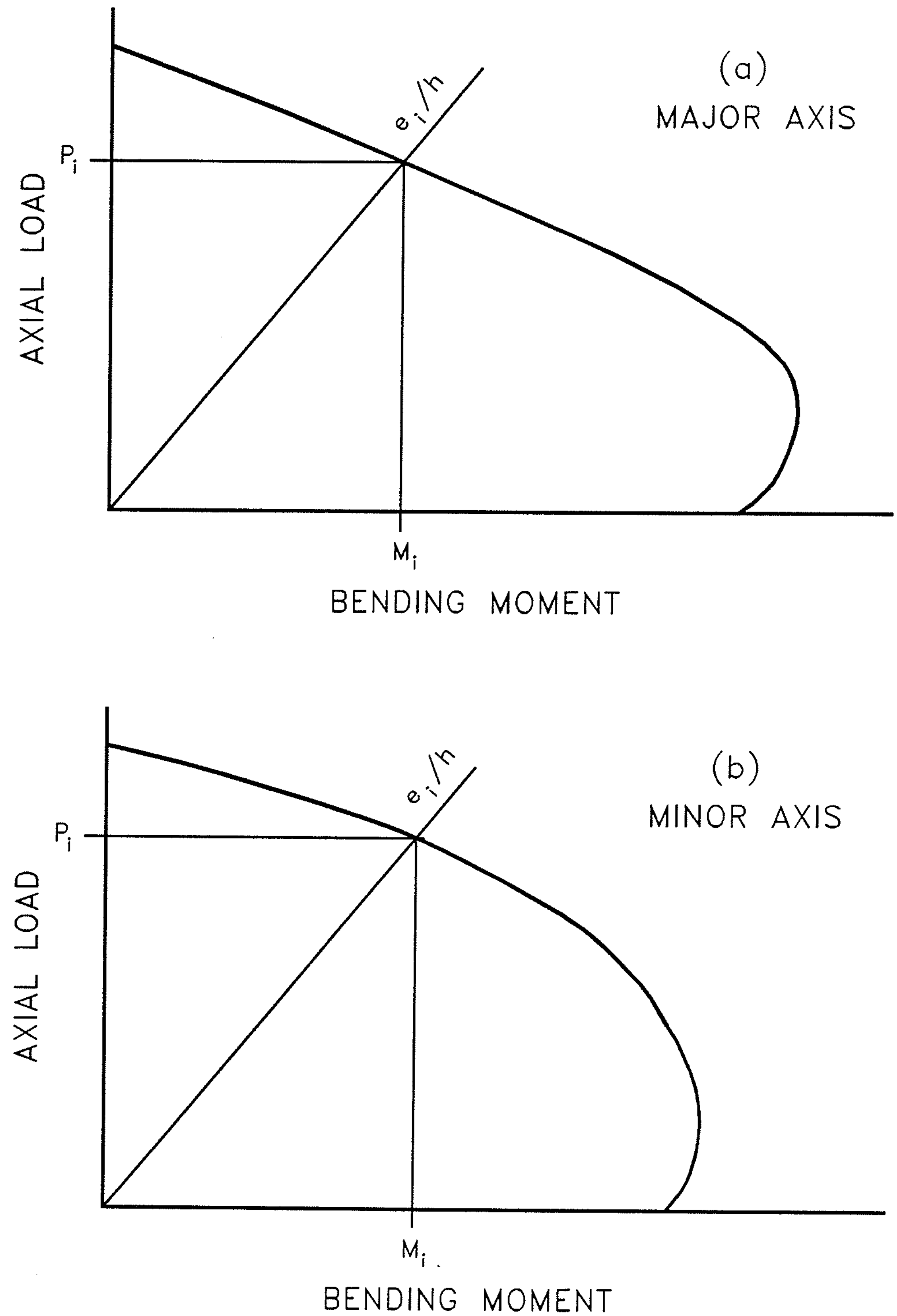

Figure 2.7 - Schematic composite cross-section and column axial load-bending moment (*P-M*) interaction diagrams for beam-columns subjected to bending about the (a) major axis and (b) minor axis of the steel section.

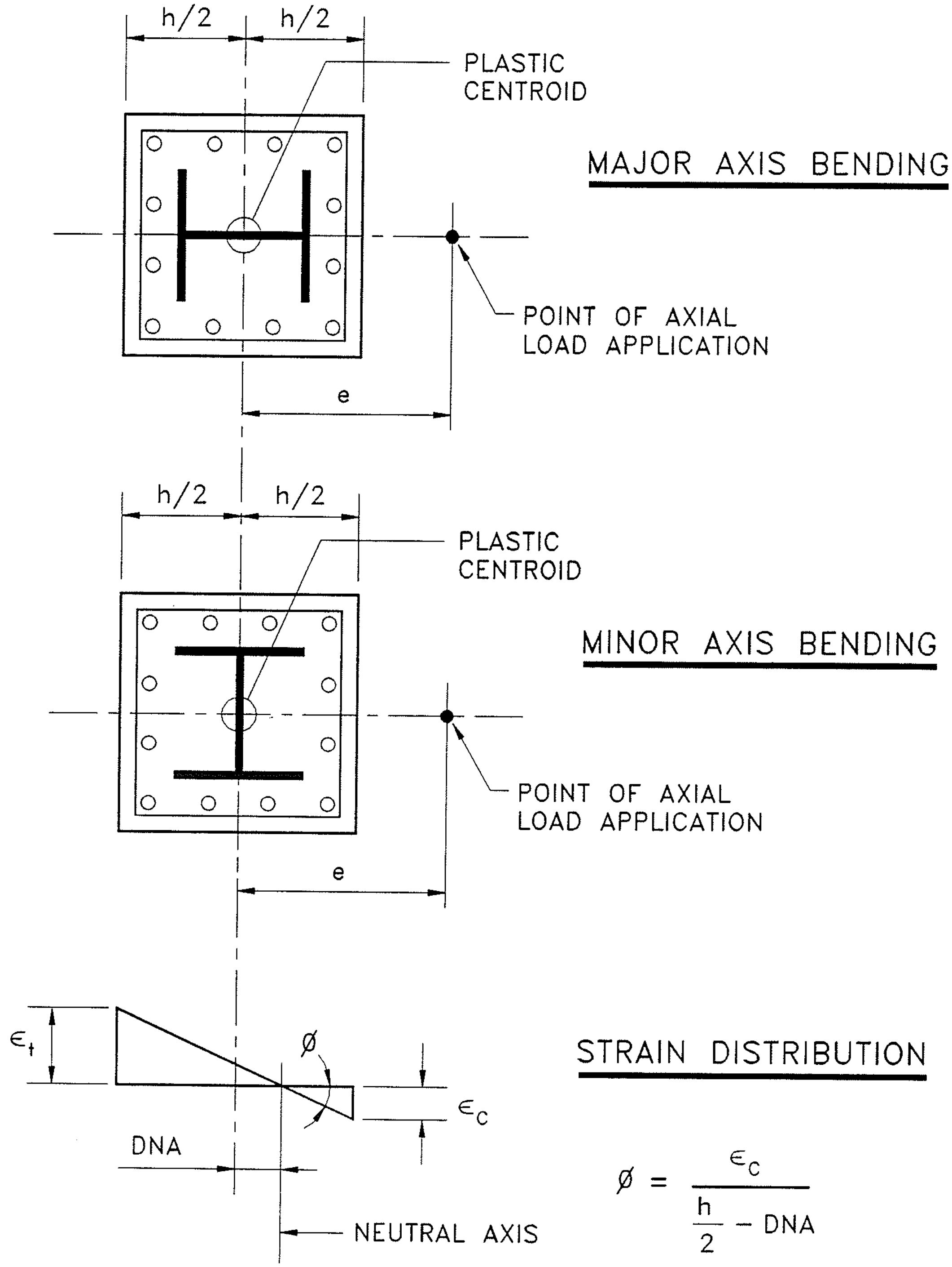

Figure 2.8 - Strain gradient in composite cross-section in which bending takes place about the major or minor axis of the steel section.

was varied and the corresponding axial force calculated. Linear interpolation and the extended Newton-Raphson technique (Kikuchi, Mirza and MacGregor 1978) was used to converge to the correct *DNA* value for each desired axial force. The bending moment corresponding to the curvature, neutral axis position and the axial force was then calculated.

The curvature was then incremented creating a new matrix of *P* versus *DNA* values and new bending moment calculated. The curvature was incremented until the concrete cover on the compressive side of the cross-section had spalled off to ensure that the maximum bending moment for the desired axial force was obtained.

However, when strain hardening was considered at low axial load levels (less than 20 percent of the pure compression capacity), the maximum bending moment occurred at very high curvature values long after the spalling of the concrete. For these cases, the tension flange of the steel section was monitored at each curvature increment and if rupture of the tension flange was imminent, no further points were calculated for that axial load level. It should be noted that the effect of strain hardening was only used for the comparison of theoretical model to experimental results discussed in Chapter 3.

This procedure, outlined in Figure 2.9, created the required M-ϕ-P relationship. The data when plotted is similar to the data plotted in Figure 2.6. When the moment versus

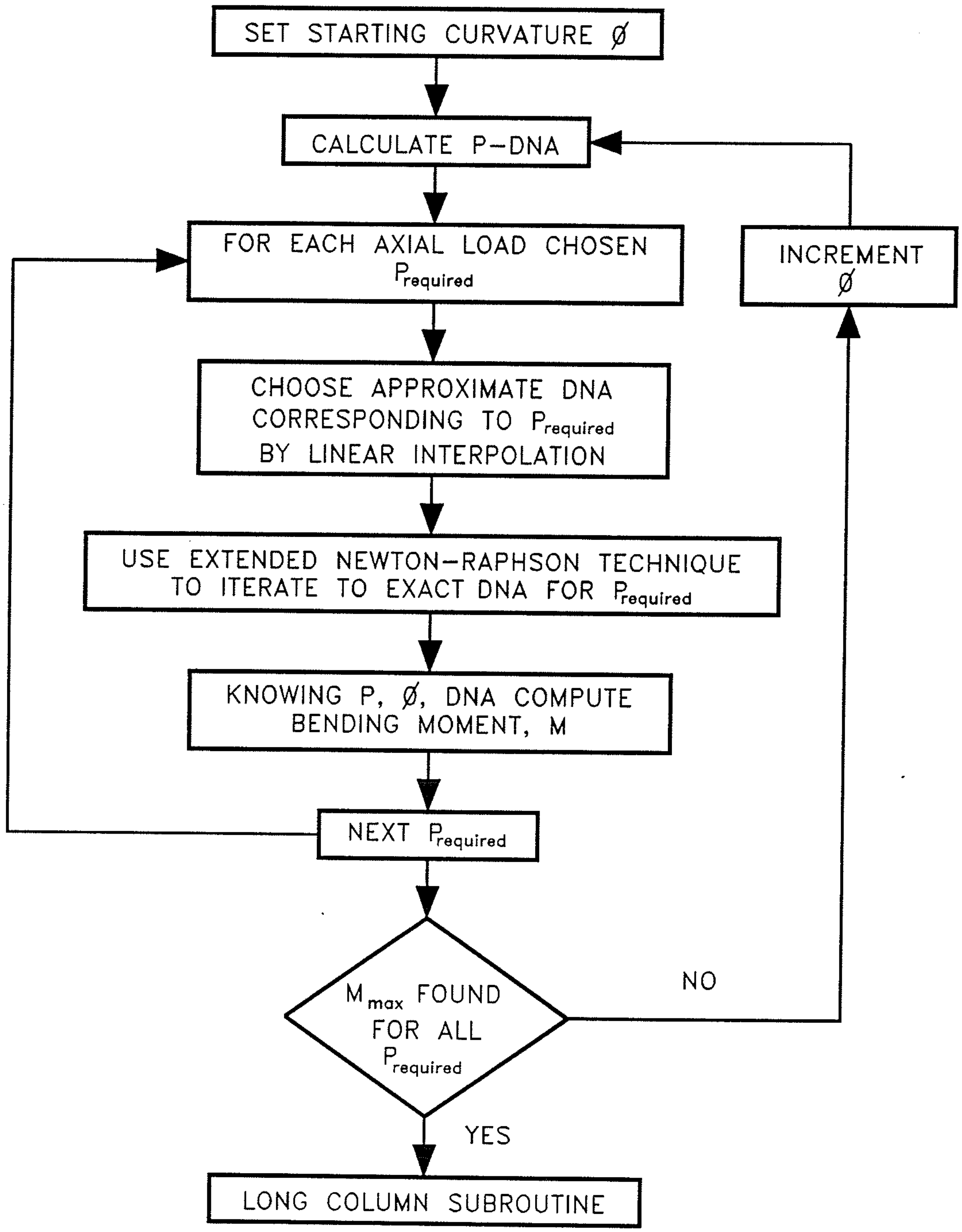

Figure 2.9 - Flow chart for computation of M-ϕ-P relationships for composite cross-section.

curvature diagrams were completed for all of the desired axial load levels, the maximum bending moment for each axial load level is stored. These bending moments paired with the corresponding axial loads form the *P-M* interaction diagram (Figure 2.7). The program then proceeds to the slender column subroutine for lengths greater than zero.

2.5 SLENDER BEAM-COLUMN STRENGTH

The bending moment capacity of a beam-column at a given axial load level is lower than the capacity of the cross-section. A beam-column of length ℓ deflects laterally when subjected to an eccentric axial load and is subjected to additional moment at its mid-height. A column bending in single curvature under equal end eccentricities was modeled in this study (Figure 1.1). Therefore, secondary moments at the mid-height caused by the axial load acting through additional eccentricity become significant in slender columns and control the maximum applied end moment.

In order to construct the slender beam-column *P-M* interaction diagram, the program calculates the maximum end moment corresponding to the desired axial load level. To be stable the internal forces at the mid-height of the beam-column and the ends must be in equilibrium with the applied external forces. As the end eccentricity is increased for the given axial load, there is a corresponding increase in lateral deflection and secondary moment until the material at mid-height fails. The long column bending moment capacity is the bending moment acting at the ends of the column at failure.

The concentric load capacity of a slender column was not utilized in examining the flexural stiffness of a beam-column. However, for the comparison of experimental results to theoretical results, described in Chapter 3, the concentric load capacity was determined.

Therefore, just as for the cross-sectional strength, the concentric axial load capacity for the slender column was calculated first in the development of the *P-M* interaction diagram. The tangent modulus theory, used by Wakabayashi (1976) and Basu (1967), was used to calculate this load. The use of the tangent modulus theory requires the assumption that no initial camber exists in the steel section, because the theory can only be applied to columns that are perfectly straight.

A concentrically loaded slender column fails by buckling before the material strength is exceeded. The ultimate buckling stress for a column of homogeneous material is given by the tangent buckling formula shown in Equation 2.13.

$$f_{cr} = \frac{\pi^2 E_t}{(k\ell/r)^2} \qquad (2.13)$$

Substituting 1.0 for the effective length factor k, and the square root of the moment of inertia divided by the area ($\sqrt{I/A}$) for the radius of gyration r, Equation 2.13 can be rewritten as:

$$P_{cr} = f_{cr}\, A = \frac{\pi^2}{\ell^2} E_t I \qquad (2.14)$$

where P_{cr} is the column buckling load.

Equation 2.14 must be applied independently to the six materials present in a composite column, each material possessing independent stress-strain curves. The sum of all six tangent buckling strengths gives the tangent buckling load for the column. Wakayabashi (1976) proposed a similar procedure. To account for the six independent materials, Equation 2.14 takes the following form:

$$P_{cr} = \sum_{i=1}^{i=6} (f_{cr_i} A_i) = \frac{\pi^2}{\ell^2} \sum_{i=1}^{i=6} (E_{t_i} I_i) \qquad (2.15)$$

An iterative technique was used to solve Equation 2.15 because the tangent elastic modulus of an element is a function of the stress in the element. This was accomplished by adjusting the axial strain in the column until the load calculated by each side of Equation 2.15 was less than 1 pound (4.45 N). Thus establishing the point on the slender column *P-M* interaction diagram that corresponds to the maximum concentric load and zero bending moment.

The method for establishing the points other than the pure compression capacity on the slender beam-column *P-M* interaction diagram determines the maximum end eccentricity sought for each desired axial load level and is described as follows:

(a) Assume a mid-height deflection of the column.

(b) Find the end curvature which corresponds to the desired deflected shape.

(c) Find the bending moment corresponding to the end curvature from the cross-section M-ϕ-P relationships and calculate the end eccentricity.

(d) Add the end eccentricity to the assumed mid-height deflection and calculate a new bending moment at the mid-height of the column.

(e) If the bending moment calculated in (d) is less than the maximum bending moment from the cross-section M-ϕ-P relationship, increase the mid-height deflection and repeat the process starting from item (a). If the bending moment calculated in (d) is greater than the maximum bending moment from the cross-section M-ϕ-P relationship, the end eccentricity calculated in item (d) from the previous iteration is used to compute the maximum end bending moment.

To represent the deflected shaped of a pin-ended column, a fourth order parabola suggested by Quast (1970) was used. The mid-height deflection is given by Equation 2.16

$$\Delta_m = \frac{\ell^2}{10}\left(\phi_m + \frac{\phi_e}{4}\right) \tag{2.16}$$

where ϕ_m and ϕ_e are the curvatures at mid-height and the column ends, respectively; ℓ is the length of the column; and

Δ_m is the mid-height deflection of the column as shown in Figure 1.1.

The total mid-height eccentricity e_t is the sum of the assumed mid-height deflection Δ_m from Equation 2.16 and the end eccentricity e as shown in Equation 2.17.

$$e_t = e + \Delta_m \tag{2.17}$$

Substitution of Equation 2.16 into 2.17 and rearranging to solve for the end eccentricity yields Equation 2.18.

$$e = e_t - \left(\frac{\ell^2}{10}\right)\left(\phi_m + \frac{\phi_e}{4}\right) \tag{2.18}$$

The mid-height eccentricity e_t can be calculated by dividing the mid-height bending moment by the axial load as shown in Equation 2.19.

$$e_t = \frac{M_m}{P} \tag{2.19}$$

Substitution of Equation 2.19 into 2.18 gives the simple relationship between the end eccentricity (e), mid-height moment (M_m), the mid-height curvature (ϕ_m) and the end curvature (ϕ_e) as shown in Equation 2.20.

$$e = \left(\frac{M_m}{P}\right) - \left(\frac{\ell^2}{10}\right)\left(\phi_m + \frac{\phi_e}{4}\right) \tag{2.20}$$

The program uses Equation 2.20 and the cross-section M-ϕ-P relations previously calculated to solve for a combination of end eccentricity, mid-height deflection and mid-height curvature that are in equilibrium. Figure 2.10 outlines the

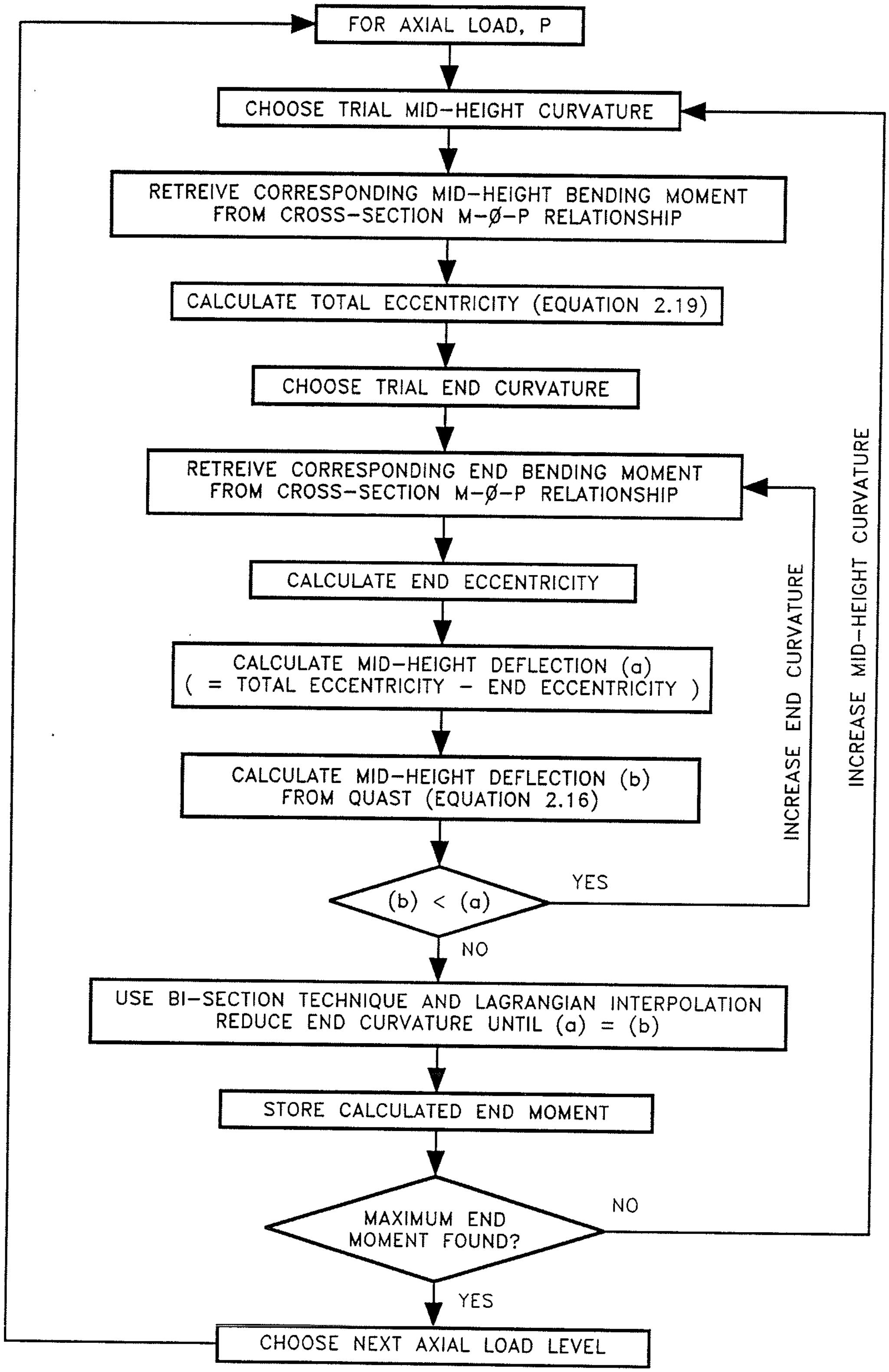

Figure 2.10 - Flow chart for computing slender column M-ϕ-P relationships.

procedure. Values for the mid-height curvature are incremented from a minimum value (the smallest curvature from the cross-section M-ϕ-P relationship corresponding to desired axial load) until a maximum end bending moment is calculated. For each mid-height curvature value assumed, values of the end curvature are tested and incremented from the minimum value until an equilibrium combination is found. The largest curvature that can be attained at mid-height is the one that corresponds to the maximum moment from the M-ϕ-P diagram for the axial load. Once all possible mid-height curvatures have been investigated, the largest end bending moment calculated becomes one point on the slender beam-column P-M interaction curve. The process is then repeated to complete the entire slender beam column P-M interaction curve.

2.6 MATERIAL STRESS-STRAIN CURVES

A composite beam-column is represented by six different materials, each characterized by a distinct stress-strain relationship as indicated earlier in Section 2.3. Three of the six materials are unconfined, partially confined and highly confined concrete. The flange and web of the rolled steel shape account for two more of the material types. The longitudinal reinforcing steel makes up the sixth material present in the cross-section. The six materials are shown in Figure 2.3.

2.6.1 Stress-Strain Curves for Concrete

The distinction between the concrete areas, defined in Section 2.3, recognizes the differences inherent in the stress-strain relationship due to the confining action of the rectangular lateral ties, the longitudinal reinforcing steel bars and the rolled steel section. Concrete confinement increases both compressive strength of concrete and ductility. Park, Priestly and Gill (1982) , Sheikh and Uzemeri (1982), and Sheikh and Yeh (1986) developed methods to determine the beneficial effects of increased compressive strength and ductility of concrete for reinforced concrete columns. Methods to determine the effect of confinement on the concrete tensile stress-strain relationship are not available. Therefore, identical tensile stress-strain relations for all types of concrete confinements was assumed. The stress-strain relationships presented in this Section are based on static loading conditions.

Based on the recommendation of Skrabek and Mirza (1990) and the findings of Llewellyn (1986), a modified version of the Kent and Park (1971) curve (Figure 2.11) for unconfined concrete was used to describe the stress-strain relationship for concrete outside the perimeter of the lateral ties in this study. Equation 2.21 represents the curve between the origin and the peak stress, and the descending branch of the curve between the peak stress and the stress at ultimate strain is described by Equation 2.22.

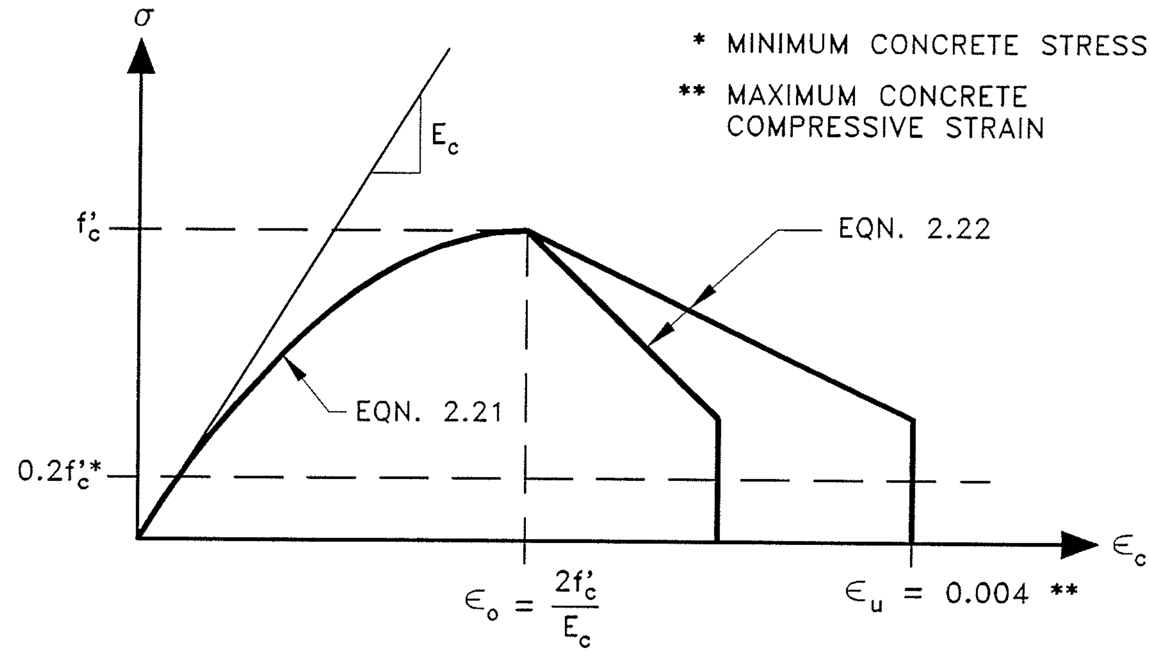

Figure 2.11 - Unconfined concrete compressive stress-strain relationship used in theoretical strength subroutine.

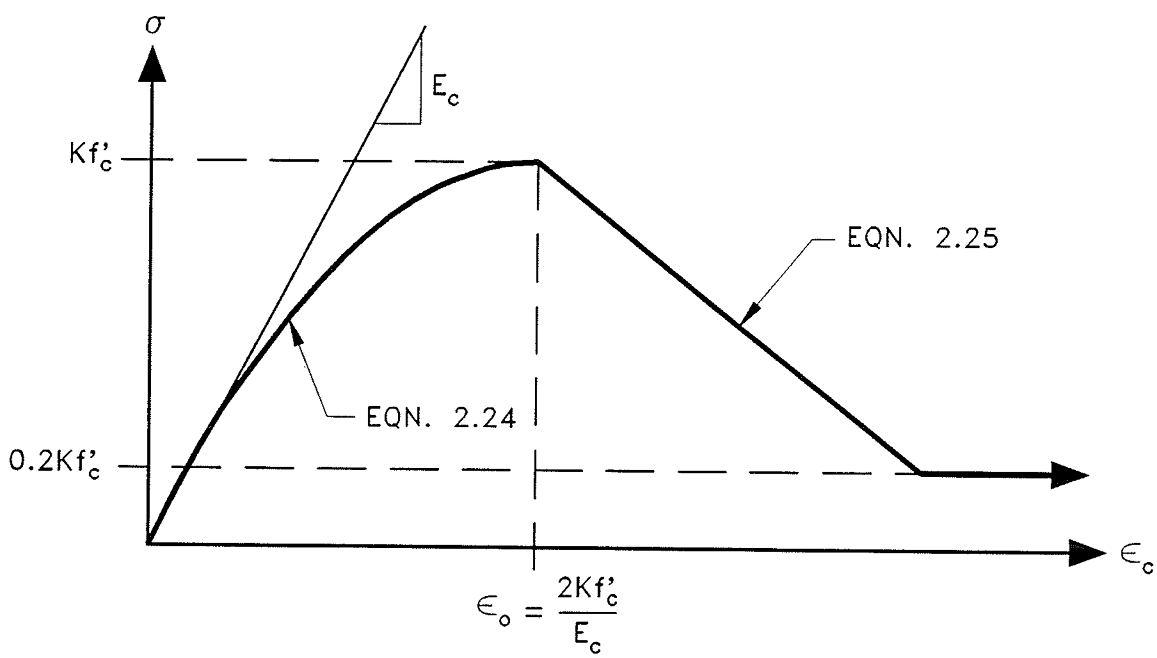

Figure 2.12 - Partially confined concrete compressive stress-strain relationship used in theoretical strength subroutine.

$$f_c = f_c' \left[\frac{2\epsilon_c}{\epsilon_o} - \left(\frac{\epsilon_c}{\epsilon_o} \right)^2 \right] \tag{2.21}$$

$$f_c = f_c' \left[1 - Z \left(\epsilon_c - \epsilon_o \right) \right] \tag{2.22}$$

where $$Z = \frac{0.5}{\epsilon_{50u} - \epsilon_o}$$

and $$\epsilon_{50u} = \frac{3 + \epsilon_o f_c'}{f_c' - 1000}$$

For SI conversion replace 3 by 0.0207 MPa and 1000 by 6.895 MPa. The strain at the peak stress (ϵ_o) *was* allowed to vary as a function of the concrete strength (Equation 2.23) rather than a constant value of 0.002 suggested by Kent and Park (1971).

$$\epsilon_o = \frac{2f_c'}{E_c} \tag{2.23}$$

For partially confined concrete Skrabek and Mirza (1990) investigated the Modified Kent and Park Curve (Park, Priestly and Gill 1982), and the Sheikh - Uzumeri Curve (1982) for their applicability to composite columns and found them to produce similar results. The Modified Kent and Park Curve (Figure 2.12) was used in this study to model the partially confined concrete in the composite cross-section, as was used by Skrabek and Mirza (1990). The Modified Kent and Park Curve assumes that the degree of confinement is a function of the concrete cylinder strength f'_c, the vertical spacing of the ties s_h, the ratio of volume of lateral ties to volume of concrete core ρ_s, and the yield strength of the horizontal ties f_{yh}. The ascending portion of the curve between the origin and the peak stress is described by Equation 2.24 while Equation 2.25 describes the descending branch of the curve.

$$f_c = Kf'_c \left[\frac{2\epsilon_c}{K\,\epsilon_o} - \left(\frac{\epsilon_c}{K\,\epsilon_o} \right)^2 \right] \tag{2.24}$$

where $K = 1 + \dfrac{\rho_s\, f_{yh}}{f'_c}$

$$f_c = Kf'_c \left[1 - Z\left(\epsilon_c - K\,\epsilon_o\right) \right] \geq 0.2Kf'_c \tag{2.25}$$

where $Z = \dfrac{0.5}{\epsilon_{50u} + \epsilon_{50h} - K\,\epsilon_o}$

and $\epsilon_{50u} = \dfrac{3 + K\,\epsilon_o f'_c}{f'_c - 1000}$

and $\epsilon_{50h} = \dfrac{3}{4}\rho_s \sqrt{\dfrac{h''}{s_h}}$

In the equation above, h'' is the out to out width of the lateral ties. For SI conversion replace 3 by 0.0207 MPa and 1000 by 6.895 MPa.

The Modified Kent and Park Curve used by Skrabek and Mirza to model the heavily confined concrete between the web and flanges of the rolled steel shape was also used in this study. The peak stress in the heavily confined concrete was assumed to be maintained at all strains beyond the peak stress. Figure 2.13 describes the assumed stress-strain curve for heavily confined concrete.

The tensile stress-strain curve used in this study is shown is Figure 2.14. A linear stress-strain relationship from the origin to the modulus of rupture was assumed with the elastic modulus for tension assumed equal to the modulus of elasticity in compression. The work of Skrabek and Mirza (1990) shows that this simple model suggested by Park and Pauley (1975), and Mirza and MacGregor (1989) was sufficient.

2.6.2 Stress-Strain Curves for Steel

An elastic-plastic stress-strain curve was assumed to describe the behaviour of both the structural steel and the longitudinal reinforcing steel. Strain-hardening was not included for the study of stiffness described in Chapter 5 and 6, but was included for calibration of the strength model described in Chapter 3. The stress-strain curve for compression was assumed to be the same as that for tension.

A second order parabola was used to describe the strain-hardening portion of the stress-strain curve. At ultimate strain the slope of the strain hardening curve was assumed to be equal to zero.

The variables used by the program to describe the stress-

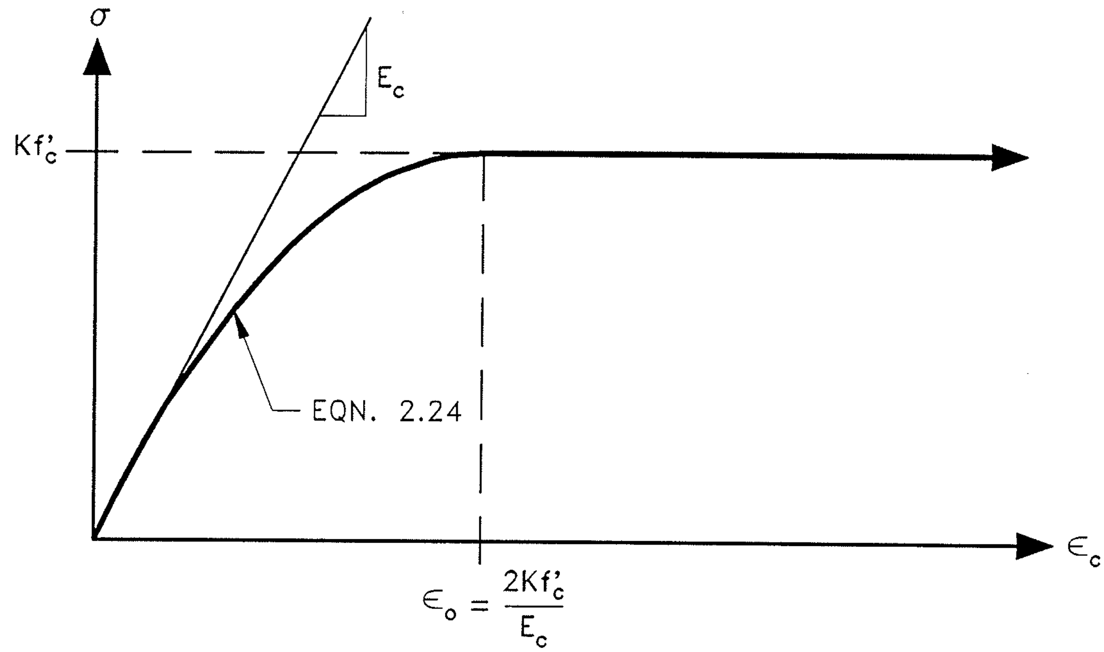

Figure 2.13 - Heavily confined concrete compressive stress-strain relationship used in theoretical strength subroutine.

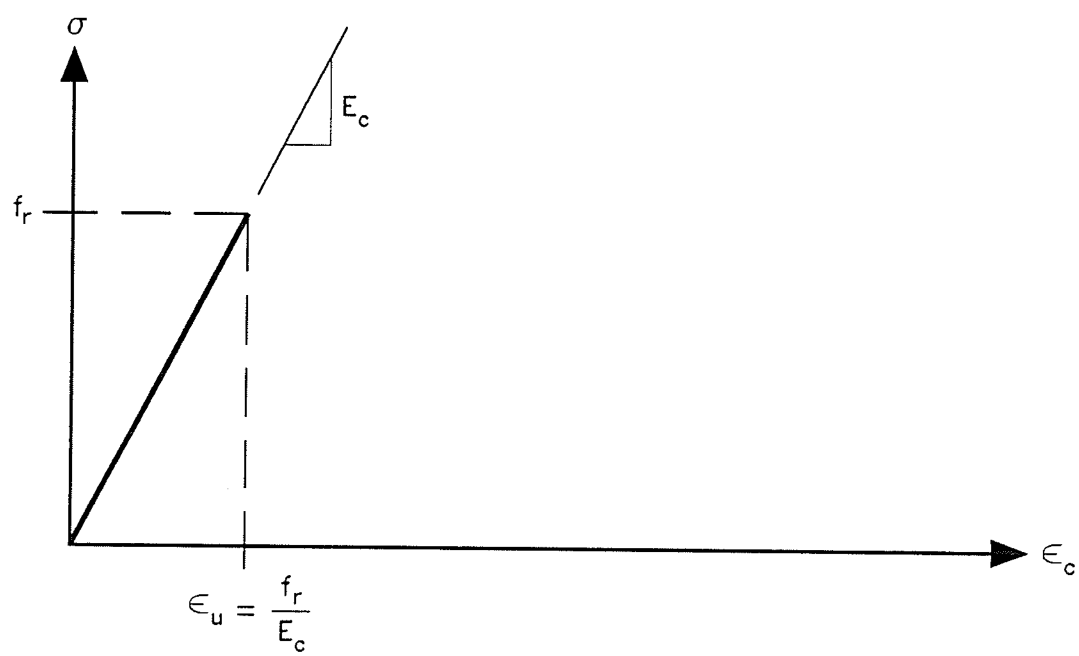

Figure 2.14 - Concrete tensile stress-strain relationship used in theoretical strength subroutine.

strain curve for structural steel shown in Figure 2.15 are the elastic modulus E_s, the yield stress f_{ys}, the strain at the onset of strain hardening ϵ_{sstrn}, the initial tangent slope of the strain hardening curve E_{sstrn}, and the ultimate stress f_{us}.

The variables used by the program to describe the stress strain curve for reinforcing steel shown in Figure 2.16 are the elastic modulus E_r, the yield stress f_{yr}, the strain at the onset of strain hardening ϵ_{rstrn}, the ultimate stress f_{ur}, and the ultimate strain ϵ_{ur}.

2.7 RESIDUAL STRESSES IN STRUCTURAL STEEL

Residual stresses are due to uneven cooling of component parts during the manufacturing process. Skrabek and Mirza (1990) found that the work of LaChance and Hays (1980), Virdi and Dowling (1973), and Mirza (1989) made it evident that residual stresses can significantly vary the strength of a composite beam-column. For this reason the effect of residual-stresses was accounted for in this study.

A detailed analysis by Skrabek and Mirza (1990) determined that using Young's (1971) model (Equation 2.26) to predict the residual stresses at the flange tips combined with the model by Galambos (1963) (Equation 2.27) to predict the residual stresses at the flange-web juncture provides the best overall prediction of measured values reported by Beedle and Tall (1960).

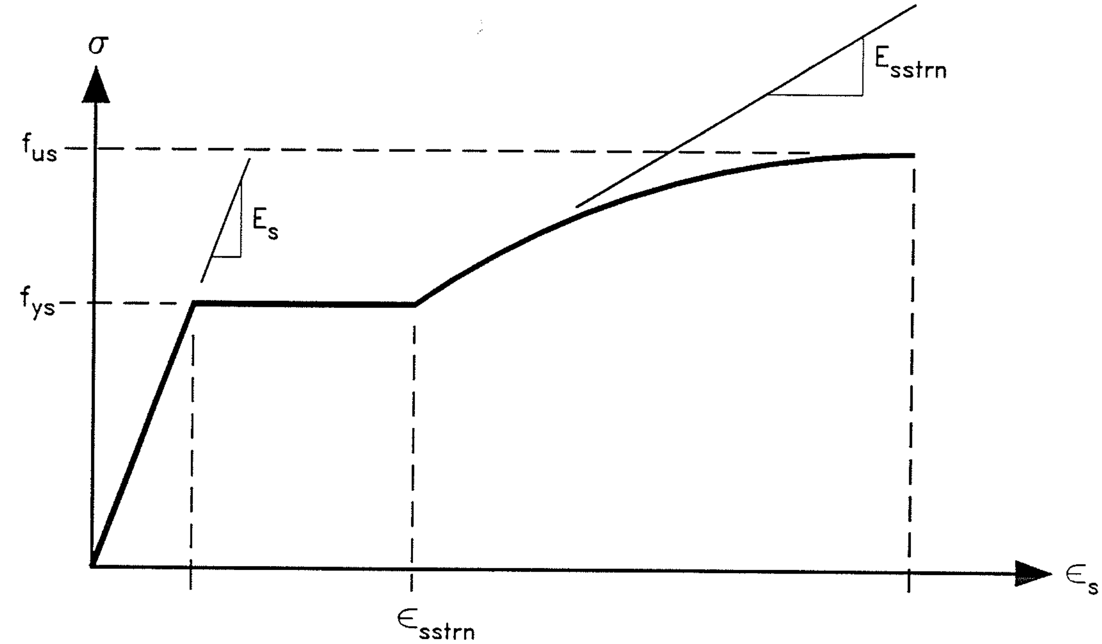

Figure 2.15 - Structural steel stress-strain relationship in tension or compression used in theoretical strength subroutine.

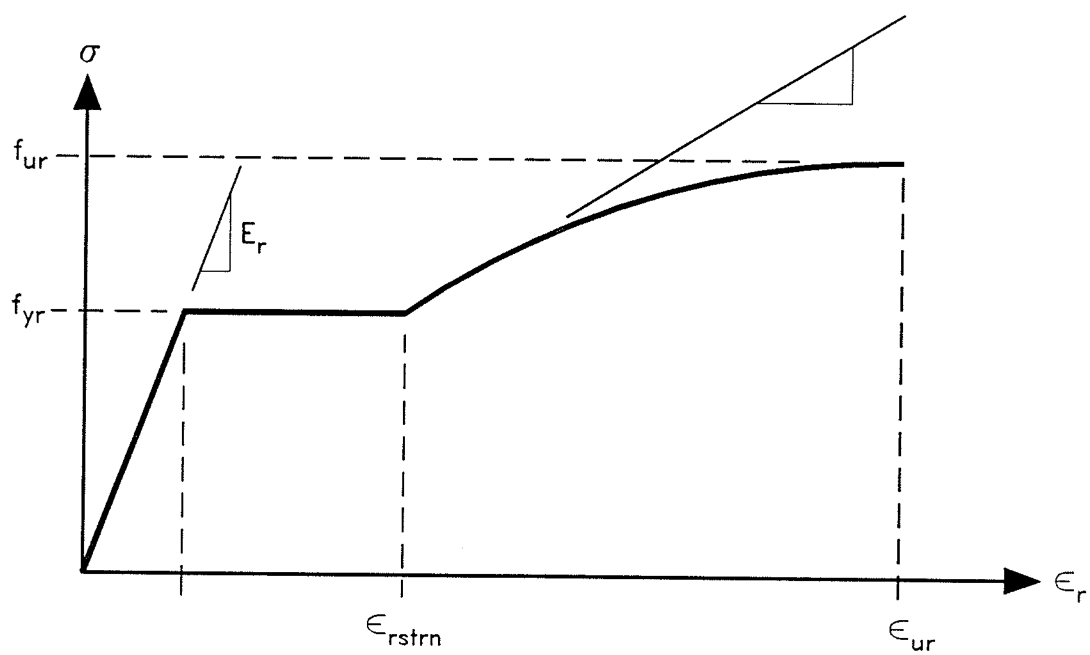

Figure 2.16 - Reinforcing steel stress-strain relationship in tension or compression used in theoretical strength subroutine.

$$\sigma_{rft} = -24{,}000\left(1 - \frac{A_w}{1.2A_f}\right) \qquad (2.26)$$

$$\sigma_{rfw} = -\sigma_{rft}\left[\frac{bt}{bt + w\ (d - 2t)}\right] \qquad (2.27)$$

A linear distribution was assumed for the residual stresses. In Equation 2.26 σ_{rft} is the residual stress at the tips of the flanges, A_w is the area of the web, and A_f is the area of both flanges of the steel section. In Equation 2.27 σ_{rfw} is the residual stress at the flange web juncture, b is the flange width, t is the flange thickness (average thickness for tapered flanges), w is the web thickness and d is the depth of the structural steel shape. For SI conversion of Equation 2.26, replace 24,000 psi by 165 MPa.

Using a trial and error method, described below, the program calculates the required residual stress at the mid-depth of the web to maintain force equilibrium of the steel section:

(a) Determine the net force in the flanges due to residual stresses.

(b) Determine whether the mid-depth of the web is in tension or in compression in order to achieve equilibrium.

(c) Calculate the mid-depth residual stress assuming a triangular stress distribution in the web (Figure 2.17(a)(i) or 2.17(b)(i)).

(d) If the residual stress computed in (c) exceeds 50 percent of the web yield stress, try a trapezoidal distribution

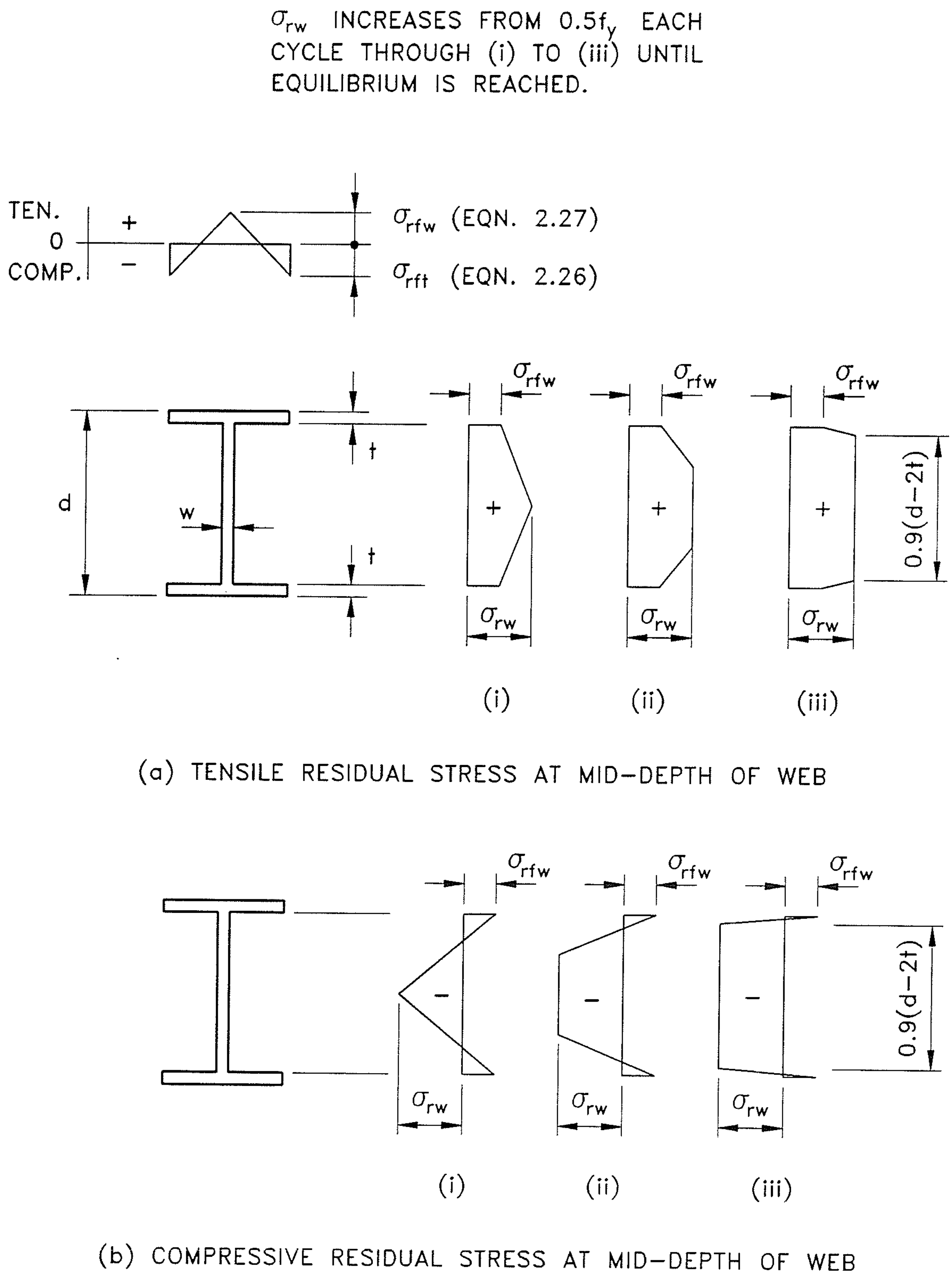

Figure 2.17 - Residual stress distribution in wide flanged steel shapes used in theoretical strength subroutine.

(Figure 2.17(a)(ii) or 2.17(b)(ii)) assuming a value of 50 percent of the web yield stress as the mid-depth stress. Increase the zone of mid-depth stress to a maximum of 90 percent of the web depth (Figure 2.17(a)(iii) or 2.17(b)(iii) or until equilibrium is achieved.

(e) If equilibrium is not reached in (d) increase the mid-depth stress by another 5 percent of the web yield stress and repeat with the trapezoidal distribution for the web residual stresses.

Item (e) is repeated until equilibrium is achieved. This procedure balanced the residual stresses in the steel section before the residual stress in the web reached yield stress level. The theoretical program can be used with or without the above-noted residual stresses in the rolled steel section depending what is desired. For this study, however, the residual stresses were included in the analysis of strength as indicated earlier.

3 - COMPARISON OF THEORETICAL MODEL TO EXPERIMENTAL RESULTS

To test the accuracy of the theoretical model, the ultimate strengths predicted by the theoretical subroutine were compared to the ultimate strengths of physical experimental test results gathered from published literature. No new tests were conducted for this study. The load cases studied for major and minor axis bending are examined individually and are discussed in detail in the Section 3.1 and 3.2. Data gathered for examination for bending about major and minor axis of the steel section included concentric loading, eccentric loading causing bending about an axis, and pure bending about an axis for columns with slenderness ratios ℓ/h (length to overall concrete cross-section depth) ranging from 2.0 to 45.0.

Problems which were encountered while interpreting the experimental results for some of the test data gathered from available literature are summarized below:

1) The specified length of some specimens was unclear, especially when haunches were used at the ends of the column. This pertains to tests conducted by Stevens (1965).
2) Information regarding the reinforcement was in some cases insufficient with respect to quantity, position, and yield strength. This pertains to tests conducted by Stevens (1965) and Bondale (1966).
3) The way the concrete strength was determined from cubes

was unclear for some test results (cube tested parallel or perpendicular to the direction of casting). This pertains to tests conducted by Stevens (1965), Bondale (1966), Procter (1967), Janss and Anslijn (1974), Janss and Piraprez (1974), Roik and Mangerig (1987), and Roik and Schwalbenhofer (1988).

4) Test specimens were in some cases very small. This pertains to tests conducted by Stevens (1965) and Bondale (1966).

For some of the physical tests, 4-inch, 6-inch and 8-inch cube specimens were tested to establish concrete strength, instead of the "standard" 6-inch diameter by 12-inch high cylinders. In these cases the strength reported was converted to an equivalent cylinder strength.

Many different factors for obtaining and equivalent cylinder strength from cube strength have been employed by other authors over the years. Roderick and Rogers (1969) and Roderick and Loke (1974) utilized Equation 3.1 recommended by Evans (1943).

$$f_c' = 1.035u - 700 \qquad (3.1)$$

in which both the cube strength (u) and the cylinder strength (f'_c) are in pounds per square inch. Virdi and Dowling (1973) reported a factor of 0.64 for converting the strength of a 6-inch cube to an equivalent cylinder. Furlong (1976) appears to have used 0.8 times the 4-inch cube strength to obtain an equivalent 6-inch cylinder strength. May and Johnson (1978) applied a factor of 0.76 for obtaining an equivalent cylinder strength from a 6-inch cube. Roik and Bergmann (1989) used 0.83 times the 4-inch cube strength and 0.85 times the 8-inch cube strength to obtain an equivalent 6-inch cylinder strength.

Eight physical tests on columns by Bondale (1966), four for major axis bending and four for minor axis bending, that were used in this study were also compared by Basu (1967) to his theoretical model. Basu's work indicated that if a ratio of the 4-inch cube strength to 6-inch cylinder strength is taken as 0.80 as opposed to 0.67, it will change the tested to theoretical strength ratio by approximately 10 percent for the eight columns tested by Bondale.

It was decided that two equations would be used, when necessary, to obtain an equivalent cylinder strength from a given cube. Equation 3.2, which is based on the statistical theory of brittle fracture of solids (Bolotin 1969), as reproduced by Mirza, Hatzinikolas and MacGregor (1979), is utilized to account for the difference in strength due to volume difference of a cube with respect to a 4-inch cube.

$$f = f_o \left[0.58 + 0.42 \left(\frac{v_o}{v} \right)^{\frac{1}{3}} \right] \qquad (3.2)$$

In Equation 3.2, f_o and v_o represent the concrete strength and volume of a 4-inch cube, and f and v are the concrete strength and volume of a cube of the desired size (6-inch in this study). L'Hermite's equation (1955) (Equation 3.3) reproduced by Neville (1973) was then applied to convert the 6-inch cube strength to that of an equivalent 6-inch diameter by 12-inch long cylinder.

$$f'_c = \left(0.76 + 0.2\log\left(\frac{f_{cu}}{2840}\right)\right) f_{cu} \tag{3.3}$$

in which f_{cu} is the 6-inch cube specimen strength and f'_c represents the 6-inch cylinder strength in psi. For SI units replace 2840 psi with 19.6 MPa.

In a number of cases only the nominal values for the strength of the structural steel and reinforcing steel were reported with the physical test data. In most cases, however, actual tests were performed to determine the yield strength of the structural steel and the reinforcing steel.

3.1 COMPARISON OF THEORETICAL STRENGTH OF COLUMNS SUBJECTED TO MAJOR AXIS BENDING TO EXPERIMENTAL RESULTS

The accuracy of the theoretical model for columns subjected to major axis bending was initially checked against 81 physical tests gathered from Bondale (1966), May and Johnson (1978), Morino et al. (1984), Procter (1967), Suzuki et al. (1983), Roik and Mangerig (1987), and Roik and Schwalbenhofer (1988). Sixteen more physical tests of columns subjected to major axis bending were located since the completion of the work by Skrabek and Mirza (1990). Five of the physical tests were eventually excluded from the comparison for reasons that will be discussed later in this section.

A brief description of the 81 physical tests used for the comparison of tested to theoretical strength for columns subjected to major axis bending is given in Table 3.1. Included with the information on material properties and specimen configuration shown in Table 3.1 is the ratio of tested to calculated ultimate strengths (strength ratio) for each of the 81 beam-column specimens. A strength ratio was taken as the ratio of the bending moment strengths for $e/h=\infty$, and the ratio of the axial load capacities for $e/h<\infty$. Detailed descriptions of material properties and specimen configuration for each beam-column are given in Table A1 of Appendix A. The plot of tested strength against the theoretical strength (Figure 3.1) indicates that the magnitude of error increases proportionally with an increase in strength, which is expected since the percentage of error remains relatively constant.

The calculated mean, coefficient of variation and coefficient of skewness for strength ratios of all beam-column specimens listed in Table 3.1 are shown in Table 3.2. The statistical analysis shown in Table 3.2 was subdivided into two categories, based on the slenderness ratio (ℓ/h). The columns with an ℓ/h less than 6.6 are assumed to be short columns and long columns are assumed to have ℓ/h greater than or equal to 6.6. The data was further categorized into four

Table 3.1 - Specimen Configuration for Composite Columns Subjected to Bending about the Major Axis used for Ratio of Test to Calculated Ultimate Strength

Author	Col. Desig.	h (in.)	b (in.)	f'_c (psi)	ρ_{ss}	ρ_{rs}	$\frac{\rho_{ss} f_{yss}}{f'_c}$	ℓ/h	e/h	Tested Strength	Theor. Strength	Strength Ratio	
Bondale (1966)	RS 60.3	6.00	3.75	4506	0.0653	0.0062	0.649	10.0	0.500	55.8	47.0	1.188	
	RS 80.2	6.00	3.75	4382	0.0653	0.0062	0.667	13.3	0.333	70.1	55.8	1.257	*
	RS 100.1	6.00	3.75	4260	0.0653	0.0062	0.687	16.7	0.167	92.3	72.9	1.265	*
	RS 120.0	6.00	3.75	4700	0.0653	0.0062	0.622	20.0	0.000	107.1	115.3	0.929	
May & Johnson (1978)	RC1	7.87	7.87	4308	0.0745	0.0028	0.727	8.1	0.112	301.2	282.2	1.067	
	RC3	7.87	7.87	3390	0.0745	0.0028	0.924	8.1	0.136	305.7	239.1	1.279	*
	RC4	7.87	7.87	5191	0.0745	0.0028	0.603	14.8	0.197	191.1	217.9	0.877	
Morino et al. (1984)	A4-90	6.30	6.30	3060	0.0870	0.0036	1.481	5.8	0.250	166.5	121.4	1.372	*
	B4-90	6.30	6.30	3393	0.0870	0.0036	1.302	14.4	0.250	114.6	104.0	1.102	
	C4-90	6.30	6.30	3379	0.0870	0.0036	1.177	21.7	0.250	93.9	83.0	1.131	
	D4-90	6.30	6.30	3074	0.0870	0.0036	1.474	28.9	0.250	64.7	63.5	1.019	
	A8-90	6.30	6.30	4872	0.0870	0.0036	0.953	5.8	0.469	118.1	98.6	1.197	
	B8-90	6.30	6.30	4829	0.0870	0.0036	0.957	14.4	0.469	94.0	84.3	1.114	
	C8-90	6.30	6.30	3567	0.0870	0.0036	1.305	21.7	0.469	68.0	62.5	1.089	
	D8-90	6.30	6.30	3321	0.0870	0.0036	1.399	28.9	0.469	50.1	49.2	1.020	
Procter (1967)	S1	11.00	8.00	4722	0.0484	0.0000	0.432	2.2	0.000	470.4	522.9	0.900	
	S2	11.00	8.00	4722	0.0484	0.0000	0.432	2.2	0.000	481.6	522.9	0.921	
	S3	12.00	8.00	5407	0.0520	0.0000	0.410	2.0	0.000	698.9	642.1	1.088	
	S4	12.00	8.00	5407	0.0520	0.0000	0.410	2.0	0.000	703.4	642.1	1.095	
	1	11.25	8.00	4722	0.0473	0.0000	0.422	11.7	0.533	132.2	127.7	1.035	
	2	11.25	8.00	4722	0.0473	0.0000	0.422	11.7	0.800	87.4	87.4	1.000	
	3	11.25	8.00	4722	0.0473	0.0000	0.422	11.7	0.000	470.4	508.0	0.926	
	4	11.25	8.00	4722	0.0473	0.0000	0.422	11.7	0.533	143.4	127.7	1.122	
	5	11.25	8.00	5407	0.0473	0.0000	0.369	11.7	0.800	91.8	90.5	1.015	
	6	12.00	8.00	5407	0.0520	0.0000	0.410	11.0	0.750	129.9	114.1	1.138	
	7	12.00	8.00	5407	0.0520	0.0000	0.410	11.0	0.500	199.4	168.6	1.183	
	8	12.00	8.00	5407	0.0520	0.0000	0.410	11.0	0.000	560.0	613.6	0.913	
	9	11.25	8.00	6007	0.0473	0.0000	0.332	11.7	0.267	268.8	243.5	1.104	
	10	11.25	8.00	6007	0.0473	0.0000	0.332	11.7	0.267	250.9	243.5	1.030	
	11	12.00	8.00	6007	0.0520	0.0000	0.369	11.0	0.000	533.1	658.5	0.810	
	12	12.00	8.00	6007	0.0520	0.0000	0.369	11.0	0.250	315.8	290.9	1.086	
Suzuki et al. (1983)	LH-000-C	8.27	8.27	4785	0.0290	0.0021	0.274	2.9	0.000	380.0	366.4	1.037	
	LH-020-C	8.27	8.27	4785	0.0290	0.0021	0.274	2.9	0.000	374.3	429.4	0.872	
	LH-040-C	8.27	8.27	4785	0.0290	0.0021	0.274	2.9	0.000	374.3	398.0	0.940	
	LH-100-C	8.27	8.27	4785	0.0290	0.0021	0.274	2.9	0.000	385.8	379.2	1.017	
	RH-000-C	8.27	8.27	4858	0.0546	0.0021	0.624	2.9	0.000	547.0	462.7	1.182	
	RH-020-C	8.27	8.27	4858	0.0546	0.0021	0.624	2.9	0.000	561.4	523.7	1.072	
	RH-040-C	8.27	8.27	4858	0.0546	0.0021	0.624	2.9	0.000	521.1	493.4	1.056	
	RH-100-C	8.27	8.27	4858	0.0546	0.0021	0.624	2.9	0.000	521.1	475.2	1.097	
	HT60-000-C	8.27	8.27	4858	0.0600	0.0021	1.035	2.9	0.000	598.8	562.8	1.064	
	HT60-020-C	8.27	8.27	4858	0.0600	0.0021	1.035	2.9	0.000	656.4	674.0	0.974	
	HT60-040-C	8.27	8.27	4858	0.0600	0.0021	1.035	2.9	0.000	662.2	639.2	1.036	
	HT60-100-C	8.27	8.27	4858	0.0600	0.0021	1.035	2.9	0.000	627.6	611.8	1.026	
	HT80-000-C	8.27	8.27	4858	0.0633	0.0021	1.480	2.9	0.000	716.9	626.3	1.145	
	HT80-020-C	8.27	8.27	4858	0.0633	0.0021	1.480	2.9	0.000	734.2	797.3	0.921	
	HT80-040-C	8.27	8.27	4858	0.0633	0.0021	1.480	2.9	0.000	728.4	759.4	0.959	
	HT80-100-C	8.27	8.27	4858	0.0633	0.0021	1.480	2.9	0.000	711.1	721.0	0.986	

Table 3.1 - Continued

Author	Col. Desig.	h (in.)	b (in.)	f'_c (psi)	ρ_{ss}	ρ_{rs}	$\frac{\rho_{ss} f_{yss}}{f'_c}$	ℓ/h	e/h	Tested Strength	Theor. Strength	Strength Ratio
Suzuki	HT80-000-CB	8.27	8.27	4423	0.0423	0.0021	1.060	2.9	0.874	110.4	104.0	1.061
et al.	HT80-020-CB	8.27	8.27	4423	0.0423	0.0021	1.060	2.9	1.062	110.4	108.7	1.016
(1983)	LH-000-B	8.27	8.27	4292	0.0290	0.0021	0.306	2.9	inf.	27.4	27.8	0.988
	LH-020-B	8.27	8.27	4597	0.0290	0.0021	0.286	2.9	inf.	29.4	32.1	0.916
	LH-040-B	8.27	8.27	4524	0.0290	0.0021	0.290	2.9	inf.	28.2	30.1	0.939
	LH-100-B	8.27	8.27	4365	0.0290	0.0021	0.301	2.9	inf.	28.2	28.0	1.008
	RH-000-B	8.27	8.27	4858	0.0546	0.0021	0.624	2.9	inf.	48.9	52.1	0.940
	RH-020-B	8.27	8.27	4858	0.0546	0.0021	0.624	2.9	inf.	54.5	56.9	0.958
	RH-040-B	8.27	8.27	4858	0.0546	0.0021	0.624	2.9	inf.	53.3	45.5	1.171
	RH-100-B	8.27	8.27	4858	0.0546	0.0021	0.624	2.9	inf.	50.9	52.3	0.974
	HT60-000-B	8.27	8.27	4814	0.0600	0.0021	1.045	2.9	inf.	68.8	73.4	0.937
	HT60-020-B	8.27	8.27	4814	0.0600	0.0021	1.045	2.9	inf.	79.2	79.7	0.993
	HT60-040-B	8.27	8.27	4814	0.0600	0.0021	1.045	2.9	inf.	77.2	76.2	1.013
	HT60-100-B	8.27	8.27	4814	0.0600	0.0021	1.045	2.9	inf.	72.0	75.9	0.949
	HT80-000-B	8.27	8.27	4771	0.0633	0.0021	1.507	2.9	inf.	93.5	98.8	0.946
	HT80-020-B	8.27	8.27	4771	0.0633	0.0021	1.507	2.9	inf.	104.2	105.3	0.989
	HT80-040-B	8.27	8.27	4771	0.0633	0.0021	1.507	2.9	inf.	101.0	102.8	0.983
	HT80-100-B	8.27	8.27	4771	0.0633	0.0021	1.507	2.9	inf.	97.9	99.6	0.983
Roik	23	11.81	11.81	6570	0.0868	0.0050	0.517	16.7	0.300	526.3	442.3	1.190
Mangeri	24	11.81	11.81	6570	0.0868	0.0050	0.517	16.7	0.500	368.3	324.8	1.134
(1987)	25	11.81	11.81	6570	0.0868	0.0050	0.517	26.7	0.300	377.8	314.4	1.202 *
	26	11.81	11.81	6570	0.0868	0.0050	0.517	26.7	0.500	200.9	238.6	0.842
Roik	V11	11.02	11.02	6351	0.0434	0.0079	0.230	12.4	0.571	171.7	169.6	1.012
Schwal'r	V12	11.02	11.02	6351	0.0434	0.0079	0.230	12.4	0.214	366.3	373.3	0.981
(1988)	V13	11.02	11.02	6786	0.0434	0.0079	0.215	12.4	0.357	322.9	272.7	1.184
	V21	11.02	11.02	6786	0.0495	0.0079	0.333	12.4	0.357	338.2	321.8	1.051
	V22	11.02	11.02	5365	0.0495	0.0079	0.421	12.4	0.571	213.8	201.7	1.060
	V23	11.02	11.02	5365	0.0495	0.0079	0.421	12.4	0.214	437.2	388.9	1.124
	V31	11.02	11.02	5902	0.0996	0.0079	0.555	12.4	0.357	384.1	383.3	1.002
	V32	11.02	11.02	5902	0.0996	0.0079	0.555	12.4	0.214	506.9	501.2	1.011
	V33	11.02	11.02	5699	0.0996	0.0079	0.575	12.4	0.571	294.3	280.8	1.048
	V41	11.02	11.02	5699	0.1441	0.0079	0.796	12.4	0.357	477.7	422.9	1.130
	V42	11.02	11.02	6119	0.1441	0.0079	0.926	12.4	0.571	344.9	359.6	0.959
	V43	11.02	11.02	6119	0.1441	0.0079	0.995	12.4	0.214	614.9	650.6	0.945

NOTE : For e/h = inf., strength is given in kip-ft (1 kip-ft = 1.356 kN-m).

For all other values of e/h, the strength is shown in kips (1 kip = 4.448 kN).

b = width of the concrete cross-section parrallel to the axis of bending;

h = depth of the concrete cross-section perpendicular to the axis of bending.

The term f_{yss} was taken as the web yield strength for computing the $\rho_{ss} f_{yss}/f'_c$ ratio.

The strain-hardening of both steels was included in the analysis.

* Excluded from final analysis.

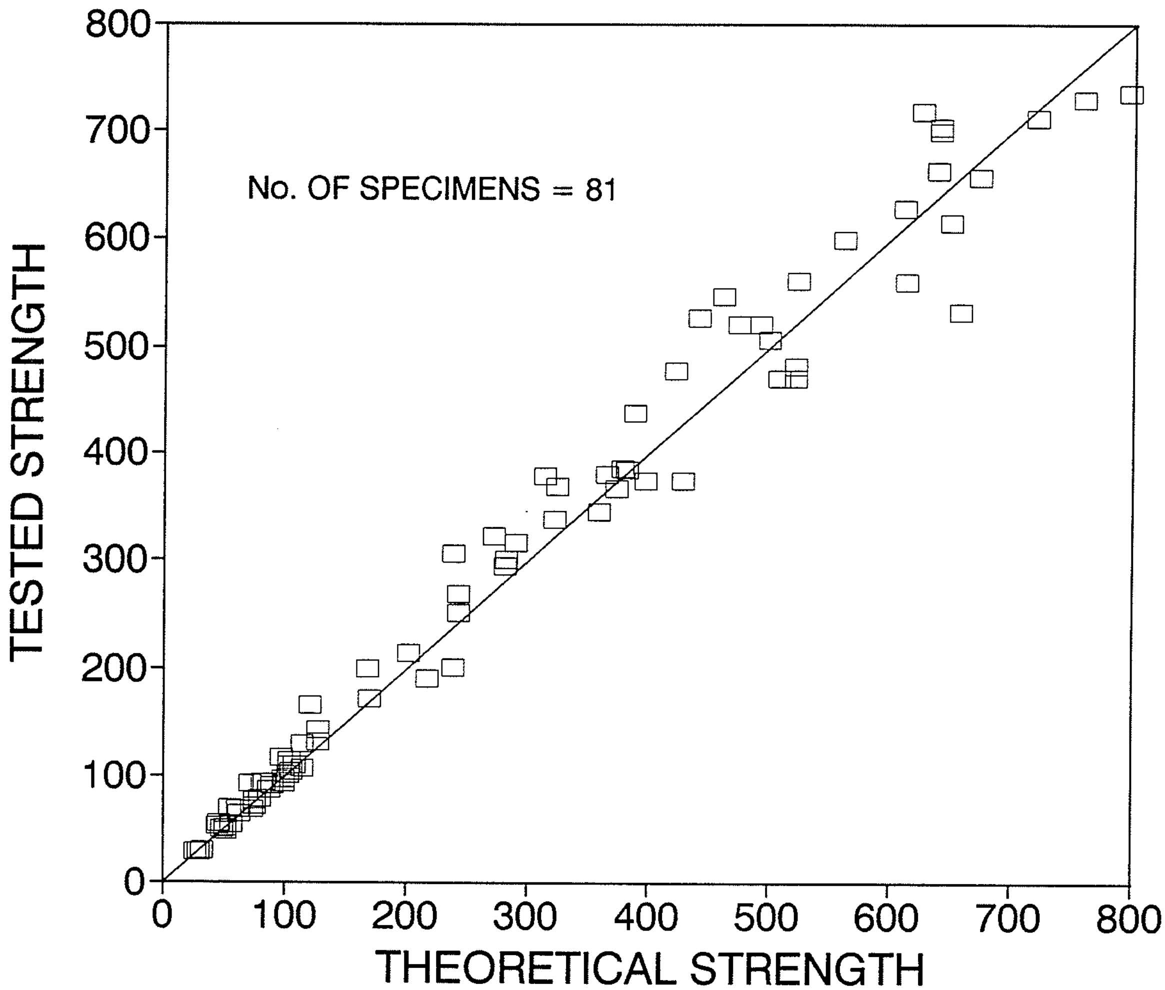

For e/h = inf., the strength is plotted in kip-ft.

For all other values of e/h, the strength is shown in kips.

Figure 3.1 - Comparison of tested strength to theoretical strength for beam-columns subjected to bending about the major axis of the steel section.

Table 3.2 - Statistical Analysis of Ratios of Tested to Calculated Strength of all Composite beam-column specimens subjected to major axis bending (Strain-harding included).

Column Type (1)	(2)	all e/h (3)	0 <= e/h <= 0.2 (4)	0.2 < e/h < 1 (5)	0 <= e/h < 1 (6)	e/h = inf. (7)
Short (ℓ/h< 6.6)	No.	40	20	4	24	16
	Mean	1.02	1.02	1.16	1.04	0.98
	CV	9.52	8.24	13.78	10.54	5.93
	Skew	1.39	0.01	0.32	0.92	2.05
Long (ℓ/h=> 6.6)	No.	41	8	33	41	0
	Mean	1.06	1.01	1.08	1.06	-
	CV	10.51	17.65	8.18	10.51	-
	Skew	-0.14	0.55	-0.24	-0.14	-
All ℓ/h	No.	81	28	37	65	16
	Mean	1.04	1.02	1.09	1.06	0.98
	CV	10.23	11.31	9.09	10.48	5.93
	Skew	0.52	0.49	0.35	0.25	2.05

Table 3.3 - Statistical Analysis of Ratios of Tested to Calculated Strength of all Composite beam-column specimens subjected to major axis bending for which strength ratio was less than or equal to 1.2 (Strain-hardening included).

Column Type (1)	(2)	all e/h (3)	0 <= e/h <= 0.2 (4)	0.2 < e/h < 1 (5)	0 <= e/h < 1 (6)	e/h = inf. (7)
Short (ℓ/h< 6.6)	No.	39	20	3	23	16
	Mean	1.01	1.02	1.09	1.03	0.98
	CV	7.85	8.24	8.64	8.43	5.93
	Skew	0.66	0.01	0.29	0.07	2.05
Long (ℓ/h=> 6.6)	No.	37	6	31	37	0
	Mean	1.04	0.92	1.07	1.04	-
	CV	9.31	9.21	7.58	9.31	-
	Skew	-0.46	0.48	-0.45	-0.46	-
All ℓ/h	No.	76	26	34	60	16
	Mean	1.03	1.00	1.07	1.04	0.98
	CV	8.71	9.32	7.57	8.94	5.93
	Skew	0.06	0.02	-0.38	-0.28	2.05

ranges of end eccentricity ratio (e/h) as described in Table 3.2.

The mean value for the ratio of tested to theoretical ultimate strength was 1.04 with a coefficient of variation of 10.23 percent when all 81 specimens were considered (Table 3.2 - Column 3). This is comparable with the mean value of 1.04 and coefficient of variation of 10.4 percent obtained by Skrabek and Mirza (1990) for 63 specimens analyzed by an earlier version of the same program. It is also comparable to a mean value of 1.04 and a coefficient of variation of 10.4 percent obtained by Virdi and Dowling (1973) for their analysis of 8 biaxially loaded composite columns.

Significant differences in the statistics for the four different ranges of end eccentricity ratio (Table 3.2 Columns 4,5,6, and 7) were noticed for certain cases. Long columns with low eccentricity ratios (e/h greater than or equal to zero and less than or equal to 0.2) have a greater coefficient of variation (17.65 percent) than the overall coefficient of variation (10.23 percent). For short columns with an intermediate eccentricity ratio (e/h greater than 0.2 and less than 1.0), the mean value (1.16) and the coefficient of variation (13.78 percent) obtained are both greater than the overall mean (1.041) and coefficient of variation (10.23).

It was decided, after successively removing data with relatively high strength ratios and recalculating the statistics, that the physical tests with a strength ratio greater than 1.20 would not be included in the statistical analysis. Using this criteria, a total of five columns were removed from the statistical analysis: RS 80.2 and RS 100.1 from Bondale, RC3 from May and Johnson, A4-90 from Morino et al., and No. 25 from Roik and Mangerig. The strength ratio plotted against e/h, ℓ/h, ρ_{ss} and $(\rho_{ss}+\rho_{rs})$ in Figures 3.2, 3.3, 3.4 and 3.5, respectively, shows the relative location of the removed data with respect to the remaining data. Removing the five columns from the statistical analysis results in a marked improvement in the mean values and coefficient of variation for each of the e/h ranges as well as for the overall statistics, except for the case of pure bending ($e/h = \infty$). This can be seen by comparing the values in Table 3.3 to those shown in Table 3.2.

Column 6 in Table 3.3, where e/h ranges from zero to 1.0, is of specific interest since eccentricity ratios ranging from 0.05 to 1.0 were used to study the effective flexural stiffness (EI) of composite columns described in Chapter 5 and 6. Here, whether the columns are short, long or all lengths combined, the mean value and the coefficient of variation do not differ significantly. Based on the mean value and coefficient of variation determined for 60 columns with all ℓ/h included (Table 3.3 Column 6), a mean value of 1.04 and a coefficient of variation of 9 percent are recommended to describe the model error for beam-columns bending about the major axis of the steel section when $e/h \leq 1.0$.

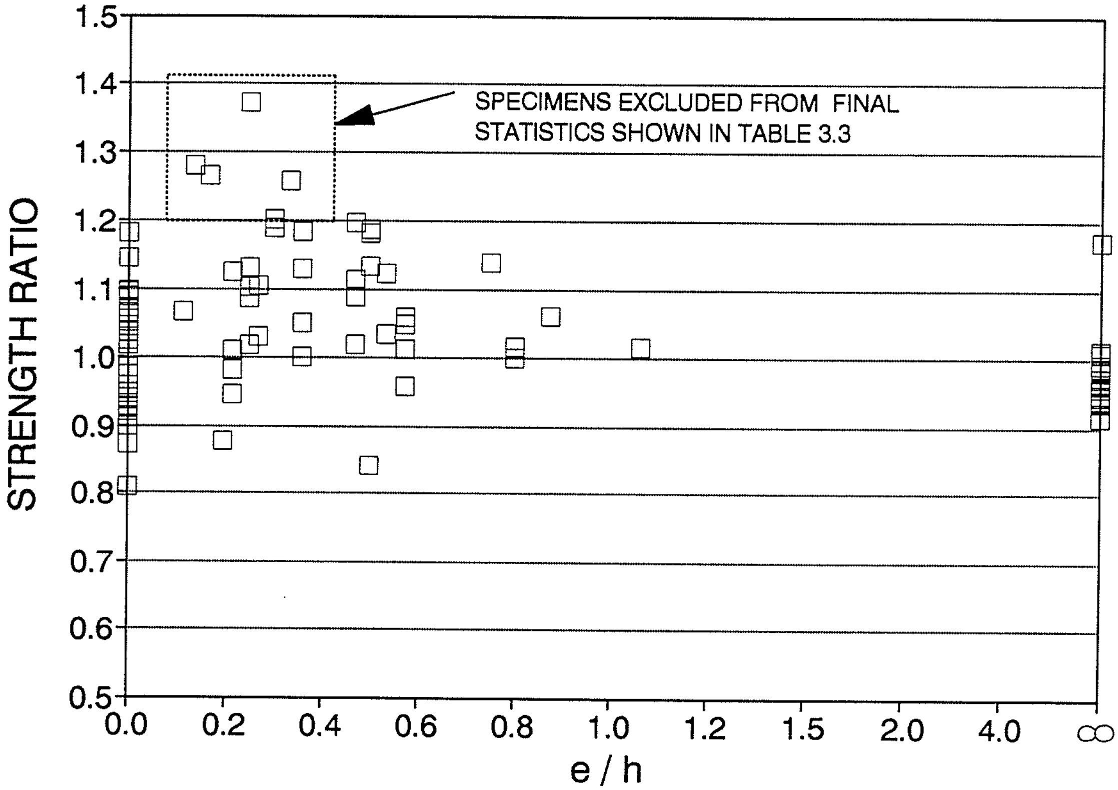

Figure 3.2 - Effect of e/h on strength ratios for beam-columns subjected to bending about the major axis of the steel section.

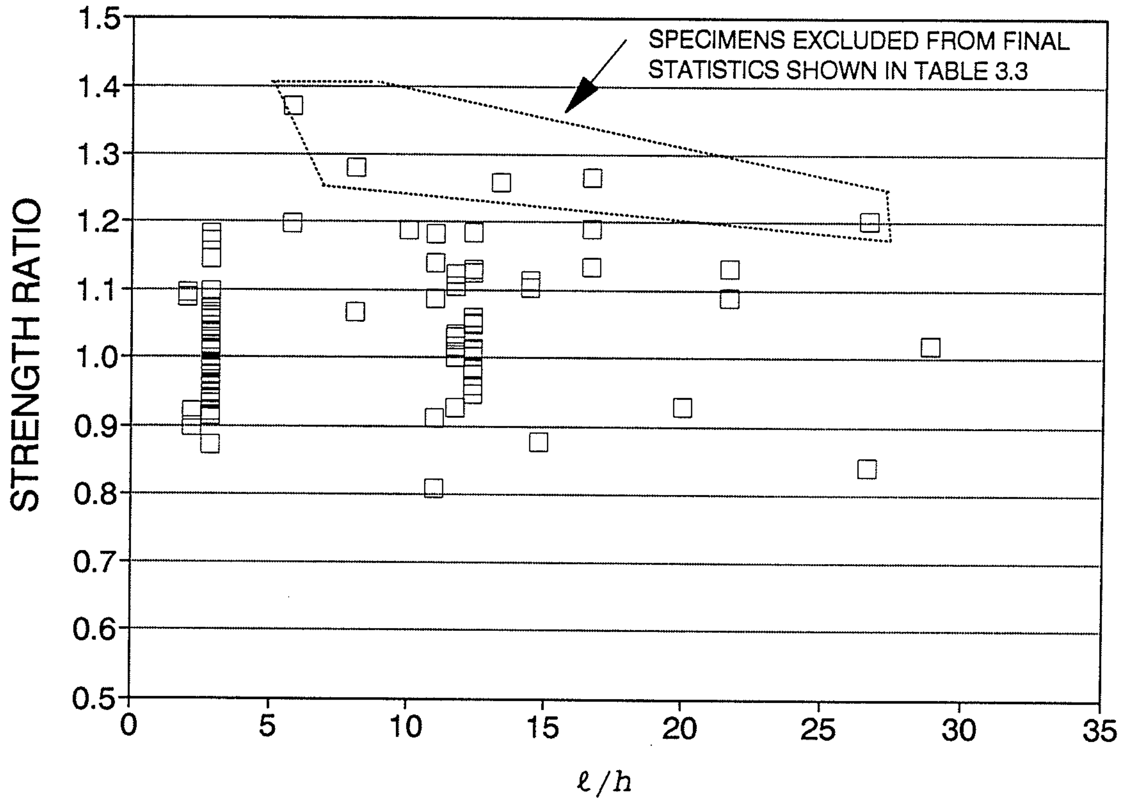

Figure 3.3 - Effect of ℓ/h on strength ratios for beam-columns subjected to bending about the major axis of the steel section.

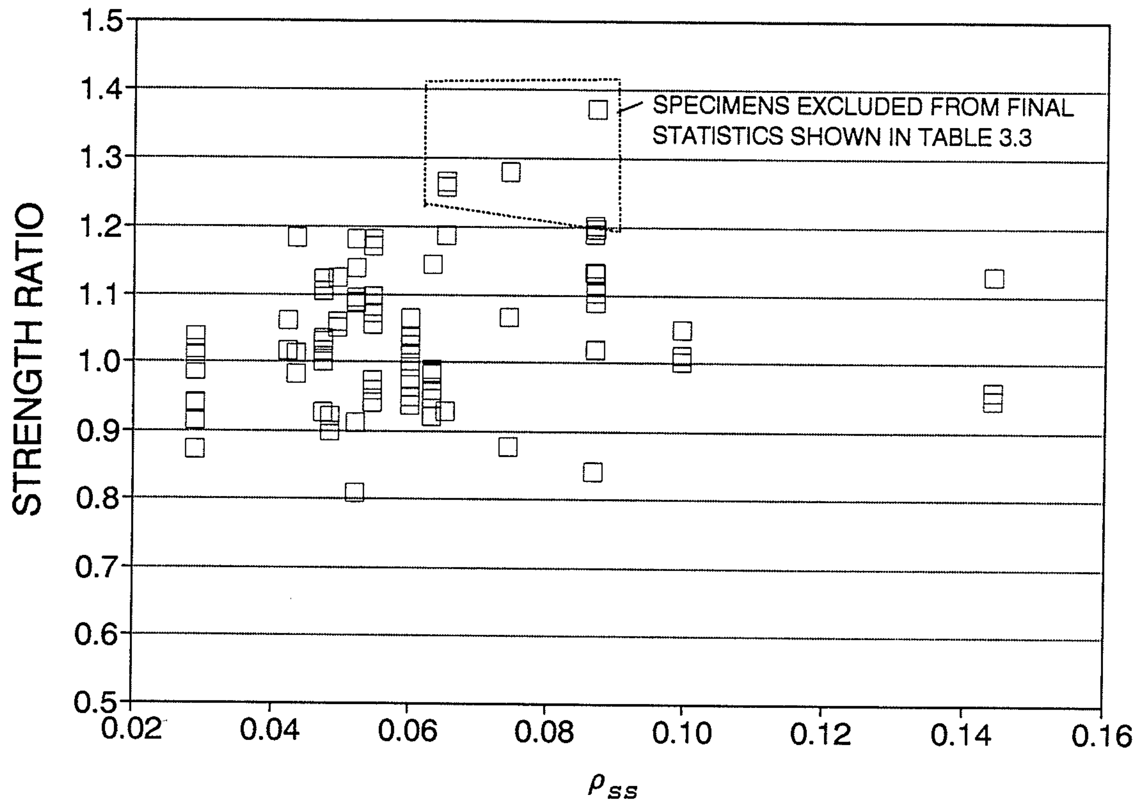

Figure 3.4 - Effect of ρ_{ss} on strength ratios for beam-columns subjected to bending about the major axis of the steel section.

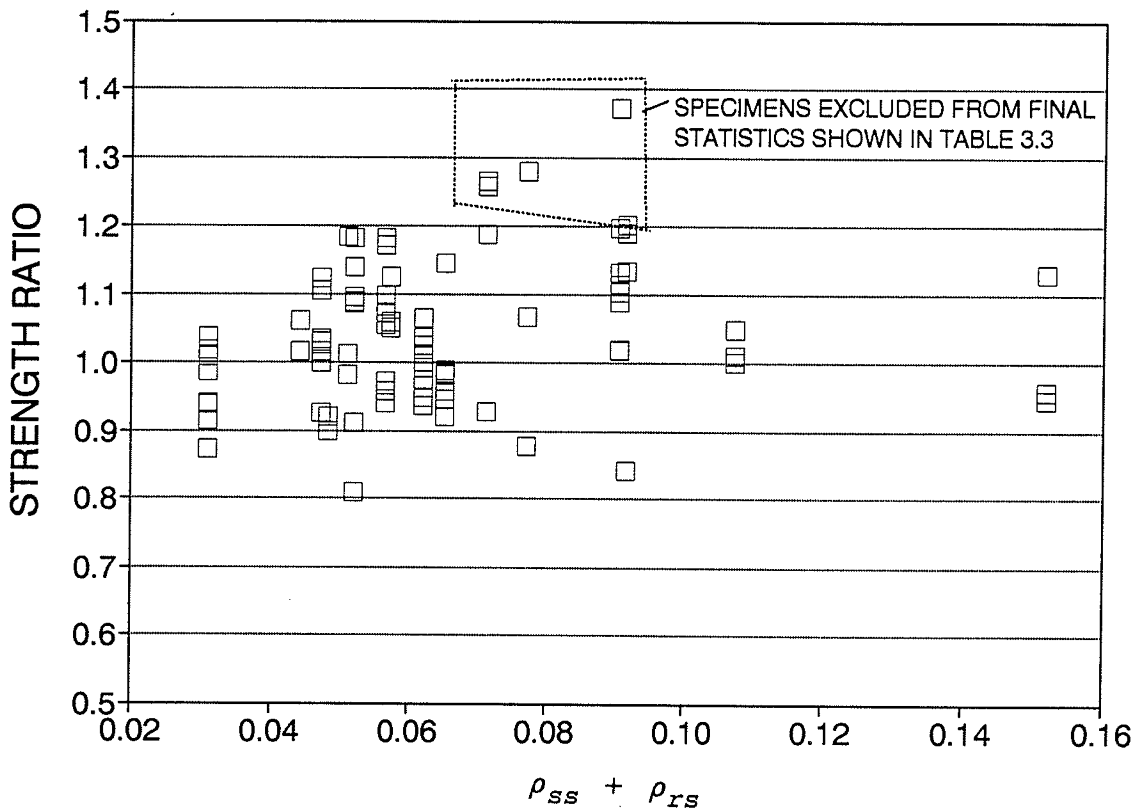

Figure 3.5 - Effect of ($\rho_{ss} + \rho_{rs}$) on strength ratios for beam-columns subjected to bending about the major axis of the steel section.

Pure bending (Column 7 in Table 3.3), where $e/h = \infty$, gives the lowest coefficient of variation (5.93 percent) compared to the other e/h ranges. The lower coefficient of variation is, probably, a result of the following:

1) The variation in concrete strength does not affect the pure bending strength as significantly as the strength under pure axial load or combined axial load and bending.
2) The laboratory test procedure for pure bending is not prone to as much experimental error as are those for axially loaded columns and columns subjected to axial load and bending.

The calculated ultimate strength considering the effect of strain hardening (Table 3.1) was compared to the calculated ultimate strength when strain hardening effect was not included (Table A2, Appendix A). Strain hardening was found to increase the predicted strength by about 20 percent for cases of pure flexure only and had little or no affect on the calculated strength of the remainder of the beam-column specimens.

The probability distribution of the strength ratios calculated for the sixty specimens ($e/h \leq 1.0$) is plotted on a normal probability paper in Figure 3.6 and is compared to a normal probability distribution using a suggested mean value of 1.04 and coefficient of variation of 9 percent. The data can be assumed to be normally distributed since the data closely follows the normal curve.

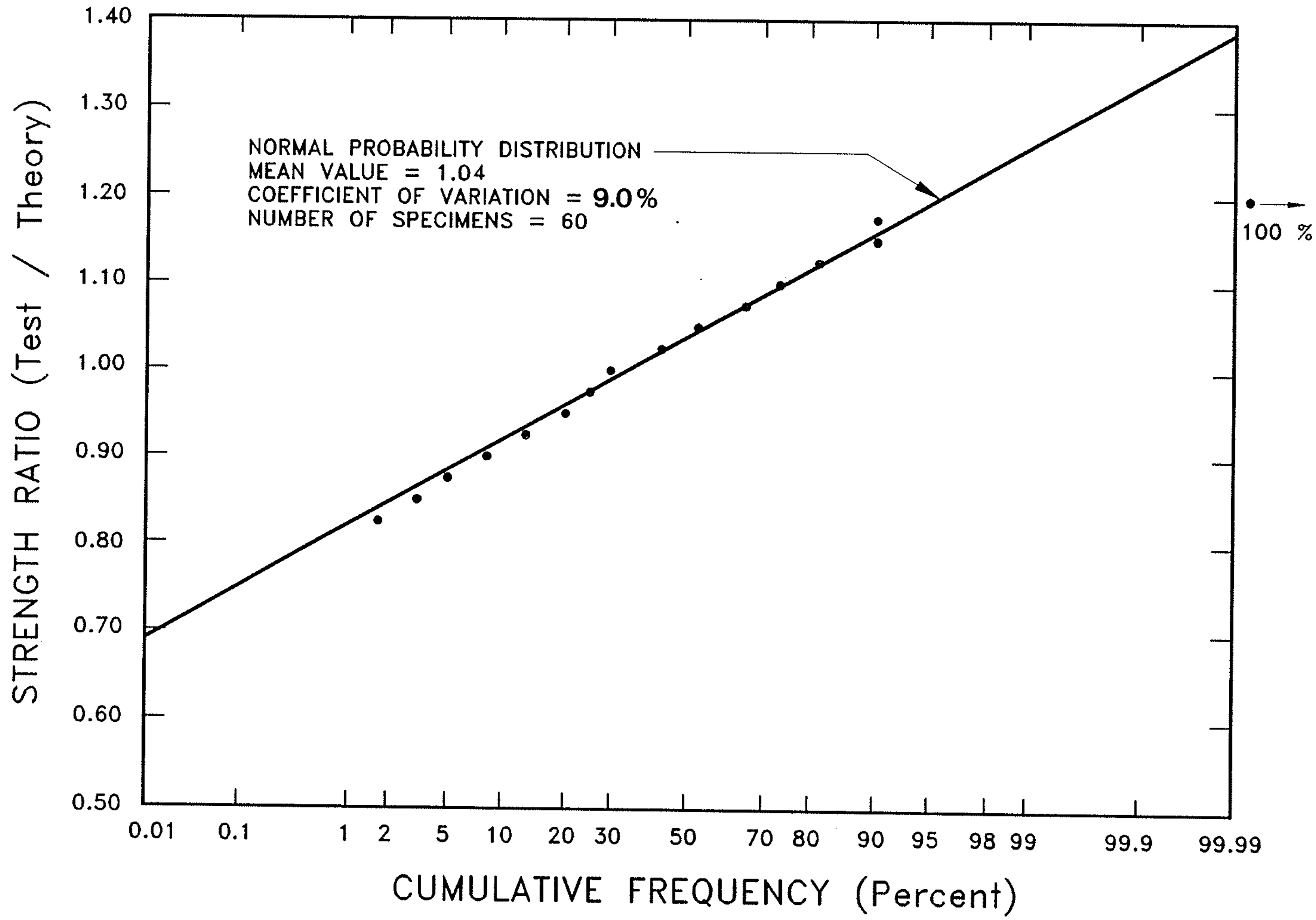

Figure 3.6 - Probability distribution of strength ratios (test/theory $\leq$ 1.20) of composite beam-column specimens (Table 3.1) bending about the major axis with $0 \leq e/h \leq 1.0$.

3.2 COMPARISON OF THEORETICAL STRENGTH OF COLUMNS SUBJECTED TO MINOR AXIS BENDING TO EXPERIMENTAL RESULTS

The accuracy of the theoretical model for columns subjected to bending about the minor axis was initially checked against 164 physical tests from Stevens (1965), Bondale (1966), May and Johnson (1978), Janss and Anslijn (1974), Janss and Piraprez (1974), Roderick and Loke (1974), Morino et al. (1984), Roik and Mangerig (1987), and Roik and Schwalbenhofer (1988).

Table 3.4 outlines the material properties and specimen configurations, and gives ratio of tested to calculated ultimate strength (strength ratio) for the 164 specimens studied. A strength ratio was taken as the ratio of the bending moment strengths for $e/h = \infty$, and the ratio of the axial load capacities for $e/h < \infty$. Detailed descriptions of material properties and specimen configuration for each beam-column specimen are given in Table A3 of Appendix A. Figure 3.7 plots the tested strength of all 164 columns against the calculated theoretical strength.

The calculated mean, coefficient of variation and coefficient of skewness for strength ratios of all beam-column specimens listed in Table 3.4 are shown in Table 3.5. The statistical analysis shown in Table 3.5 was subdivided into two categories based on to the slenderness ratio (ℓ/h). The columns with ℓ/h less than 6.6 are assumed to be short columns and long columns are assumed to have ℓ/h greater than or equal

Table 3.4 - Specimen Configuration for Composite Columns Subjected to Bending about the Minor Axis used for Ratio of Tested to Calculated Ultimate Strength.

Author	Col. Desig.	b (in.)	h (in.)	f'_c (psi)	ρ_{ss}	ρ_{rs}	$\frac{\rho_{ss} f_{yss}}{f'_c}$	ℓ/h	e/h	Tested Strength	Theor. Strength	Strength Ratio	
Stevens (1965)	CV2	7.00	6.50	1115	0.1291	0.0000	4.175	12.6	0.115	134.4	98.0	1.3714	*
	CV3	7.00	6.50	1900	0.1291	0.0000	2.450	12.6	0.115	161.3	110.6	1.4586	*
	CV4	7.00	6.50	2491	0.1291	0.0000	1.869	12.6	0.115	179.2	122.4	1.4636	*
	CV5	7.00	6.50	3058	0.1291	0.0000	1.523	12.6	0.115	201.6	134.5	1.4989	*
	CV6	7.00	6.50	3672	0.1291	0.0000	1.268	12.6	0.123	228.5	142.6	1.6025	*
	AE1	7.00	6.50	2046	0.1291	0.0000	2.275	4.3	0.154	165.8	137.4	1.2065	*
	AE2	7.00	6.50	2679	0.1291	0.0000	1.738	7.1	0.154	163.5	135.6	1.2056	*
	AE3	7.00	6.50	2566	0.1291	0.0000	1.814	12.6	0.154	141.1	105.9	1.3321	*
	AE4	7.00	6.50	2906	0.1291	0.0000	1.602	18.2	0.154	118.7	88.5	1.3409	*
	AE5	7.00	6.50	2305	0.1291	0.0000	2.020	23.7	0.154	98.6	63.2	1.5588	*
	AE6	7.00	6.50	2010	0.1291	0.0000	2.317	7.1	0.000	291.2	257.0	1.1333	*
	AE7	7.00	6.50	2083	0.1291	0.0000	2.235	7.1	0.077	224.0	176.8	1.2673	*
	AE8	7.00	6.50	2157	0.1291	0.0000	2.158	18.2	0.077	161.3	108.5	1.4860	*
	AE9	7.00	6.50	1467	0.1291	0.0000	3.174	23.7	0.231	78.4	44.6	1.7563	*
	AE10	7.00	6.50	1900	0.1291	0.0000	2.450	23.7	0.308	72.8	42.2	1.7263	*
	AE11	7.00	6.50	2305	0.1291	0.0000	2.020	16.6	inf.	20.9	19.4	1.0760	
	FE1	16.00	12.00	2083	0.0996	0.0041	1.580	15.0	0.000	985.6	814.6	1.2099	*
	FE2	16.00	12.00	2268	0.0996	0.0041	1.451	15.0	0.000	1055.0	846.1	1.2470	*
	FE3	16.00	12.00	2083	0.0996	0.0041	1.580	15.0	0.083	672.0	479.5	1.4016	*
	FE4	16.00	12.00	1936	0.0996	0.0041	1.699	15.0	0.167	486.1	331.9	1.4645	*
	FE5	16.00	12.00	2454	0.0996	0.0041	1.341	15.0	0.167	515.2	365.7	1.4089	*
	FE6	16.00	12.00	2231	0.0996	0.0041	1.475	15.0	0.250	360.6	278.6	1.2943	*
	FE7	16.00	12.00	2231	0.0996	0.0041	1.475	15.0	0.333	295.7	234.9	1.2587	*
	FE8	16.00	12.00	2342	0.0996	0.0041	1.405	15.0	0.417	262.1	206.1	1.2717	*
	FE9	16.00	12.00	2268	0.0996	0.0041	1.451	15.0	0.500	230.7	178.9	1.2897	*
	FE10	16.00	12.00	2604	0.0996	0.0041	1.264	15.0	0.583	199.4	168.4	1.1836	*
	FE11	16.00	12.00	2529	0.0996	0.0041	1.301	15.0	0.667	168.0	149.9	1.1211	*
	FE12	16.00	12.00	2529	0.0996	0.0041	1.301	10.0	inf.	131.4	128.6	1.0219	
	B1	5.00	3.50	2120	0.0674	0.0000	1.310	13.1	0.000	82.9	64.7	1.2802	*
	B2	5.00	3.50	1467	0.0674	0.0000	1.894	18.3	0.000	61.2	42.6	1.4352	*
	B3	5.00	3.50	1827	0.0674	0.0000	1.520	23.4	0.000	64.1	38.0	1.6881	*
	B4	5.00	3.50	1610	0.0674	0.0000	1.725	28.6	0.000	44.4	27.6	1.6070	*
	B5	5.00	3.50	2083	0.0674	0.0000	1.334	33.7	0.000	51.5	25.0	2.0649	*
	B6	5.00	3.50	1791	0.0674	0.0000	1.551	38.9	0.000	36.7	18.4	1.9922	*
	B7	5.00	3.50	2305	0.0674	0.0000	1.205	44.0	0.000	34.5	17.0	2.0244	*
	A1	7.00	6.50	1900	0.1291	0.0000	2.861	1.4	0.000	358.4	304.0	1.1791	*
	A2	7.00	6.50	1682	0.1291	0.0000	3.231	7.1	0.000	313.6	259.2	1.2099	*
	A3	7.00	6.50	1900	0.1291	0.0000	2.861	12.6	0.000	322.6	239.7	1.3456	*
	A4	7.00	6.50	2046	0.1291	0.0000	2.656	12.6	0.000	302.4	246.2	1.2282	*
	A5	7.00	6.50	1864	0.1291	0.0000	2.917	18.2	0.000	293.4	200.7	1.4623	*
	A6	7.00	6.50	2216	0.1291	0.0000	2.453	23.7	0.000	235.2	164.3	1.4314	*
	RE1a	7.00	6.50	2010	0.1291	0.0000	2.814	18.2	0.000	300.2	214.7	1.3978	*
	RE1b	7.00	6.50	1791	0.1291	0.0000	3.158	18.2	0.000	280.0	206.5	1.3558	*
	RE2a	7.00	6.50	1900	0.1291	0.0000	2.976	18.2	0.000	275.5	217.4	1.2676	*
	RE2b	7.00	6.50	2305	0.1291	0.0000	2.453	18.2	0.000	268.8	230.9	1.1640	*
	RE3a	7.00	6.50	2231	0.1291	0.0043	2.535	18.2	0.000	313.6	271.9	1.1535	*
	RE3b	7.00	6.50	1900	0.1291	0.0043	2.976	18.2	0.000	277.8	260.2	1.0674	*
	RE4a	7.00	6.50	1973	0.1291	0.0000	2.866	18.2	0.000	271.0	209.5	1.2937	*
	RE4b	7.00	6.50	1827	0.1291	0.0000	3.095	18.2	0.000	284.5	204.1	1.3936	*

Table 3.4 - Continued

Author	Col. Desig.	b (in.)	h (in.)	f'_c (psi)	ρ_{ss}	ρ_{rs}	$\frac{\rho_{ss} f_{yss}}{f'_c}$	ℓ/h	e/h	Tested Strength	Theor. Strength	Strength Ratio	
Stevens	FA1	16.00	12.00	1864	0.0996	0.0000	1.759	3.0	0.000	1070.7	899.4	1.1905	*
(1965)	FA2	16.00	12.00	2010	0.0996	0.0000	1.631	6.0	0.000	1008.0	912.8	1.1044	*
	FA3	16.00	12.00	1755	0.0996	0.0000	1.868	9.0	0.000	943.0	817.3	1.1539	*
	FA4	16.00	12.00	1973	0.0996	0.0000	1.661	12.0	0.000	954.2	807.0	1.1825	*
	FA5	16.00	12.00	1973	0.0996	0.0000	1.661	15.0	0.000	949.8	738.5	1.2861	*
Bondale	RW 60.3	6.00	3.75	4665	0.0653	0.0099	0.627	16.0	0.800	17.9	14.9	1.2019	*
(1966)	RW 80.2	6.00	3.75	5557	0.0653	0.0099	0.526	21.3	0.533	21.7	19.1	1.1370	
	RW 100.1	6.00	3.75	4488	0.0653	0.0099	0.652	26.7	0.267	20.8	20.8	1.0030	
	RW 120.0	6.00	3.75	3927	0.0653	0.0099	0.745	32.0	0.000	52.9	53.0	0.9969	
May (1978)	RC5	7.87	7.87	5278	0.0745	0.0294	0.594	14.3	0.100	185.5	231.2	0.8021	
Janss	1.1	9.45	9.45	6014	0.0747	0.0079	0.514	17.8	0.000	483.3	528.9	0.9139	
Anslijn	1.2	9.45	9.45	5517	0.0747	0.0079	0.560	17.8	0.000	489.8	506.8	0.9665	
(1974)	1.3	9.45	9.45	5263	0.0747	0.0079	0.563	17.8	0.000	470.0	491.5	0.9563	
	2.1	9.45	9.45	5263	0.0747	0.0079	0.603	14.5	0.000	527.4	564.9	0.9336	
	2.2	9.45	9.45	4507	0.0747	0.0079	0.704	14.5	0.000	489.8	517.9	0.9458	
	2.3	9.45	9.45	5517	0.0747	0.0079	0.575	14.5	0.000	580.3	581.6	0.9978	
	3.1	9.45	9.45	5957	0.0747	0.0079	0.502	10.4	0.000	591.3	680.8	0.8685	
	3.2	9.45	9.45	6014	0.0747	0.0079	0.497	10.3	0.000	503.1	685.2	0.7342	*
	3.3	9.45	9.45	5263	0.0747	0.0079	0.568	10.4	0.000	527.4	634.0	0.8318	
	4.1	9.45	9.45	5263	0.0747	0.0079	0.568	5.4	0.000	573.8	658.3	0.8715	
	4.2	9.45	9.45	4507	0.0747	0.0079	0.663	5.3	0.000	556.0	604.2	0.9201	
	4.3	9.45	9.45	5574	0.0747	0.0079	0.536	5.2	0.000	617.9	618.0	0.9997	
	5.1	9.45	9.45	4870	0.0747	0.0079	0.844	14.5	0.000	529.7	585.6	0.9045	
	5.2	9.45	9.45	5277	0.0747	0.0079	0.778	14.5	0.000	591.3	611.3	0.9673	
	5.3	9.45	9.45	4982	0.0747	0.0079	0.825	14.5	0.000	556.0	592.9	0.9378	
	6.1	9.45	9.45	4870	0.0747	0.0079	1.116	17.8	0.000	529.7	517.0	1.0244	
	6.2	9.45	9.45	5277	0.0747	0.0079	1.030	17.8	0.000	485.3	541.0	0.8971	
	6.3	9.45	9.45	4996	0.0747	0.0079	1.088	17.8	0.000	558.2	524.6	1.0642	
	7.1	9.45	9.45	4968	0.0747	0.0079	1.064	14.5	0.000	556.0	624.1	0.8908	
	7.2	9.45	9.45	5291	0.0747	0.0079	0.999	14.5	0.000	589.1	648.3	0.9086	
	7.3	9.45	9.45	4996	0.0747	0.0079	1.058	14.5	0.000	578.0	626.6	0.9225	
	8.1	9.45	9.45	5263	0.0747	0.0079	1.029	10.4	0.000	547.2	759.3	0.7207	*
	8.2	9.45	9.45	6014	0.0747	0.0079	0.900	10.4	0.000	531.7	816.8	0.6509	*
	8.3	9.45	9.45	5957	0.0747	0.0079	0.909	10.4	0.000	573.8	812.9	0.7058	*
	9.1	12.60	8.27	4507	0.0497	0.0067	0.436	16.6	0.000	514.1	497.1	1.0342	
	9.2	12.60	8.27	5957	0.0497	0.0067	0.330	16.6	0.000	569.3	592.9	0.9601	
	9.3	12.60	8.27	5291	0.0497	0.0067	0.371	16.6	0.000	463.3	549.6	0.8430	
	10.1	12.60	8.27	5263	0.0497	0.0067	0.669	16.6	0.000	518.6	579.1	0.8956	
	10.2	12.60	8.27	4968	0.0497	0.0067	0.709	16.6	0.000	609.1	557.6	1.0923	
	10.3	12.60	8.27	4982	0.0497	0.0067	0.707	16.6	0.000	531.7	559.2	0.9508	
	11.1	9.45	9.45	5390	0.0747	0.0079	0.575	14.4	0.167	251.6	257.9	0.9755	
	11.2	9.45	9.45	5574	0.0747	0.0079	0.556	14.4	0.167	264.8	262.9	1.0072	
	11.3	9.45	9.45	4772	0.0747	0.0079	0.650	14.4	0.167	240.5	240.1	1.0018	
	12.1	9.45	9.45	5390	0.0747	0.0079	0.979	14.4	0.167	264.8	271.9	0.9739	
	12.2	9.45	9.45	5207	0.0747	0.0079	1.013	14.4	0.167	251.6	243.7	1.0321	
	12.3	9.45	9.45	4772	0.0747	0.0079	1.106	14.4	0.167	222.8	253.3	0.8796	

Table 3.4 - Continued

Author	Col. Desig.	b (in.)	h (in.)	f'_c (psi)	ρ_{ss}	ρ_{rs}	$\frac{\rho_{ss} f_{yss}}{f'_c}$	ℓ/h	e/h	Tested Strength	Theor. Strength	Strength Ratio	
Janss	13.1	12.60	8.27	5574	0.0497	0.0067	0.352	11.6	0.190	269.1	277.3	0.9703	
Anslijn	13.2	12.60	8.27	5207	0.0497	0.0067	0.377	11.7	0.190	234.0	264.6	0.8845	
(1974)	13.3	12.60	8.27	5094	0.0497	0.0067	0.386	11.7	0.190	229.5	259.5	0.8846	
Janss	1	12.60	8.27	4724	0.0497	0.0067	0.426	16.6	0.000	606.8	515.2	1.1779	
Piraprez	3	12.60	8.27	4724	0.0497	0.0067	0.426	6.1	0.000	591.3	628.1	0.9414	
(1974)	5	12.60	8.27	5161	0.0497	0.0067	0.390	16.6	0.000	617.9	544.3	1.1352	
	7	12.60	8.27	5161	0.0497	0.0067	0.390	6.1	0.000	646.4	665.6	0.9713	
	9	12.60	8.27	5534	0.0497	0.0067	0.364	16.6	0.000	428.0	568.8	0.7524	*
	11	12.60	8.27	5534	0.0497	0.0067	0.364	6.1	0.000	461.3	697.6	0.6612	*
	13	12.60	8.27	4992	0.0497	0.0067	0.403	20.4	0.000	419.2	478.9	0.8753	
	15	12.60	8.27	5110	0.0497	0.0067	0.394	20.4	0.000	441.2	484.5	0.9107	
	17	12.60	8.27	5043	0.0497	0.0067	0.399	20.4	0.000	437.0	481.4	0.9077	
	19	12.60	8.27	4741	0.0497	0.0067	0.425	11.8	0.000	575.8	599.4	0.9606	
	23	12.60	8.27	4573	0.0497	0.0067	0.440	11.8	0.000	600.1	586.3	1.0236	
	27	12.60	8.27	4108	0.0497	0.0067	0.490	11.8	0.000	551.7	549.4	1.0042	
	2	9.45	9.45	4724	0.0747	0.0079	0.622	14.5	0.000	518.6	521.3	0.9949	
	4	9.45	9.45	4724	0.0747	0.0079	0.622	5.3	0.000	522.9	615.4	0.8496	
	6	9.45	9.45	5161	0.0747	0.0079	0.570	14.5	0.000	538.4	549.2	0.9805	
	8	9.45	9.45	5161	0.0747	0.0079	0.570	5.3	0.000	545.0	646.8	0.8426	
	10	9.45	9.45	5534	0.0747	0.0079	0.531	14.5	0.000	481.1	572.6	0.8401	
	12	9.45	9.45	5534	0.0747	0.0079	0.531	5.3	0.000	503.1	660.6	0.7616	*
	14	9.45	9.45	4992	0.0747	0.0079	0.589	17.8	0.000	403.9	479.1	0.8431	
	16	9.45	9.45	5110	0.0747	0.0079	0.575	17.8	0.000	533.9	484.1	1.1029	
	18	9.45	9.45	5043	0.0747	0.0079	0.583	17.8	0.000	472.3	481.3	0.9812	
	21	9.45	9.45	4741	0.0747	0.0079	0.620	10.3	0.000	573.8	593.5	0.9667	
	25	9.45	9.45	4573	0.0747	0.0079	0.643	10.3	0.000	547.2	580.9	0.9420	
	29	9.45	9.45	4108	0.0747	0.0079	0.716	10.3	0.000	448.0	545.2	0.8217	
	20	12.60	8.27	4741	0.0497	0.0067	0.425	11.7	0.190	269.1	248.0	1.0852	
	24	12.60	8.27	4573	0.0497	0.0067	0.440	11.7	0.190	231.8	241.5	0.9598	
	28	12.60	8.27	4108	0.0497	0.0067	0.490	11.7	0.190	236.0	224.3	1.0521	
	22	9.45	9.45	4741	0.0747	0.0079	0.620	10.2	0.167	264.8	275.5	0.9614	
	26	9.45	9.45	4573	0.0747	0.0079	0.643	10.2	0.167	218.5	269.5	0.8106	
	30	9.45	9.45	4108	0.0747	0.0079	0.716	10.2	0.167	280.1	251.4	1.1143	
Roderick	SE 1	8.00	7.00	3690	0.0525	0.0000	0.603	12.0	0.000	273.0	268.1	1.0184	
& Loke	SE 2	8.00	7.00	4280	0.0525	0.0000	0.520	12.0	0.057	211.0	211.2	0.9993	
(1974)	SE 3	8.00	7.00	3910	0.0525	0.0000	0.569	12.0	0.114	129.0	139.7	0.9235	
	SE 4	8.00	7.00	3880	0.0525	0.0000	0.551	12.0	0.000	264.0	275.3	0.9591	
	SE 5	8.00	7.00	3710	0.0525	0.0000	0.576	12.0	0.057	195.0	188.4	1.0349	
	SE 6	8.00	7.00	3280	0.0525	0.0000	0.730	12.0	0.114	108.0	122.1	0.8844	
	SE 7	8.00	7.00	4200	0.0525	0.0000	0.491	12.0	0.214	88.0	88.3	0.9967	
	SE 8	8.00	7.00	4140	0.0525	0.0000	0.500	12.0	0.000	290.0	285.8	1.0148	
	SE 9	8.00	7.00	4580	0.0525	0.0000	0.453	17.1	0.029	201.0	213.6	0.9409	
	SE10	8.00	7.00	4310	0.0525	0.0000	0.480	17.1	0.057	135.0	168.1	0.8031	
	SE11	8.00	7.00	3250	0.0525	0.0000	0.690	17.1	0.114	88.0	92.2	0.9547	
	SE12	8.00	7.00	4280	0.0525	0.0000	0.485	17.1	0.214	67.0	70.2	0.9543	
	SE13	8.00	7.00	3070	0.0263	0.0000	0.368	12.0	0.000	180.0	192.9	0.9333	
	SE14	8.00	7.00	2890	0.0263	0.0000	0.391	12.0	0.057	116.0	134.0	0.8659	
	SE15	8.00	7.00	3810	0.0263	0.0000	0.296	12.0	0.114	108.0	126.3	0.8551	

Table 3.4 - Continued

Author	Col. Desig.	b (in.)	h (in.)	f'_c (psi)	ρ_{ss}	ρ_{rs}	$\frac{\rho_{ss} f_{yss}}{f'_c}$	ℓ/h	e/h	Tested Strength	Theor. Strength	Strength Ratio	
Morino et al. (1984)	A4-90	6.30	6.30	3060	0.0870	0.0036	1.481	5.8	0.250	113.0	88.4	1.2791	*
	B4-90	6.30	6.30	3393	0.0870	0.0036	1.302	14.4	0.250	83.6	69.1	1.2090	*
	C4-90	6.30	6.30	3379	0.0870	0.0036	1.177	21.7	0.250	61.7	52.4	1.1773	
	D4-90	6.30	6.30	3074	0.0870	0.0036	1.474	28.9	0.250	46.4	37.1	1.2502	*
	A8-90	6.30	6.30	4872	0.0870	0.0036	0.953	5.8	0.469	77.4	66.7	1.1608	
	B8-90	6.30	6.30	4829	0.0870	0.0036	0.957	14.4	0.469	59.5	53.7	1.1068	
	C8-90	6.30	6.30	3567	0.0870	0.0036	1.305	21.7	0.469	39.7	36.8	1.0779	
	D8-90	6.30	6.30	3321	0.0870	0.0036	1.399	28.9	0.469	30.3	28.2	1.0759	
Roik Mangerig (1987)	7	11.81	11.81	6570	0.0868	0.0050	0.517	10.0	0.100	1023.1	789.0	1.2967	*
	8	11.81	11.81	6570	0.0868	0.0050	0.517	10.0	0.300	502.0	406.4	1.2352	*
	9	11.81	11.81	6570	0.0868	0.0050	0.517	16.7	0.100	824.6	587.6	1.4034	*
	10	11.81	11.81	6570	0.0868	0.0050	0.517	16.7	0.300	410.9	316.3	1.2989	*
	11	11.81	11.81	6570	0.0868	0.0050	0.517	26.7	0.100	455.0	334.8	1.3588	*
	12	11.81	11.81	6570	0.0868	0.0050	0.517	26.7	0.300	223.9	206.8	1.0827	*
Roik Schwal'r (1988)	V102	11.02	11.02	5956	0.0495	0.0079	0.370	12.6	0.357	252.2	236.3	1.0674	
	V111	11.02	11.02	6015	0.0495	0.0314	0.358	12.6	0.357	394.9	347.9	1.1351	
	V112	11.02	11.02	6015	0.0495	0.0314	0.358	12.6	0.214	565.9	478.7	1.1822	
	V113	11.02	11.02	6015	0.0495	0.0314	0.358	12.6	0.000	1032.8	1069.1	0.9660	
	V121	11.02	11.02	6015	0.0434	0.0314	0.251	12.6	0.571	256.1	237.7	1.0772	
	V122	11.02	11.02	6015	0.0434	0.0314	0.251	12.6	0.714	182.9	196.6	0.9305	
	V123	11.02	11.02	6015	0.0434	0.0314	0.251	12.6	0.357	345.4	333.2	1.0367	

NOTE : For e/h = inf., strength is given in kip-ft (1 kip-ft = 1.356 kN-m).

For all other values of e/h, the strength is shown in kips (1 kip = 4.448 kN).

b = width of the concrete cross-section parrallel to the axis of bending;

h = depth of the concrete cross-section perpendicular to the axis of bending.

The term f_{yss} was taken as the web yield strength for computing the $\rho_{ss} f_{yss}/f'_c$ ratio.

The strain-hardening of both steels was included in the analysis.

* Excluded from final analysis.

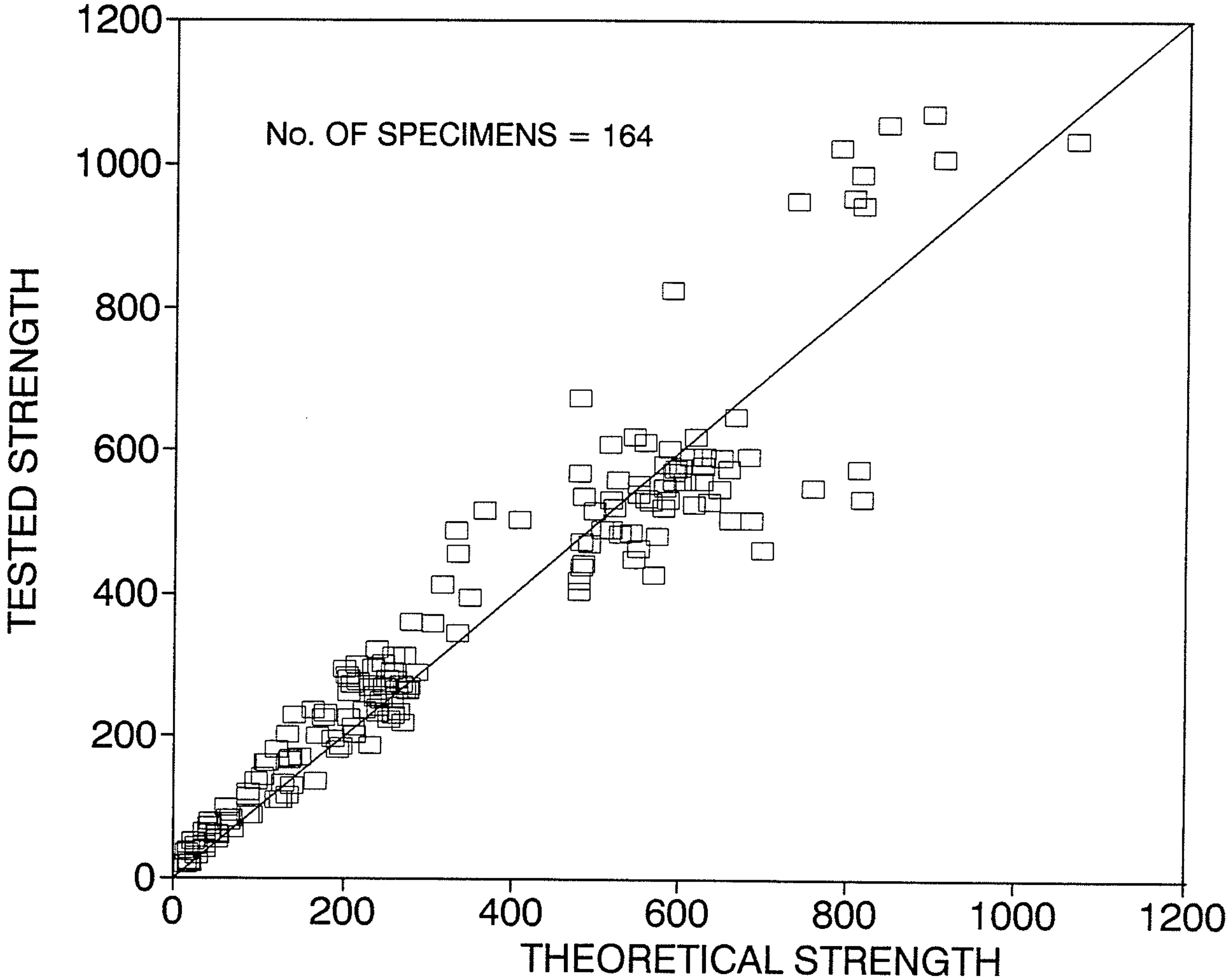

For e/h = inf., the strength is plotted in kip-ft.

For all other values of e/h, the strength is shown in kips.

Figure 3.7 - Comparison of tested strength to theoretical strength for beam-columns subjected to bending about the minor axis of the steel section.

Table 3.5 - Statistical Analysis of Ratios of Tested to Calculated Strength of all Composite beam-column specimens subjected to minor axis bending (Strain-hardening included).

Column Type (1)	(2)	all e/h (3)	0 <= e/h <= 0.2 (4)	0.2 < e/h < 1 (5)	0 <= e/h < 1 (6)	e/h = inf. (7)
Short (ℓ/h< 6.6)	No.	15	13	2	15	-
	Mean	1.00	0.96	1.22	1.00	-
	CV	18.43	17.73	6.86	18.43	-
	Skew	-0.09	0.02	0.00	-0.09	-
Long (ℓ/h=> 6.6)	No.	149	119	28	147	2
	Mean	1.12	1.10	1.18	1.12	1.05
	CV	22.87	24.40	15.92	23.00	3.65
	Skew	1.19	1.22	1.62	1.17	0.00
All ℓ/h	No.	164	132	30	162	2
	Mean	1.11	1.09	1.19	1.11	1.05
	CV	22.77	24.25	15.41	22.88	3.65
	Skew	1.18	1.25	1.62	1.17	0.00

to 6.6. The data was further categorized into four ranges of end eccentricity ratio (e/h) as described in Table 3.5.

The mean value for the ratio of tested to theoretical ultimate strength was 1.11 with a coefficient of variation of 22.77 percent when all 164 specimens were considered (Table 3.5 - Column 3). These values do not correlate to the mean value of 1.04 and coefficient of variation of 10.23 percent obtained for the 81 beam-column specimens subjected to the major axis bending and analyzed in the Section 3.1.

A review of the strength ratios in Table 3.4 shows Stevens' test data to be overly conservative with a wide variation in strength ratios ranging from 1.04 to 2.06. A parametric study of the data was then carried out using different variables. The purpose was to compare the strength ratios obtained from Stevens' data to those obtained for the data of the other authors. Figures 3.8, 3.9, 3.10, and 3.11 plot the strength ratios for Stevens' data and the rest of the data against e/h, ℓ/h, f'_c, and $\rho_{ss}f_{yss}/f'_c$, respectively, where ρ_{ss} = the structural steel ratio, and f_{yss} = the yield strength of the structural steel. Comparisons of Figures 3.8(a) and (b), 3.9(a) and (b), 3.10(a) and (b), and 3.11(a) and (b) indicate that Stevens' data is consistently different from the others. Stevens' 54 specimens alone gave a mean value of 1.36 and a coefficient of variation of 17.09 percent. This is significantly different from a mean value of 0.98 and a coefficient of variation of 14.34 percent obtained for the

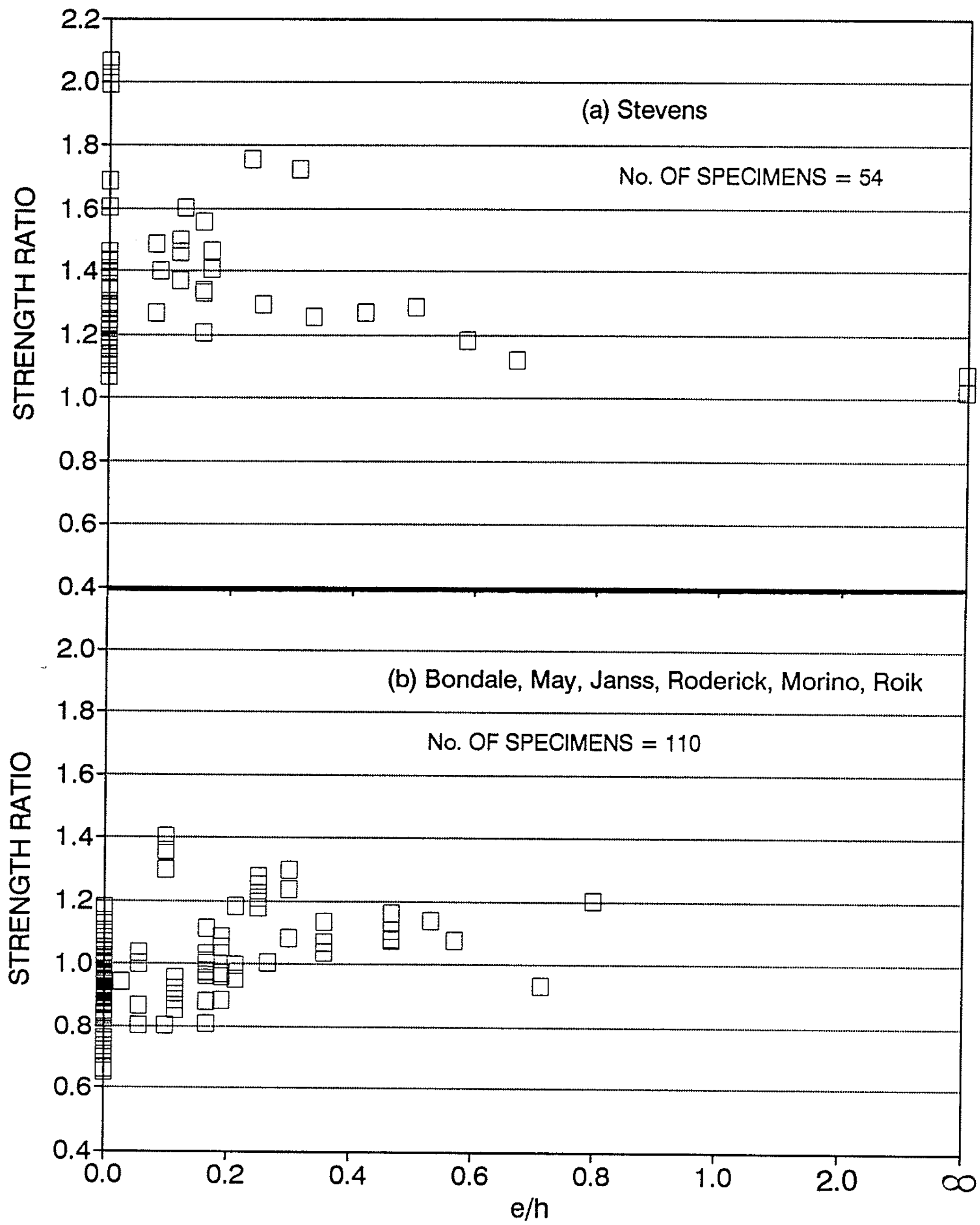

Figure 3.8 - Effect of *e/h* on strength ratios for (a) Stevens' data and (b) data of other authors.

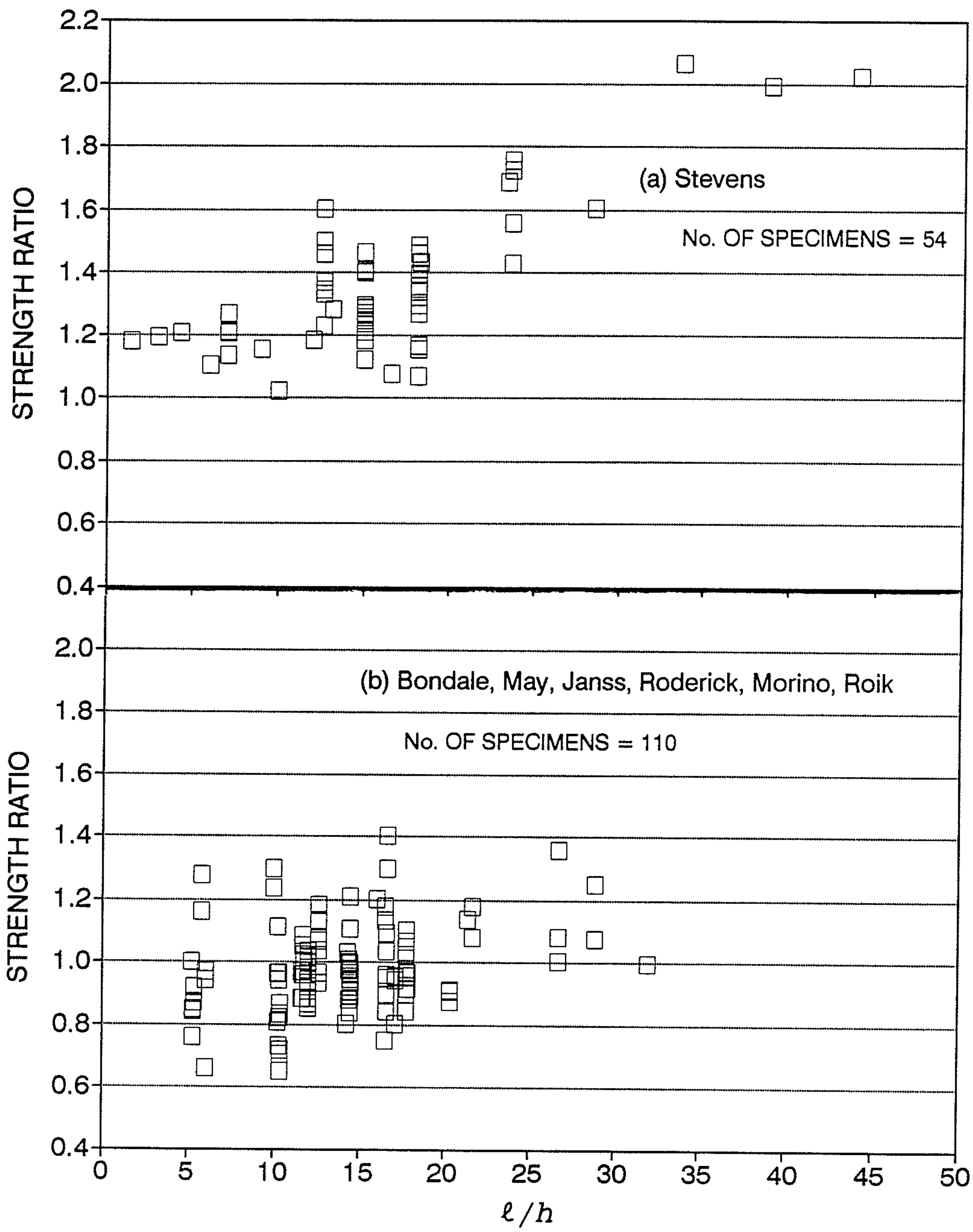

Figure 3.9 - Effect of ℓ/h on strength ratios for (a) Stevens' data and (b) data of other authors.

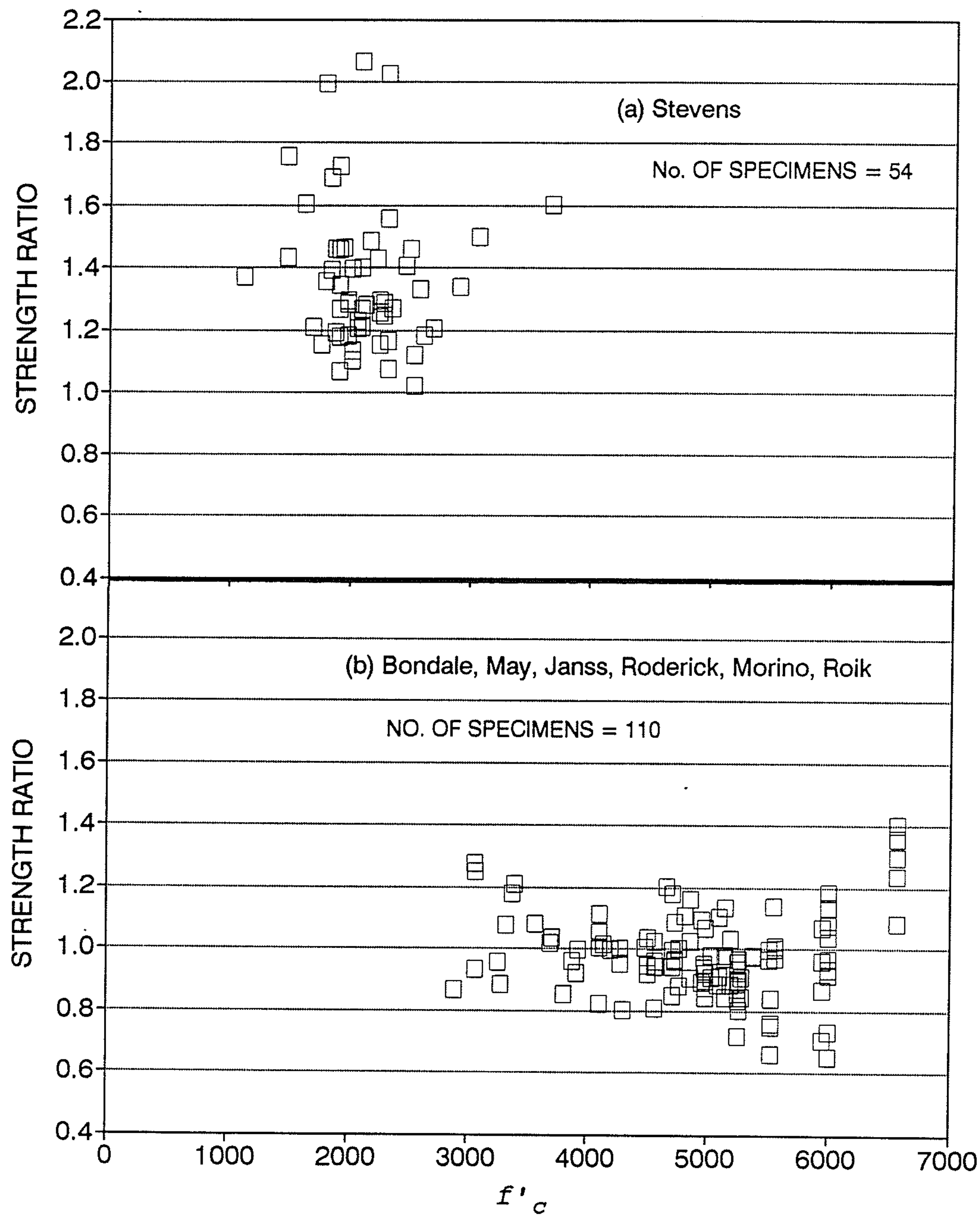

Figure 3.10 - Effect of f'_c on strength ratios for (a) Stevens' data and (b) data of other authors.

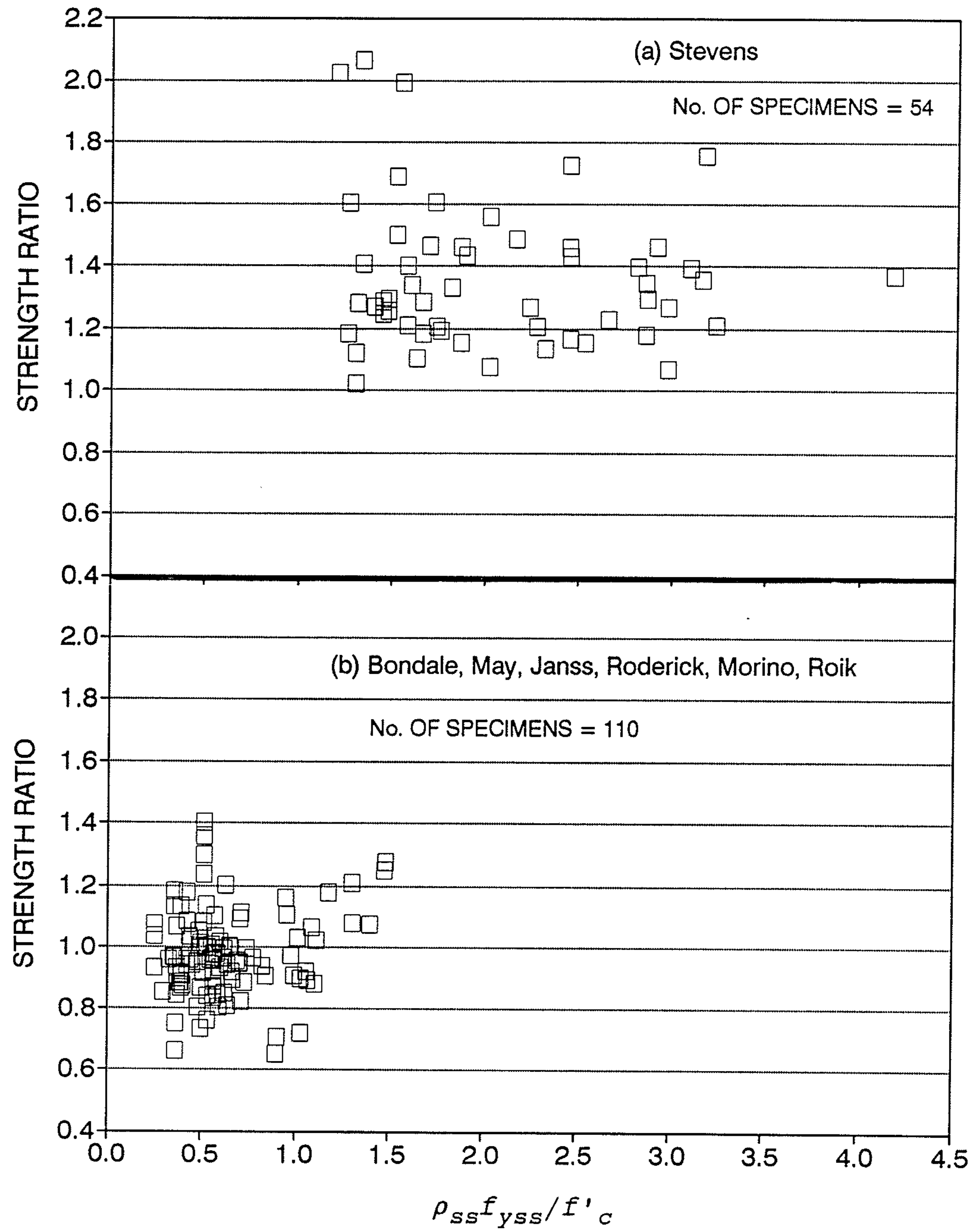

Figure 3.11 - Effect of $\rho_{ss}f_{yss}/f'_c$ on strength ratios for (a) Stevens' data and (b) data of other authors.

remaining 110 specimens.

Basu (1966) used 26 of Stevens' column specimens(CV, AE, and FE series in Table 3.4) and found that using a factor of 0.8 instead of 0.67 to obtain equivalent cylinder strength from a 4-inch cube gave 10 percent better agreement with his theoretical model. Roderick and Rogers (1969) on the other hand, analyzed Stevens' twelve specimens from FE series (Table 3.4) and suggested that the yield strength of 32.9 ksi (227 MPa) reported by Stevens' for the 12-inch by 6-inch structural steel section is somewhat low in comparison to the nominal yield strength of 35.8 ksi (247 MPa) specified for that section.

Figure 3.10 (a) shows that the concrete strength f'_c for almost all of Stevens' specimens is less than 3000 psi. This indicates an apparent problem either with obtaining an equivalent cylinder strength using Equation 3.2 and 3.3 or with the cube test data reported by Stevens. The latter is suspected to contribute to the problem, because Equation 3.2 and 3.3 were used to convert the cube strength to the cylinder strength for many of the remaining specimens and gave reasonable results.

Other problems that were encountered in determining the material properties and cross-section configuration for the test specimens reported by Stevens' data are summarized below:

1) The specified length of some of the specimens was unclear.

2) Information regarding the reinforcement was insufficient with respect to quantity, position, and yield strength.

3) The way the concrete strength was determined from cubes was unclear (cube tested parallel or perpendicular to the direction of casting).

4) Two sets of concrete cubes were cast, one set stored with the beam-column specimens and the other stored in water, gave significantly different results.

Stevens' data indicates that the theoretical model is quite conservative. More favourable results could have been obtained if the water stored cube strengths were multiplied by a factor of 0.8 to obtain an equivalent cylinder strength rather than using the approximately 0.67 times the strength obtained from the cubes stored with the test specimens. Consequently, it was decided that it would be acceptable not to use Stevens' data in this study, with the exception of the two tests in pure flexure (AE11 and FE12 in Table 3.4). Flexural tests results were retained because the strength is not as significantly affected by concrete strength and unsupported length as is in the case of beam-columns subjected to combined axial load and bending. A plot of tested strength versus theoretical strength for the remaining 112 specimens is shown in Figure 3.12.

The statistics for strength ratios of the remaining 112 specimens resulted in a mean value of 0.98 and a coefficient of variation of 14.23 percent (Table 3.6 - Column 3). This

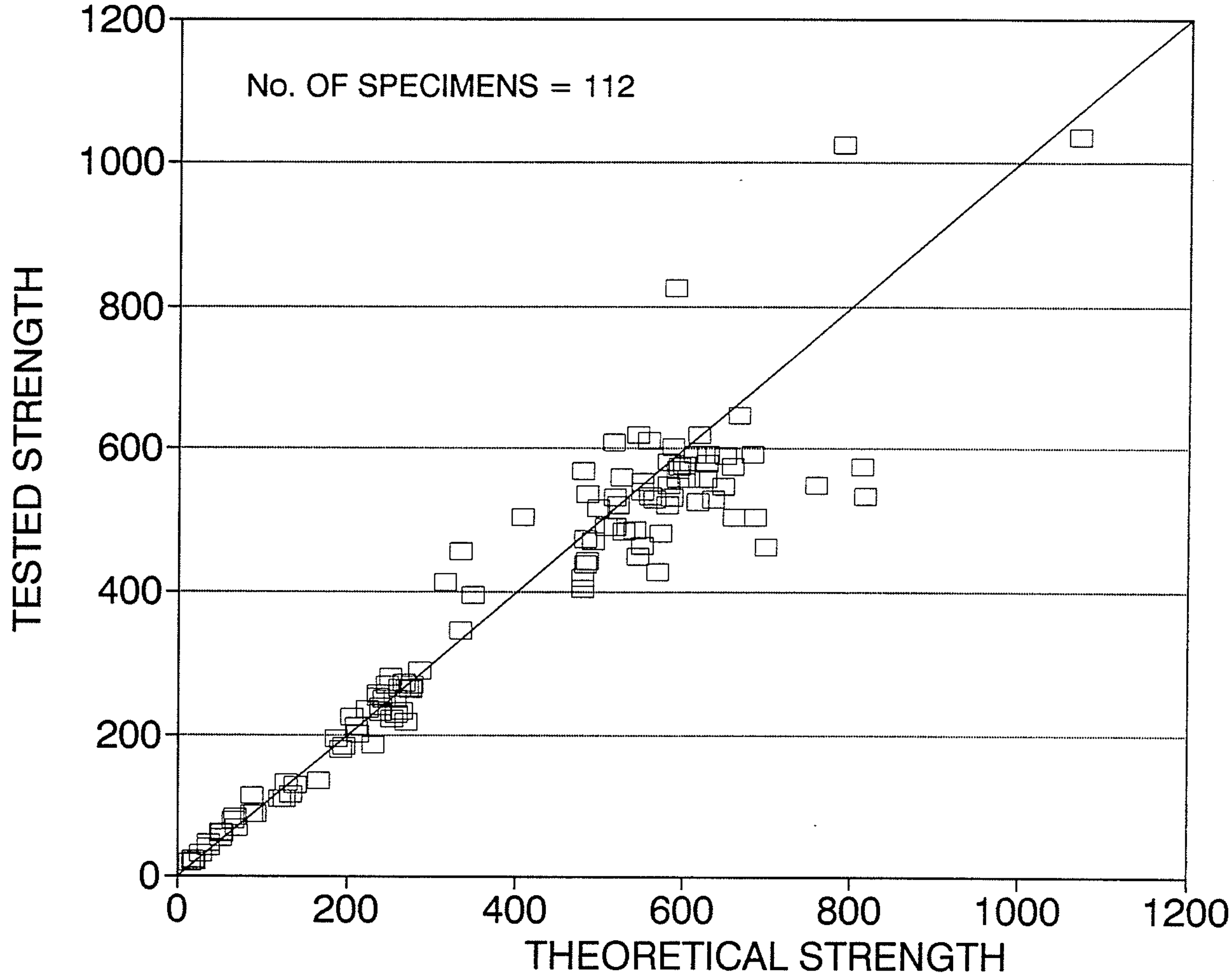

For e/h = inf., the strength is plotted in kip-ft.

For all other values of e/h, the strength is shown in kips.

Figure 3.12 - Comparison of tested strength to theoretical strength for beam-columns subjected to minor axis bending other than those tested by Stevens in which $e/h \leq \infty$.

Table 3.6 - Statistical Analysis of Ratios of Tested to Calculated Strengths for Composite beam-columns subjected to minor axis bending other than those tested by Stevens in which e/h < inf. (Strain-hardening included).

Column Type (1)	(2)	all e/h (3)	0 <= e/h <= 0.2 (4)	0.2 < e/h < 1 (5)	0 <= e/h < 1 (6)	e/h = inf. (7)
Short (ℓ/h< 6.6)	No.	11	9	2	11	-
	Mean	0.93	0.87	1.22	0.93	-
	CV	18.57	12.29	6.86	18.57	-
	Skew	0.48	-0.58	0.00	0.48	-
Long (ℓ/h=> 6.6)	No.	101	79	20	99	2
	Mean	0.99	0.95	1.11	0.99	1.05
	CV	13.73	13.20	9.05	13.85	3.65
	Skew	0.48	0.86	0.00	0.51	0.00
All ℓ/h	No.	112	88	22	110	2
	Mean	0.98	0.95	1.12	0.98	1.05
	CV	14.23	13.35	9.14	14.34	3.65
	Skew	0.43	0.77	-0.07	0.46	0.00

Table 3.7 - Statistical Analysis of Ratios of Tested to Calculated Strengths for Composite beam-column specimens subjected to minor axis bending for which the strength ratio ranged from 0.8 to 1.2 (Strain-hardening included).

Column Type (1)	(2)	all e/h (3)	0 <= e/h <= 0.2 (4)	0.2 < e/h < 1 (5)	0 <= e/h < 1 (6)	e/h = inf. (7)
Short (ℓ/h< 6.6)	No.	8	7	1	8	-
	Mean	0.94	0.91	1.16	0.94	-
	CV	11.02	6.70	-	11.02	-
	Skew	0.88	0.09	-	0.88	-
Long (ℓ/h=> 6.6)	No.	87	71	14	85	2
	Mean	0.97	0.95	1.07	0.97	1.05
	CV	9.26	8.46	7.26	9.30	3.65
	Skew	0.26	0.32	-0.21	0.30	0.00
All ℓ/h	No.	95	78	15	93	2
	Mean	0.97	0.95	1.07	0.97	1.05
	CV	9.39	8.38	7.30	9.42	3.65
	Skew	0.32	0.36	-0.30	0.37	0.00

compares reasonably well with the mean value of 1.04 and a coefficient of variation of 10.23 percent obtained for strength ratios of 81 beam-column specimens subjected to major axis bending and analyzed in the Section 3.1. This also compares with the mean value of 1.04 and coefficient of variation of 10.4 percent obtained by Virdi and Dowling (1973) for eight biaxially loaded composite columns.

Differences in statistics for the four different ranges of end eccentricity ratio (Table 3.6 Columns 4, 5, 6, and 7) and the overall statistics (Table 3.6 Column 3) are significant for some cases. For short columns with low to intermediate eccentricity ratios (Columns 4, 5 and 6 in Table 3.6), the mean value and coefficient of variation fluctuate considerably for each range of end eccentricity ratio. Long columns with intermediate eccentricity ratios (Column 5 in Table 3.6) have a much higher mean value than the overall mean value.

It was decided that all data with a strength ratio greater than 1.20 or less than 0.8 be excluded from the final analysis. This is consistent with what was done for the calibration of the theoretical model for beam-columns subjected to major axis bending and described in Section 3.1. Using this criteria, a total of 17 specimens were removed from the final statistical analysis: RS 60.3 from Bondale; 3.2, 8.1, 8.2 and 8.3 from Janss and Anslijn; 9, 11 and 12 from Janss and Piraprez; A4-90, B4-90 and D4-90 from Morino et al.;

and all 6 beam-column specimens from Roik and Mangerig. All tests from Roik and Mangerig were excluded since five out of six of these tests were outside the limits of 0.8 and 1.2. The strength ratios plotted against e/h, ℓ/h, ρ_{ss}, and $\rho_{ss}+\rho_{rs}$ in Figures 3.13, 3.14, 3.15 and 3.16, respectively, show the relative locations of the excluded data with respect to the remaining data. The resulting statistics in Table 3.7 of the remaining 95 specimens shows a marked improvement in the mean value and coefficient of variation for each of the e/h ranges as well as for the overall statistics over the values shown in Table 3.6.

Column 6 in Table 3.7, where e/h ranges from zero to 1.0, is of specific interest since eccentricity ratios ranging from 0.05 to 1.0 were used to study the effective flexural stiffness (EI) of composite columns described in Chapters 5 and 6. Here, whether the columns are short, long or all lengths combined, the mean value and the coefficient of variation do not differ significantly. Based on the mean value and coefficient of variation, determined for 93 columns with all ℓ/h included (Table 3.7 Column 6), a mean value of 1.0 with a coefficient of variation of 10 percent are recommended to describe the model error for beam-columns bending about the minor axis of the steel section when $e/h \leq$ 1.0.

Pure bending (Column 7 in Table 3.7), where $e/h = \infty$, gives the lowest coefficient of variation (3.65 percent)

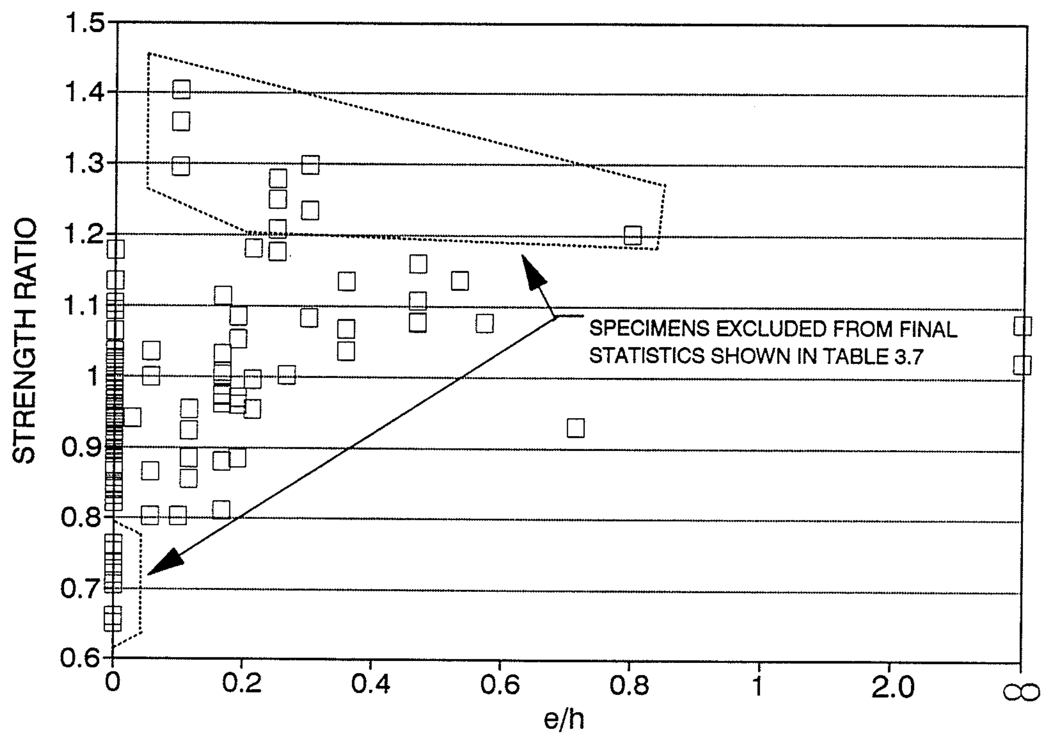

Figure 3.13 - Effect of *e/h* on strength ratios for beam-columns subjected to bending about the minor axis of the steel section.

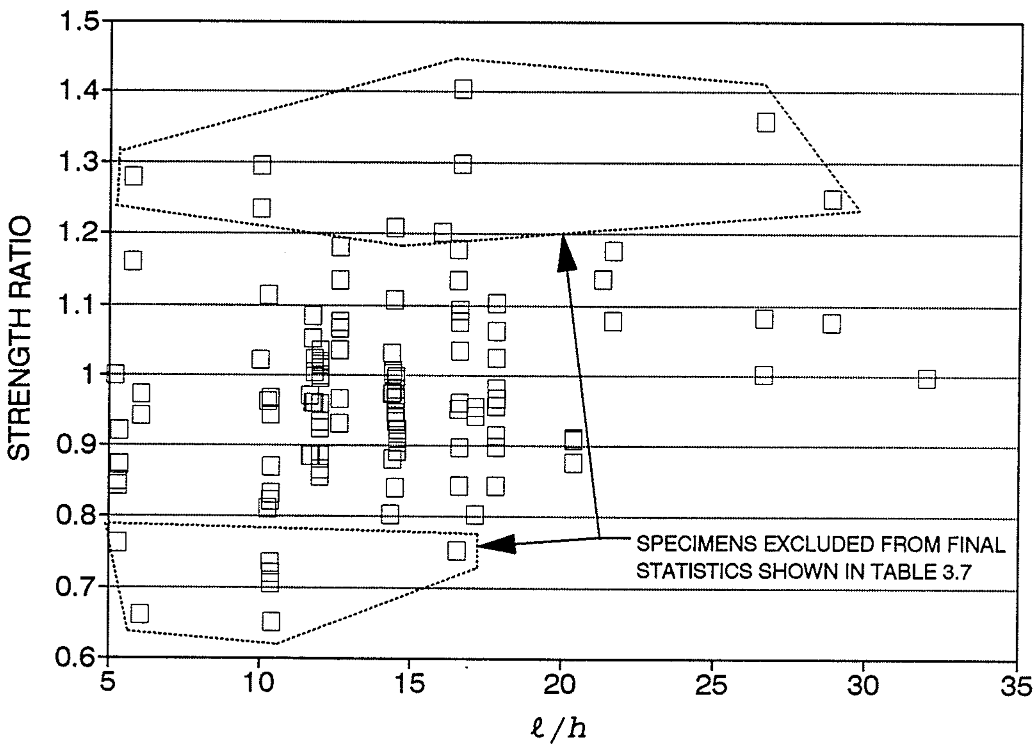

Figure 3.14 - Effect of ℓ/h on strength ratios for beam-columns subjected to bending about the minor axis of the steel section.

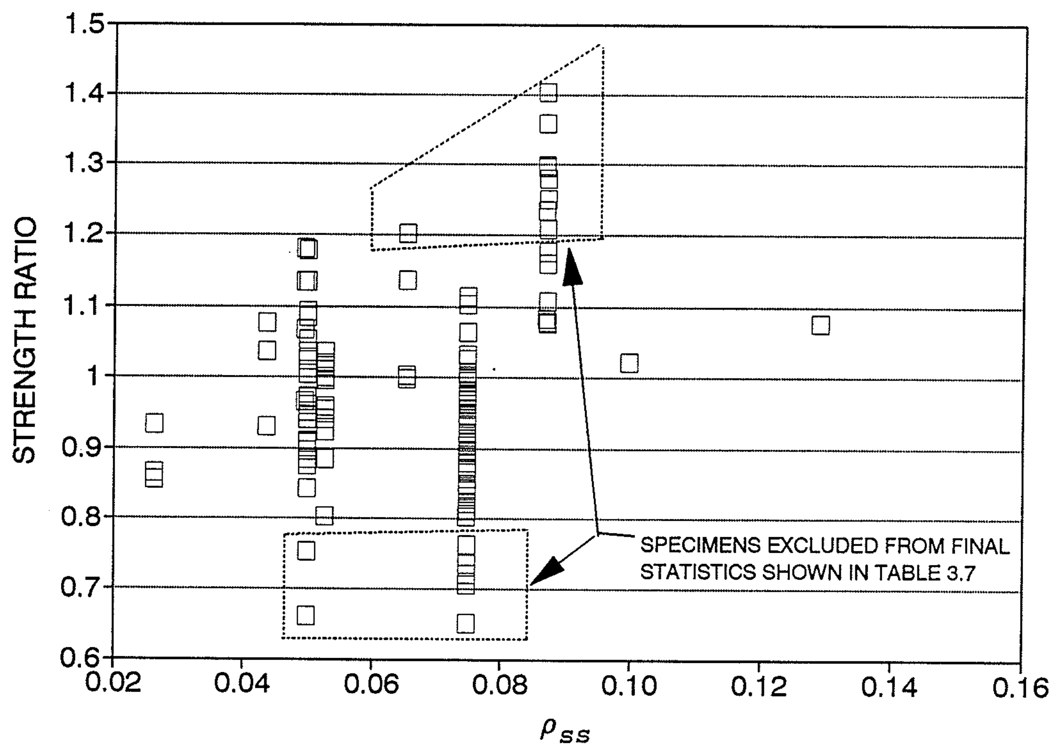

Figure 3.15 - Effect of ρ_{ss} on strength ratios for beam-columns subjected to bending about the minor axis of the steel section.

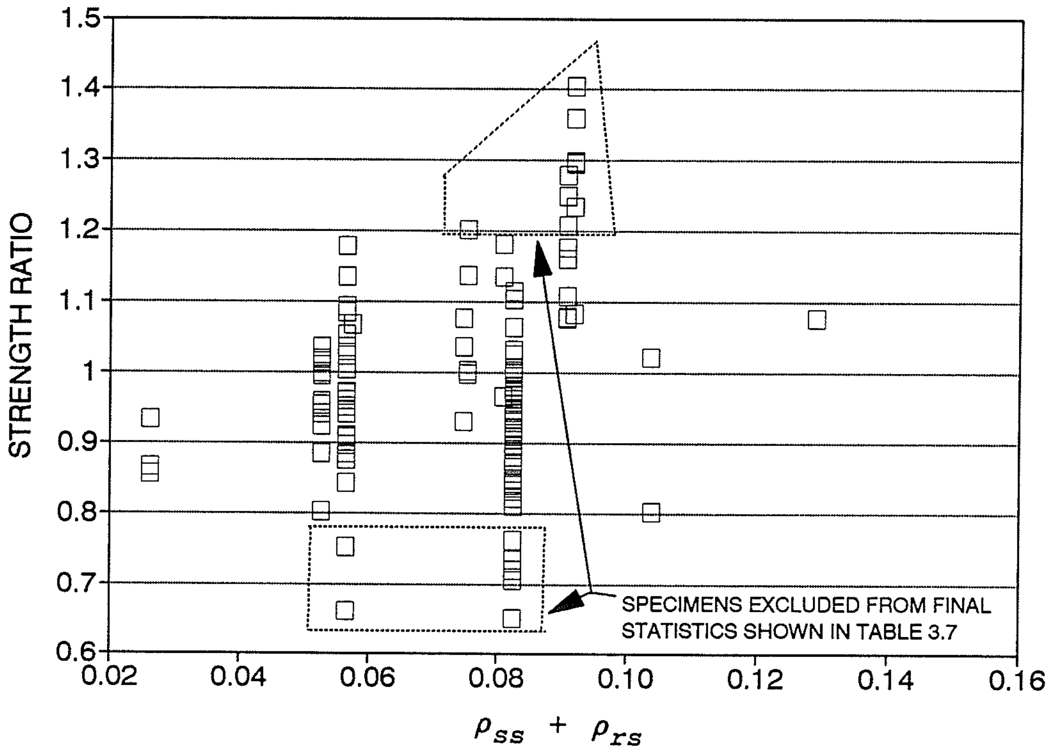

Figure 3.16 - Effect of $(\rho_{ss} + \rho_{rs})$ on strength ratios for beam-columns subjected to bending about the minor axis of the steel section.

compared to the other e/h ranges. This is the same trend exhibited by beam-columns subjected to pure bending about the major axis described in Section 3.1.

The calculated ultimate strength considering the effect of strain-hardening was compared to the calculated ultimate strength when strain hardening was not included. Strain hardening was found to have no affect on the calculated strength of the beam-columns when $e/h < \infty$. Strain hardening had some effect on the strength of beam-columns subjected to pure bending. The resulting calculated ultimate bending strength without the effect of strain-hardening for each of Stevens' two beam-columns, AE11 and FE12, are 17.63 kip-ft and 127.4 kip-ft, respectively.

The probability distribution of the strength ratios calculated for the 93 specimens ($e/h \leq 1.0$) is plotted on a normal probability paper in Figure 3.17 and is compared to a normal probability distribution using the suggested mean value of 1.00 and coefficient of variation of 10 percent. The data can be assumed to be normally distributed since the data closely follows the normal curve.

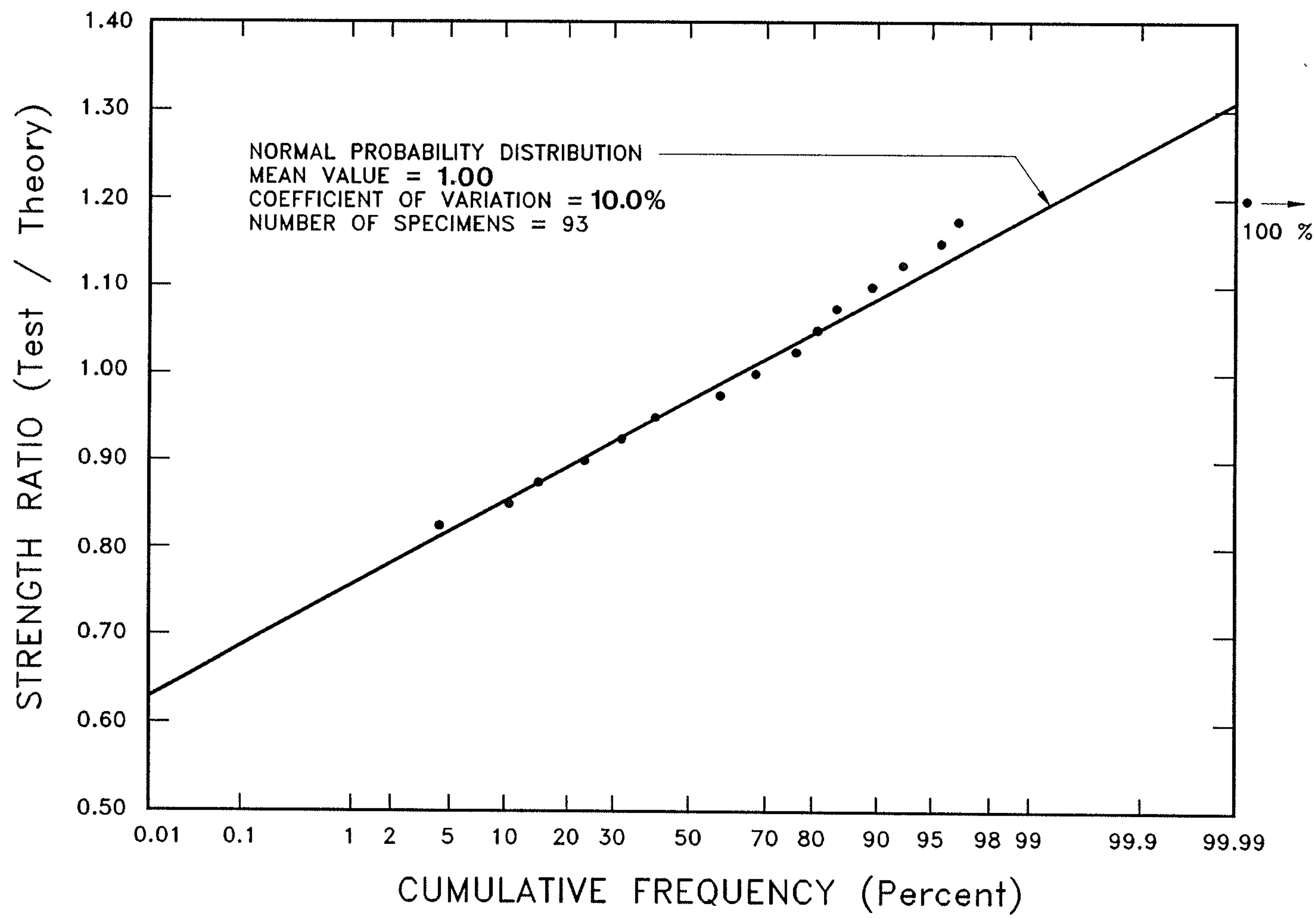

Figure 3.17 - Probability distribution of strength ratios ($0.8 \leq$ test/theory ≤ 1.20) of composite beam-column specimens (Table 3.4) bending about the minor axis with $0 \leq e/h \leq 1.0$.

4 - ACI AND AISC FLEXURAL STIFFNESSES

4.1 ACI CODE EFFECTIVE FLEXURAL STIFFNESS

Equation 4.1 is specified by the ACI Building Code (1989) and CSA Code A23.3 (1984) to determine the effective flexural stiffness of slender composite columns subjected to short term loading.

$$EI = 0.2E_cI_g + E_sI_{ss} \tag{4.1}$$

In the above equation, E_c is the modulus of elasticity for concrete, I_g is the moment of inertia for the gross concrete cross section, E_s is the modulus of elasticity for steel, and I_{ss} is the moment of inertia of the structural steel shape taken about the centroidal axis of the composite cross-section.

4.2 AISC-LRFD CODE EFFECTIVE FLEXURAL STIFFNESS

The AISC LRFD-Specification (AISC Code 1986) for the design of Structural Steel Buildings does not compute the effective flexural stiffness (EI) of a composite beam-column as does the ACI code. The procedure, described in detail later in this section, was developed to obtain effective flexural stiffness from the AISC interaction equations. The AISC EI so computed is comparable to the ACI EI and theoretical EI.

First, the equations given in the AISC Code (1986) were rearranged to establish axial load-bending moment (P-M) relationships for slender beam-column strength and cross-section strength. The bending moment from each of the two interaction diagrams for a given axial load level was then computed and used to determine the AISC moment magnification factor, similar to the one described in the ACI code. Finally, the moment magnification equation, given in the ACI Building Code, was rearranged to solve for AISC *EI*. The procedure outlined above simply uses the ACI moment magnifier approach in reverse order and the AISC interaction equations for composite columns.

4.2.1 AISC Axial Load-Bending Moment Relationship

The AISC Code (Chapter H) limits the strength interaction for structural steel members subjected to combined axial load and bending moment according to Equation 4.2 and 4.3.

For $\dfrac{P_u}{\phi_c\, P_n} \geq 0.2$

$$\frac{P_u}{\phi_c\, P_n} + \frac{8}{9}\left(\frac{M_{ux}}{\phi_b\, M_{nx}} + \frac{M_{uy}}{\phi_b\, M_{ny}}\right) \leq 1.0 \qquad (4.2)$$

For $\dfrac{P_u}{\phi_c\, P_n} < 0.2$

$$\frac{P_u}{2\phi_c\, P_n} + \left(\frac{M_{ux}}{\phi_b\, M_{nx}} + \frac{M_{uy}}{\phi_b\, M_{ny}}\right) \leq 1.0 \qquad (4.3)$$

The modifications required in these equations to obtain the strength interaction for composite columns are described later in this section. Essentially, Equations 4.2 and 4.3 can be used to describe the axial load-bending moment interaction relationship for a beam-column of any length ℓ.

In Equations 4.2 and 4.3, P_u is the required compressive strength in kips; P_n is the nominal compressive strength in kips for a column of length ℓ determined in accordance with Section E2 of the AISC Code; M_u is the required flexural strength calculated including the second order effects; M_n is the nominal flexural strength of the cross section; ϕ_c and ϕ_b are resistance factors for compression and bending. In this study the major and minor axis bending cases were each considered separately and the resistance factors were set equal to 1.0. Equation 4.2 and 4.3 take the following form:

$$\text{For } \frac{P_u}{P_n} \geq 0.2 \qquad \frac{P_u}{P_n} + \frac{8}{9}\left(\frac{M_u}{M_n}\right) \leq 1.0 \tag{4.4}$$

$$\text{For } \frac{P_u}{P_n} < 0.2 \qquad \frac{P_u}{2P_n} + \left(\frac{M_u}{M_n}\right) \leq 1.0 \tag{4.5}$$

Schematic P-M interaction curves resulting from Equations 4.4 and 4.5 for bending about one axis are given in Figure 4.1.

The nominal compressive strength (P_n) for a steel column is defined in Chapter E (Section E2) of the AISC Code as:

$$P_n = A_g F_{cr} \tag{4.6}$$

$$\text{For } \lambda_c \leq 1.5 \qquad F_{cr} = (0.658^{\lambda_c^2}) F_y \tag{4.7}$$

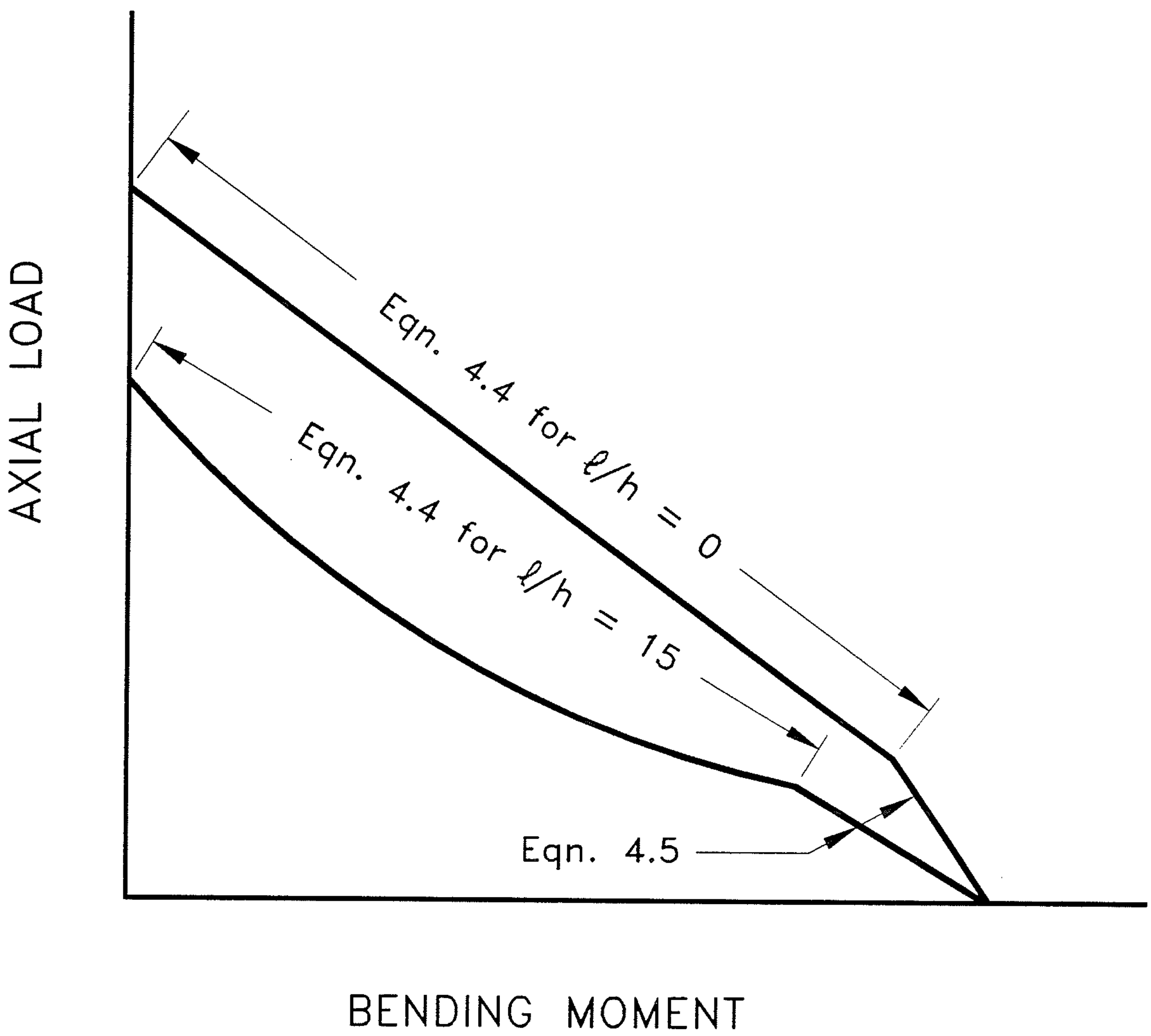

Figure 4.1 - Schematic cross-section and column axial load-bending moment (*P-M*) interaction diagrams developed from AISC interaction equations for beam-columns bending about one axis of the steel section.

For $\lambda_c > 1.5$ $$F_{cr} = \left[\frac{0.877}{\lambda_c^2}\right]F_y \tag{4.8}$$

and $$\lambda_c = \frac{K\ell}{r\pi}\sqrt{\frac{F_y}{E}} \tag{4.9}$$

in which A_g is the gross cross section area of the steel member, in.^{2}; F_y is the specified yield strength, ksi; E is the modulus of elasticity, ksi; K is the effective length factor, which was taken equal to 1.0 for this study; ℓ is the unbraced length, inches; and r is the governing radius of gyration about the plane of buckling, inches.

For structures designed on the basis of first-order elastic analysis, Equation 4.10 is used (in lieu of second-order analysis) to obtain the required flexural moment (M_u) that accounts for the second-order effects of column length and lateral translation.

$$M_u = B_1 M_{nt} + B_2 M_{\ell t} \tag{4.10}$$

where B_1 is a moment magnifier to account for second-order length effects and is described by Equation 4.11 and M_{nt} is the required flexural strength (kip-in.) in a member assuming no lateral translation of the frame.

$$B_1 = \frac{C_m}{1 - \dfrac{P_u}{P_e}} \geq 1.0 \tag{4.11}$$

The product of the moment magnifier B_2 and $M_{\ell t}$, the required flexural strength for the member due to lateral translation of the frame, were equal to zero because lateral translation was not considered in this study. In Equation 4.11, the coefficient $C_m = 0.6 - 0.4(M_1/M_2)$ accounts for end moment conditions for compression members braced against lateral translation. M_1/M_2 is the ratio of the smaller bending moment to the larger bending moment acting at opposite ends of the unbraced length and in the plane of bending being considered. For single curvature bending, M_1 and M_2 are equal and opposite and, therefore, C_m becomes equal to 1.0. Finally, P_e is defined by the equation:

$$P_e = \frac{A_g F_y}{\lambda_c^2} \tag{4.12}$$

In the present form, Equations 4.2 through 4.12, described above are for structural steel beam-columns. To obtain the design strength of a composite beam-column, the AISC Code modifies the properties of the structural steel according to the following provisions:

(a) Replace A_g with A_s, the area of the gross steel shape.

(b) Replace r with r_m, the greater of the radius of gyration of the steel shape or 0.3 times the overall depth of the composite section in the plane of buckling.

(c) Replace F_y with a modified yield stress F_{my} and replace E with a modified modulus of elasticity E_m, as described by Equations 4.13 and 4.14.

$$F_{my} = F_y + c_1 F_{yr}(A_r/A_s) + c_2 f'_c(A_c/A_s) \qquad (4.13)$$

$$E_m = E + c_3 E_c(A_c/A_s) \qquad (4.14)$$

in which A_c is the area of concrete, in.^{2}; A_r is the area of the longitudinal reinforcing bars, in.^{2} ; A_s is the area of the steel section, in.^{2}; E is the modulus of elasticity for steel, ksi; E_c is the Modulus of elasticity for concrete calculated as $57000\sqrt{f'_c}$, ksi; F_y is the specified yield strength of the steel shape, ksi; F_{yr} is the specified yield strength of the longitudinal reinforcing bars, ksi; f'_c is the specified compressive strength of the concrete, ksi; and coefficients c_1, c_2 and c_3 are equal to 0.7, 0.6, and 0.2 respectively.

(d) The nominal flexural strength (M_n) is calculated using Equation 4.15 described in Chapter I (Section I4) of the AISC Code.

$$M_n = M_p = ZF_y + \frac{1}{3}(h_2 - 2c_r)A_r F_{yr} + \left(\frac{h_2}{2} - \frac{A_w F_y}{1.7 f'_c h_1}\right) A_w F_y \qquad (4.15)$$

This is an approximate formula obtained from the plastic stress distribution for the composite section. In Equation 4.15, A_w is the web area of the encased steel shape, in.^{2}; Z is the plastic section modulus of the steel section, in.^{3}; c_r is the average distance from the compression face to longitudinal reinforcement in that face and distance from tension face to longitudinal reinforcement in the face, inches; h_1 is the width of the cross section parallel to the axis of bending, inches; and h_2 is the depth of the cross section perpendicular to the axis of bending, inches.

Substituting Equation 4.10 and then Equation 4.11 into Equations 4.4 and 4.5 yields:

For $\frac{P_u}{P_n} \geq 0.2$

$$\frac{P_u}{P_n} + \frac{8}{9}\left(\frac{M_{nt}}{M_n\ (1 - \frac{P_u}{P_e})}\right) \leq 1.0 \qquad (4.16)$$

For $\frac{P_u}{P_n} < 0.2$

$$\frac{P_u}{2P_n} + \left(\frac{M_{nt}}{M_n\ (1 - \frac{P_u}{P_e})}\right) \leq 1.0 \qquad (4.17)$$

Instead of generating a series of values to determine the *P-M* relationship and then interpolating for a desired end eccentricity ratio (e/h), a closed form solution was used. In the present form, Equations 4.16 and 4.17 cannot be readily solved using simple algebraic manipulation since each equation has two unknowns, M_{nt} and P_u. Knowing the value of end eccentricity (e) from the desired e/h ratio, the term P_u times e was substituted for M_{nt} into Equations 4.16 and 4.17, leaving each equation with only one unknown variable (P_u) in

Equation 4.18 and 4.19.

For $\frac{P_u}{P_n} \geq 0.2$

$$\frac{P_u}{P_n} + \frac{8}{9}\left(\frac{P_u e}{M_n\ (1 - \frac{P_u}{P_e})}\right) = 1.0 \qquad (4.18)$$

For $\frac{P_u}{P_n} < 0.2$

$$\frac{P_u}{2P_n} + \left(\frac{P_u e}{M_n\ (1 - \frac{P_u}{P_e})}\right) = 1.0 \qquad (4.19)$$

Both sides of Equations 4.18 and 4.19 were then multiplied by $(1 - P_u/P_e)$ to give:

For $\frac{P_u}{P_n} \geq 0.2$

$$\frac{P_u}{P_n} - \frac{P_u^2}{P_n P_e} + \frac{8}{9}\frac{P_u e}{M_n} = 1.0 - \frac{P_u}{P_e} \qquad (4.20)$$

For $\frac{P_u}{P_n} < 0.2$

$$\frac{P_u}{2P_n} - \frac{P_u^2}{2P_n P_e} + \frac{P_u e}{M_n} = 1.0 - \frac{P_u}{P_e} \qquad (4.21)$$

Rearranging Equations 4.20 and 4.21, gathering terms of P_u and multiplying through by -1.0 results in the following expressions:

For $\dfrac{P_u}{P_n} \geq 0.2$

$$\left(\frac{1}{P_n P_e}\right) P_u^2 + \left(-\frac{1}{P_n} - \frac{8}{9}\frac{e}{M_n} - \frac{1}{P_e}\right) P_u + (1.0) = 0 \qquad (4.22)$$

For $\dfrac{P_u}{P_n} < 0.2$

$$\left(\frac{1}{2P_n P_e}\right) P_u^2 + \left(-\frac{1}{2P_n} - \frac{e}{M_n} - \frac{1}{P_e}\right) P_u + (1.0) = 0 \qquad (4.23)$$

in which e is calculated from the desired e/h ratio and is an input to Equations 4.22 and 4.23; P_n, P_e and M_n are values that can be readily determined using the equations stated earlier and the given cross-section properties and column length. Equations 4.22 and 4.23 are in the form of a general quadratic equation: $ax^2 + bx + c = 0$, where $x = P_u$ and a, b and c are the constants indicated within parentheses in Equations 4.22 and 4.23. The solution for a general quadratic equation shown below was then used to determine P_u:

$$P_u = x = \frac{-b \pm \sqrt{b^2 - 4ac}}{2a} \qquad (4.24)$$

Equation 4.24 gives two solutions due to the plus and minus signs used in the numerator of the equation. It was determined that the minus sign gives the correct solution because the other solution (with a plus sign) for P_u is greater than the pure axial load capacity of the cross-section ($\ell = 0$).

Equations 4.22, 4.23 and 4.24 were used to solve for the axial load P_u for each desired eccentricity for a slender column. M_{nt} (M_{col}) was then taken equal to P_u times e. To maintain consistency with the terms in Section 2.1, M_{col} was used to represent the overall slender column bending moment capacity and M_{cs} to represent the cross-section bending moment capacity. P_u was then substituted into either equation 4.16 or 4.17 depending on the ratio of P_u/P_n, the column length was set equal to zero, M_{cs} was used to replace M_{nt}, and the equation was rearranged to solve for M_{cs}. Note that for a cross-section (column of length zero) P_e tends to infinity. Therefore, P_u/P_e becomes zero, making the solution a matter of simple algebra.

4.2.2 Computation of AISC Effective Flexural Stiffness

To facilitate a direct comparison to the ACI method of determining the effective flexural stiffness, it was determined that an equivalent moment magnification factor, similar to the one utilized by the ACI Code, could be computed from the interaction diagrams and formulation described in Section 4.2.1.

The ACI magnified factored moment M_c is defined by

$$M_c = \delta_b M_{2b} + \delta_s M_{2s} \tag{4.25}$$

Equation 4.25 is identical to Equation 4.10 taken from the

AISC Code. In Equation 4.25, δ_b is a moment magnifier to account for second-order length effects as computed from Equation 4.26; M_{2b} is the moment resulting from gravity loads. The product of the moment magnifier δ_s and M_{2s}, the moment resulting from lateral loads, was equal to zero because lateral loads were not considered in this study.

$$\delta_b = \frac{C_m}{1 - \dfrac{P_u}{\phi P_c}} \geq 1.0 \tag{4.26}$$

In Equation 4.26, C_m is the equivalent uniform moment diagram factor and is equal to $0.6 - 0.4(M_{1b}/M_{2b})$; M_{1b}/M_{2b} is the ratio of smaller bending moment to larger bending moment acting at opposite ends of the unbraced length and in the plane of bending being considered. For single curvature, M_{1b} and M_{2b} are equal and opposite and C_m becomes equal to 1.0. P_u is the factored axial load; ϕ is the resistance factor which was taken equal to 1.0 in this study; and P_c is defined by:

$$P_c = \frac{\pi^2 EI}{(k\ \ell_u)^2} \tag{4.27}$$

in which ℓ_u is the unsupported length of the column and k is the effective length factor taken equal to 1.0 for the type of beam columns considered.

Substituting into Equation 4.25, M_{col} for M_{2b}, M_{cs} for M_c, and δ_b from Equation 4.26, and setting $C_m = 1.0$, $\phi = 1.0$, and $\delta_s M_{2s} = 0$ gives the following expression:

$$M_{cs} = \left(\frac{1}{1 - \frac{P_u}{P_c}} \right) M_{col} \tag{4.28}$$

Equation 4.28 was rearranged to solve for P_c (Equation 4.29).

$$P_c = \frac{P_u}{\left(1 - \frac{M_{col}}{M_{cs}} \right)} \tag{4.29}$$

Equating Equation 4.27 to Equation 2.29, setting k = 1.0, and then solving for EI gives the effective flexural stiffness for the AISC Code:

$$EI = \frac{P_u \, \ell_u^2}{\pi^2 \left(1 - \frac{M_{col}}{M_{cs}} \right)} \tag{4.30}$$

The terms P_u, M_{col} and M_{cs} were obtained from the closed form solution to the column axial load-bending moment interaction diagrams, shown in Figure 4.2 and explained in Section 4.2.1. A short computer program was written to compute the EI employing the procedure outlined in this Section and Section 4.2.1.

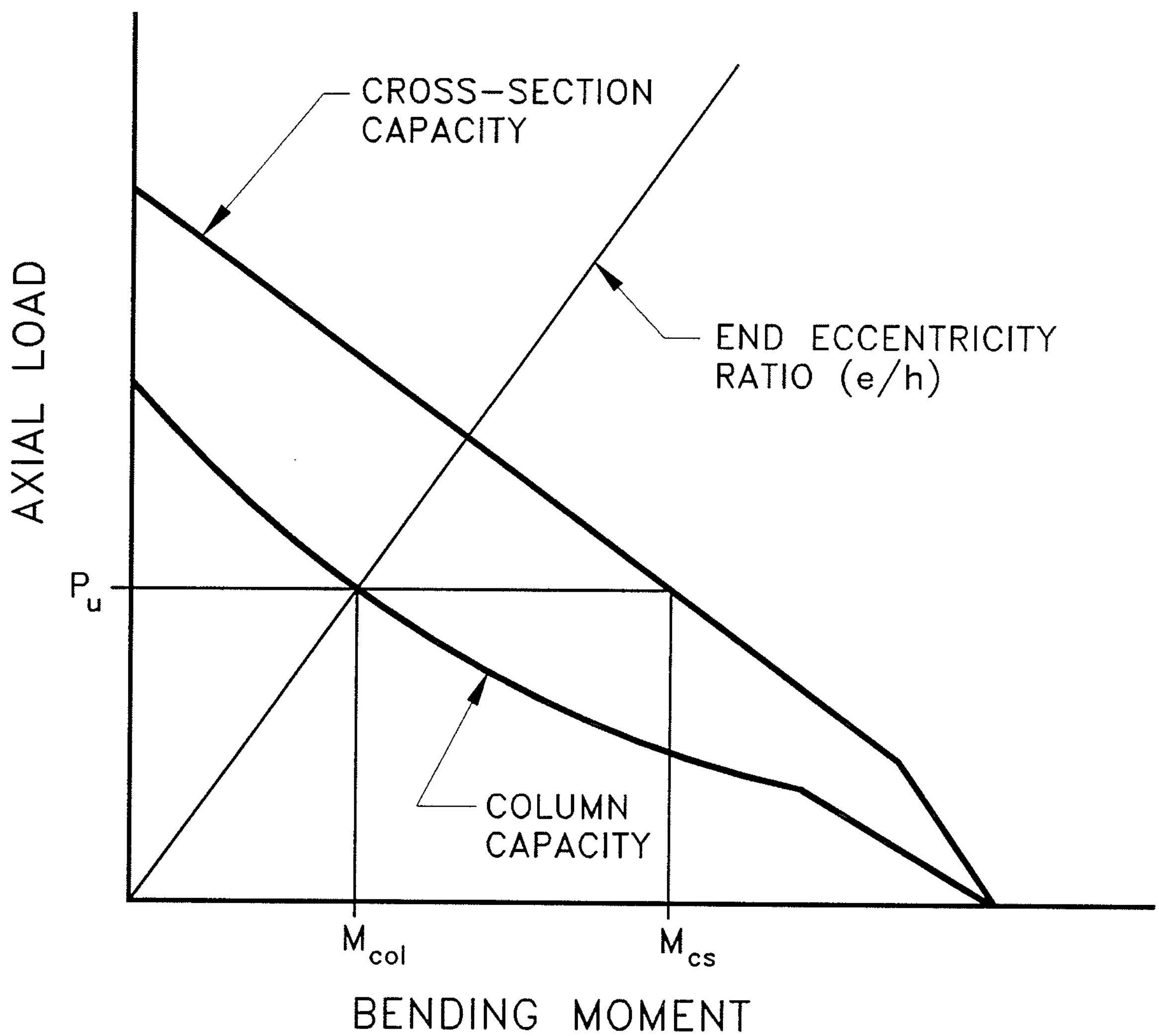

Figure 4.2 - Schematic cross-section and column axial load-bending moment interaction diagrams used to develop an equivalent AISC flexural stiffness.

5 - EVALUATION OF EFFECTIVE STIFFNESS FOR BEAM-COLUMNS SUBJECTED TO MAJOR AXIS BENDING

5.1 DESCRIPTION OF BEAM-COLUMNS STUDIED

In an attempt to study the full range of variables, 11880 composite beam-columns were used to evaluate the theoretical stiffness of beam-columns bending about the major axis. Each column had a different combination of the specified properties. The specified nominal concrete strengths f'_c, the structural steel yield strengths f_{yss}, the reinforcing steel ratios ρ_{rs}, the structural steel ratios ρ_{ss} and the size of structural steel shapes used in this study are listed in Table 5.1. The values shown in the table represent the practical ranges of these variables used in the construction industry. The overall concrete cross-section had a size of 22 inches by 22 inches; the details of the cross-section are given in Figure 5.1.

The ACI and AISC Code requirements for composite columns influenced the selection of the cross section parameters used in this study. For composite beam-columns neither the ACI nor the AISC Code specifies a maximum amount for the structural steel core. However, the AISC Code states that to qualify as a composite column the structural steel ratio (ρ_{ss}) must be greater than or equal to 4 percent. The ACI Building Code requires that a minimum of 1 percent to a maximum of 8 percent of longitudinal reinforcing (ρ_{rs}) be included with the

Table 5.1 - Specified properties of composite beam-columns studied*

Properties	Specified Values	Number of Specified Values
f'_c , psi	4000; 5000; 6000; 8000	4
f_{yss} , psi	36000; 44000; 50000	3
ρ_{rs} , %	1.09; 1.96; 3.17	3
structural steel	section / ρ_{ss} , % W12 x 170 / 10.33 W12 x 120 / 7.29 W12 x 72 / 4.36 W10 x 112 / 6.80 W10 x 68 / 4.13 W8 x 67 / 4.07	6
ℓ/h	10; 15; 20; 25; 30	5
e/h	0.05; 0.1; 0.2; 0.3; 0.4; 0.5 0.6; 0.7; 0.8; 0.9; 1.0	11

* Total number of columns equals (4 x 3 x 3 x 6 x 5 x 11 =) 11880 with each column having a different combination of specified properties shown above. All columns had a cross section size of 22 x 22 in. with lateral ties conforming to ACI 318-89 Clause 10.14.8.

Note: 1.0 in. = 25.4 mm; 1000 psi = 6.895 MPa.

STEEL SECTION					LONGITUDINAL REINFORCING									
								Corner Rebars			Add'l Rebars		Total Area of Rebars	
Designation	A_{ss} (in.^{2})	d_{ss} (in.)	b_f (in.)	ρ_{ss} (%)	Y (in.)	Max. bar dia. for Z=1.0 in.	Max. bar dia. for lap	Bar Dia. (in.)	No. Req.	Clear Dist. Z (in.)	Bar Dia. (in.)	No. Req.	(in.^{2})	ρ_{rs} (%)
W12 x 170	50.0	14.03	12.57	10.33	1.99	1.90	1.72	1.693	4	1.342	1.000	8	15.32	3.17
(W310 x 253)								1.000	4	2.167	1.000	8	9.48	1.96
								0.750	4	2.465	0.750	8	5.28	1.09
W12 x 120	35.3	13.12	12.32	7.29	2.44	2.20	1.84	1.693	4	1.706	1.000	8	15.32	3.17
(W310 x 179)								1.000	4	2.540	1.000	8	9.48	1.96
								0.750	4	2.841	0.750	8	5.28	1.09
W12 x 72	21.1	12.25	12.04	4.36	2.88	2.60	1.98	1.693	4	2.097	1.000	8	15.32	3.17
(W310 x 107)								1.000	4	2.934	1.000	8	9.48	1.96
								0.750	4	3.236	0.750	8	5.28	1.09
W10 x 112	32.9	11.36	10.41	6.80	3.32	3.30	2.80	1.693	4	3.002	1.000	8	15.32	3.17
(W250 x 167)								1.000	4	11.521	1.000	8	9.48	1.96
								0.750	4	11.823	0.750	8	5.28	1.09
W10 x 68	20.0	10.40	10.13	4.13	3.80	3.70	2.94	1.693	4	3.427	1.000	8	15.32	3.17
(W250 x 101)								1.000	4	4.263	1.000	8	9.48	1.96
								0.750	4	4.565	0.750	8	5.28	1.09
W8 x 67	19.7	9.00	8.28	4.07	4.50	4.60	3.86	1.693	4	4.581	1.000	8	15.32	3.17
(W200 x 100)								1.000	4	5.417	1.000	8	9.48	1.96
								0.750	4	5.719	0.750	8	5.28	1.09

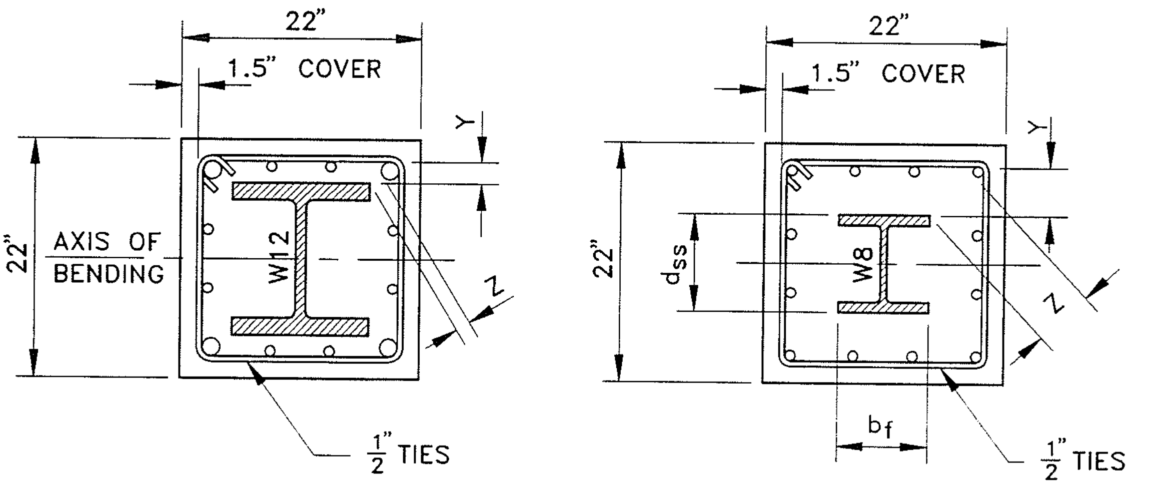

Figure 5.1 - Details of composite column cross-section for columns subject to bending about the major axis.

structural steel core. Difficulty in lap splicing the reinforcing bars reduces the maximum limit of ρ_{rs} to about 3 to 4 percent when a relatively large structural steel core is encased. The reinforcing steel ratio is, therefore, usually expected to range from 1 to 3 percent. Even three percent reinforcing steel will restrict ρ_{ss} to a maximum of about 10 percent, giving a range of ρ_{ss} about 4 to 10 percent. The AISC Code (Chapter I, Section I2) specifies that f'_c be restricted to range from 3000 psi to 8000 psi and that the maximum yield strength for structural steel and reinforcing bars shall not exceed 55,000 psi in calculating the strength of the column. The ACI Building Code, on the other hand, specifies that f'_c shall not be less than 2500 psi (Clause 10.14.8.1) and that the design yield strength of the structural steel shall not exceed 50,000 psi (Clause 10.14.8.2), but no restriction is placed on the design yield strength of the reinforcing steel. With these requirements in mind, the strengths for concrete and structural steel shown in Table 5.1 were selected. The yield strength of the reinforcing bars was taken as 60 ksi for all of the cross section arrangements, because this represents the standard strength of reinforcing bars used in the construction industry. Figure 5.1 shows the cross section arrangements that were used in this study.

Utilizing six different sizes of structural steel shapes (Figure 5.1) provided the means to study the effect of concrete cover over the structural steel section. The ratio of the depth of the structural steel shape to the depth of the concrete cross-section d_{ss}/h was used as an index for concrete cover over structural steel.

Table 5.1 shows that eleven end eccentricity ratios e/h ranging from 0.05 to 1.0 were used. This is consistent with the findings of Mirza and MacGregor (1982) that, for reinforced concrete buildings, e/h usually varies from 0.1 to 0.65. Five slenderness ratios ℓ/h were chosen to represent the range of ℓ/h for columns in braced frames designed in accordance with ACI 318-89 Clause 10.11.

As the purpose of this study is to simulate the actual stiffness EI of beam-columns described by nominal cross-sectional properties, the specified nominal values for material strength and cross-sectional properties will not provide an accurate estimation of EI. Mean values established by Skrabek and Mirza (1990) corresponding to the nominal specified properties were, therefore, used to compute the theoretical stiffness for each column. Table 5.2 lists the mean values corresponding to the specified nominal values.

The short-term theoretical effective flexural stiffness EI for each of the 11,880 columns studied was computed using Equation 2.7, the cross-section and slender column interaction diagrams described in Section 2.2, and the mean values of the variables specified in Table 5.2. The simulated column stiffness data were then statistically analyzed for examining the current ACI column stiffness, the equivalent AISC column

Table 5.2 - Mean Values of Variables Used for Computing Theoretical Strength and Stiffness.

(a) Concrete

Nominal Strength f'_c (psi)	Mean Values		
	Compressive Strength f_c (psi)	Modulus of Rupture f_r (psi)	Elastic Modulus E_c (ksi)
4,000	3,388	445	3,260
5,000	4,013	485	3,537
6,000	4,641	523	3,795
8,000	5,904	591	4,263

(b) Structural Steel Strength*

Nominal Strength f_y (psi)	Mean Values	
	Static Yield Strength	
	Web f_{ysw} (psi)	Flange f_{ysf}
36,000	39,240	0.95 f_{ysw}
44,000	47,960	0.95 f_{ysw}
50,000	54,500	0.95 f_{ysw}

(c) Residual Stresses in Structural Steel

Steel Shape	Flange Tip (psi)	Flange - web Juncture (psi)
W12 x 170 (W310 x 253)	-18,367	11,792
W12 x 120 (W310 x 179)	-17,983	11,267
W12 x 72 (W310 x 107)	-17,896	11,152
W10 x 112 (W250 x 167)	-18,576	12,089
W10 x 68 (W250 x 101)	-18,384	11,816
W8 x 67 (W200 x 100)	-18,465	11,931

* Note: Modulus of Elasticity for Structural Steel, E_s = 29,000 ksi

Table 5.2 - continued

(d) Structural Steel Dimensions

	Section Depth d	Flange Width b	Flange Thickness t	Web Thickness w
Ratio of Actual to Specified Dimensions	1.000	1.005	0.976	1.017

(e) Reinforcing Steel

Nominal Strength f_y (psi)	Static Yield Strength f_{ys} (psi)	Elastic Modulus E_s (ksi)
60,000	66,800	29,000

(f) Deviation of Overall Beam-Column Dimensions from Nominal Specified Dimensions

Length (in.)	0.0
Cross-Section Depth (in.)	+0.06
Cross-Section Width (in.)	+0.06
Concrete Cover to Lateral Ties (in.)	+0.33
Spacing of Lateral Ties (in.)	0.0

stiffness, and for developing the proposed design equations for *EI*.

5.2 EXAMINATION OF ACI AND AISC STIFFNESSES

The ACI Building Code and the comparable AISC Code equivalent flexural stiffnesses (Equation 4.1 and 4.30 described in Chapter 4) were compared with the theoretical *EI* data generated for all of the 11,880 composite columns subjected to bending about the major axis of the steel section. The nominal values of variables shown in Table 5.1 and Figure 5.1 were used for computing the ACI and AISC *EI* values. Note the theoretical *EI* values were computed using the mean values of variables shown in Table 5.2.

The histograms in Figure 5.2 show the ratios of theoretical *EI* to design *EI* (EI_{th}/EI_{des}). The results shown in Figure 5.2 (a) were computed based on EI_{des} taken equal to the ACI *EI* equation (Equation 4.1) and those shown in Figure 5.2(b) were based on EI_{des} set equal to AISC *EI* expression (Equation 4.30). Figure 5.2 that includes data for all ρ_{rs} values (1.09, 1.96, 3.17 percent) indicates that relatively high mean stiffness ratios and coefficients of variation (*CV*) are obtained from both the ACI and AISC equations (mean value = 1.39, *CV* = 22.8 percent; and mean value = 1.45, *CV* = 22.8 percent for Equations 4.1 and 4.30, respectively). This means that the ACI and AISC equations on the average predict conservative *EI* values which are about 40 percent lower than

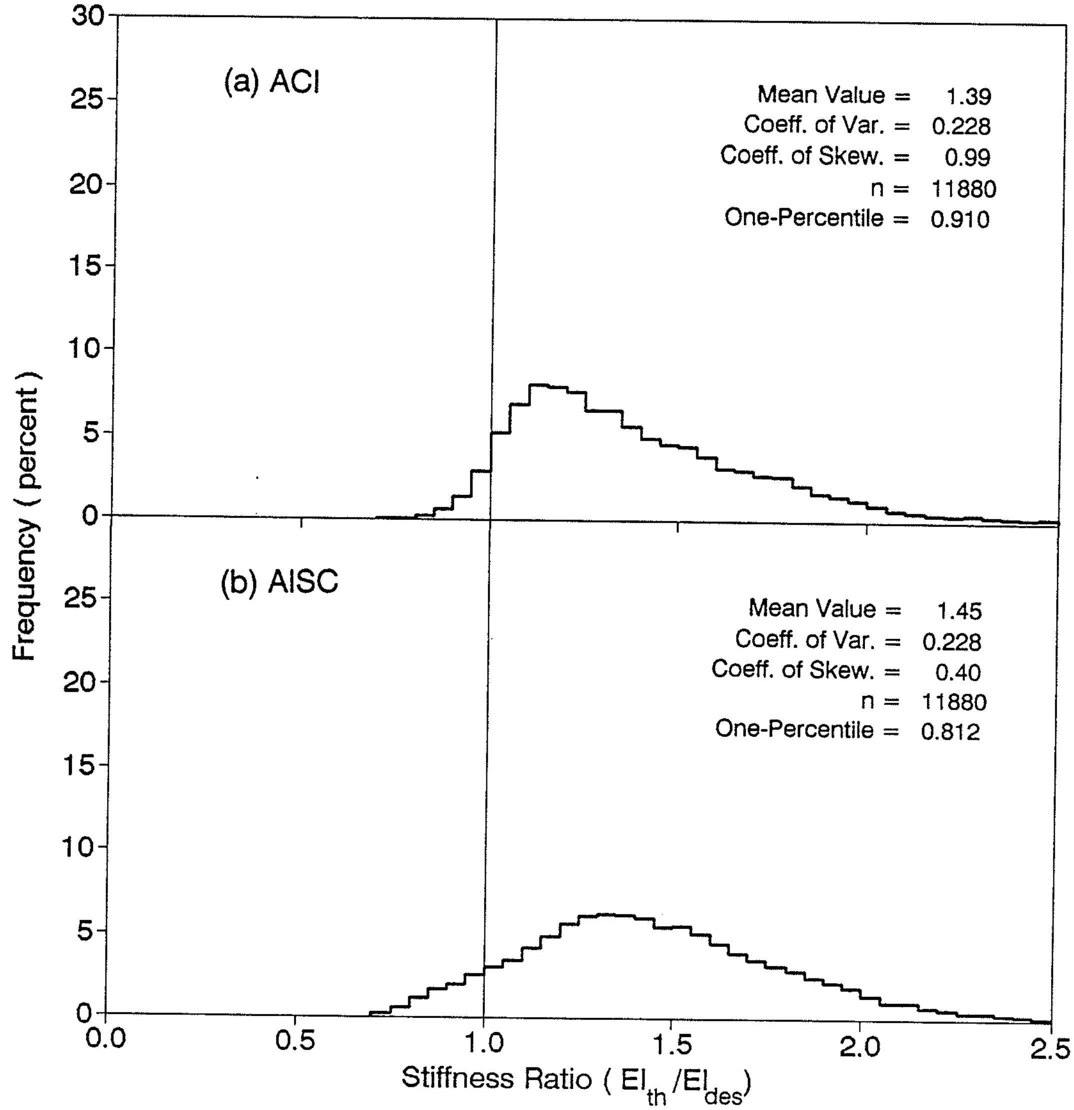

Figure 5.2 - Frequency histogram comparing ACI and AISC stiffness equations with theoretical results for all columns bending about major axis.

the theoretically predicted values.

The ACI equation, however, does not account for differences in the reinforcing steel ratio ρ_{rs}. A second comparison showing only the data where ρ_{rs} = 1 percent was plotted in Figure 5.3 for both the ACI and AISC stiffnesses. Mean values of 1.21 and 1.26 were obtained for ACI and AISC, respectively, along with coefficients of variation similar to those in Figure 5.2. This significant change in mean value indicates that the ACI and AISC design equations were most likely calibrated for the minimum required reinforcement ratio. This also appears to confirm the general belief that ACI and AISC equations are, in most cases, on the safe side. For a significant number of columns studied, however, both the ACI and AISC *EI* deviated substantially from the corresponding theoretically computed *EI*. This is because the ACI and AISC design equations do not include all the parameters that affect the stiffness of slender columns. The ACI equation does not account for the longitudinal reinforcing steel whereas the AISC design equations modify the properties of a composite column to that of an "equivalent steel" column in which cracking of the concrete is not considered.

It is evident from Figures 5.2 and 5.3 and the related discussions that there appears to be a need for modification in the existing ACI stiffness equation and AISC strength interaction equations used for the design of composite beam-columns.

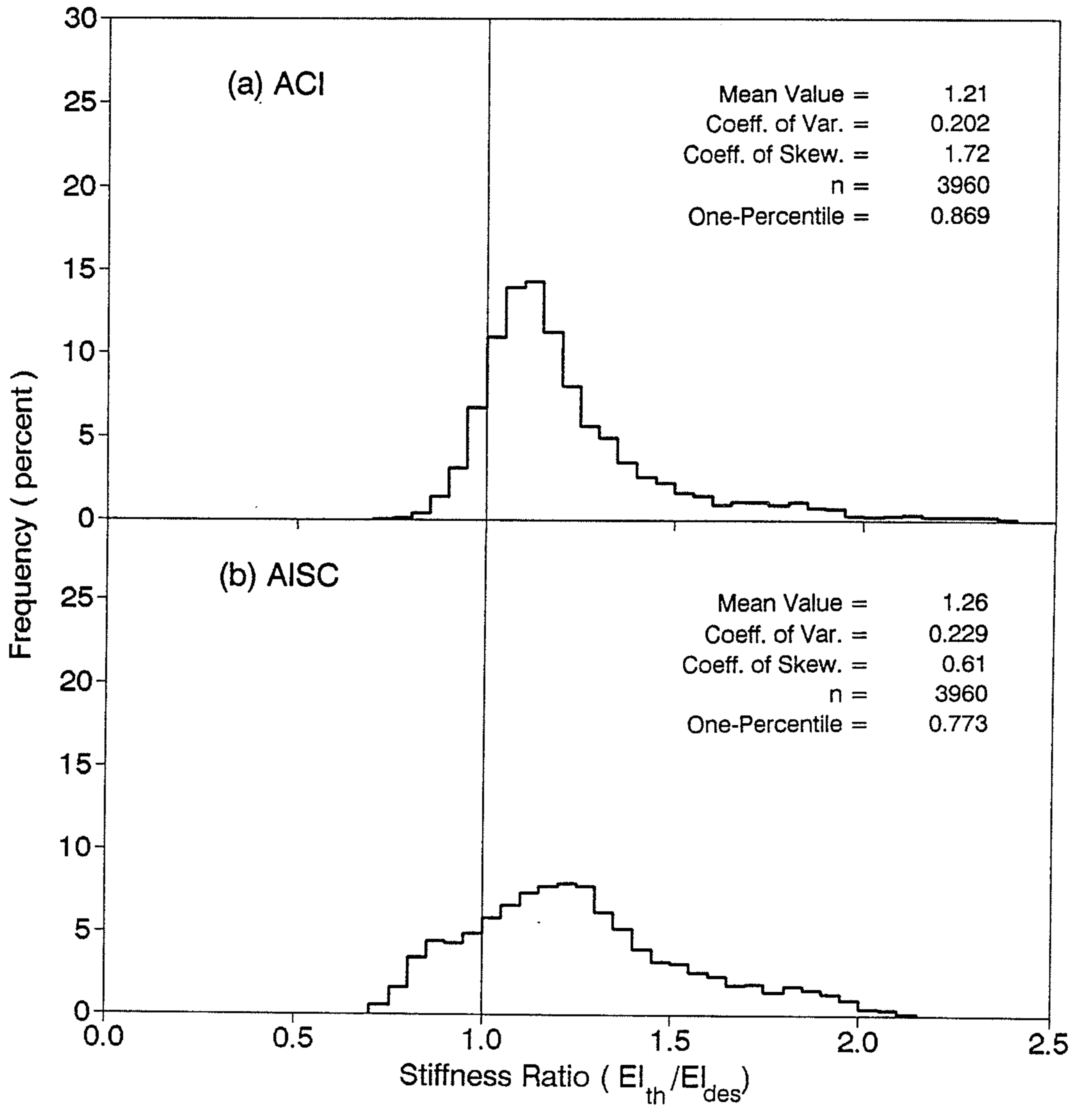

Figure 5.3 - Frequency histogram comparing ACI and AISC stiffness equations with theoretical results for columns bending about major axis where ρ_{rs} = 1.09 percent.

5.3 DEVELOPMENT OF PROPOSED DESIGN EQUATIONS FOR SHORT-TERM EI

Mirza (1990) among others pointed out that the effective flexural stiffness of a slender reinforced concrete column is significantly affected by cracking along its length and inelastic actions in the concrete and reinforcing steel. This is also expected for a composite column although to a lesser degree, because the structural steel core is expected to stiffen the concrete cross-section. However, the inelastic actions within the encased structural steel shape affect the overall stiffness of a composite column. *EI* is then represented by a complex function of a number of variables that cannot be readily transformed into a unique and simple analytical solution. The objective in this study is to develop simple equations for *the EI* of composite columns, similar to the ones that were produced by Mirza (1990) for reinforced concrete columns. Multiple linear regression analysis was chosen to evaluate *EI* from the generated theoretical stiffness data.

5.3.1 Variables Used for Regression Analysis

The variables used in this study were divided into two major groups: (A) variables that affect the contribution of concrete to the overall effective stiffness; and (B) variables that influence the contribution of structural and reinforcing steel to the overall effective stiffness of a composite beam-column.

Group A consists of five subgroups, similar to those described by Mirza(1990): (1) end eccentricity ratio e/h or P_u/P_o (subgroup X_1), in which P_u is the factored axial load acting on the slender column and P_o is the pure axial load capacity of the cross-section; (2) slenderness ratio ℓ/h or ℓ/r (subgroup X_2), where r is the radius of gyration calculated according to the ACI Building Code Equation (10-13) reproduced here as Equation 5.1; (3) steel index ρ_{ss}, or ρ_{rs}, or $\rho_g = (\rho_{ss} + \rho_{rs})$, or ρ_{rs}/ρ_{ss}, or $\rho_{ss}f_{yss}/f'_c$, or $\rho_{rs}f_{yrs}/f'_c$, or $(\rho_{ss}f_{yss} + \rho_{rs}f_{yrs})/f'_c$ (subgroup X_3), where ρ_g is the total steel ratio and f_{yrs} is the specified yield strength of the reinforcing steel; (4) stiffness index I_{rs}/I_{ss}, or I_{ss}/I_g, or I_{rs}/I_g, or $(I_{ss} + I_{rs})/I_g$ (subgroup X_4) where I_g = the moment of inertia of the gross concrete cross-section neglecting structural and reinforcing steel; and (5) concrete cover index d_{ss}/h (subgroup X_5) where d_{ss}, the depth of the structural steel section, is divided by the overall depth of the composite cross-section perpendicular to the axis of bending being considered.

$$r = \sqrt{\frac{(E_cI_g/5) + E_sI_{ss}}{(E_cA_g/5) + E_sA_{ss}}} \qquad (5.1)$$

In Equation 5.1, A_g equals the area of the gross concrete cross-section neglecting structural and reinforcing steel and A_{ss} equals the gross cross-sectional area of the structural steel section. The Group A variables are listed in Table 5.3.

Group B, on the other hand, consists of two variables, $E_s I_{ss}$ and $E_s I_{rs}$, that were considered to have a significant affect on the overall effective stiffness of a composite column.

Mirza and MacGregor (1989) found that for reinforced concrete slender columns the variables in the first and second subgroup of group A are important in the study of the strength and behaviour of slender columns. Mirza (1990) verified this in his analysis of the flexural stiffness of rectangular reinforced concrete columns. The third subgroup variables of Group A took into consideration the influence of the quantity of steel in proportion to the area of concrete cross-section. The fourth subgroup was intended to examine the effects of relative stiffnesses of steel and concrete. The fifth and final subgroup of Group A was included to investigate the effect of concrete cover to the structural steel shape on column stiffness.

The variables within an individual subgroup of Group A were considered as dependent variables, while variables between the subgroups were taken as independent variables. For example, e/h was considered dependent on P_u/P_o but was taken independent of variables related to slenderness ratio, steel index, stiffness index, and concrete cover index. The variables of Group B were always considered independent variables. A maximum of one variable from any of the chosen

Table 5.3 - Variable combinations used for regression analysis - Major Axis Bending

Variable Combination Number	Group "A" Variables: X_1 End Eccentricity Ratio		X_2 Slenderness Ratio		X_3 Steel Index							X_4 Stiffness Index				X_5 Concrete Cover Index	Standard Error	Multiple Correlation Coefficient
	e/h	P_u/P_o	ℓ/h	ℓ/r	ρ_{ss}	ρ_{rs}	ρ_g	$\frac{\rho_{rs}}{\rho_{ss}}$	$\frac{\rho_{ss} f_{yss}}{f'_c}$	$\frac{\rho_{rs} f_{yrs}}{f'_c}$	(11)+(12)	$\frac{I_{rs}}{I_{ss}}$	$\frac{I_{ss}}{I_g}$	$\frac{I_{rs}}{I_g}$	$\frac{I_{rs}+I_{ss}}{I_g}$	d_{ss}/h	S_e*	R_c
(1)	(2)	(3)	(4)	(5)	(6)	(7)	(8)	(10)	(11)	(12)	(13)	(14)	(15)	(16)	(17)	(18)	(19)	(20)
1	X		X					X						X		X	0.049	0.966
2	X		X					X						X			0.049	0.965
3	X		X					X				X					0.050	0.964
4	X		X					X					X				0.049	0.966
5	X		X					X							X		0.049	0.966
6	X		X					X									0.050	0.963
7	X		X		X												0.050	0.964
8	X		X			X											0.049	0.965
9	X		X				X										0.050	0.964
10	X		X						X								0.050	0.964
11	X		X							X							0.049	0.965
12	X		X								X						0.050	0.964
13	X		X														0.050	0.964
14	X			X													0.051	0.962
15		X	X														0.056	0.955
16		X		X													0.058	0.952
17	X																0.056	0.955
18		X															0.072	0.925
19			X														0.080	0.904
20				X													0.081	0.903
21						X											0.083	0.897
22								X									0.084	0.896
23													X				0.083	0.898
24														X			0.083	0.897
25																X	0.083	0.897

* S_e was computed for the constant α_k.

subgroups of Group A was, therefore, used for a particular regression analysis of the theoretical stiffness data. When one variable from each subgroup of Group A and both variables from Group B are included into the regression analysis, Equation 2.2 becomes:

$$EI = (\alpha_k + \alpha_1 X_1 + \alpha_2 X_2 + \alpha_3 X_3 + \alpha_4 X_4 + \alpha_5 X_5) E_c (I_g - I_{ss}) + \alpha_{ss} E_s I_{ss} + \alpha_{rs} E_s I_{rs} \tag{5.2a}$$

in which α_k is a constant (equivalent to the intercept of a simple linear equation). The remaining α values are dimensionless reduction factors corresponding to independent variables X_1, X_2, X_3, X_4, X_5, $E_s I_{ss}$ and $E_s I_{rs}$. X_1 through X_5 represent one variable chosen from each of the subgroups (i.e. end eccentricity ratio, slenderness ratio, steel index, stiffness index, and concrete cover index) in Group A.

The combination of Group A variables used for different regression analyses are given in Table 5.3. Group B variables were included in all regression analyses shown in Table 5.3.

The prediction accuracy for a particular regression equation was based on the standard error S_e, a measure of sampling variability, and the multiple correlation coefficient R_c, an index of relative strength of the relationship. The smaller the value of S_e the smaller the sampling variability of the regression equation. An R_c value equal to zero signifies no correlation, and $R_c = \pm 1.0$ indicates 100 percent correlation. R_c values greater than +1.0 and less than -1.0 are not possible. The calculated values of S_e and R_c for each regression analysis are also given in Table 5.3. To reduce the relative magnitude of the standard error S_e, both sides of Equation 5.2a were divided by $E_c(I_g - I_{ss})$ to "normalize" the equation. This also allowed the S_e obtained in this study to be compared to the S_e obtained by Mirza (1990) for reinforced concrete columns. The normalized version of Equation 5.2a is:

$$\frac{EI}{E_c(I_g - I_{ss})} = \alpha_k + \alpha_1 X_1 + \alpha_2 X_2 + \alpha_3 X_3 + \alpha_4 X_4 + \alpha_5 X_5 + \alpha_{ss}\frac{E_s I_{ss}}{E_c(I_g - I_{ss})} + \alpha_{rs}\frac{E_s I_{rs}}{E_c(I_g - I_{ss})} \tag{5.2b}$$

Note that S_e in this study was computed for α_k.

5.3.2 Regression Analysis

Table 5.3 shows the S_e and R_c values calculated for 25 regression equations. The insignificant changes in S_e and R_c for the first thirteen variable combinations indicate that variables other than those used in combination 13 (e/h and ℓ/h) do not significantly influence the EI of slender columns. A correlation analysis confirmed that this was due to the fact that the variables in subgroups X_3 and X_4 were included explicitly or implicitly in the format of the regression equations, Equations 5.2a and 5.2b.

Variable combinations 13 to 16 involving e/h, P_u/P_o, ℓ/h, and ℓ/r proved that e/h and ℓ/h are the most significant pair of variables from Group A influencing EI. The ratios ℓ/h and ℓ/r are obviously correlated, however, ℓ/h is much simpler to compute. A correlation analysis of the variables used in combinations 13 to 16, including the Group B variables, confirmed Mirza's observation indicating that: (a) no correlation exists between e/h and ℓ/h (or ℓ/r) ratios; (b) there is some correlation between P_u/P_o and ℓ/h (or ℓ/r) ratios; and (c) a strong correlation exists between P_u/P_o and e/h ratios. This means that e/h and ℓ/h (or ℓ/r) are independent variables and P_u/P_o is dependent on e/h.

Finally, combinations 17 through 25 show that when only one of the variables in Group A was combined with the two variables in Group B, e/h is the most significant variable from Group A.

In summary, the lowest S_e and highest R_c values among the regression equations concerning two variables and one variable from Group A, combined with the two variables from Group B, were obtained for variable combinations 13 and 17, respectively. The resulting regression equations are:

$$EI = (0.313 + 0.00334\, \ell/h - 0.203\, e/h)\, E_c(I_g - I_{ss}) + 0.792 E_s I_{ss} + 0.788 E_s I_{rs} \qquad (5.3)$$

$$EI = (0.379 - 0.203\, e/h)\, E_c(I_g - I_{ss}) + 0.792 E_s I_{ss} + 0.788 E_s I_{rs} \qquad (5.4)$$

Equations 5.3 and 5.4 are similar in format to regression Equations 5.5 and 5.6 developed by Mirza (1990) for reinforced concrete columns.

$$EI = (0.294 + 0.00323\, \ell/h - 0.299\, e/h)\, E_c I_g + E_s I_{rs} \qquad (5.5)$$

$$EI = (0.358 - 0.299\, e/h)\, E_c I_g + E_s I_{rs} \qquad (5.6)$$

Both sets of equations show that with an increase in e/h ratio there is a corresponding decrease in EI for a column. This is because an increase in e/h means a corresponding increase in bending moment and tension stresses at the outer fibre, resulting in more cracking of the column. The coefficient of 0.203 associated with e/h in Equations 5.3 and 5.4 for composite columns is about 2/3 of that in Equations 5.5 and 5.6 for reinforced concrete columns. This is due to the structural steel shape in composite columns interrupting the continuity of the cracks that remain unarrested in reinforced concrete columns. Equations 5.3 and 5.5 indicate that for an increase in ℓ/h ratio there is an increase in EI. Mirza (1990) suggests that this is because in a longer column the cracks are likely to be more widely spaced with more concrete in between the cracks contributing to the EI of the column. The coefficients of 0.792 and 0.788 related to E_sI_{ss} and E_sI_{rs}, respectively, in Equations 5.3 and 5.4 indicate "softening" of structural and reinforcing steel. This is the result of elastic-plastic nature of the stresses developed in the structural steel and the reinforcing steel at ultimate load.

For composite columns S_e = 0.050 and R_c = 0.964 were obtained for Equation 5.3. This compares to an S_e = 0.058 and R_c = 0.86 reported by Mirza (1990) for Equation 5.5. For the second composite column equation (Equation 5.4) S_e equals 0.056 and R_c equals 0.955. The corresponding values reported by Mirza for Equation 5.6 were 0.061 and 0.84.

A scatter diagram (Figure 5.4) shows the values of *EI* computed from Equations 5.3 and 5.4 plotted against the corresponding theoretical *EI*. Regression *EI* from Equation 5.3 is shown in Figure 5.4 (a), and Figure 5.4 (b) is for Equation 5.4. Both equations exhibit reasonable correlation with the theoretical *EI* values when compared to the line of unity labelled as 45° line. Equation 5.3 produced somewhat, but not very significantly, better results.

The histograms and related statistical data for the ratio of theoretical *EI* to regression *EI* (EI_{th}/EI_{reg}) developed from all the columns studied (n = 11,880) are virtually identical for Equations 5.3 and 5.4, as shown in Figure 5.5. EI_{reg} in Figure 5.5(a) was taken from Equation 5.3 and that in Figure 5.5(b) from Equation 5.4. Both equations give mean values of 1.00. The coefficient of variation (*CV*) for Equation 5.3 is 0.075 and 0.080 for Equation 5.4. This represents a very significant improvement when compared to mean values of 1.39 and 1.45 shown in Figure 5.2 for the ACI and AISC stiffness equations, respectively, and *CV* of 0.228 obtained for both ACI and AISC equations.

The histograms and statistical data for the columns where the longitudinal reinforcement ratio (ρ_{rs}) is one percent (n=3960), shown in Figure 5.6, again indicates that the two equations give almost the same results. Both equations give mean values of 0.99. The *CV* for Equation 5.3 is 0.088 and 0.091 for Equation 5.4. This still represents a very

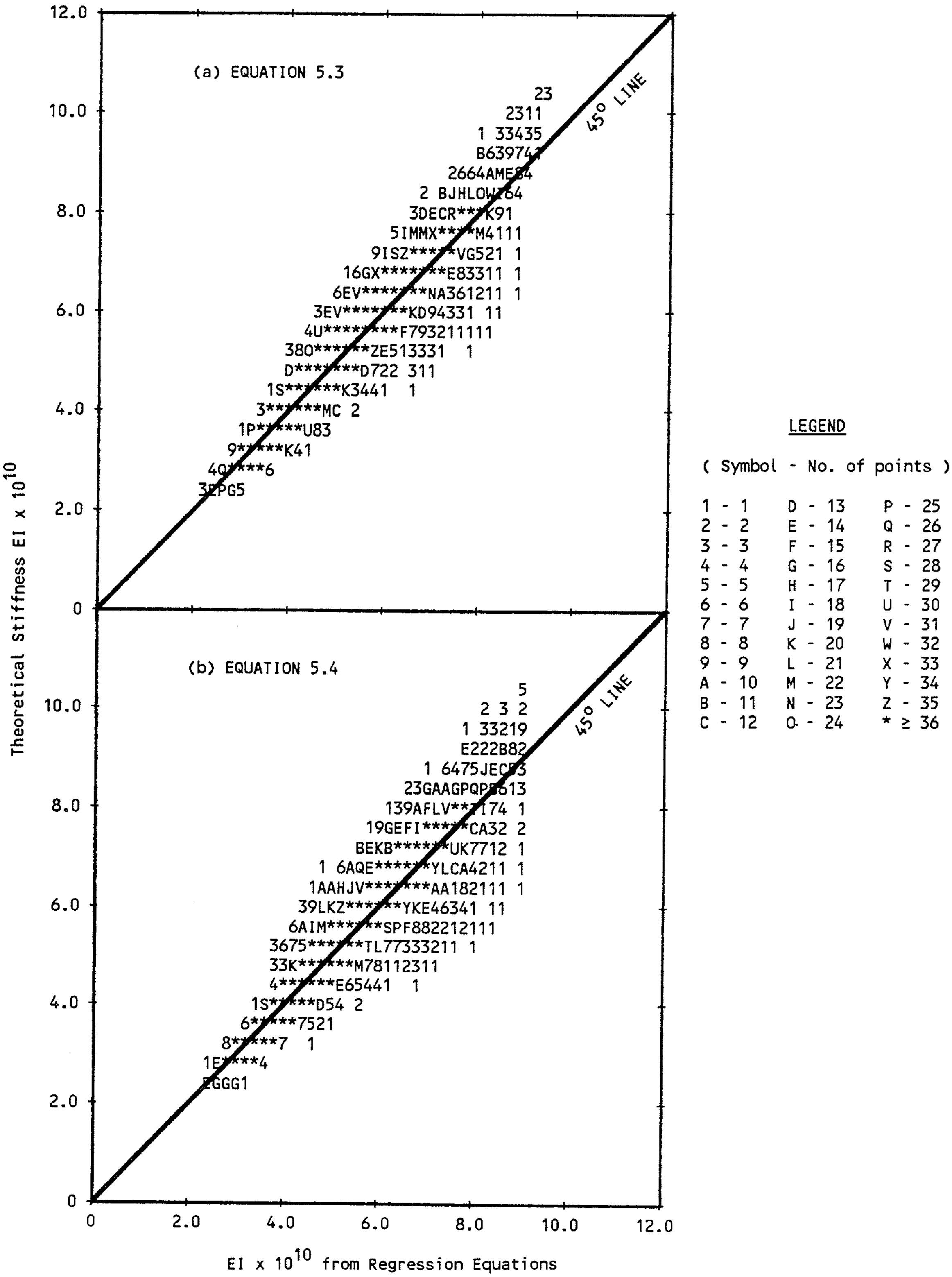

Figure 5.4 - Comparison of selected regression equations with theoretical data for all columns bending about major axis.

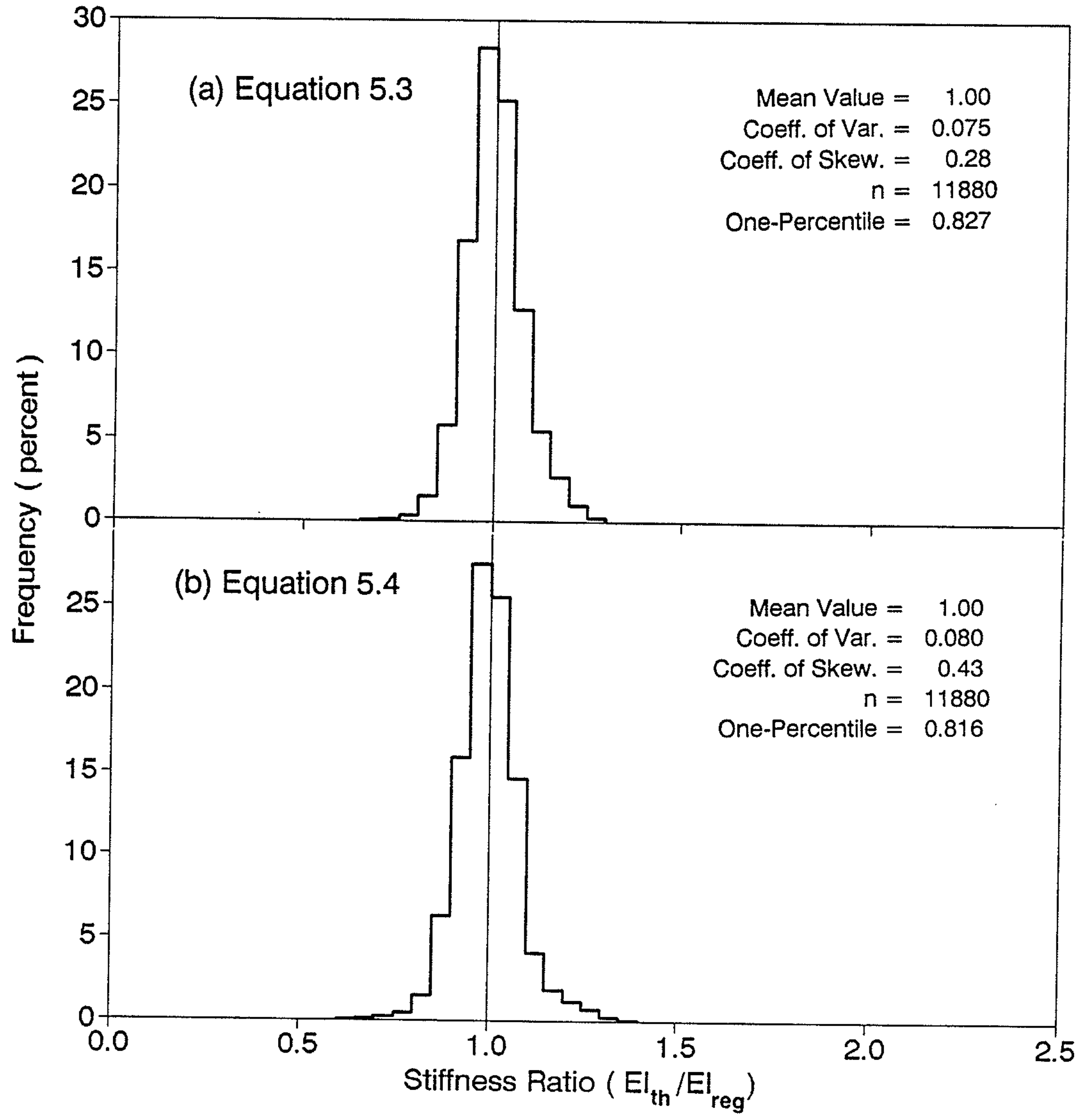

Figure 5.5 - Frequency histograms comparing selected regression equations with theoretical data for all columns bending about major axis.

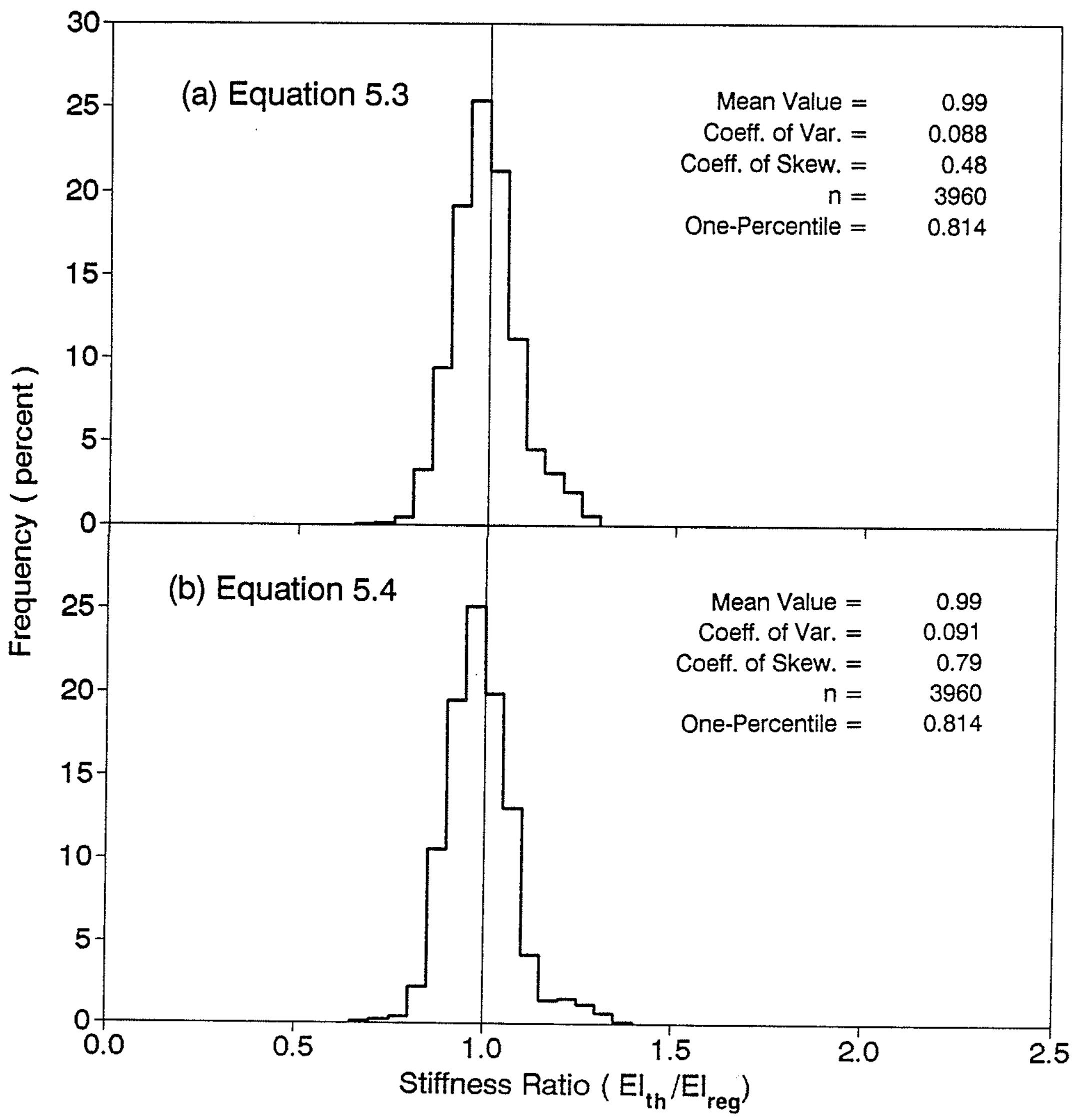

Figure 5.6 - Frequency histograms comparing selected regression equations with theoretical data for columns bending about major axis where ρ_{rs} = 1.09 percent.

significant improvement over the mean values of 1.21 and 1.26, and the coefficients of variation of 0.202 and 0.229 obtained from the ACI and AISC stiffness equations shown in Figure 5.3.

5.3.3 Proposed Design Equations

Equations 5.7 and 5.8, proposed for design use, were simplified from Equations 5.3 and 5.4.

$$EI = [(0.27 + 0.003\,\ell/h - 0.2\,e/h)\,E_c(I_g - I_{ss}) + 0.8E_s(I_{ss} + I_{rs})] \geq E_sI_{ss} \tag{5.7}$$

$$EI = [(0.3 - 0.2\,e/h)\,E_c(I_g - I_{ss}) + 0.8\,E_s(I_{ss} + I_{rs})] \geq E_sI_{ss} \tag{5.8}$$

These compare to Equations 5.9 and 5.10 suggested by Mirza (1990) for reinforced concrete columns.

$$EI = [(0.27 + 0.003\,\ell/h - 0.3\,e/h)\,E_cI_g + E_sI_{rs}] \geq E_sI_{rs} \tag{5.9}$$

$$EI = [(0.3 - 0.3\,e/h)\,E_cI_g + E_sI_{rs}] \geq E_sI_{rs} \tag{5.10}$$

At ℓ/h of 10, Equations 5.7 and 5.8 yield the same results. For values of $\ell/h > 10$, Equation 5.8 is more conservative than Equation 5.7. However, Equation 5.8 is less conservative than Equation 5.7 for $\ell/h < 10$. For very large e/h ratios ($e/h >$ 1.5 in Equation 5.8), a lower limit of E_sI_{ss} is used for both equations to insure that the effective stiffness of the composite column is at least equal to that of the encased structural steel shape.

Histograms and statistical data were prepared using the proposed design equations for all the columns studied (n=11880). The histograms for the ratios of theoretical *EI* to design *EI* (EI_{th}/EI_{des}) are plotted in Figure 5.7. EI_{des} in Figure 5.7(a) was taken from Equation 5.7 and that in Figure 5.7(b) from Equation 5.8. As expected, Figure 5.7 indicates that the stiffness ratios (EI_{th}/EI_{des}) for Equation 5.8 (Figure 5.7 (b)) are more conservative than those for Equation 5.7 (Figure 5.7(a)).

The histograms and statistical data prepared for the columns having one percent reinforcing steel (n=3960), using the proposed design equations, are shown in Figure 5.8. The results are similar to those obtained for the data plotted in Figure 5.7.

5.4 ANALYSIS OF STIFFNESS DATA

5.4.1 Overview of Stiffness Ratio Statistics

An overview of the stiffness ratio (EI_{th}/EI_{des}) statistics computed for different design equations are given in Table 5.4 for all data and in Table 5.5 for beam-columns having a reinforcing steel ratio of one percent. To calculate the stiffness ratio of a column, EI_{th} was taken as the computed theoretical stiffness and EI_{des} was calculated from Equations 5.7, 5.8, 4.1 and 4.30. Equations 5.7 and 5.8 are the proposed design equations, Equation 4.1 is the ACI design equation, and Equation 4.30 is the stiffness expression developed from the AISC strength interaction curves.

Tables 5.4 and 5.5 give the coefficient of variation,

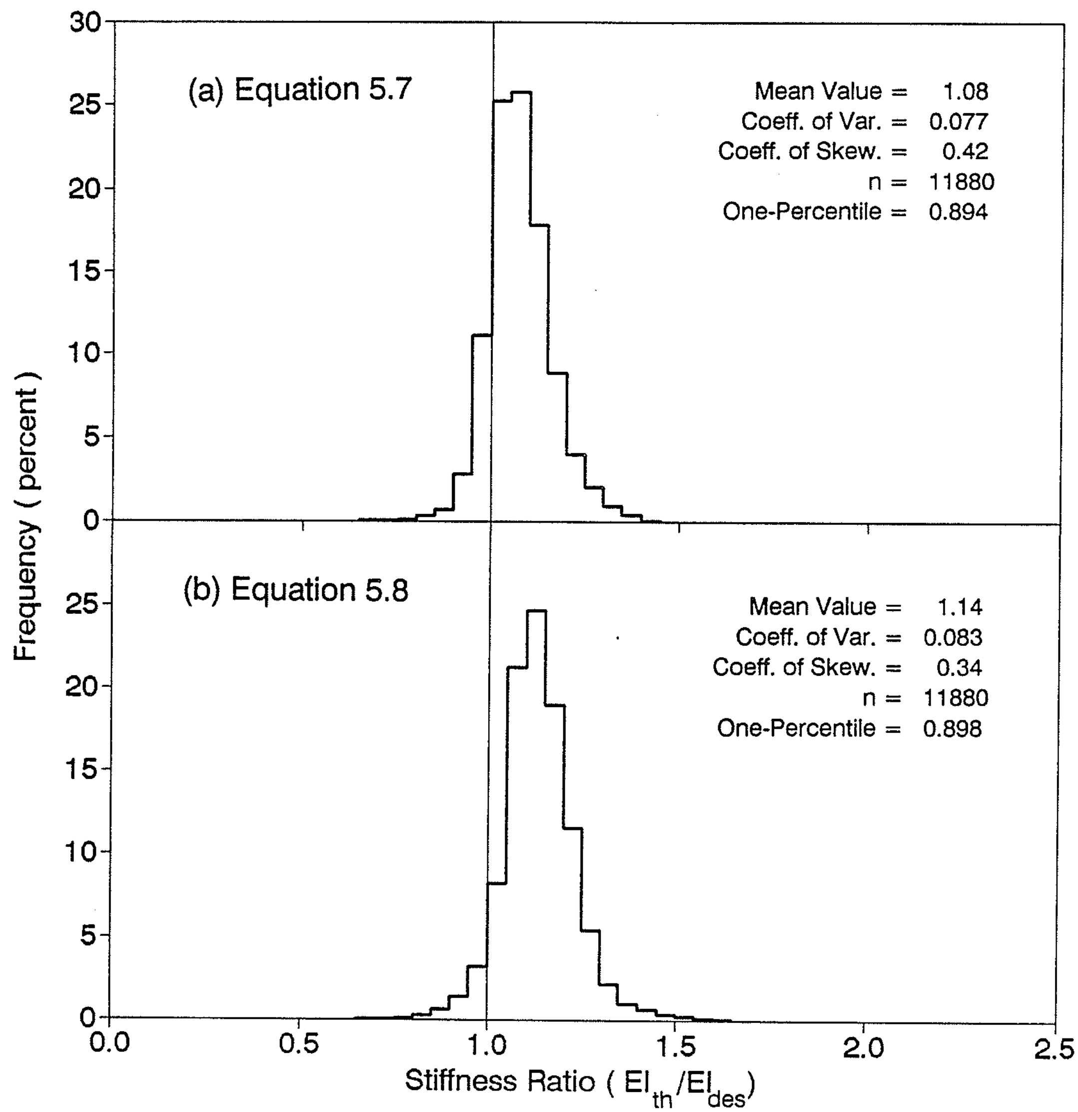

Figure 5.7 - Frequency histograms comparing proposed design equations with theoretical data for all columns bending about major axis.

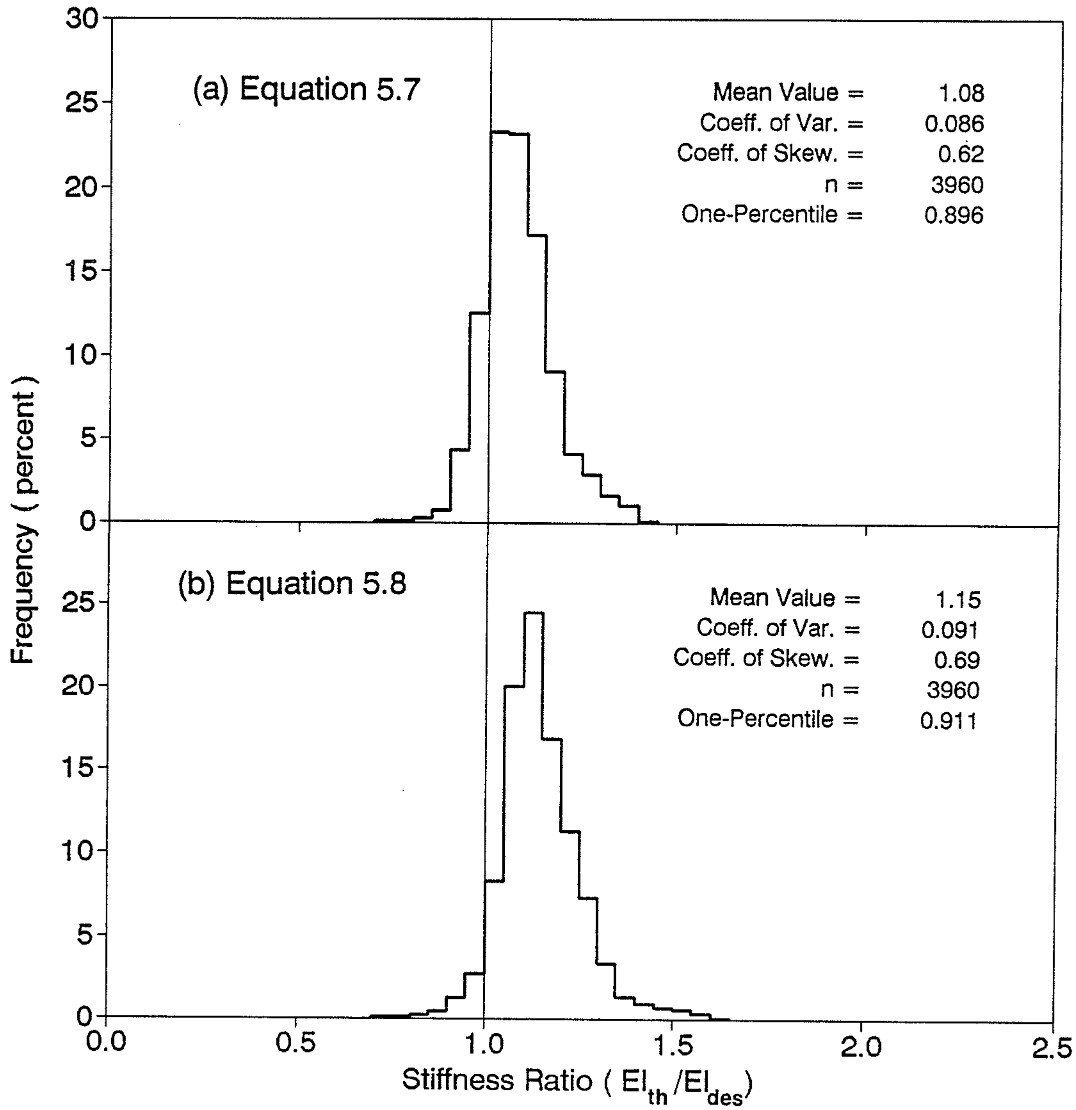

Figure 5.8 - Frequency histograms comparing proposed design equations with theoretical data for columns bending about major axis where ρ_{rs} = 1.09 percent.

Table 5.4 - Stiffness Ratio Statistics for Different Design Equations for all Beam-Columns Subjected to Major Axis Bending

Group Number (1)	Slenderness Ratio ℓ/h (2)	Eccentricity Ratio e/h (3)	Proposed Equations Eq. 5.7 (4)	Proposed Equations Eq. 5.8 (5)	ACI Eq. 4.1 (6)	AISC Eq. 4.30 (7)	Number of Columns (8)
(a) Coefficient of Variation							
A1	10	0.05 - 1.0	0.095	0.095	0.224	0.277	2376
A2	15		0.068	0.072	0.227	0.251	2376
A3	20		0.063	0.067	0.228	0.223	2376
A4	25		0.071	0.072	0.226	0.198	2376
A5	30		0.079	0.079	0.225	0.181	2376
A6	10 - 30		0.077	0.083	0.228	0.228	11880
B1	10	0.1 - 0.7	0.077	0.077	0.222	0.233	1512
B2	15		0.065	0.067	0.219	0.212	1512
B3	20		0.051	0.052	0.206	0.184	1512
B4	25		0.045	0.042	0.194	0.166	1512
B5	30		0.046	0.039	0.187	0.155	1512
B6	10 - 30		0.062	0.060	0.206	0.193	7560
(b) Mean Stiffness Ratio							
A1	10	0.05 - 1.0	1.073	1.073	1.309	1.445	2376
A2	15		1.088	1.119	1.370	1.440	2376
A3	20		1.088	1.149	1.407	1.433	2376
A4	25		1.073	1.163	1.423	1.441	2376
A5	30		1.056	1.174	1.434	1.477	2376
A6	10 - 30		1.076	1.136	1.389	1.447	11880
B1	10	0.1 - 0.7	1.065	1.065	1.358	1.527	1512
B2	15		1.075	1.104	1.407	1.518	1512
B3	20		1.061	1.118	1.423	1.487	1512
B4	25		1.039	1.121	1.424	1.473	1512
B5	30		1.017	1.124	1.427	1.488	1512
B6	10 - 30		1.051	1.106	1.408	1.499	7560

Table 5.4 - continued

Group Number (1)	Slenderness Ratio ℓ/h (2)	Eccentricity Ratio e/h (3)	Proposed Equations Eq. 5.7 (4)	Proposed Equations Eq. 5.8 (5)	ACI Eq. 4.1 (6)	AISC Eq. 4.30 (7)	Number of Columns (8)
			(c) Five-Percentile				
A1	10	0.05 - 1.0	0.900	0.900	0.930	0.865	2376
A2	15		0.975	0.996	0.981	0.890	2376
A3	20		0.995	1.047	1.016	0.931	2376
A4	25		0.976	1.063	1.040	1.000	2376
A5	30		0.948	1.067	1.057	1.080	2376
A6	10 - 30		0.959	0.993	0.998	0.941	11880
B1	10	0.1 - 0.7	0.936	0.936	0.956	1.002	1512
B2	15		0.977	0.999	1.010	1.029	1512
B3	20		0.987	1.040	1.046	1.056	1512
B4	25		0.967	1.057	1.070	1.095	1512
B5	30		0.935	1.062	1.086	1.143	1512
B6	10 - 30		0.958	0.996	1.027	1.069	7560
			(d) One-Percentile				
A1	10	0.05 - 1.0	0.787	0.787	0.848	0.764	2376
A2	15		0.923	0.939	0.905	0.795	2376
A3	20		0.967	1.013	0.950	0.824	2376
A4	25		0.943	1.036	0.975	0.875	2376
A5	30		0.911	1.047	0.993	0.972	2376
A6	10 - 30		0.894	0.898	0.910	0.812	11880
B1	10	0.1 - 0.7	0.883	0.883	0.877	0.859	1512
B2	15		0.938	0.951	0.930	0.881	1512
B3	20		0.961	1.003	0.970	0.923	1512
B4	25		0.934	1.031	0.999	0.980	1512
B5	30		0.902	1.042	1.017	1.054	1512
B6	10 - 30		0.915	0.935	0.933	0.920	7560

Table 5.5 - Stiffness Ratio Statistics for Different Design Equations for Beam-Columns Subjected to Major Axis Bending for which ρ_{rs} = 1.09 percent.

Group Number (1)	Slenderness Ratio ℓ/h (2)	Eccentricity Ratio e/h (3)	Proposed Equations Eq. 5.7 (4)	Proposed Equations Eq. 5.8 (5)	ACI Eq. 4.1 (6)	AISC Eq. 4.30 (7)	Number of Columns (8)
			(a) Coefficient of Variation				
A1	10	0.05 - 1.0	0.094	0.094	0.186	0.280	792
A2	15		0.071	0.075	0.194	0.257	792
A3	20		0.075	0.077	0.202	0.229	792
A4	25		0.087	0.086	0.205	0.196	792
A5	30		0.096	0.093	0.208	0.169	792
A6	10 - 30		0.086	0.091	0.202	0.229	3960
B1	10	0.1 - 0.7	0.079	0.079	0.185	0.228	504
B2	15		0.071	0.072	0.180	0.206	504
B3	20		0.061	0.060	0.162	0.170	504
B4	25		0.057	0.050	0.146	0.137	504
B5	30		0.058	0.046	0.136	0.116	504
B6	10 - 30		0.071	0.064	0.163	0.177	2520
			(b) Mean Stiffness Ratio				
A1	10	0.05 - 1.0	1.083	1.083	1.143	1.249	792
A2	15		1.093	1.129	1.195	1.249	792
A3	20		1.089	1.159	1.227	1.244	792
A4	25		1.073	1.176	1.245	1.252	792
A5	30		1.054	1.189	1.258	1.287	792
A6	10 - 30		1.078	1.147	1.214	1.256	3960
B1	10	0.1 - 0.7	1.077	1.077	1.196	1.326	504
B2	15		1.078	1.110	1.232	1.318	504
B3	20		1.057	1.121	1.241	1.293	504
B4	25		1.032	1.125	1.243	1.282	504
B5	30		1.008	1.129	1.247	1.298	504
B6	10 - 30		1.050	1.113	1.232	1.304	2520

Table 5.5 - continued

Group Number (1)	Slenderness Ratio ℓ/h (2)	Eccentricity Ratio e/h (3)	Proposed Equations Eq. 5.7 (4)	Proposed Equations Eq. 5.8 (5)	ACI Eq. 4.1 (6)	AISC Eq. 4.30 (7)	Number of Columns (8)
			(c) Five-Percentile				
A1	10	0.05 - 1.0	0.913	0.913	0.878	0.785	792
A2	15		0.978	1.005	0.931	0.812	792
A3	20		0.984	1.048	0.966	0.849	792
A4	25		0.954	1.061	0.993	0.902	792
A5	30		0.923	1.063	1.012	0.994	792
A6	10 - 30		0.946	1.003	0.950	0.842	3960
B1	10	0.1 - 0.7	0.944	0.944	0.907	0.883	504
B2	15		0.976	1.004	0.957	0.921	504
B3	20		0.973	1.040	0.995	0.952	504
B4	25		0.944	1.050	1.018	1.012	504
B5	30		0.912	1.052	1.034	1.069	504
B6	10 - 30		0.942	1.003	0.971	0.957	2520
			(d) One-Percentile				
A1	10	0.05 - 1.0	0.786	0.786	0.802	0.732	792
A2	15		0.923	0.939	0.873	0.761	792
A3	20		0.959	1.013	0.927	0.802	792
A4	25		0.928	1.034	0.952	0.846	792
A5	30		0.897	1.039	0.973	0.939	792
A6	10 - 30		0.896	0.910	0.869	0.773	3960
B1	10	0.1 - 0.7	0.888	0.888	0.837	0.784	504
B2	15		0.930	0.959	0.893	0.825	504
B3	20		0.947	1.005	0.934	0.873	504
B4	25		0.925	1.029	0.972	0.947	504
B5	30		0.891	1.036	0.993	1.032	504
B6	10 - 30		0.906	0.942	0.892	0.860	2520

mean, five-percentile and one-percentile values for each of the different design equations. For statistical analysis, the beam-columns studied are divided into two groups: Group A includes all columns and Group B includes only the columns with usual e/h values ($0.1 \le e/h \le 0.7$). The statistics provided within each of these groups are based on subgroups that were taken according to ℓ/h ratio but also include the statistics for the overall sample.

After reviewing Tables 5.4 and 5.5 the following observations are made:

(1) The coefficients of variation for the proposed design equations are considerably lower and remain relatively constant compared to those for the ACI or AISC equations.

(2) The mean stiffness ratios for the ACI and AISC equations tend to be significantly more conservative than those for the proposed design equations.

(3) A comparison of Table 5.4 (for all data) and Table 5.5 (for beam-columns having one percent reinforcing steel) shows that the mean, five-percentile and one-percentile stiffness ratios for the ACI and AISC equations are subjected to greater variations due to ρ_{rs} than are those for the proposed design equations.

(4) All of the design equations gave five-percentile and one-percentile values that, in most cases, exceeded 0.86 and 0.8, respectively. The AISC expression, however, in a majority of cases resulted in five-percentile and one-

percentile values less than those obtained for Equation 5.7, Equation 5.8 and the ACI equation (Equation 4.1).

Figure 5.9 shows the cumulative frequency distribution of stiffness ratios (EI_{th}/EI_{des}) for the different design equations plotted on normal probability paper. The curves in Figure 5.9 represent the data for all 11,880 columns studied. The curves for Equation 5.7, Equation 5.8 and the ACI equation (Equation 4.1) follow one another fairly closely from 0.1-percentile to 10-percentile values of stiffness ratio, whereas the AISC expression (Equation 4.30) is somewhat less conservative in this region. However, both the ACI and AISC expressions become progressively more conservative than either of the proposed design equations as the percentile values increase, as indicated by Figure 5.9.

5.4.2 Effect of Variables on Stiffness Ratios

The effects that each of the variables listed in Table 5.3 has on the mean, five-percentile, and one-percentile values of stiffness ratios (EI_{th}/EI_{des}) obtained from the proposed design equations (Equations 5.7 and 5.8), ACI equation (Equation 4.1) and AISC equation (Equation 4.30) were examined in detail.

Figures 5.10, 5.11 and 5.12 examine the effect of e/h on mean, five-percentile, and one-percentile (minimum in case of Figure 5.12) stiffness ratios. Figure 5.10 is plotted for all data (n = 11,880), Figure 5.11 includes beam-columns having

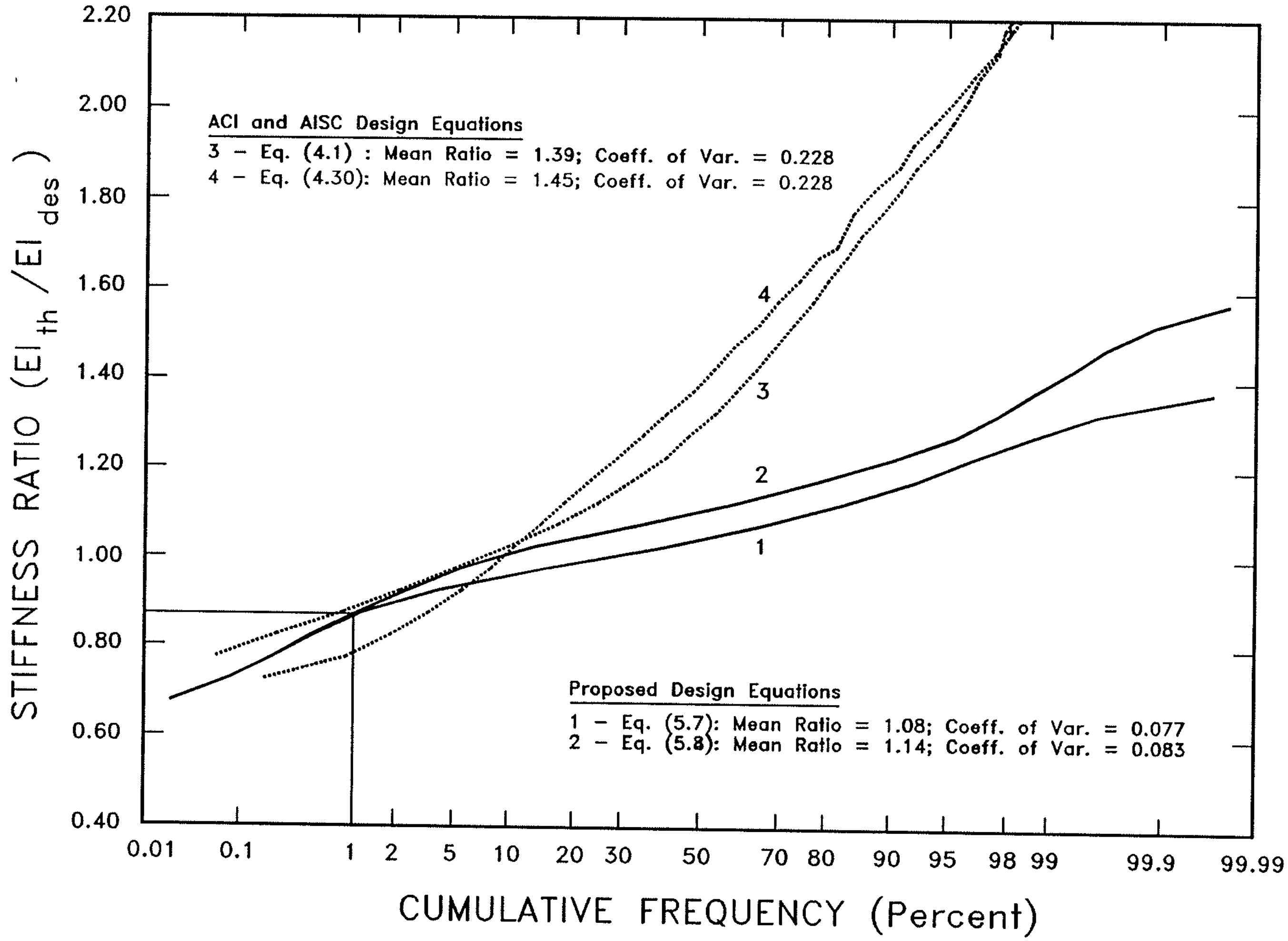

Figure 5.9 - Probability distribution of stiffness ratios computed from data for all columns bending about major axis (n = 11880).

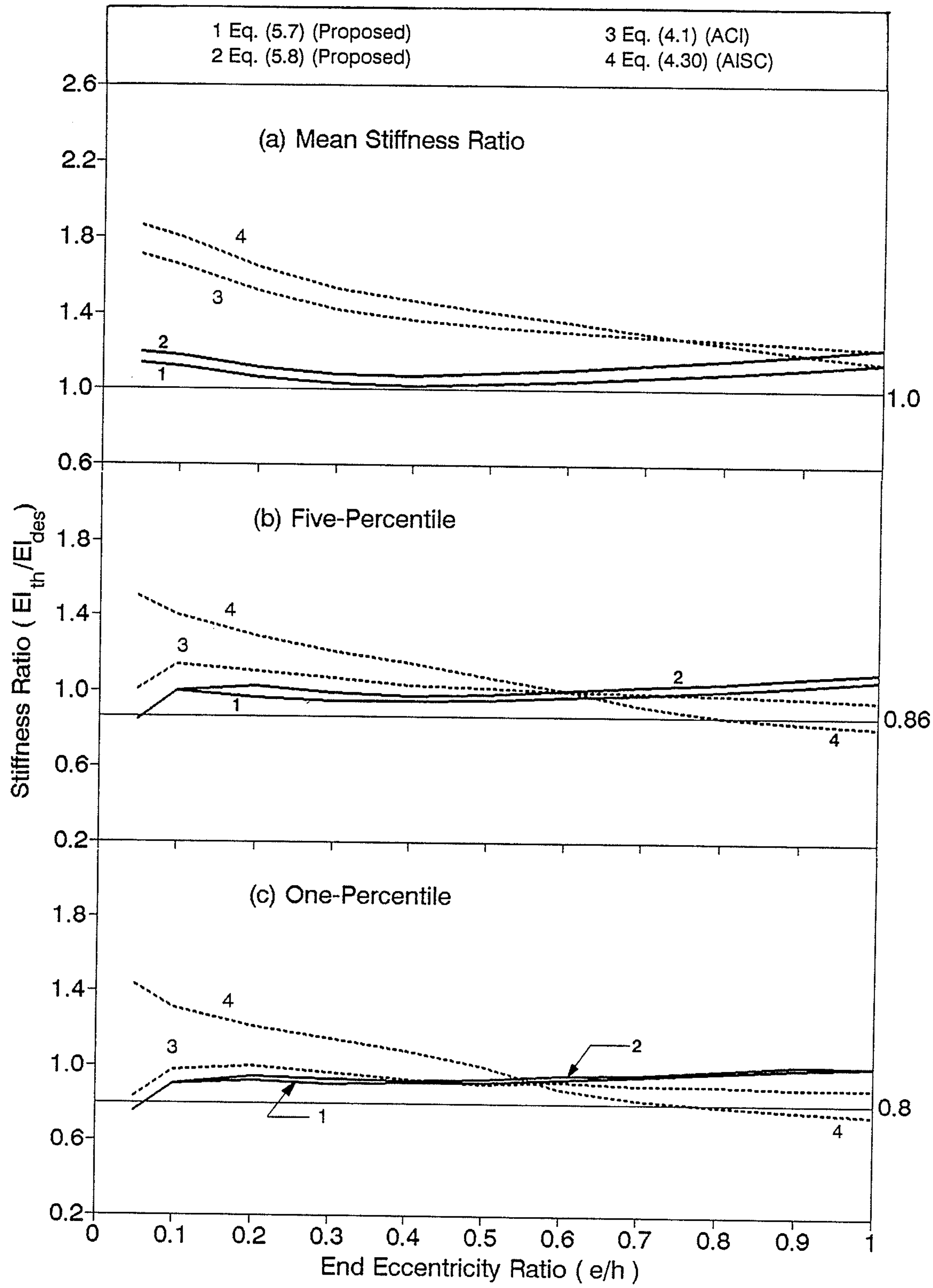

Figure 5.10 - Effect of end eccentricity ratio on stiffness ratio for different design equations for all columns bending about major axis (n = 1080 for each e/h ratio equal to 0.05, 0.1, 0.2, 0.3, 0.4, 0.5, 0.6, 0.7, 0.8, 0.9 and 1.0).

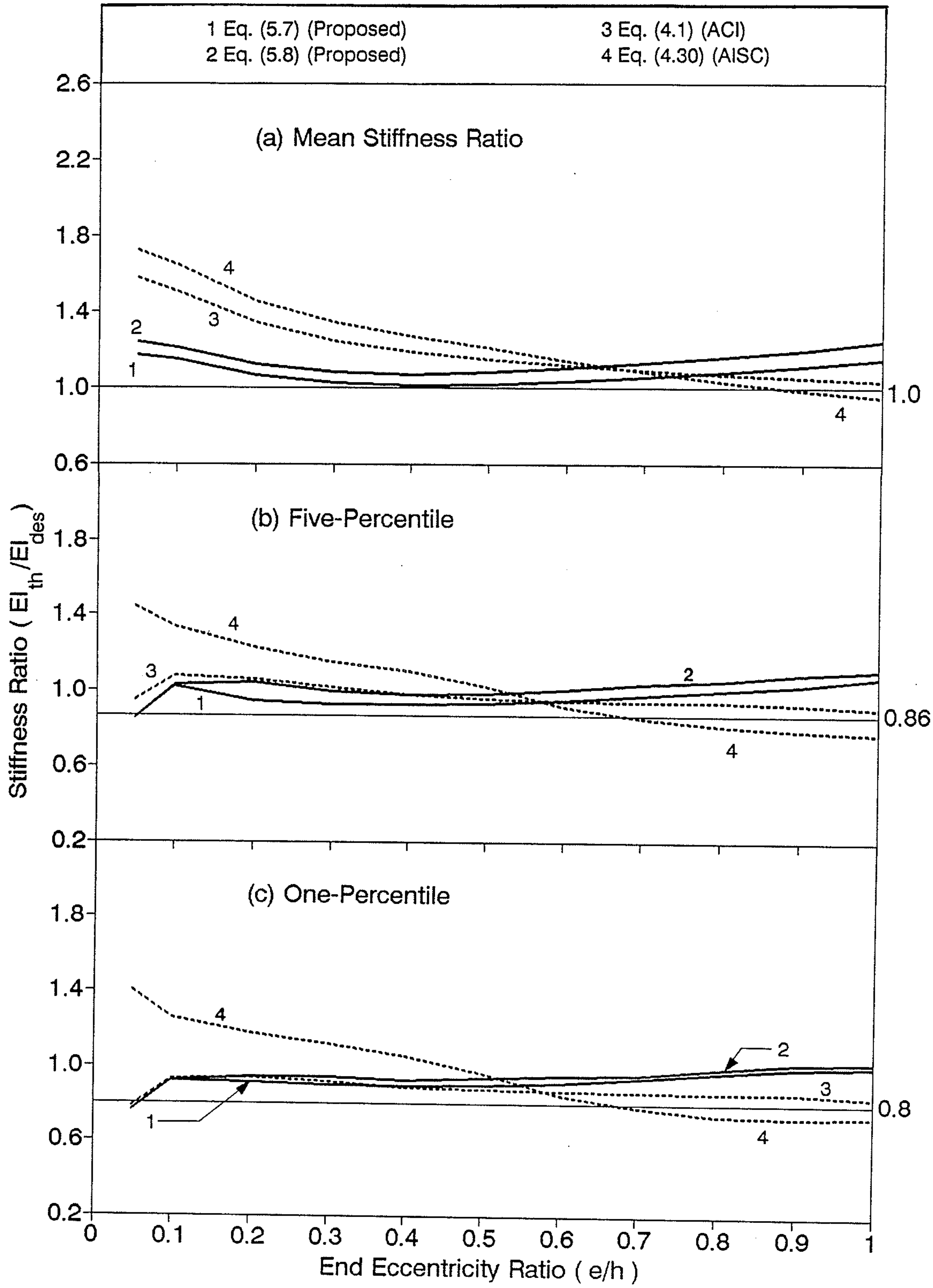

Figure 5.11 - Effect of end eccentricity ratio on stiffness ratio for different design equations for columns bending about major axis where ρ_{rs} = 1.09 percent (n = 360 for each e/h ratio equal to 0.05, 0.1, 0.2, 0.3, 0.4, 0.5, 0.6, 0.7, 0.8, 0.9 and 1.0).

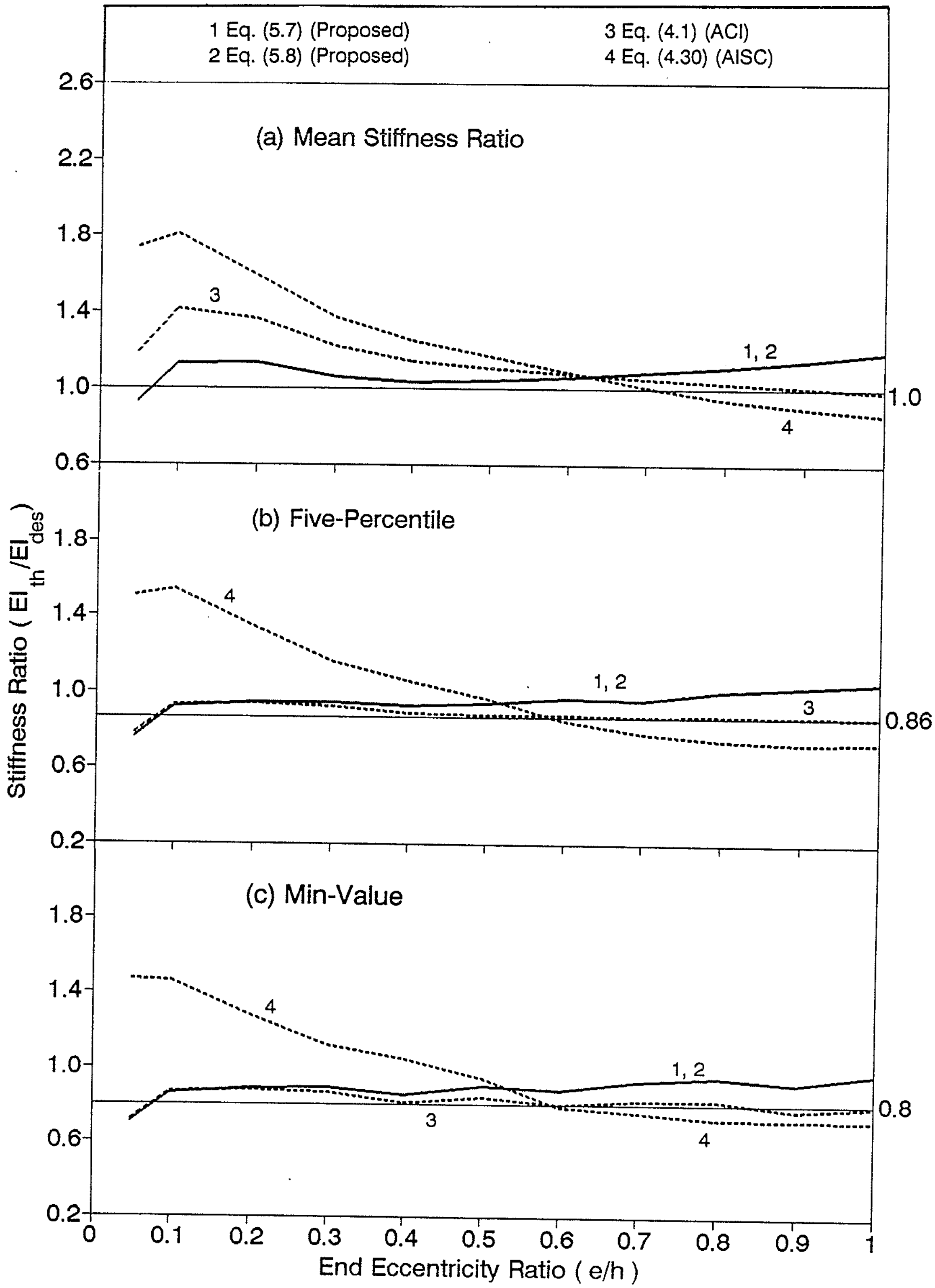

Figure 5.12 - Effect of end eccentricity ratio on stiffness ratio for different design equations for columns bending about major axis where ρ_{rs} = 1.09 percent and ℓ/h = 10 (n = 72 for each e/h ratio equal to 0.05, 0.1, 0.2, 0.3, 0.4, 0.5, 0.6, 0.7, 0.8, 0.9 and 1.0).

ρ_{rs} = 1 percent (n = 3960), and Figure 5.12 considers beam-columns with ρ_{rs} = 1 percent and ℓ/h = 10 (n = 792). Minimum values in place of one-percentile values are used for Figure 5.12 because each e/h ratio represents only 72 beam-columns. An examination of these figures indicates that proposed design equations (Equations 5.7 and 5.8) produce mean, five-percentile and one-percentile values that are relatively constant for the entire range of e/h studied. The ACI and AISC expressions produce stiffness ratios that varied with e/h. This is because neither equation uses e/h as a variable. The mean stiffness ratios for the ACI equation appear to be overly conservative at low e/h ratios, however, the ACI stiffness ratio does closely follow the five-percentile and one-percentile stiffness ratios produced by the proposed stiffness equations. Mirza (1990) pointed out that, for establishing safety in design equations, the five-percentile and one-percentile values are more important than the mean value. The proposed design equations and the ACI equation gave mean, five-percentile and one-percentile (or minimum in case of Figure 5.12) values that exceeded 1.0, 0.86 and 0.80,respectively, for most e/h ratios shown in Figures 5.10, 5.11 and 5.12. The AISC expression (Equation 4.30), on the other hand, is more conservative than the other equations for the five-percentile and one-percentile values at low e/h but these values drop below 0.86 and 0.80 at high e/h. Figure 5.12 shows that for beam-columns having ρ_{rs} = 1 percent and

$\ell/h = 10$, the mean stiffness ratio for the AISC expression is less that 1.0 when $e/h > 0.7$.

Figure 5.13 illustrates the effect of the axial load ratio (P_u/P_o) on the stiffness ratios resulting from different design equations. The axial load ratio was not a controlled variable in this study, i.e. there are as many different axial load ratios as the number of beam-columns studied. This required grouping of stiffness ratios into a number of ranges of P_u/P_o values. The statistics for stiffness ratios in each range of P_u/P_o values were then determined. Grouping the stiffness ratios according to axial load ratio resulted in having a significantly different number of columns in each of the ranges of P_u/P_o. For example, less columns were grouped in the range of 0.7 to 0.9 P_u/P_o (n = 285) than in the range of 0.2 to 0.25 P_u/P_o (n = 1648). The ranges of P_u/P_o ratios were set at 0.05-0.1, 0.1-0.15, 0.15-0.2, 0.2-0.25, 0.25-0.3, 0.3-0.35, 0.35-0.4, 0.4-0.5, 0.5-0.6, 0.6-0.7, 0.7-0.9. The mean P_u/P_o ratio for each range is plotted against the mean, five-percentile and one-percentile stiffness ratios for each corresponding range. Figure 5.13 shows that the mean stiffness ratios for the ACI and AISC equations tend to be again more conservative than for the proposed design equations. This is expected since there is a strong correlation between P_u/P_o and e/h. At P_u/P_o ratio greater than 0.7, the mean, five-percentile and one-percentile stiffness ratios for the proposed design equations are slightly less

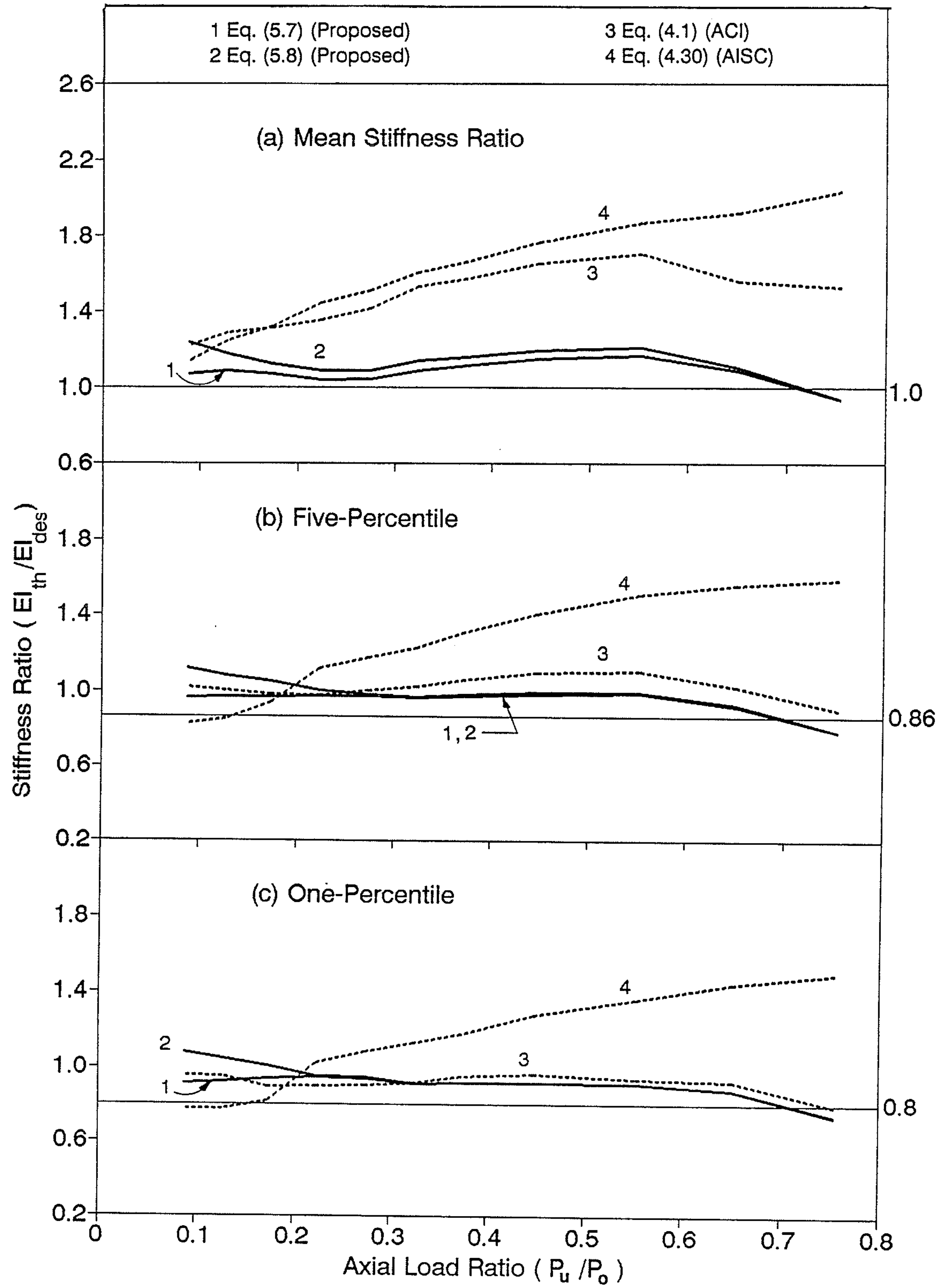

Figure 5.13 - Effect of axial load ratio on stiffness ratio for different design equations for all columns bending about major axis (n varies for each P_u/P_o ratio; total n = 11,880).

than 1.0, 0.86, and 0.80, respectively. Figures 5.14 and 5.15 show that by excluding the values of P_u/P_o for beam-columns where either e/h equals 0.05 or ℓ/h equals 10 eliminates the values of P_u/P_o greater than 0.7. This is expected because high P_u/P_o occurs at very low e/h or ℓ/h ratios.

An examination of Figure 5.16 concerning slenderness in terms of ℓ/h ratio indicates that there is no significant difference in the five-percentile and one-percentile stiffness ratios for the four design equations. Relatively constant but different values of mean, five-percentile and one-percentile stiffness ratios were obtained for all four design equations, even though only Equation 5.7 includes ℓ/h as a variable. This suggests that ℓ/h is not as significant as initially considered. The AISC expression, however, yields the lowest five-percentile and one-percentile values when $\ell/h \leq 25$. The mean value for the ACI and AISC stiffness expressions are again more conservative than the proposed design equations.

Figure 5.17 shows the effect of slenderness using ℓ/r ratio. The ACI expression for radius of gyration (Equation 5.1) was used to determine r. One hundred and twenty different values of ℓ/r for 11,880 beam-columns studied necessitated the grouping of ℓ/r into ranges. The ranges of ℓ/r ratio were set at 30-40, 40-50, 50-60, 60-70, 70-80, 80-90, 90-100, 100-110, 110-140. The mean ℓ/r ratio for each range is plotted against the mean, five-percentile and one-percentile stiffness ratios for each corresponding range,

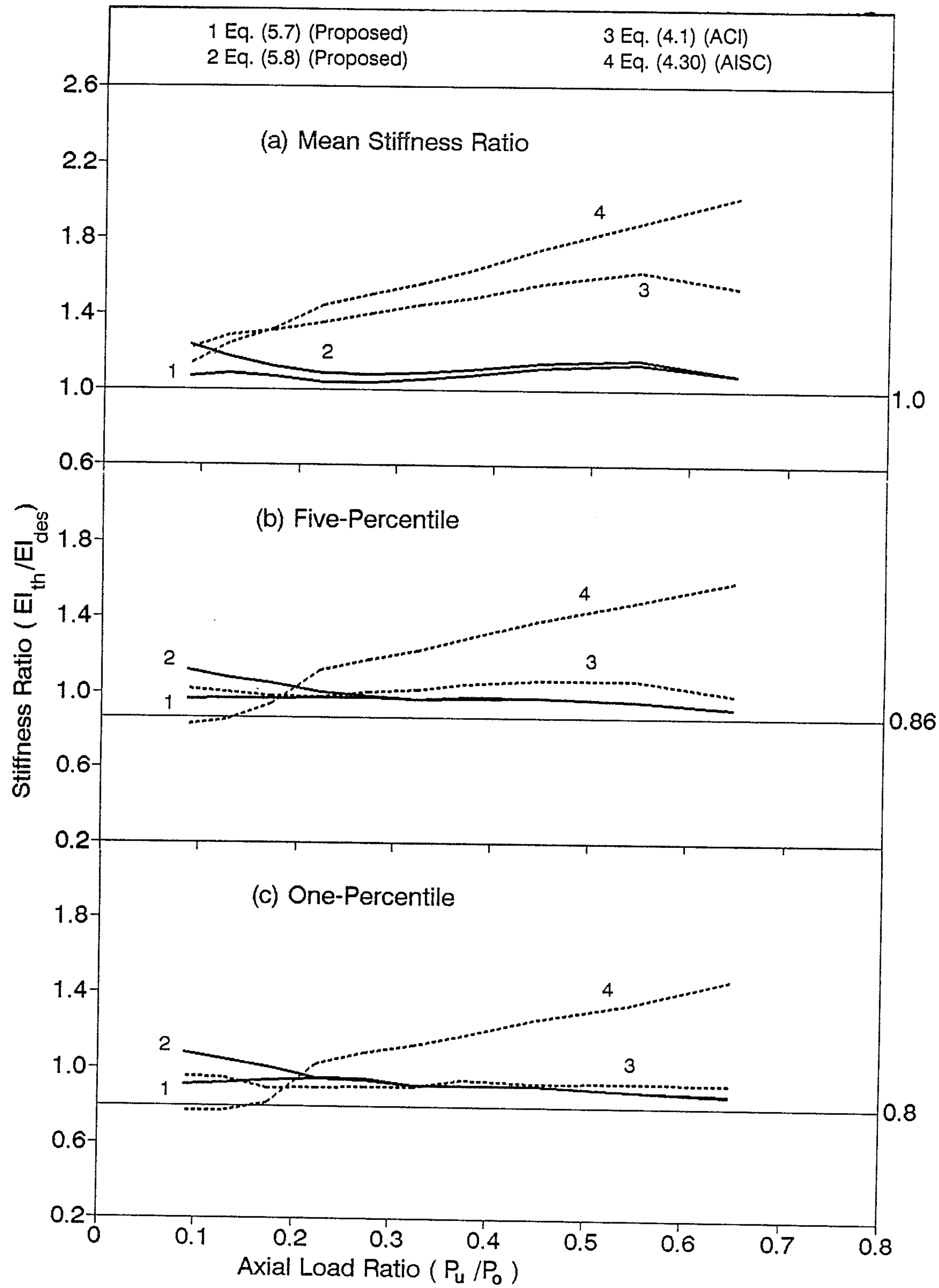

Figure 5.14 - Effect of axial load ratio on stiffness ratio for different design equations in which columns bending about major axis with e/h = 0.05 not included (n varies for each P_u/P_o ratio; total n = 10,800).

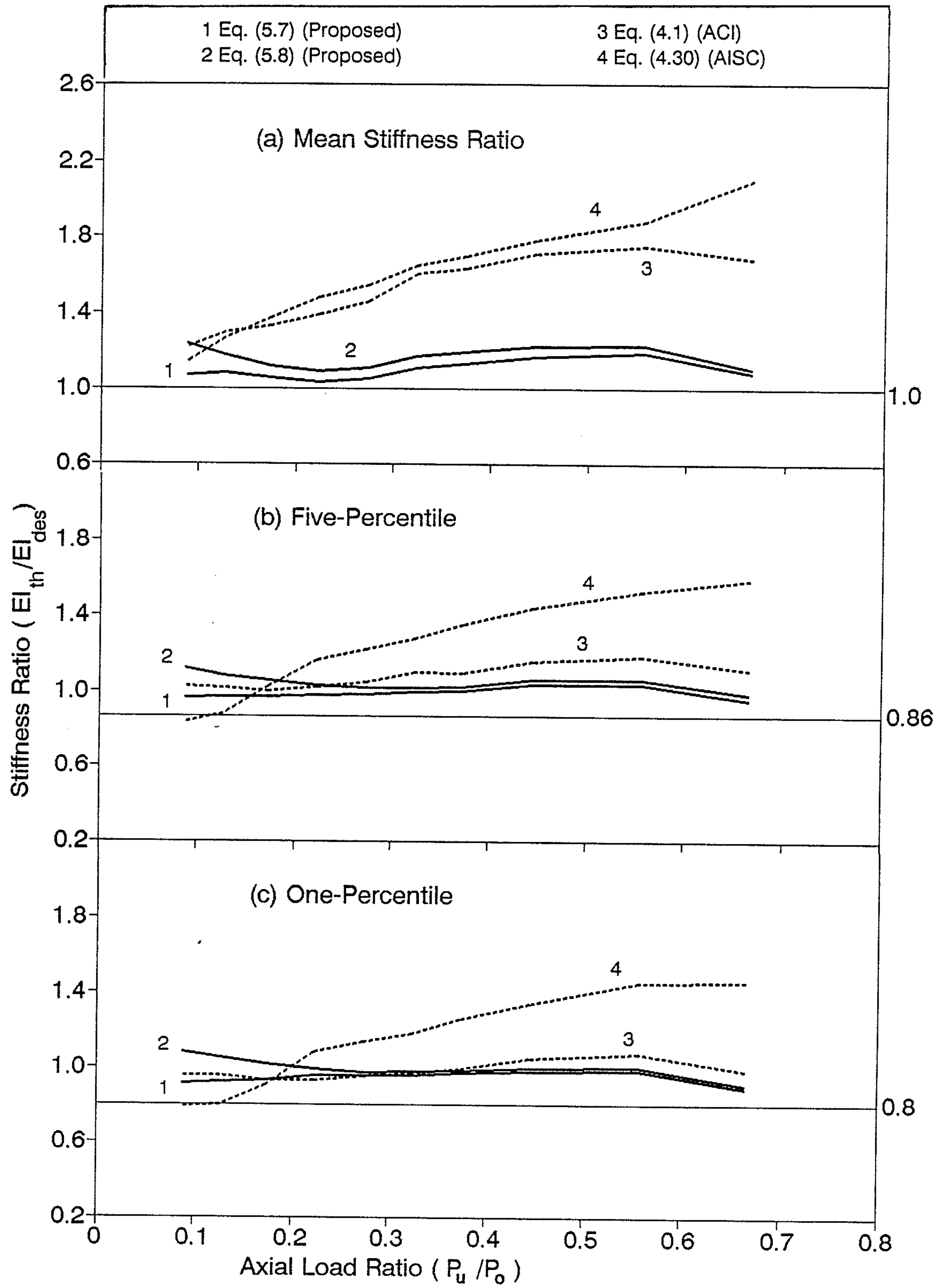

Figure 5.15 - Effect of axial load ratio on stiffness ratio for different design equations in which columns bending about major axis with ℓ/h = 10 not included (n varies for each P_u/P_o ratio; total n = 9,504).

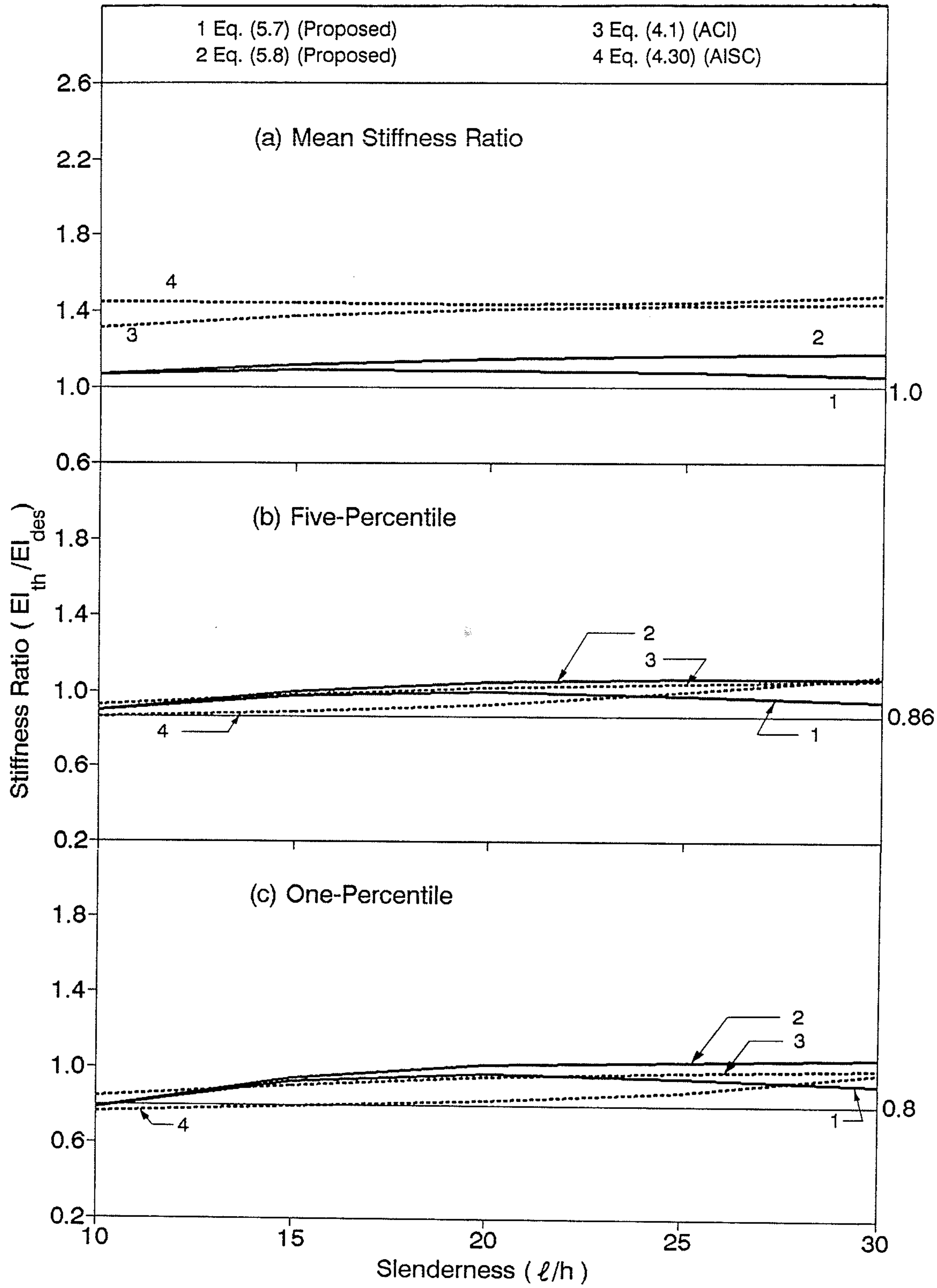

Figure 5.16 - Effect of slenderness ratio (ℓ/h) on stiffness ratio for different design equations for all columns bending about major axis (n = 2376 for each ℓ/h ratio equal to 0.05, 0.1, 0.2, 0.3, 0.4, 0.5, 0.6, 0.7, 0.8, 0.9 and 1.0).

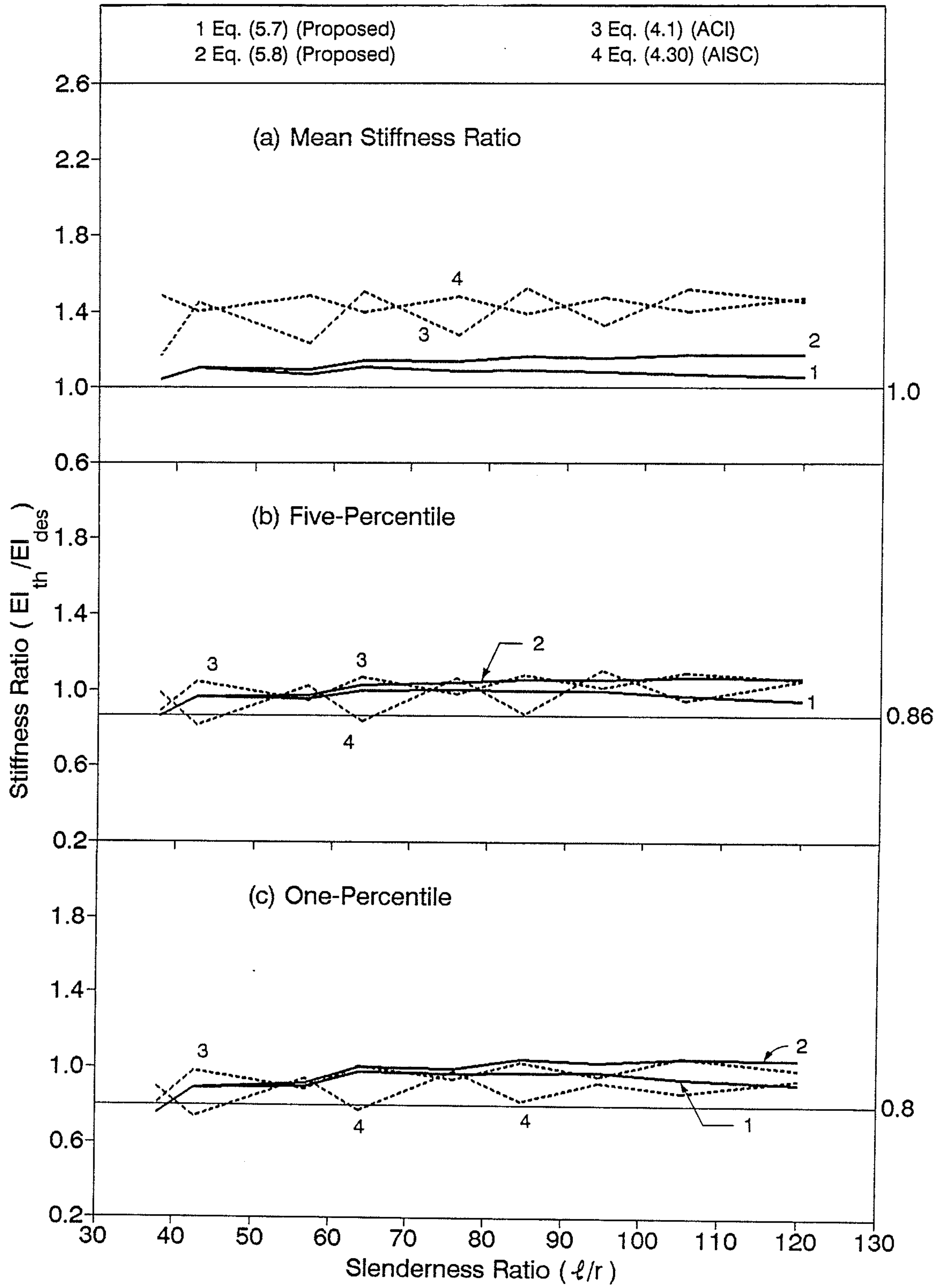

Figure 5.17 - Effect of slenderness ratio (ℓ/r) on stiffness ratio for different design equations for all columns bending about major axis (n varies for each range of ℓ/r ratio; total n = 11,880).

similar to what was done to study the effect of P_u/P_o. The apparent zig-zag nature of the plots in Figure 5.17 for the ACI equation is, probably, caused by grouping of ℓ/r and due to the fact that the contribution of reinforcing steel to beam-column stiffness is not included in Equation 4.1. For the AISC expression, even though the area of the reinforcing steel is included in computing the equivalent cross-section properties, the full effect of the reinforcing steel is not accounted for in determining the nominal axial load capacity of a beam-column. The mean, five-percentile and one-percentile stiffness ratios appear to follow the trends stated previously for ℓ/h ratio.

The effect of longitudinal reinforcing steel in terms of ρ_{rs} is shown in Figure 5.18. The stiffness ratios for the ACI and AISC expressions increase proportionally with the reinforcing steel ratio. This is because the ACI expression (Equation 4.1) does not account for the effect of reinforcing steel. This also suggests that the AISC expression does not properly account for the effect of reinforcing steel.

Figure 5.19 shows the effect of structural steel in terms of ρ_{ss} on the stiffness ratios. Figure 5.20 shows the effect of ρ_{ss} on stiffness ratios of beam-columns having reinforcing steel of only one percent. Both figures indicate that the ACI and AISC expressions are more susceptible to the effect of ρ_{ss} than the proposed equations. This influence is due to the proportion of stiffness the reinforcing steel contributes to

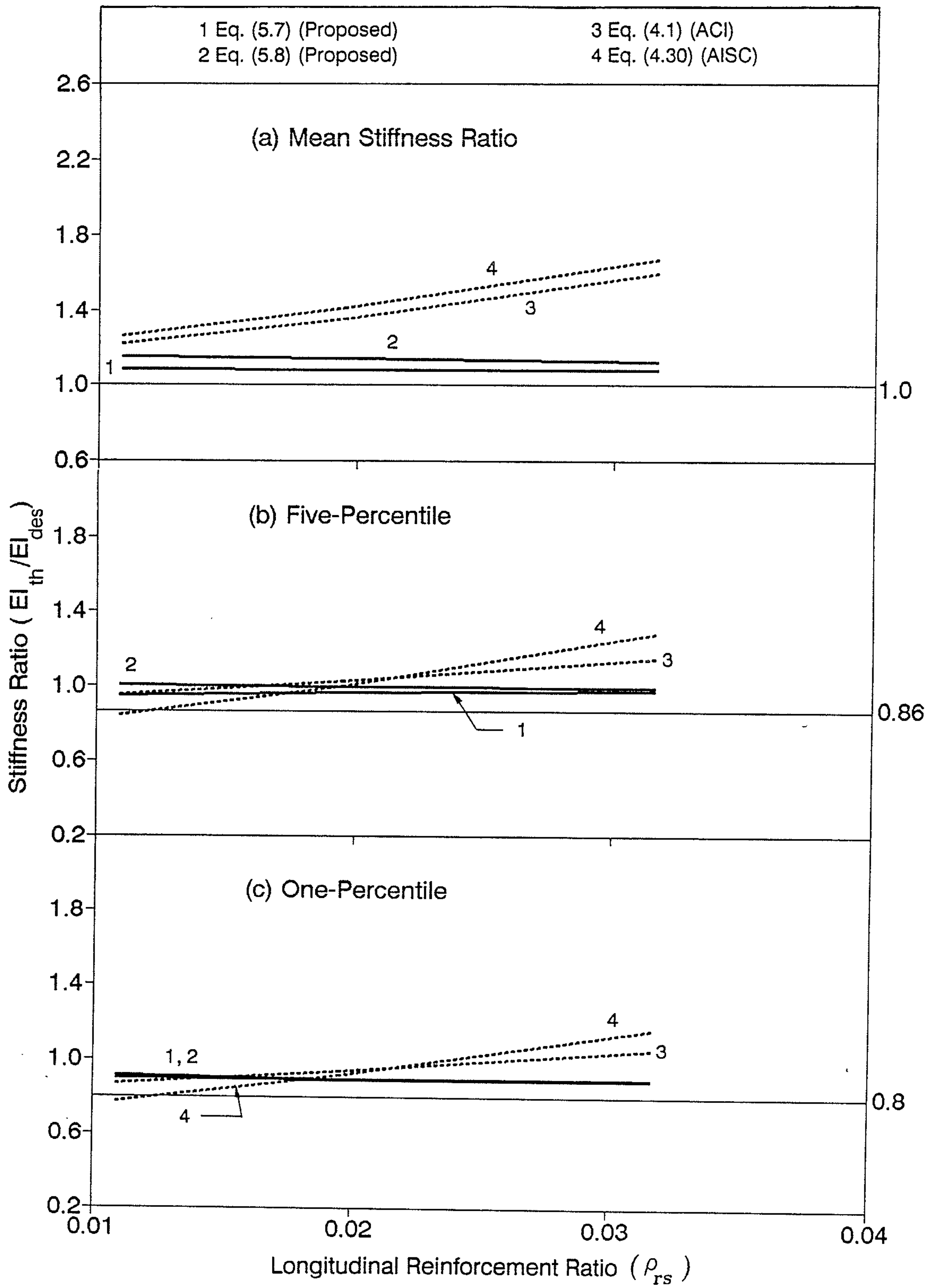

Figure 5.18 - Effect of longitudinal reinforcement ratio on stiffness ratio for different design equations for all columns bending about major axis (n = 3960 for each ρ_{rs} ratio equal to 1.09, 1.96 and 3.17 percent).

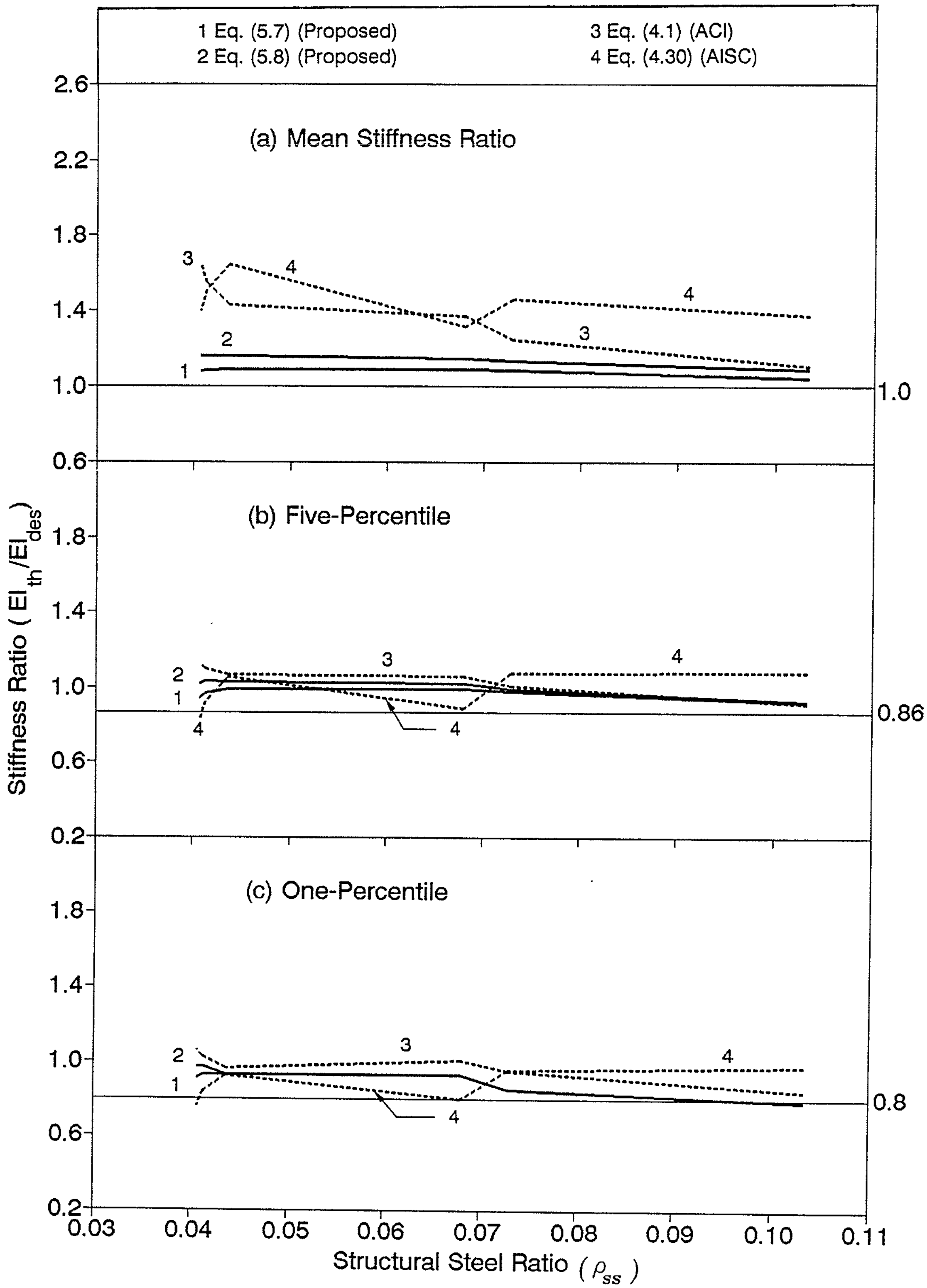

Figure 5.19 - Effect of structural steel ratio on stiffness ratio for different design equations for all columns bending about major axis (n = 1980 for each ρ_{ss} ratio equal to 4.07, 4.13, 4.36, 6.80, 7.29 and 10.33 percent).

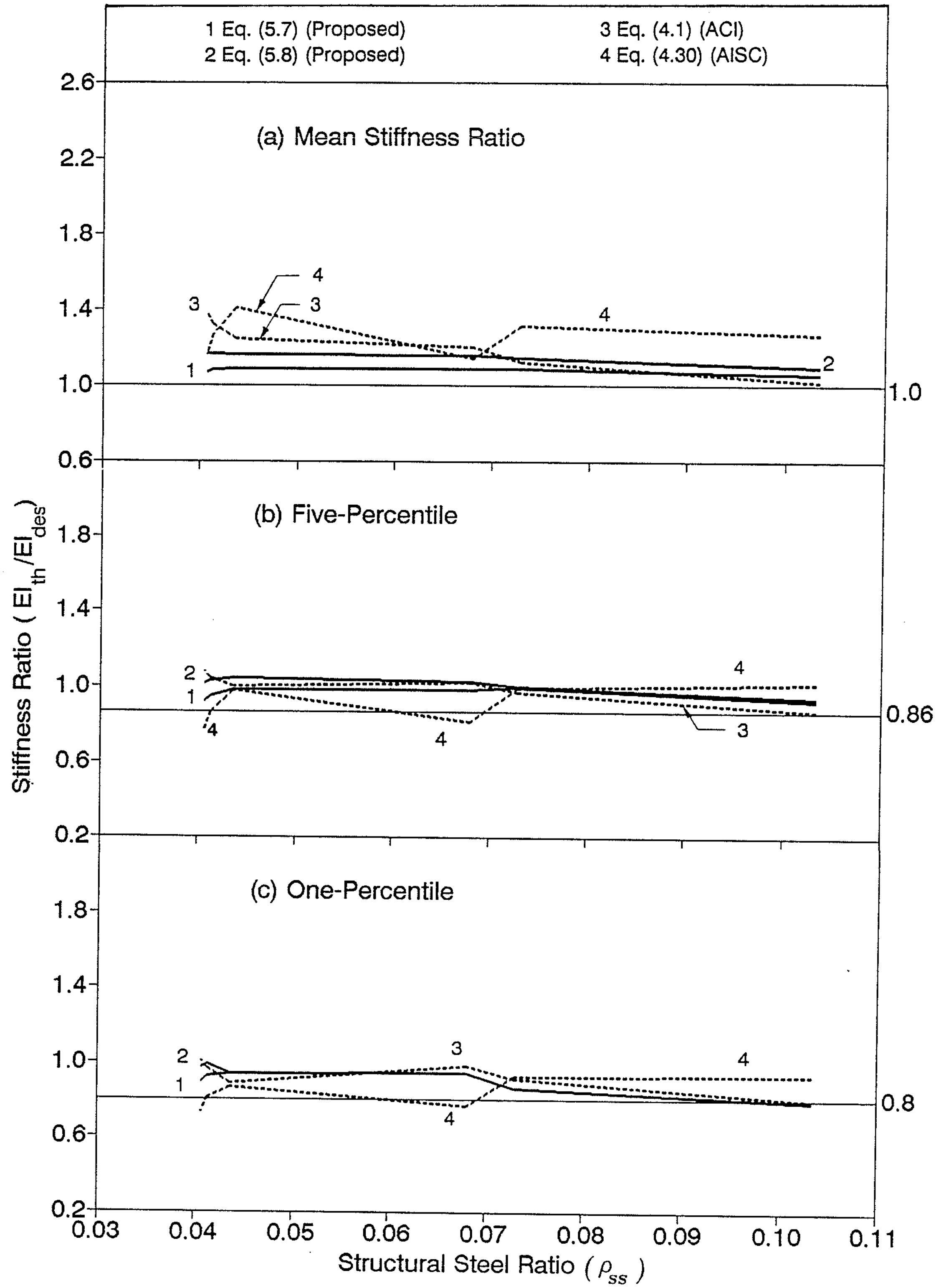

Figure 5.20 - Effect of structural steel ratio on stiffness ratio for different design equations for columns bending about major axis where ρ_{rs} = 1.09 percent (n = 660 for each ρ_{ss} ratio equal to 4.07, 4.13, 4.36, 6.80, 7.29 and 10.33 percent).

the overall stiffness in relation to the stiffness contributed by the structural steel section. For example, three steel shapes with significantly different moments of inertia were used to give a structural steel ratio of approximately 4 percent (actual values 4.07, 4.13 and 4.36 percent). This means when the ACI equation is used, a composite column containing a steel section with a relatively small moment of inertia gives a more conservative result than a column with a stiffer steel section.

Figure 5.21 concerning the effect of gross steel ratio ρ_g confirms the inconsistency of the ACI and AISC expressions for determining *EI*. Fluctuations appearing in the stiffness ratios for the proposed design equations are quite minor compared to the irregularities resulting from the ACI and AISC equations. This observation is also true for the effect of ρ_{rs}/ρ_{ss} (ratio of reinforcing steel to structural steel) as indicated by Figure 5.22. In both figures, all four design equations produced mean, five-percentile and one-percentile values of stiffness ratios that for most cases exceeded 1.0, 0.86, 0.80, respectively.

Figures 5.23, 5.24 and 5.25 examine the effects of the structural steel index $\rho_{ss}f_{yss}/f'_c$, the reinforcing steel index $\rho_{rs}f_{yrs}/f'_c$ and the gross steel index $(\rho_{ss}f_{yss}+\rho_{rs}f_{yrs})/f'_c$. Figures 5.23, 5.24, and 5.25, respectively, represent 72, 12, and 216 possible combinations of the related steel index. This resulted in stiffness ratios in Figures 5.23 and 5.25

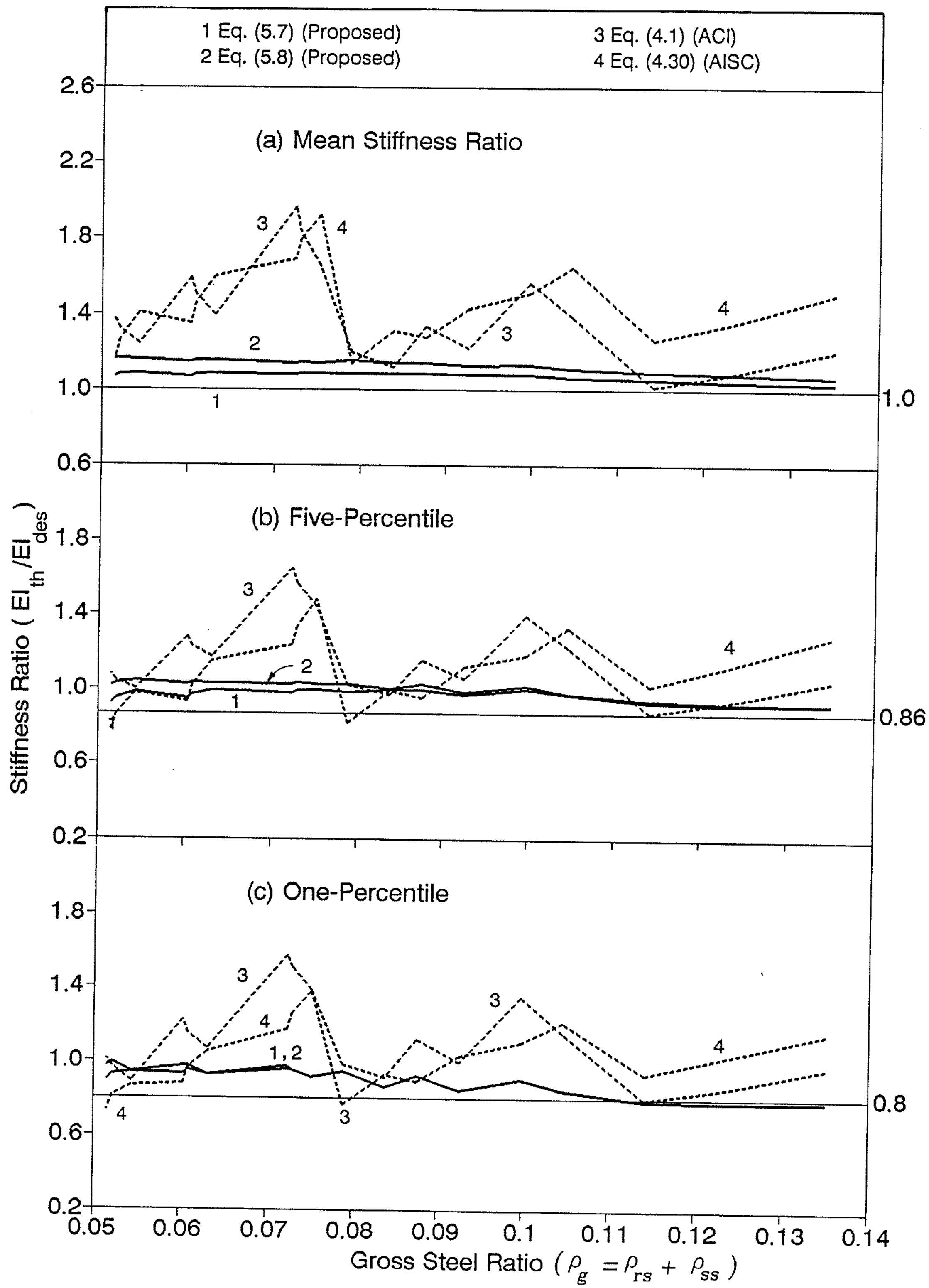

Figure 5.21 - Effect of gross steel ratio on stiffness ratio for different design equations for all columns bending about major axis (n = 660 for each ρ_g=(ρ_{rs}+ρ_{ss}) ratio equal to 5.16, 5.22, 5.45, 6.03, 6.09, 6.32, 7.24, 7.30, 7.53, 7.89, 8.38, 8.76, 9.25, 9.97, 10.46, 11.42, 12.29 and 13.50 percent).

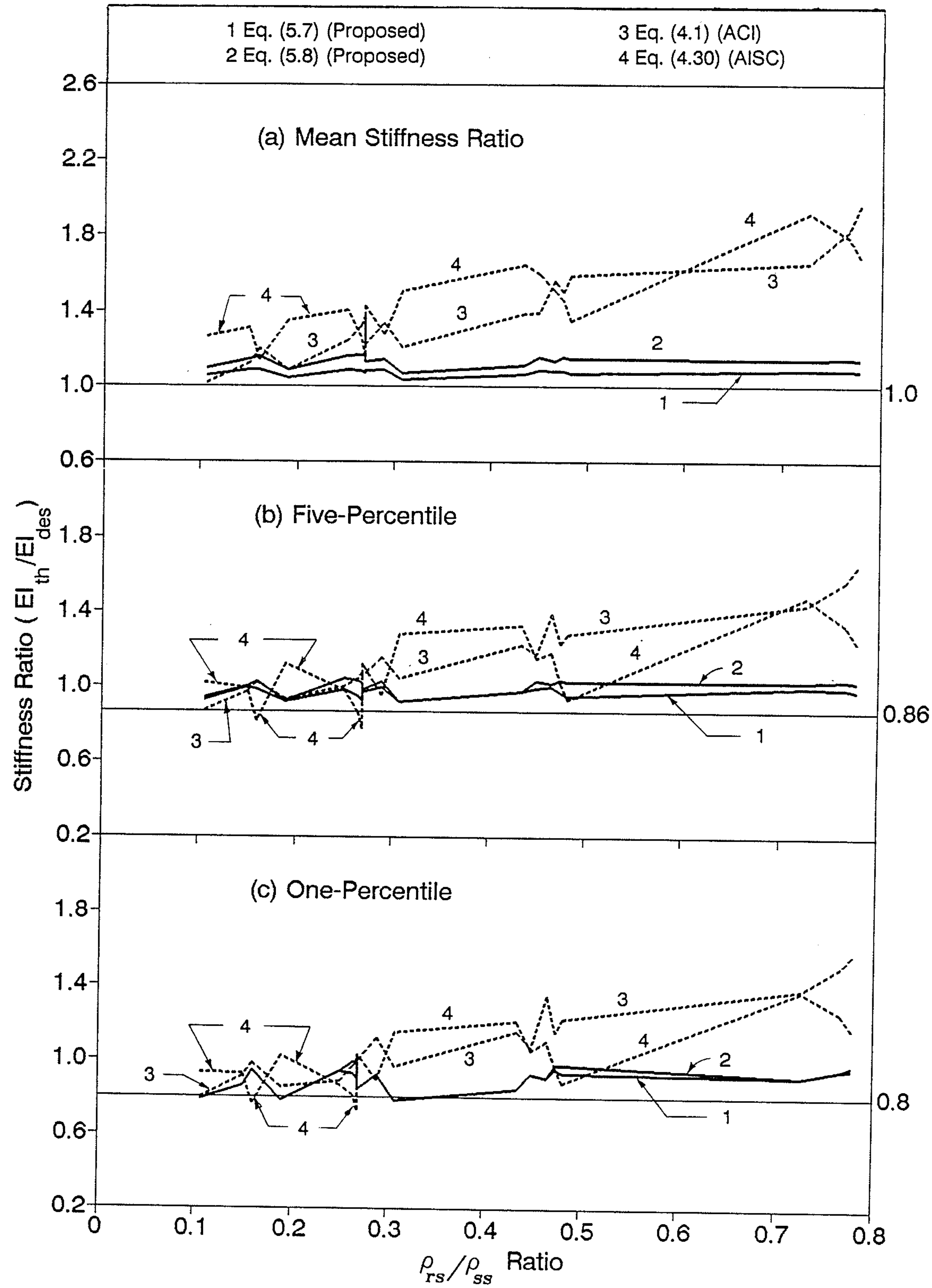

Figure 5.22 - Effect of ρ_{rs}/ρ_{ss} ratio on stiffness ratio for different design equations for all columns bending about major axis (n = 660 for each ρ_{rs}/ρ_{ss} ratio equal to 0.106, 0.150, 0.160, 0.190, 0.250, 0.264, 0.268, 0.269, 0.288, 0.306, 0.434, 0.449, 0.466, 0.474, 0.481, 0.726, 0.766 and 0.788).

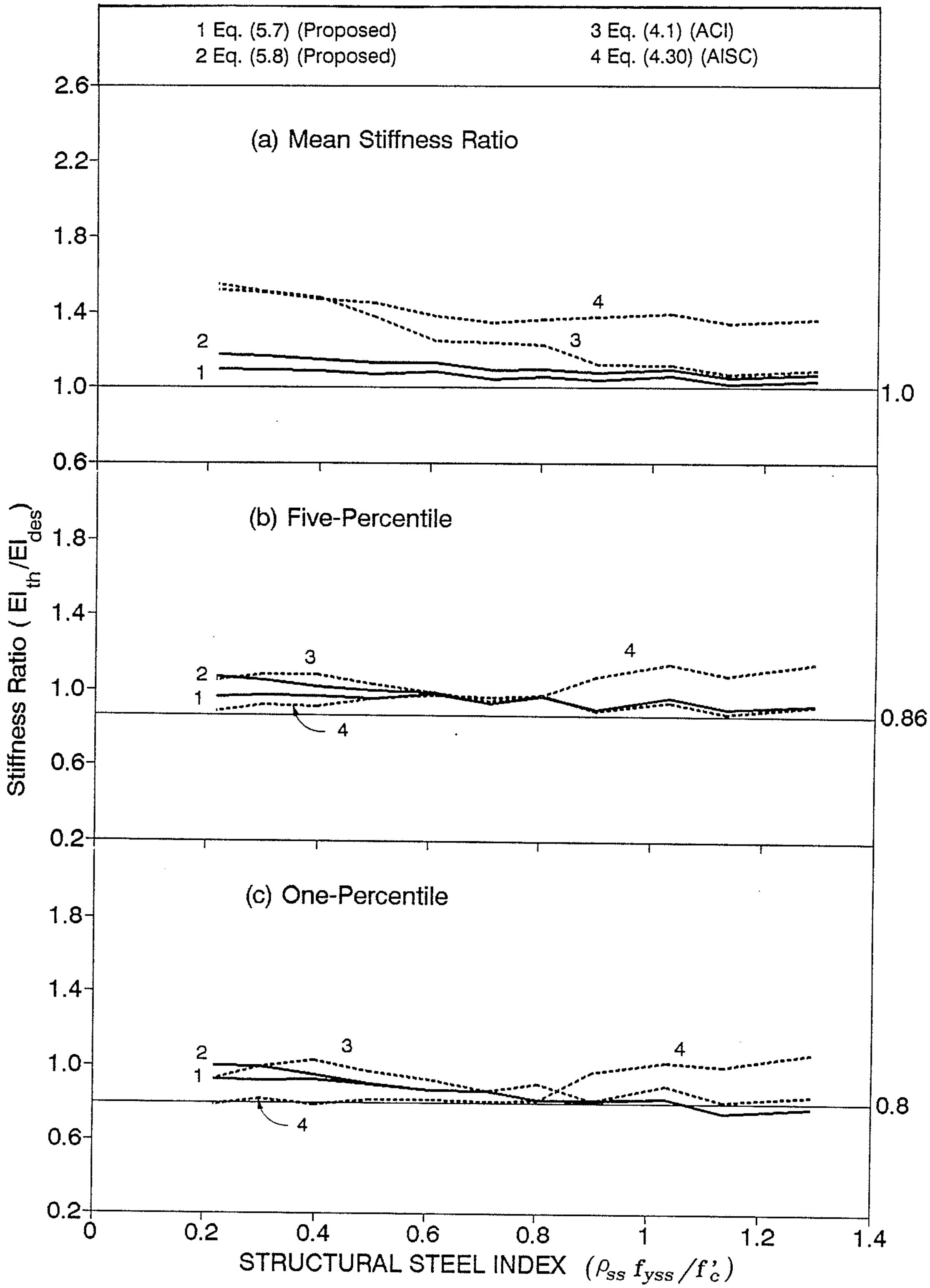

Figure 5.23 - Effect of structural steel index on stiffness ratio for different design equations for all columns bending about major axis (n varies for each $\rho_{ss}f_{yss}/f'_c$ range; total n = 11,880).

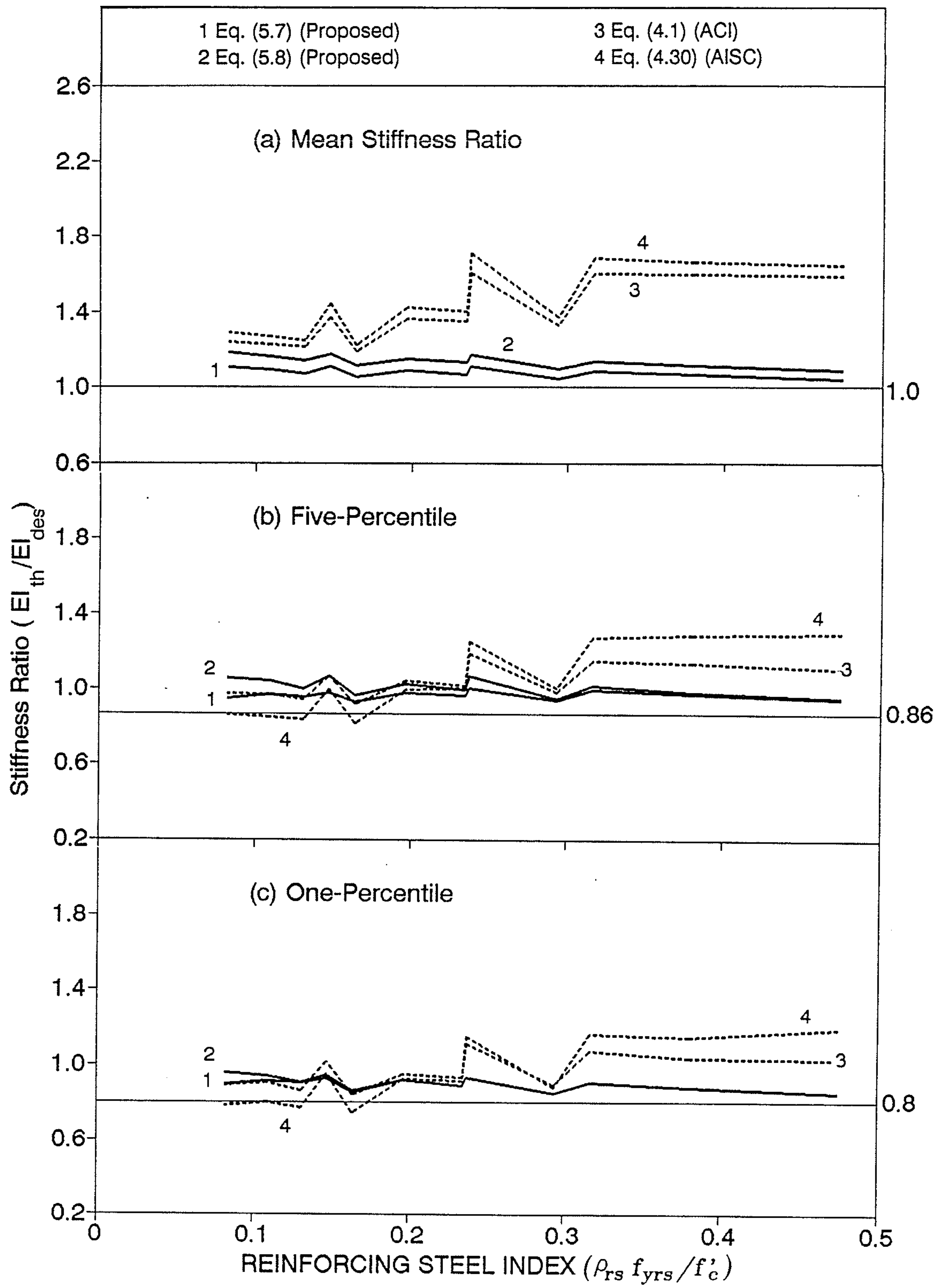

Figure 5.24 - Effect of reinforcing steel index on stiffness ratio for different design equations for all columns bending about major axis (n=990 for each $\rho_{rs}f_{yrs}/f'_c$ equal to 0.082, 0.109, 0.131, 0.147, 0.164, 0.196, 0.235, 0.237, 0.294, 0.317, 0.380 and 0.475).

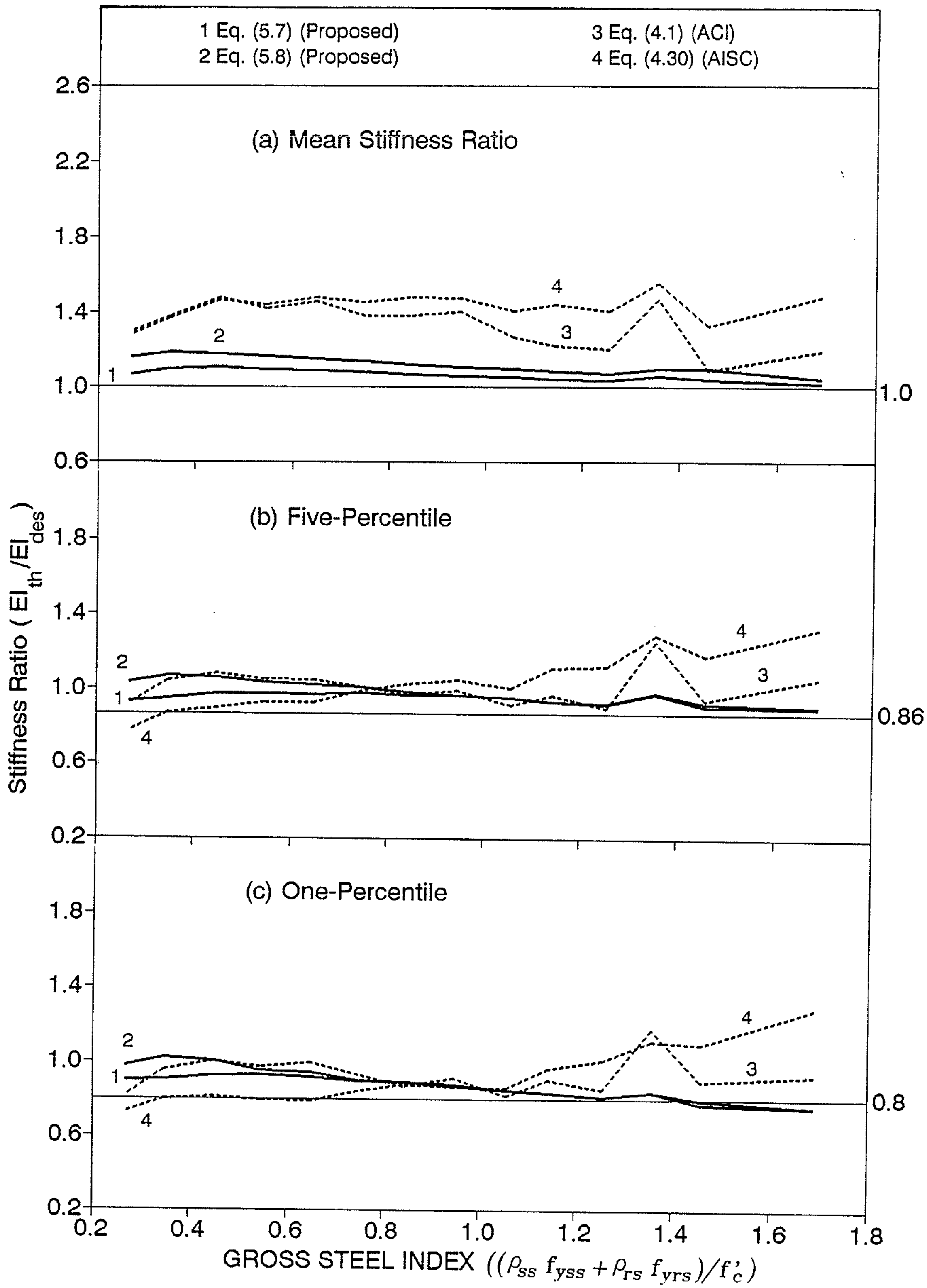

Figure 5.25 - Effect of gross steel index on stiffness ratio for different design equations for all columns bending about major axis (n varies for each $(\rho_{ss}f_{yss}+\rho_{rs}f_{yrs})/f'_c$ range; total n = 11,880).

being plotted for ranges of $\rho_{ss}f_{yss}/f'_c$ and $(\rho_{ss}f_{yss}+\rho_{rs}f_{yrs})/f'_c$, each range with a different number of stiffness ratios for statistical calculations. The ranges for $\rho_{ss}f_{yss}/f'_c$ plotted in Figure 5.23 were set at 0.20-0.25, 0.25-0.35, 0.35-0.45, 0.45-0.55, 0.55-0.65, 0.65-0.75, 0.75-0.85, 0.85-0.95, 0.95-1.05, 1.05-1.15, 1.15-1.25, 1.25-1.35; and those for $(\rho_{ss}f_{yss}+\rho_{rs}f_{yrs})/f'_c$ plotted in Figure 5.25 were set at 0.2-0.3, 0.3-0.4, 0.4-0.5, 0.5-0.6, 0.6-0.7, 0.7-0.8, 0.8-0.9, 0.9-1.00, 1.00-1.10, 1.10-1.20, 1.20-1.30, 1.30-1.40, 1.40-1.50, 1.50-1.60, 1.60-1.80. The mean steel index for each range is plotted against the mean, five-percentile and one-percentile stiffness ratios for each corresponding range. These figures show that the fluctuations in stiffness ratios for the proposed design equations are subtle compared to the fluctuations occurring for the ACI and AISC expressions.

The effects of I_{rs}/I_{ss}, I_{ss}/I_g, I_{rs}/I_g and $(I_{ss} + I_{rs})/I_g$ on stiffness ratios (EI_{th}/EI_{des}) are respectively shown in Figures 5.26, 5.27, 5.28, and 5.29. The trends shown in these figures are similar to those discussed for Figures 5.18 to 5.25 related to the steel indices. This is particularly true when Figure 5.21 is compared to Figure 5.26 and 5.29, and Figure 5.18 to Figure 5.28. As expected, Figures 5.27 and 5.28 indicate that the ACI equation is more conservative when the moment of inertia of the steel section is relatively small or when the moment of inertia of reinforcing steel is relatively large compared to the moment of inertia of the

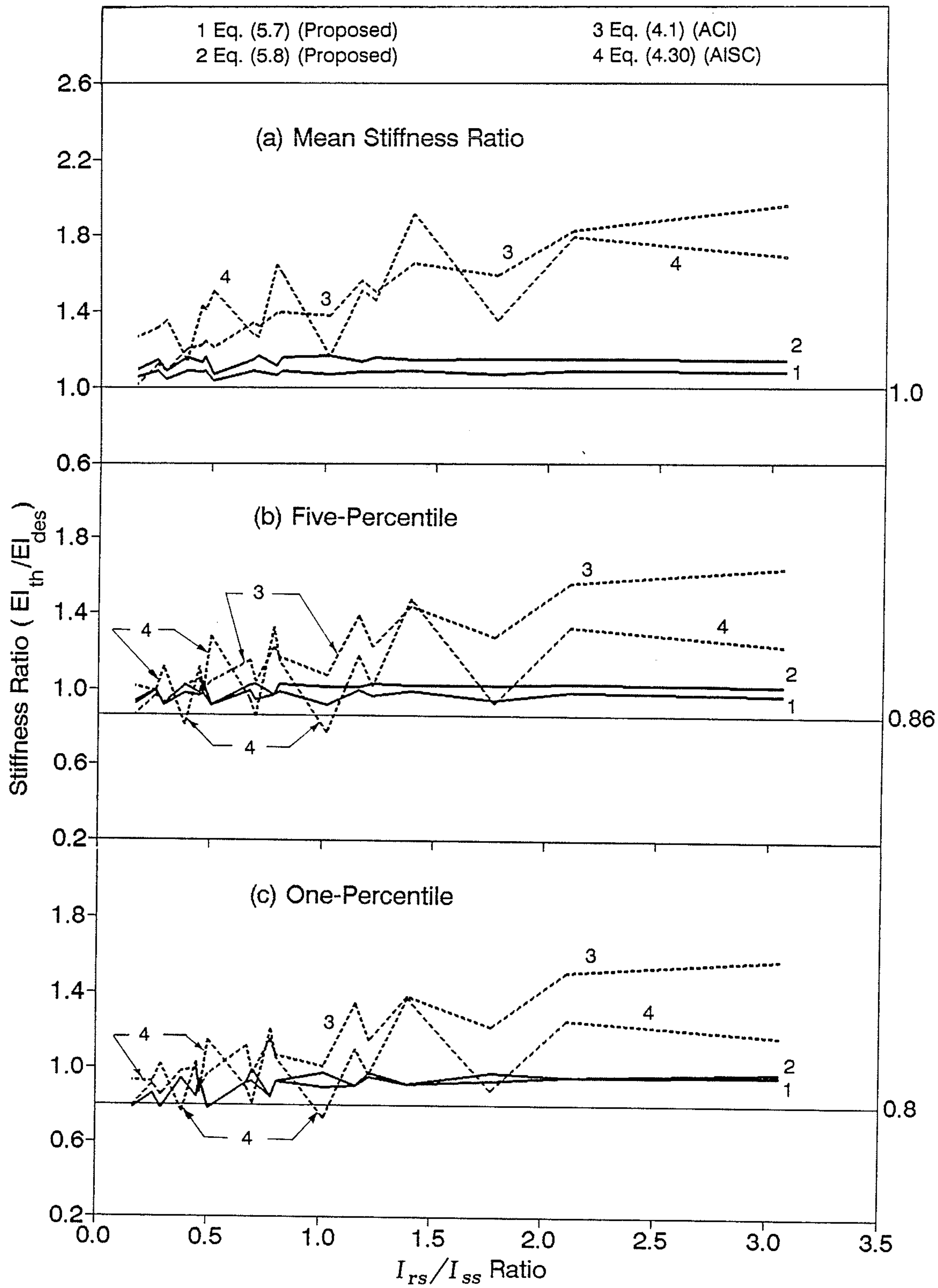

Figure 5.26 - Effect of I_{rs}/I_{ss} ratio on stiffness ratio for different design equations for all columns bending about major axis (n=660 for each I_{rs}/I_{ss} ratio equal to 0.17, 0.26, 0.29, 0.39, 0.45, 0.46, 0.50, 0.67, 0.70, 0.78, 0.81, 1.02, 1.16, 1.22, 1.39, 1.77, 2.11 and 3.06).

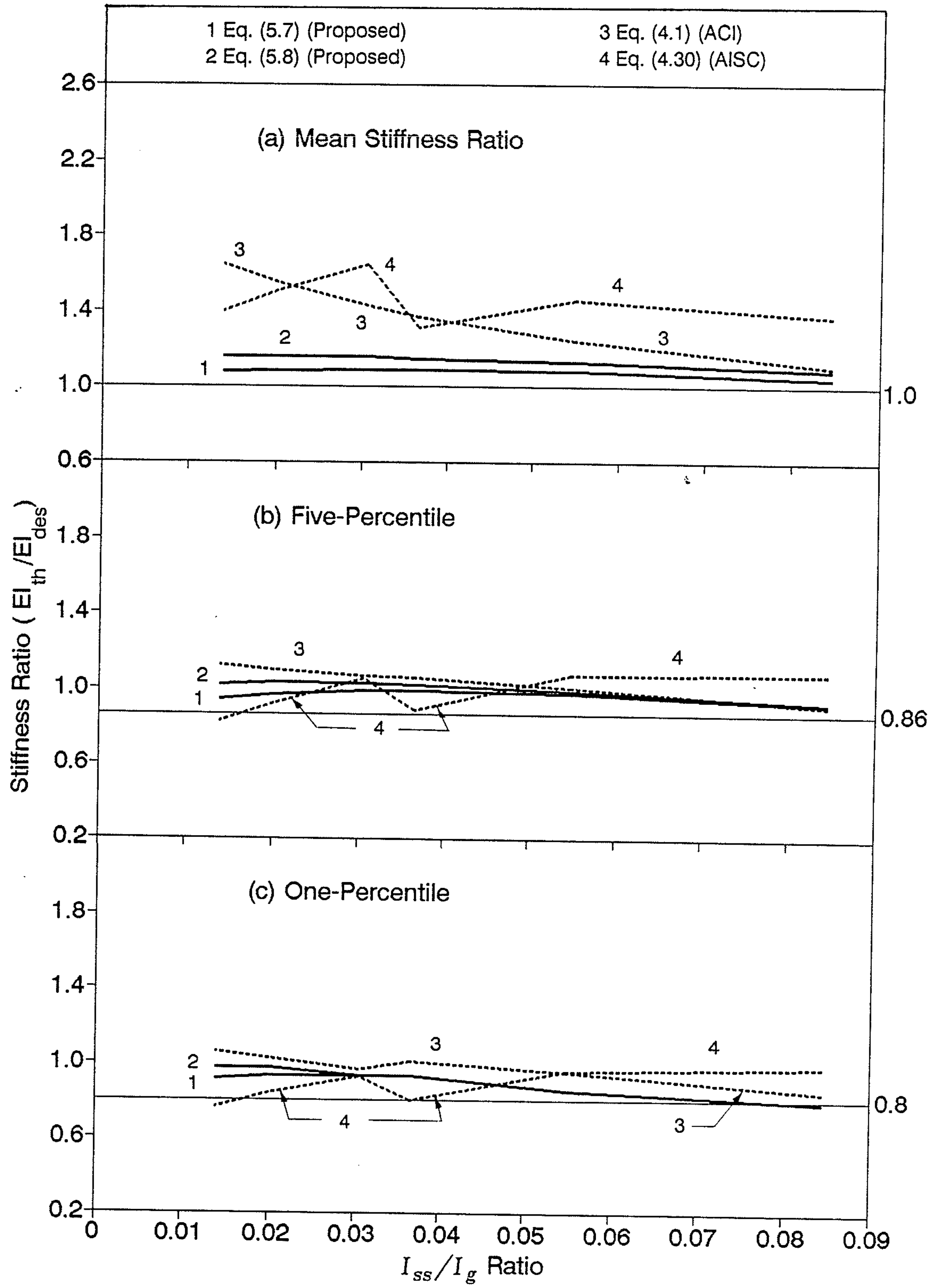

Figure 5.27 - Effect of I_{ss}/I_g ratio on stiffness ratio for different design equations for all columns bending about major axis (n=1980 for each I_{ss}/I_g ratio equal to 0.014, 0.020, 0.031, 0.037, 0.055 and 0.085).

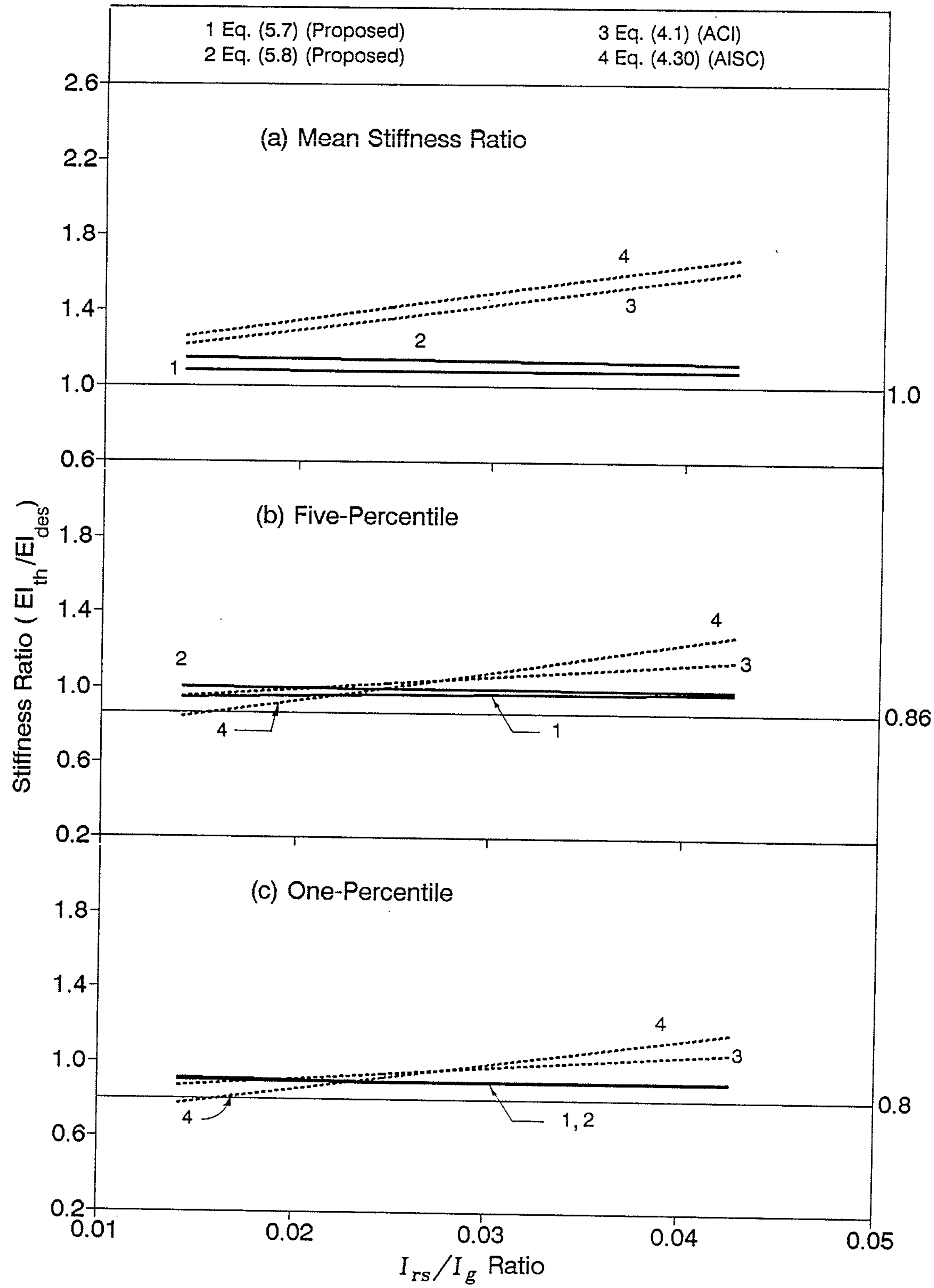

Figure 5.28 - Effect of I_{rs}/I_g ratio on stiffness ratio for different design equations for all columns bending about major axis (n=3960 for each I_{rs}/I_g ratio equal to 0.014, 0.025, 0.043).

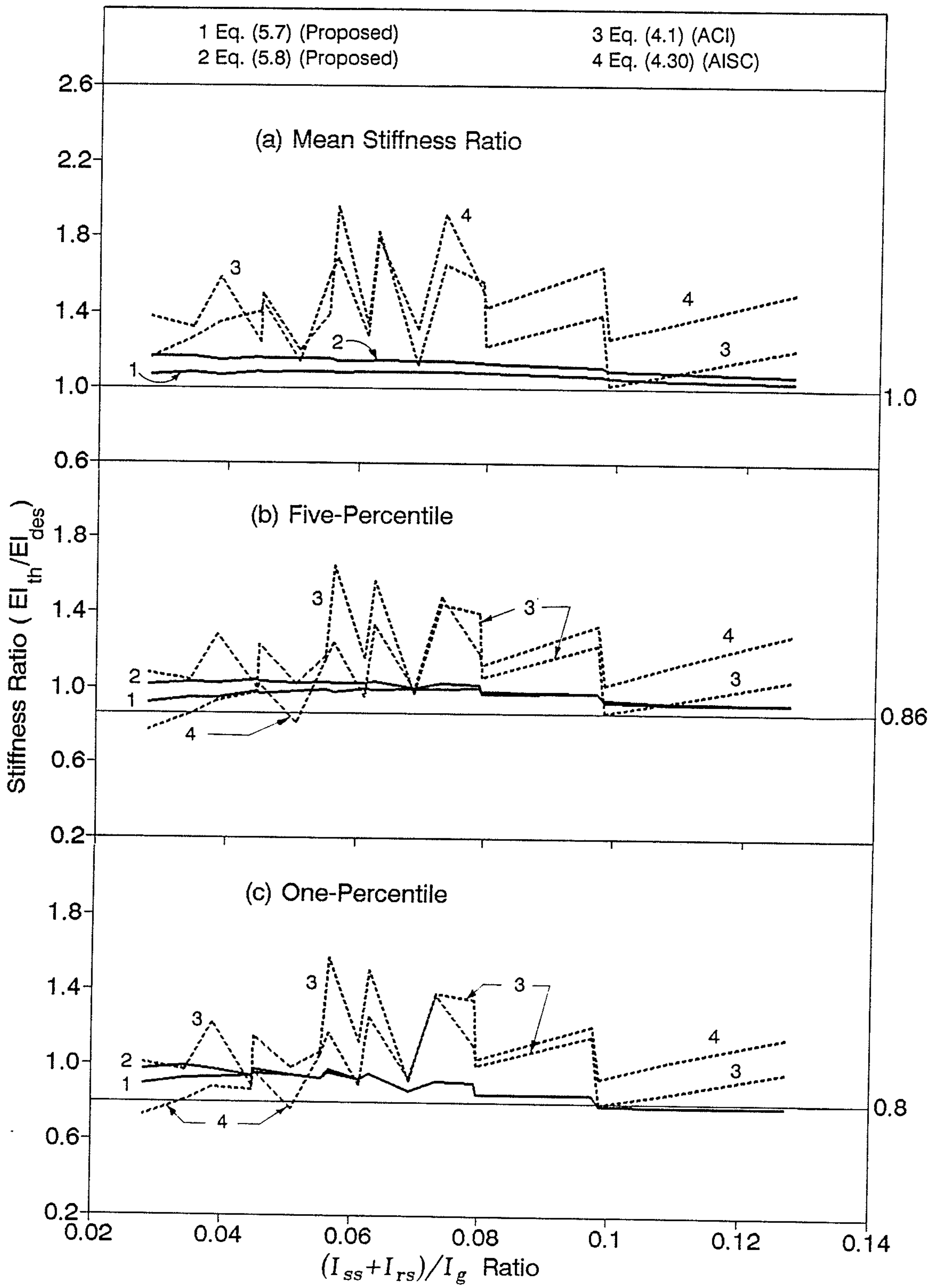

Figure 5.29 - Effect of $(I_{ss}+I_{rs})/I_g$ ratio on stiffness ratio for different design equations for all columns bending about major axis (n=660 for each $(I_{ss}+I_{rs})/I_g$ ratio equal to 0.028, 0.034, 0.039, 0.0447, 0.0449, 0.051, 0.055, 0.057, 0.061, 0.063, 0.069, 0.073, 0.079, 0.080, 0.097, 0.099, 0.109 and 0.127)

gross cross-section.

Figure 5.30 examines the effect of d_{ss}/h (ratio of depth of structural steel section to the overall depth of the composite cross section) on stiffness ratios. As expected, the results are somewhat similar to those obtain from Figure 5.27 plotted for the effect of I_{ss}/I_g. The proposed design equations produce practically constant values of mean, five-percentile and one-percentile stiffness ratios over the entire range of d_{ss}/h plotted, while the ACI and AISC equations are subject to variations for different values of d_{ss}/h.

The following can be summarized from the data plotted in Figures 5.10 to 5.30 and the related discussions:

(1) The proposed design equations (Equations 5.7 and 5.8) were not significantly affected by any of the variables investigated, while the ACI and AISC expressions (Equations 4.1 and 4.30) were significantly affected by most of these same variables.

(2) The ACI design equation produced results that are compatible to the results of the proposed design equations for the five-percentile and one-percentile stiffness ratios plotted against many of the variables. This is particularly apparent when considering the affect of e/h and ℓ/h, the variables used in the proposed design expressions.

(3) The AISC equation, in many cases, gives the most conservative results for mean stiffness ratios and the

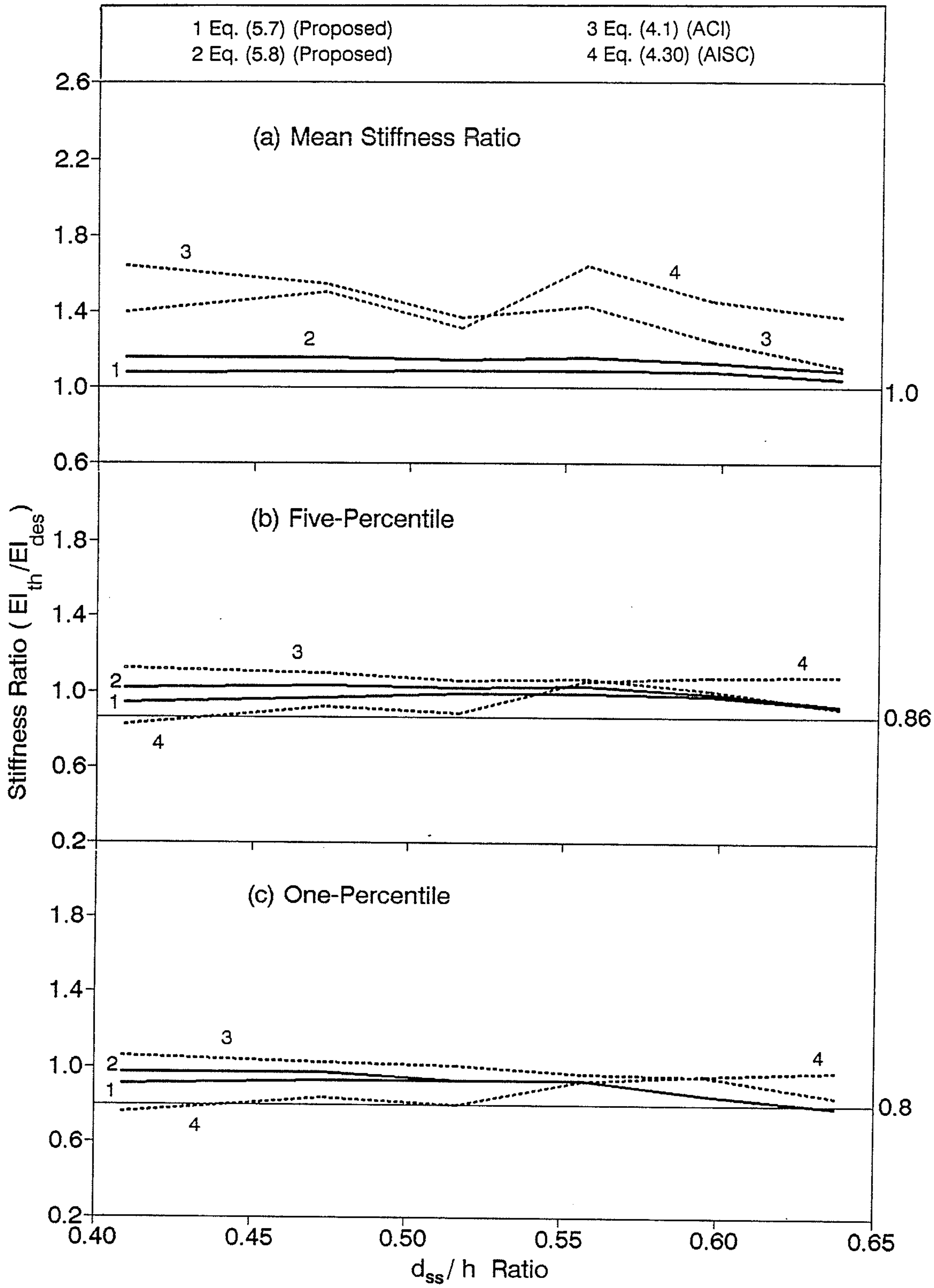

Figure 5.30 - Effect of d_{ss}/h ratio on stiffness ratio for different design equations for all columns bending about major axis (n=1980 for each d_{ss}/h ratio equal to 0.41, 0.47, 0.52, 0.56, 0.60 and 0.64).

least conservative values for the five-percentile and one-percentile stiffness ratios.

5.4.3 Stiffness Ratios Produced by Proposed Design Equations for Usual Columns

For composite beam-columns, neither the ACI Code nor the AISC Code sets an upper limit on the amount of structural steel. However, the AISC Code states that to qualify as a composite column the structural steel ratio (ρ_{ss}) must be greater than or equal to 4 percent. The ACI Building code requires that a minimum of 1 percent to a maximum of 8 percent of longitudinal reinforcing (ρ_{rs}) be included with the structural steel core. Difficulty in lap splicing the reinforcing bars reduces the maximum limit of ρ_{rs} to about 3 percent when a relatively large structural steel core is encased. The reinforcing steel ratio is, therefore, usually expected to range from 1 to 3 percent. Even three percent reinforcing steel will restrict ρ_{ss} to a maximum of about 10 percent, giving the ρ_{ss} range of about 4 to 10 percent. Mirza and MacGregor (1982) determined that the end eccentricity ratio for columns in reinforced concrete buildings usually ranged from 0.1 to 0.65. Therefore, the usual columns in this study were defined as those for which e/h = 0.1, 0.2, 0.3, 0.4, 0.5, 0.6, or 0.7, and ρ_{ss} = 4.2 (actual values = 4.07, 4.13, 4.36), 7.0 (actual values of 6.80, 7.29), or 10.3 (actual value = 10.33) percent, and ρ_{rs} equal to 1.09, 1.96, or 3.17 percent.

Figures 5.31 (a) to (e) examine the variations in mean and minium values of the stiffness ratios with respect to e/h computed from Equation 5.7 and plotted for ℓ/h = 10, 15, 20, 25 and 30, respectively. The number of values available for plotting each point were 36, 72 and 108 for ρ_{ss} = 10.3, 7.0 and 4.2 percent, respectively. The one-percentile values were not plotted in these figures because the minimum values represented 2.8, 1.4 and 0.93 percentiles. The mean stiffness ratios exceeded 1.0 for most of the columns for all ℓ/h, while the minimum values exceeded 0.8 in all cases. Only for ℓ/h =10 and ρ_{ss} = 10.3 percent and for ℓ/h =30 and ρ_{ss} = 4.2 percent, the mean stiffness ratio were less than 1.0. This indicated by Figures 5.31(a) to (e).

Equation 5.8 is identical to Equation 5.7 for ℓ/h = 10, and becomes more conservative as ℓ/h increases. This becomes evident by Figures 5.31(f), (g), (h), and (i) plotted for Equation 5.8.

The following conclusions appear to be valid for columns with e/h = 0.1 to 0.7, ρ_{ss} = 4.2 to 10.3 percent, ρ_{rs} = 1.1 to 3.2 percent, and ℓ/h = 10 to 30:

(1) The mean and minimum stiffness ratios for Equation 5.7 or 5.8 may be taken as 1.0 and 0.8, respectively;

(2) The proposed design equations (Equations 5.7 and 5.8) are not subject to significant variation due to e/h, ρ_{ss} or ℓ/h ratios.

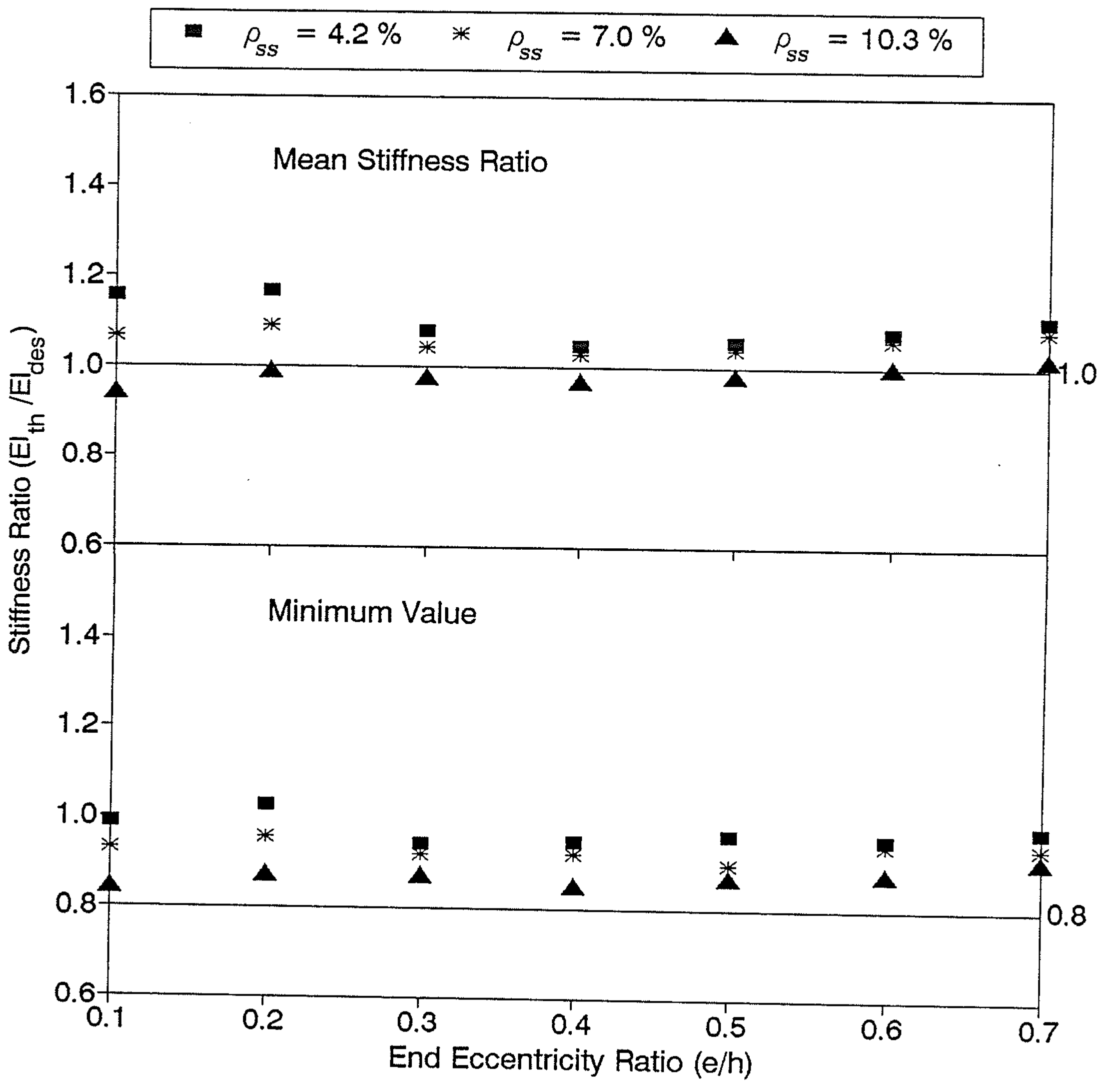

Figure 5.31(a) - Stiffness ratios obtained from proposed design equations, Eq. (5.7) or (5.8), for usual columns bending about major axis with ℓ/h = 10 (for each combination of e/h and ρ_{ss} ratios plotted n=108 for ρ_{ss}=4.2 percent, n=72 when ρ_{ss}=7.0 percent and n=36 when ρ_{ss}=10.3 percent).

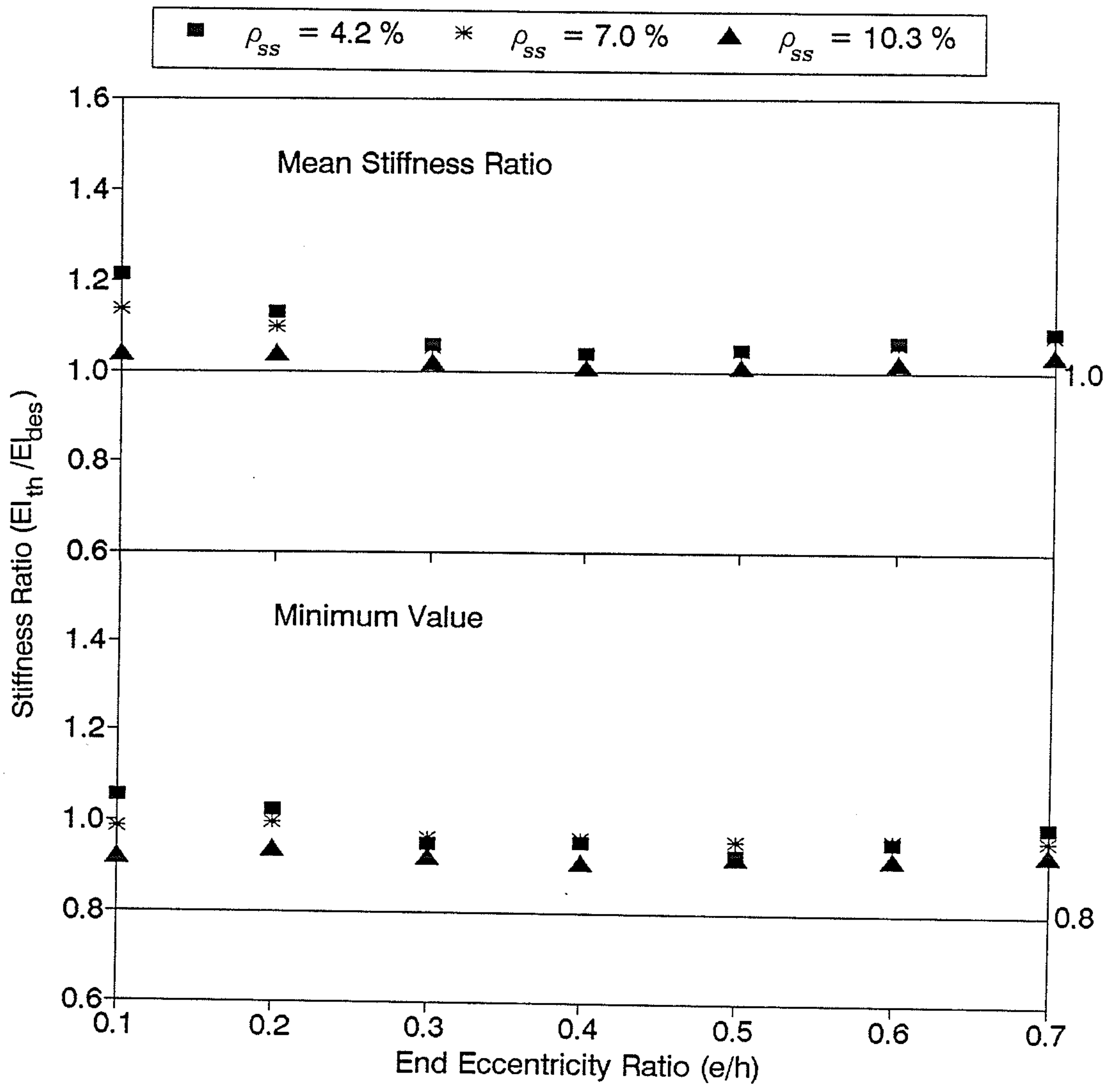

Figure 5.31(b) - Stiffness ratios obtained from proposed design Equation (5.7) for usual columns bending about major axis with ℓ/h = 15 (for each combination of e/h and ρ_{ss} ratios plotted n = 108 for ρ_{ss}=4.2 percent, n=72 when ρ_{ss}=7.0 percent and n=36 when ρ_{ss}=10.3 percent).

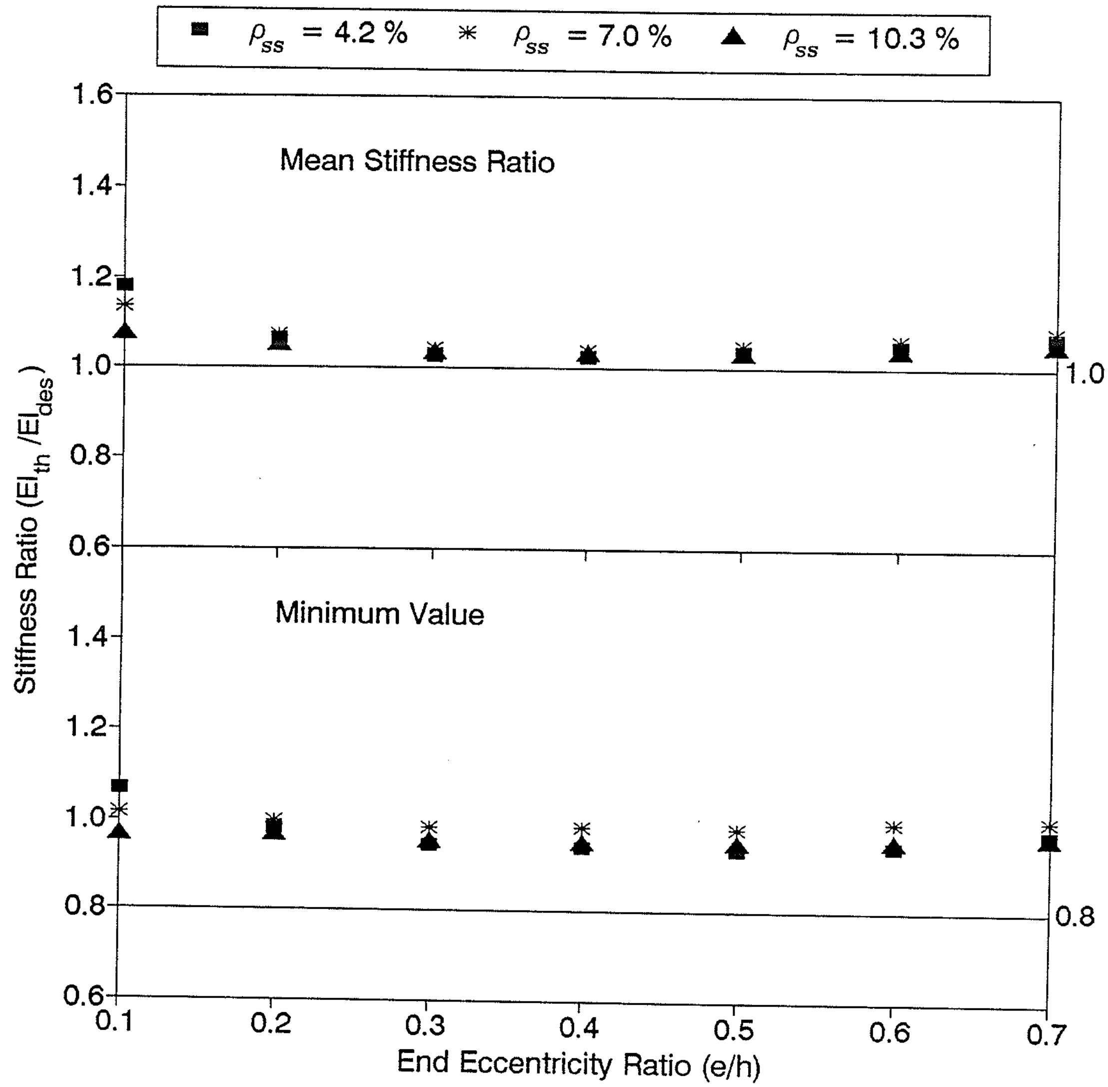

Figure 5.31(c) - Stiffness ratios obtained from proposed design Equation (5.7) for usual columns bending about major axis with ℓ/h = 20 (for each combination of e/h and ρ_{ss} ratios plotted n = 108 for ρ_{ss}=4.2 percent, n=72 when ρ_{ss}=7.0 percent and n=36 when ρ_{ss}=10.3 percent).

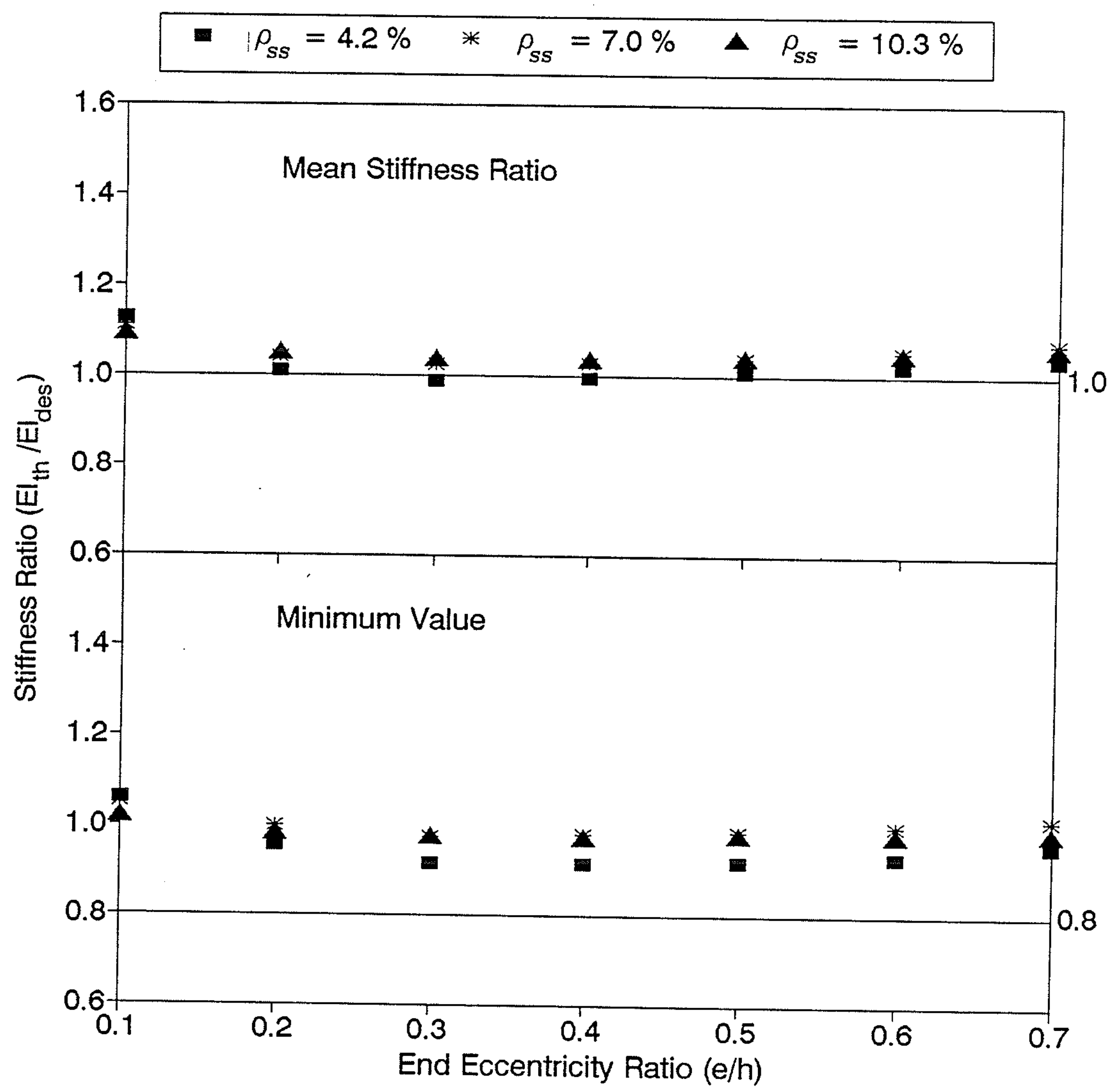

Figure 5.31(d) - Stiffness ratios obtained from proposed design Equation (5.7) for usual columns bending about major axis with ℓ/h = 25 (for each combination of e/h and ρ_{ss} ratios plotted n = 108 for ρ_{ss}=4.2 percent, n=72 when ρ_{ss}=7.0 percent and n=36 when ρ_{ss}=10.3 percent).

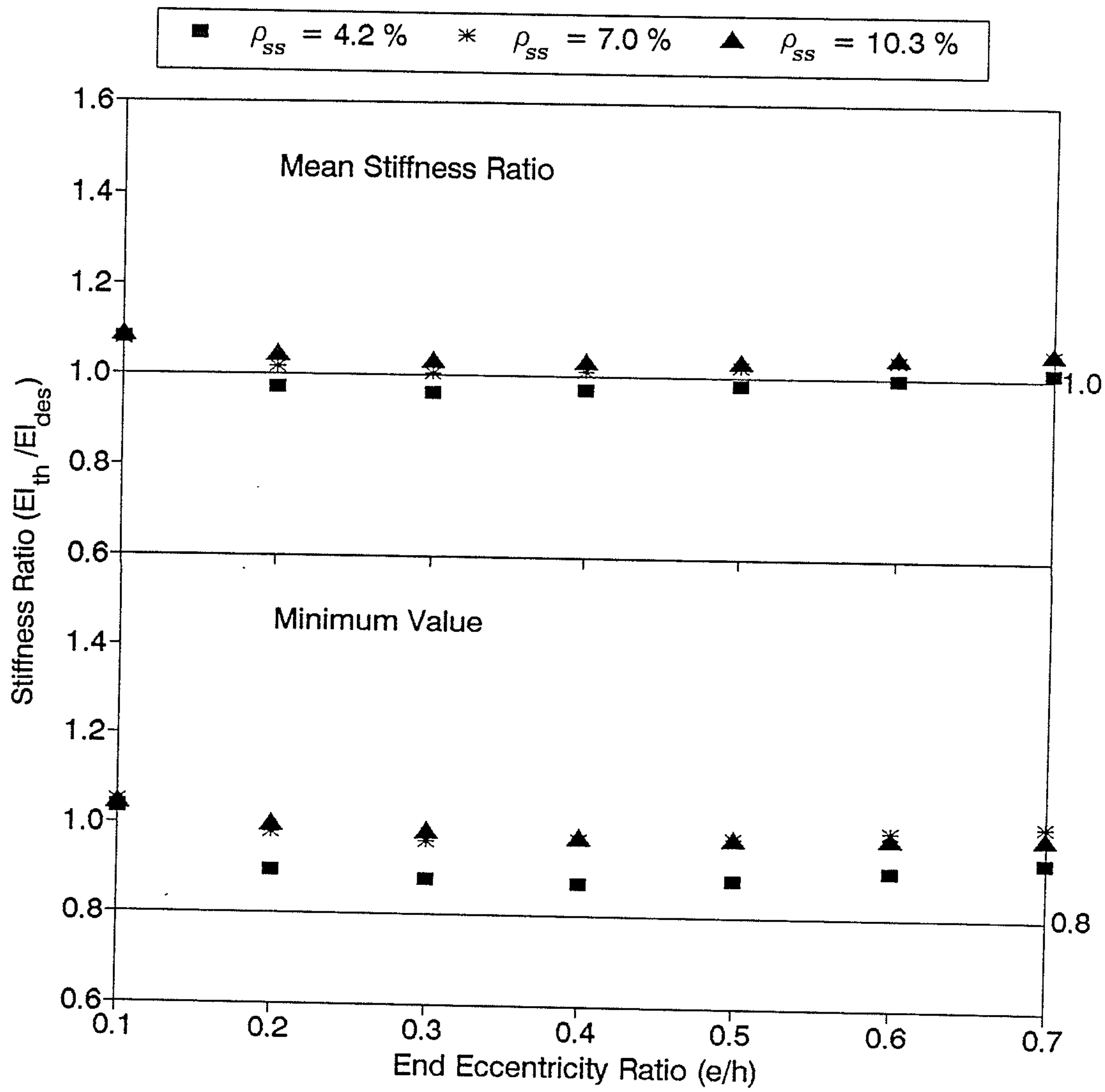

Figure 5.31(e) - Stiffness ratios obtained from proposed design Equation (5.7) for usual columns bending about major axis with ℓ/h = 30 (for each combination of e/h and ρ_{ss} ratios plotted n = 108 for ρ_{ss}=4.2 percent, n=72 when ρ_{ss}=7.0 percent and n=36 when ρ_{ss}=10.3 percent).

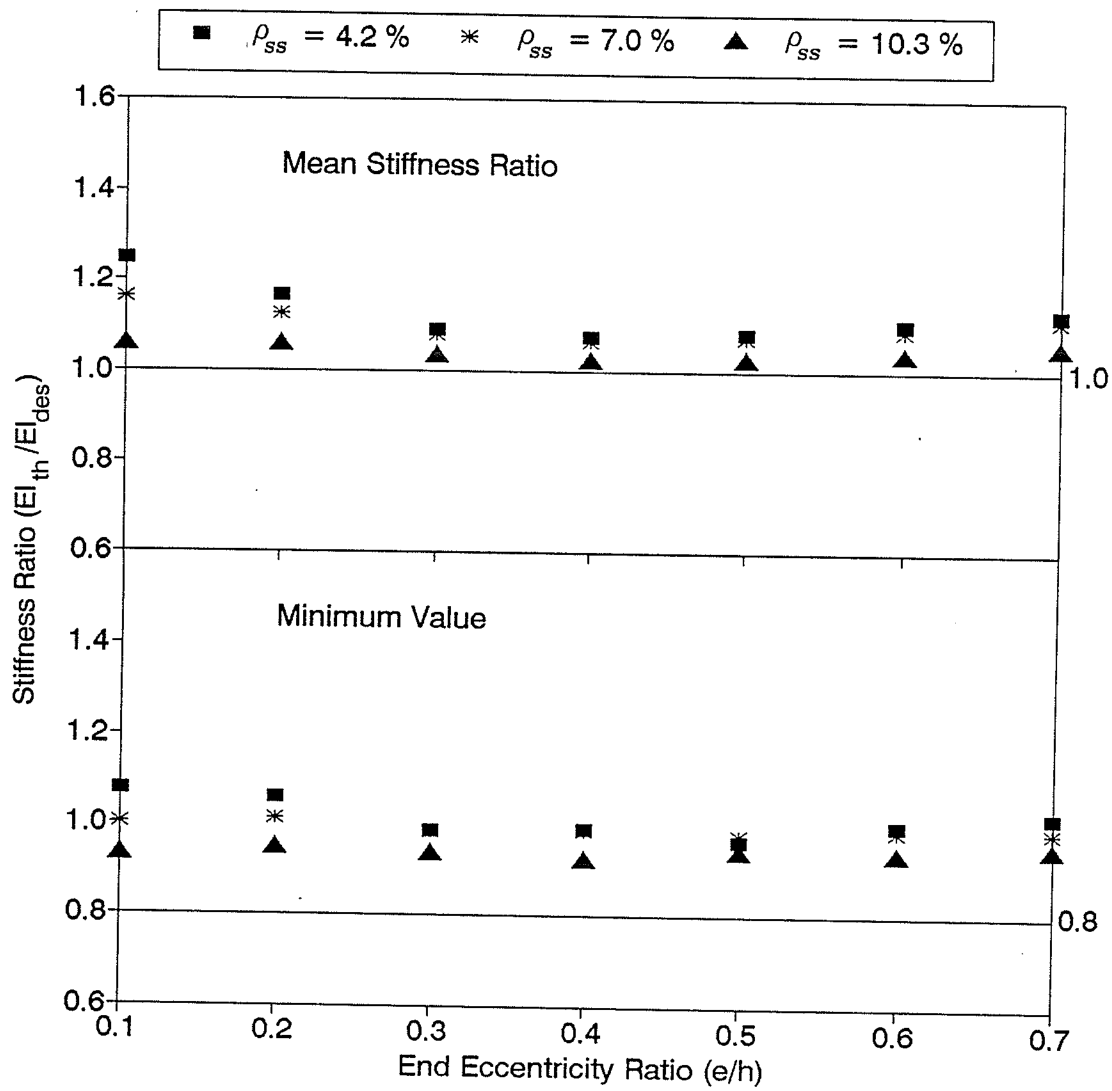

Figure 5.31(f) - Stiffness ratios obtained from proposed design Equation (5.8) for usual columns bending about major axis with ℓ/h = 15 (for each combination of e/h and ρ_{ss} ratios plotted n = 108 for ρ_{ss}=4.2 percent, n=72 when ρ_{ss}=7.0 percent and n=36 when ρ_{ss}=10.3 percent).

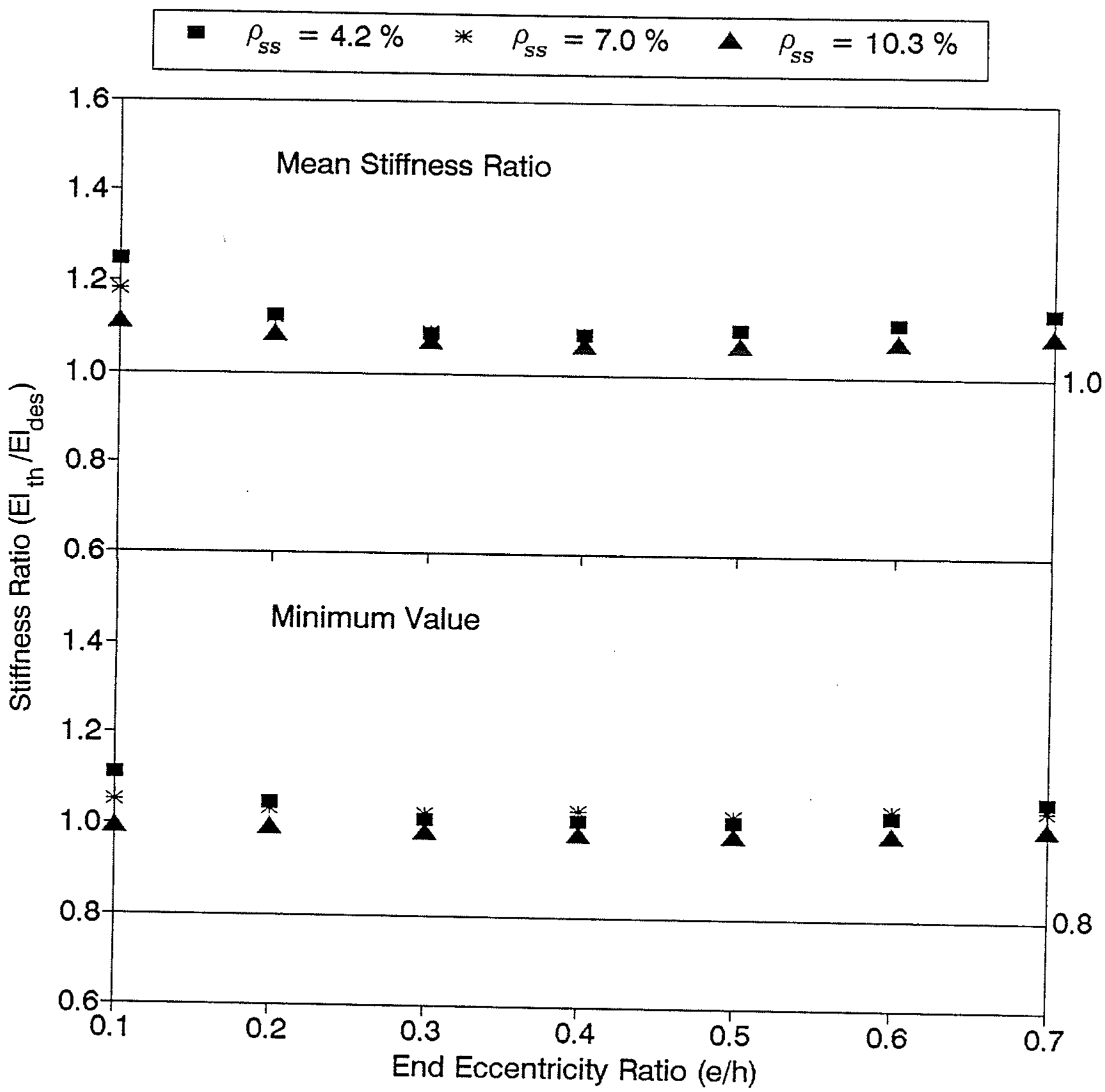

Figure 5.31(g) - Stiffness ratios obtained from proposed design Equation (5.8) for usual columns bending about major axis with ℓ/h = 20 (for each combination of e/h and ρ_{ss} ratios plotted n = 108 for ρ_{ss}=4.2 percent, n=72 when ρ_{ss}=7.0 percent and n=36 when ρ_{ss}=10.3 percent).

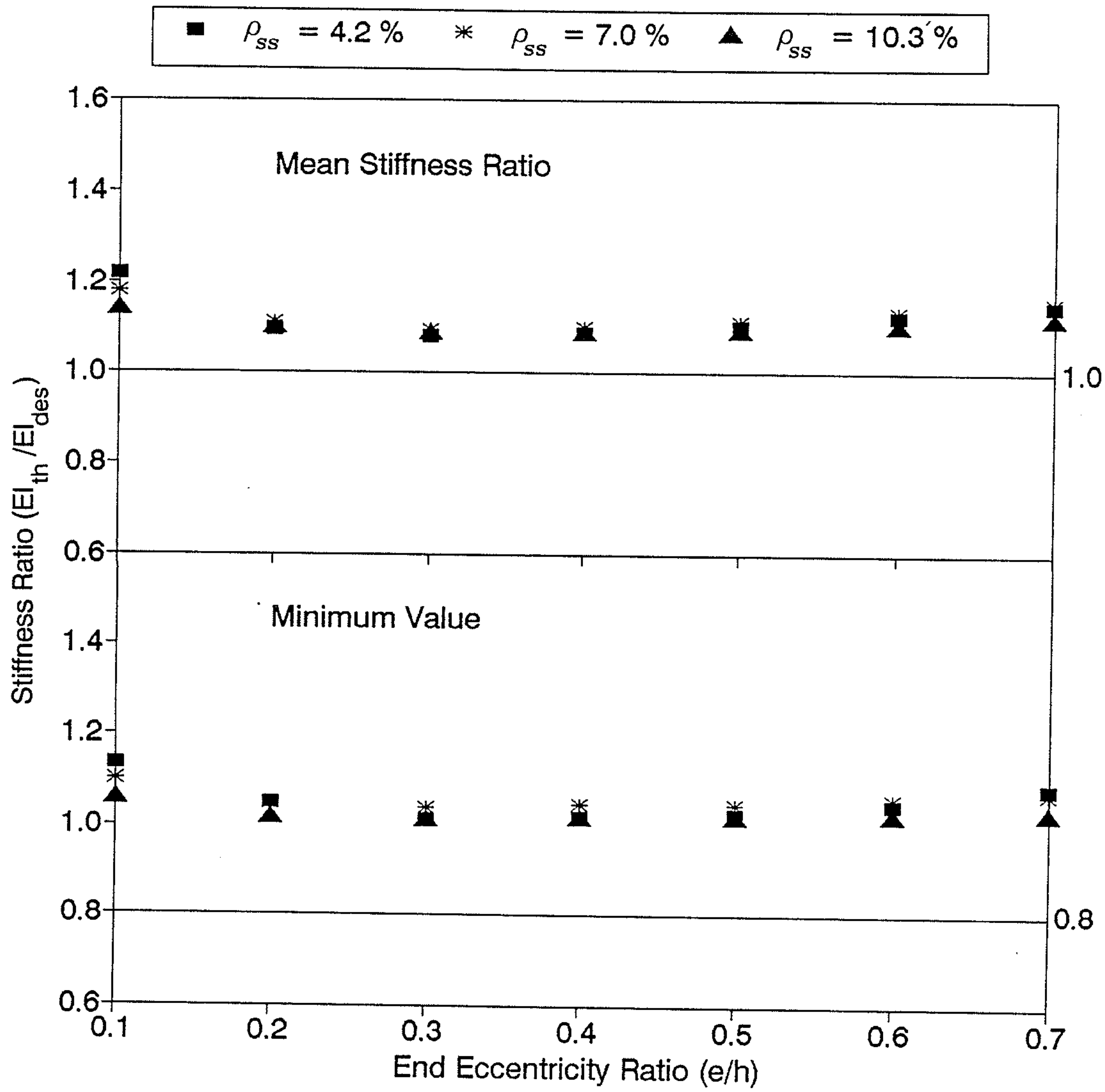

Figure 5.31(h) - Stiffness ratios obtained from proposed design Equation (5.8) for usual columns bending about major axis with ℓ/h = 25 (for each combination of e/h and ρ_{ss} ratios plotted n = 108 for ρ_{ss}=4.2 percent, n=72 when ρ_{ss}=7.0 percent and n=36 when ρ_{ss}=10.3 percent).

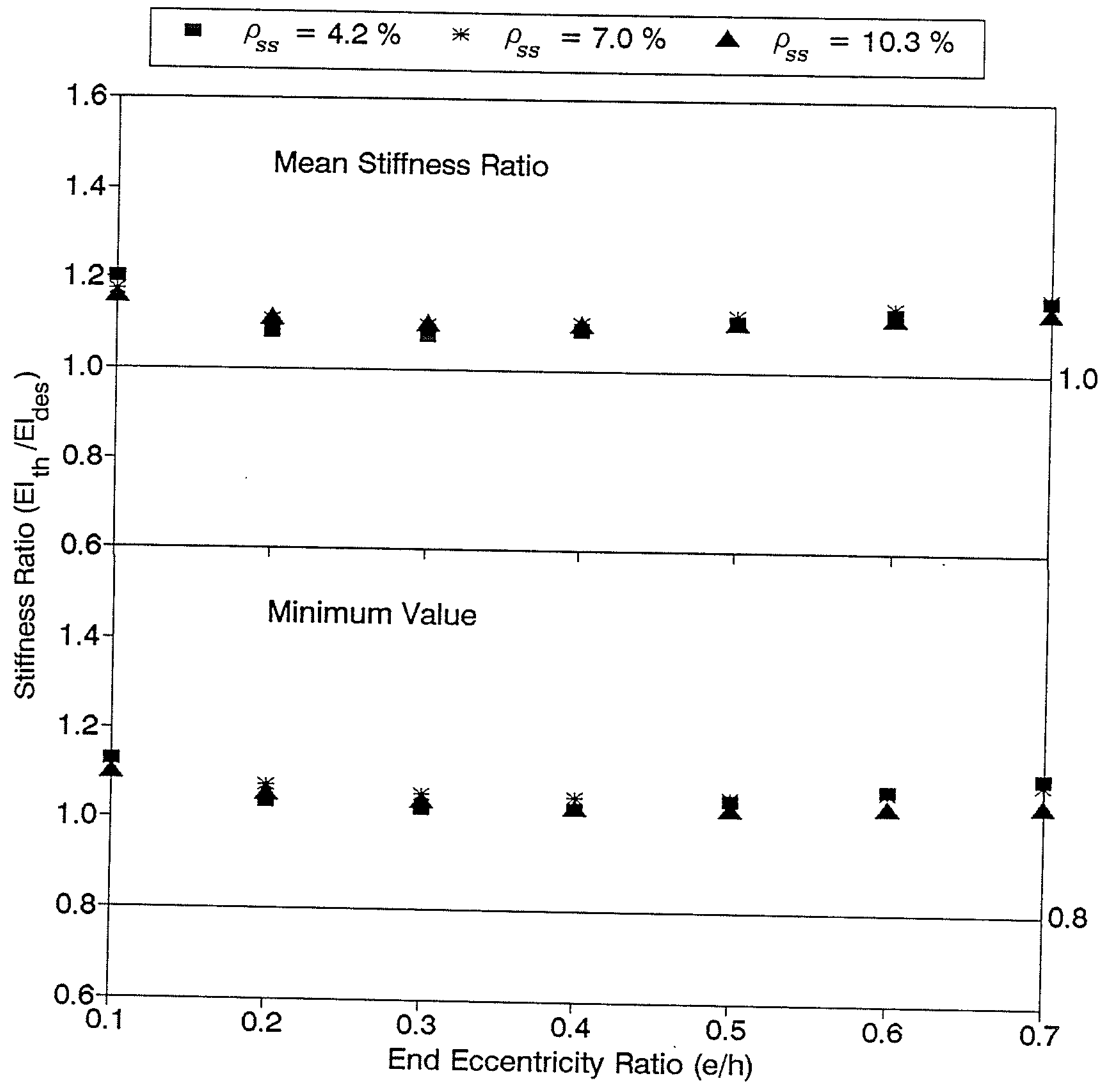

Figure 5.31(i) - Stiffness ratios obtained from proposed design Equation (5.8) for usual columns bending about major axis with ℓ/h = 30 (for each combination of e/h and ρ_{ss} ratios plotted n = 108 for ρ_{ss}=4.2 percent, n=72 when ρ_{ss}=7.0 percent and n=36 when ρ_{ss}=10.3 percent).

5.5 THEORETICALLY CALCULATED CRITICAL BUCKLING LOAD

The ratio of axial load acting on the column to critical buckling load, given as P_u/P_{cr}, is used by ACI (Equation 4.26) and AISC (Equation 4.11) to evaluate the second order effects of slenderness.

The frequency histogram and statistics shown in Figure 5.32 and Table 5.6 represent the critical load ratio $P_{u(th)}/P_{cr(th)}$ for 10800 columns with e/h ranging from 0.1 to 1.0. $P_{u(th)}$ is the computed theoretical axial load capacity and $P_{cr(th)}$ is calculated by substituting the computed theoretical effective flexural stiffness EI_{th} in Equation 2.4, yielding:

$$P_{cr(th)} = \frac{\pi^2 EI_{th}}{\ell^2} \tag{5.11}$$

Table 5.6 lists the mean value of 0.326, standard deviation of 0.177 and coefficient of variation of 0.544 for the range of critical load ratios shown in Figure 5.32. The critical load ratios of 0.4, 0.5, 0.6, 0.7 and 0.8 represent the 68th, 83rd, 92nd, 97th, and 99.9th percentiles, respectively, as indicated in Figure 5.32.

For design purposes, it is proposed that the mean value plus one standard deviation, 0.5, be used as the upper limit for P_u/P_{cr}. This means that 83 percent of the beam-columns used for plotting Figure 5.32 would be considered practical columns. The suggested upper limit of 0.5 for P_u/P_{cr} is plotted in Figures 5.33(a) and 5.33(b) to examine the effects

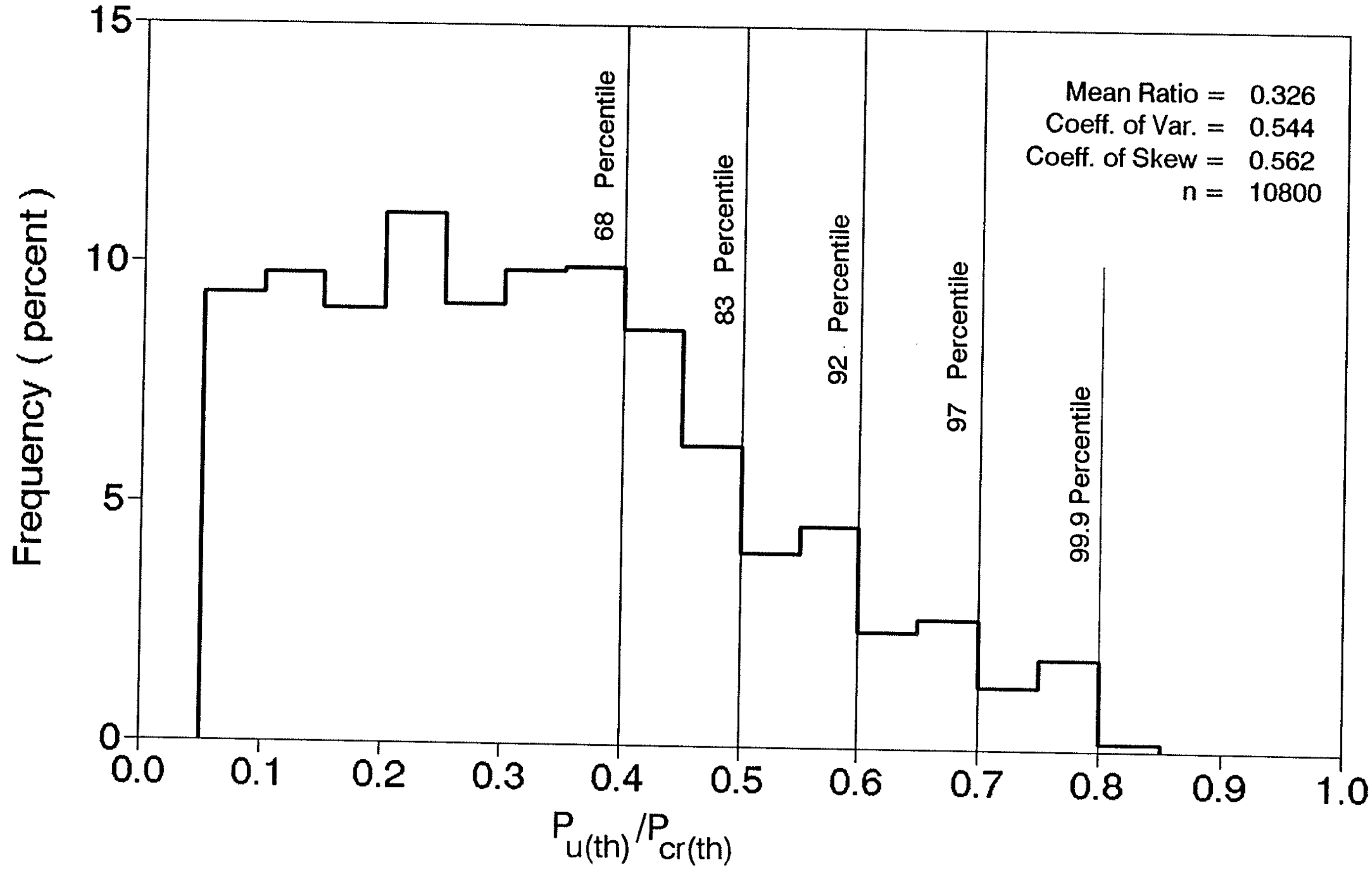

Figure 5.32 - Frequency histogram for critical load ratio for all columns bending about major axis other than those for which $e/h = 0.05$.

Table 5.6 - Statistics for critical load ratio $P_{u(th)}/P_{cr(th)}$

NUMBER OF COLUMNS STUDIED = 10800
COLUMNS WITH e/h = 0.05 NOT INCLUDED

STATISTICAL EVALUATION

MEAN-VALUE	STND-DEV.	COEF.VAR	COEF. SKEW.	KURTOSIS
0.32603	0.17721	0.54355	0.56240	2.65146

MIN-VALUE	MAX-VALUE	MEDIAN
0.05597	0.80593	0.30823

ONE-PERCENTILE	FIVE-PERCENTILE
0.06611	0.07960

MOMENTS ABOUT THE MEAN

2ND-MOMENT	3RD-MOMENT	4TH-MOMENT
0.3140179E-01	0.3129976E-02	0.2615016E-02

CUMULATIVE FREQUENCY TABLE

CLASS-NO.	LOWER-LIMIT	UPPER-LIMIT	%CUM-FREQ.	GROSS-NO.	%FREQ.	No.
1	0.00000	0.04999	0.00000	0	0.00000	0
2	0.05000	0.09999	9.35185	1010	9.35185	1010
3	0.10000	0.14999	19.12963	2066	9.77778	1056
4	0.15000	0.19999	28.15741	3041	9.02778	975
5	0.20000	0.24999	39.18518	4232	11.02778	1191
6	0.25000	0.29999	48.32407	5219	9.13889	987
7	0.30000	0.34999	58.18518	6284	9.86111	1065
8	0.35000	0.39999	68.13889	7359	9.95370	1075
9	0.40000	0.44999	76.76852	8291	8.62963	932
10	0.45000	0.49999	83.00926	8965	6.24074	674
11	0.50000	0.54999	87.02778	9399	4.01852	434
12	0.55000	0.59999	91.60185	9893	4.57407	494
13	0.60000	0.64999	94.02778	10155	2.42593	262
14	0.65000	0.69999	96.71296	10445	2.68519	290
15	0.70000	0.74999	98.00000	10584	1.28704	139
16	0.75000	0.79999	99.86111	10785	1.86111	201
17	0.80000	0.84999	100.00000	10800	0.13889	15
18	0.85000	0.89999	100.00000	10800	0.00000	0

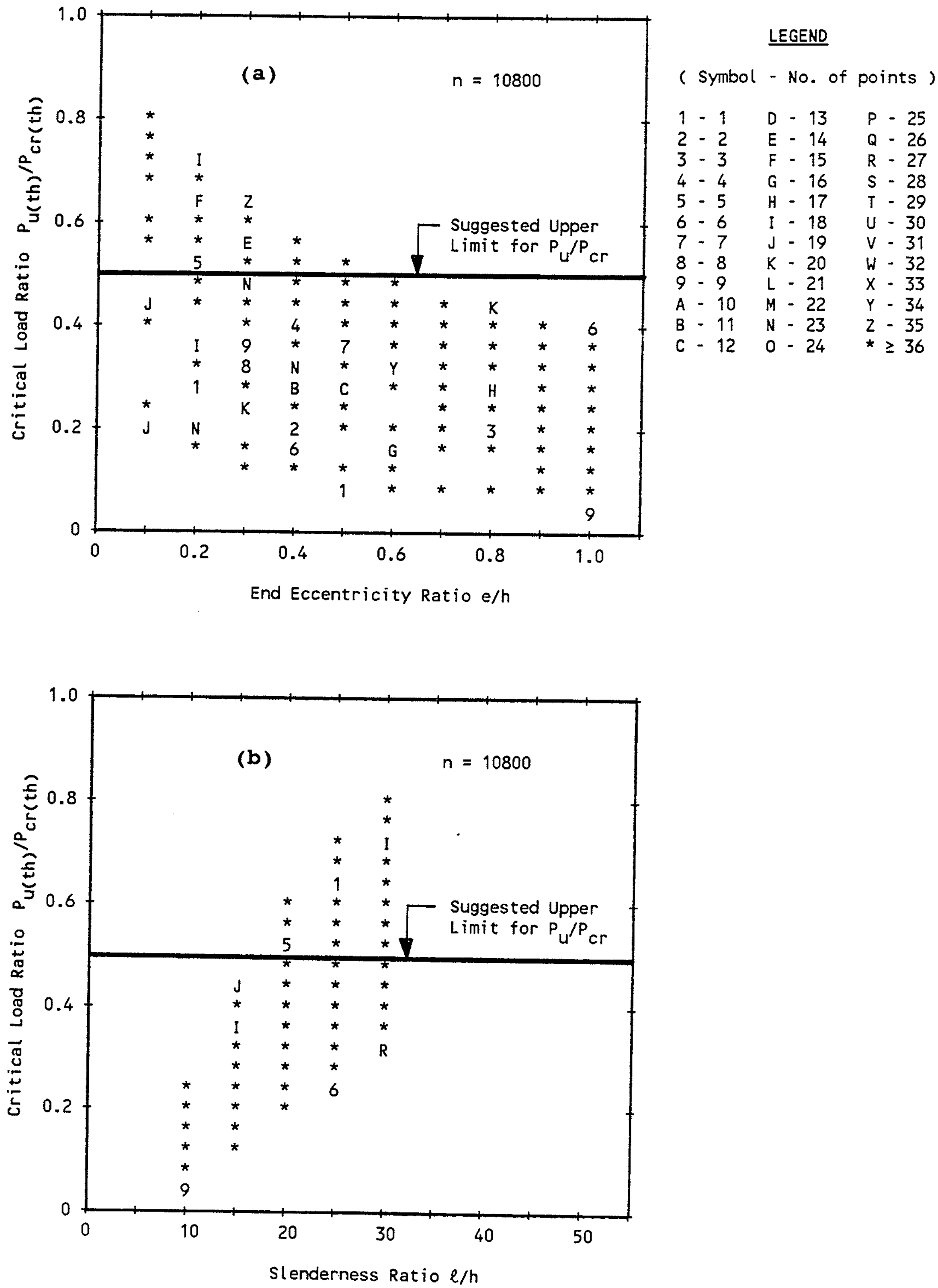

Figure 5.33 - Effect of (a) end eccentricity ratio and (b) slenderness ratio on critical load for all columns bending about the major axis other than those for which $e/h = 0.05$.

of e/h and ℓ/h on $P_{u(th)}/P_{cr(th)}$. Figures 5.33(a) and 5.33(b) indicate that some columns with low e/h, high ℓ/h, or both have $P_{u(th)}/P_{cr(th)}$ ratio greater than the suggested upper limit. This means that the suggested upper limit would control the design of very slender columns in lower storeys of high-rise buildings.

5.6 ANOTHER LOOK AT THE AISC EFFECTIVE STIFFNESS

The somewhat low stiffness ratios (EI_{th}/EI_{des}) obtained in some cases for the AISC expression (Equation 4.30) raised some concerns. This prompted a further examination of the AISC interaction equations.

A comparison of the ratios of the theoretical ultimate strength $P_{u(th)}$ to the AISC ultimate strength $P_{u(AISC)}$ was undertaken to assess the accuracy of the AISC interaction equations (Equation 4.16 and 4.17) used for predicting the beam-column strength. Figure 5.34(a) plotted from the data for all beam-columns studied shows that the probability distribution of the strength ratios yield a mean value of 1.31, coefficient of variation of 0.14, and one-percentile value of 1.01. This is clearly an improvement over the probability distribution properties of the stiffness ratios (mean value = 1.45, coefficient of variation of 0.23, and one-percentile value = 0.81) obtained from the same beam-column data and shown in Figure 5.2(b).

For the strength ratio data shown in Figure 5.34(b) for

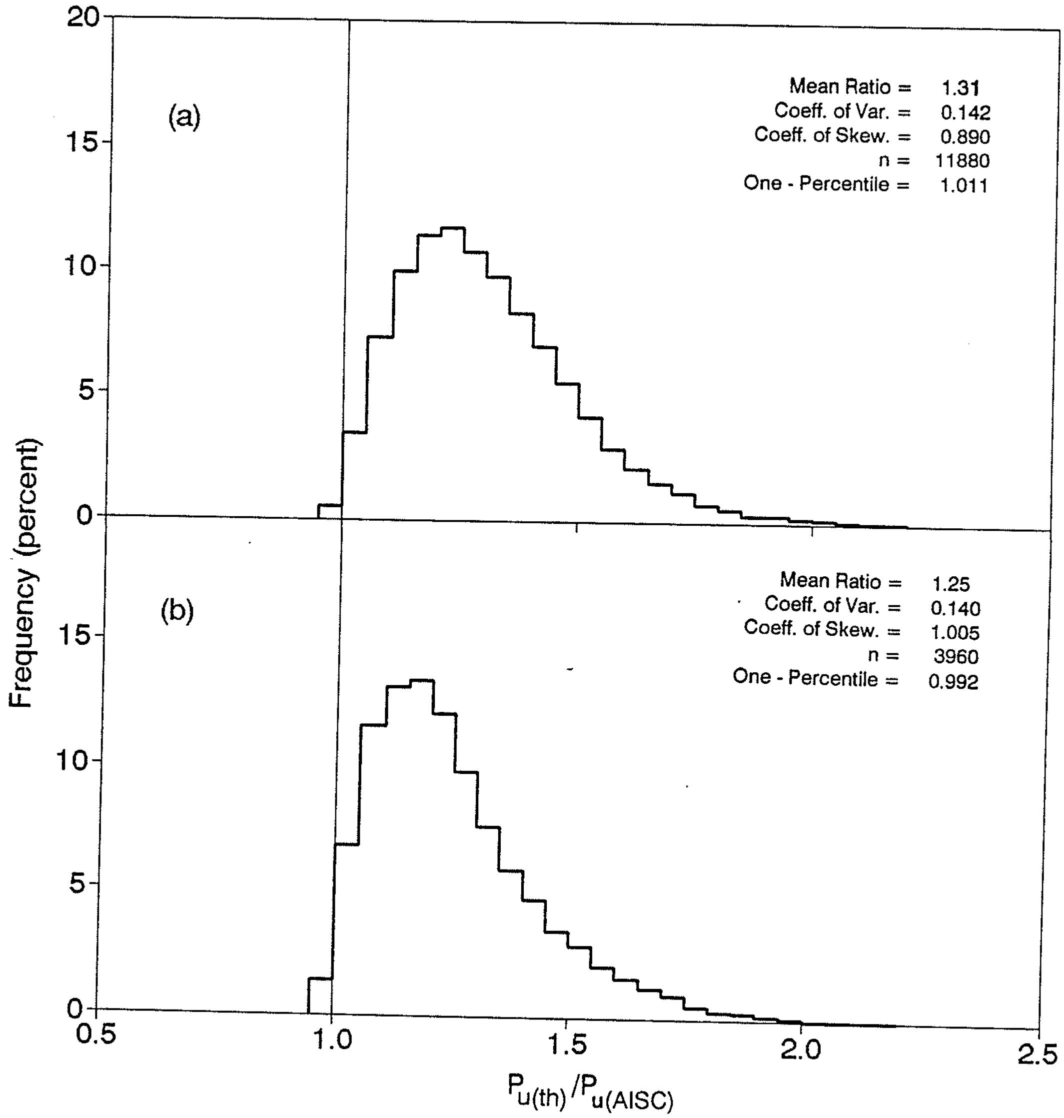

Figure 5.34 - Frequency histogram for ratio of theoretical ultimate strength to AISC ultimate strength for columns bending about the major axis: (a) ρ_{rs} = 1.09, 1.96 and 3.17 percent; and (b) ρ_{rs} = 1.09 percent.

beam-columns having only 1 percent of reinforcing steel, the mean value of 1.25, coefficient of variation of 0.14, and one-percentile value of 0.99 were obtained. Again, this is a considerable improvement over the comparable values (1.26, 0.23, and 0.77) shown in Figure 5.3(b) for stiffness ratios.

The above-noted differences in strength ratios and stiffness ratios are expected since the stiffness of a composite beam-column is more susceptible to concrete cracking and material nonlinearities than its strength.

Figures 5.35 and 5.36 show the strength ratios plotted against e/h for all the data and for data from beam-columns having ρ_{rs} of 1 percent. Both figures show mean, five-percentile and one-percentile values above 1.0, 0.86, and 0.80, respectively.

From the data plotted in Figure 5.34, 5.35, and 5.36 and the related discussion, it is concluded that the AISC method produces safe design for composite beam-columns subjected to bending about the major axis of the steel section.

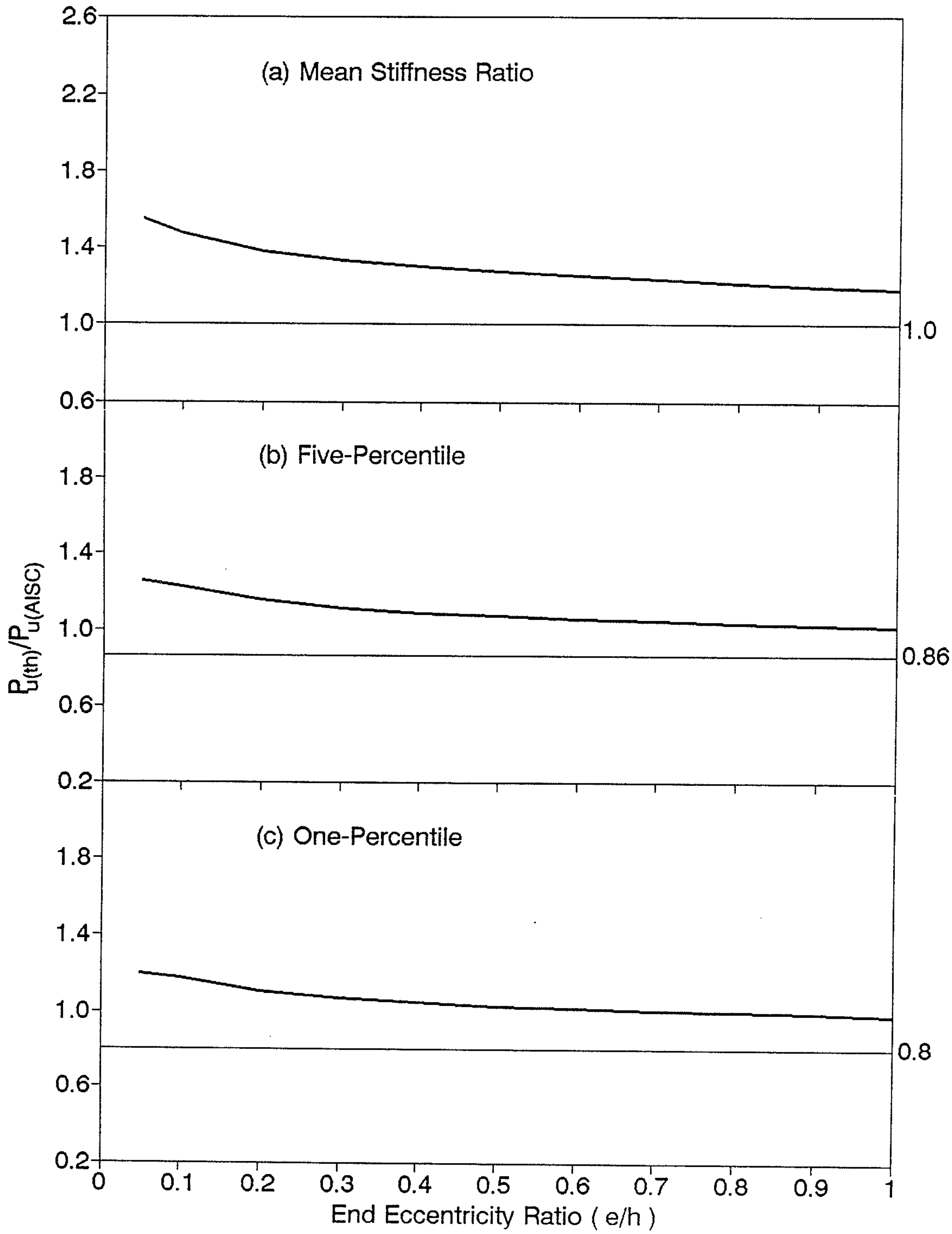

Figure 5.35 - Effect of end eccentricity ratio on ratio of theoretical ultimate strength to AISC ultimate strength for columns bending about the major axis (n = 1080 for each *e/h* ratio equal to 0.05, 0.1, 0.2, 0.3, 0.4, 0.5, 0.6, 0.7, 0.8, 0.9 and 1.0).

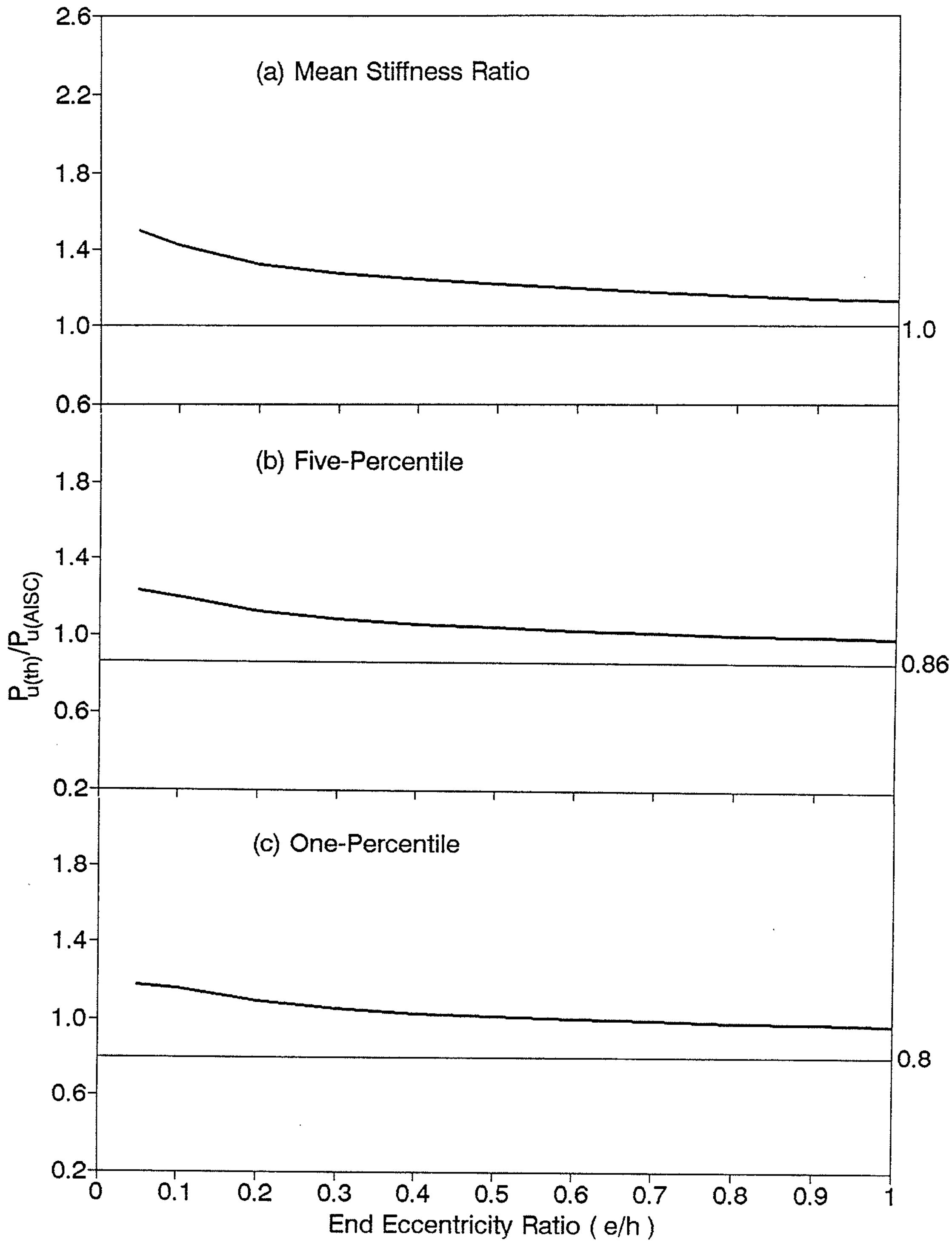

Figure 5.36 - Effect of end eccentricity ratio on ratio of theoretical ultimate strength to AISC ultimate strength for columns bending about the major axis where ρ_{rs} = 1.09 percent (n = 360 for each e/h ratio equal to 0.05, 0.1, 0.2, 0.3, 0.4, 0.5, 0.6, 0.7, 0.8, 0.9 and 1.0).

6 - EVALUATION OF EFFECTIVE STIFFNESS FOR BEAM-COLUMNS SUBJECTED TO MINOR AXIS BENDING

6.1 DESCRIPTION OF BEAM-COLUMNS STUDIED

To obtain a parametric study equivalent to the study of major axis bending, 11880 composite beam-columns were used to evaluate the theoretical stiffness of columns bending about the minor axis. Each column had a different combination of the specified properties. The specified nominal concrete strengths f'_c, the structural steel yield strengths f_{yss}, the reinforcing steel ratios ρ_{rs}, the structural steel ratios ρ_{ss} and the size of structural steel shapes used in this study are listed in Table 6.1. The values shown in the table represent the practical ranges of these variables used in the construction industry. The overall concrete cross-section had a size of 22 inches by 22 inches; the details of the cross-section are given in Figure 6.1.

The ACI and AISC Code requirements for composite columns influenced the selection of the cross section parameters used in this study. For composite beam-columns neither the ACI nor the AISC Code specifies a maximum amount for the structural steel core. However, the AISC Code states that to qualify as a composite column the structural steel ratio (ρ_{ss}) must be greater than or equal to 4 percent. The ACI Building Code requires that a minimum of 1 percent to a maximum of 8 percent of longitudinal reinforcing (ρ_{rs}) be included with the

Table 6.1 - Specified properties of composite beam-columns studied*

Properties	Specified Values	Number of Specified Values
f'_c , psi	4000; 5000; 6000; 8000	4
f_{yss} , psi	36000; 44000; 50000	3
ρ_{rs} , %	1.09; 1.96; 3.17	3
structural steel	section / ρ_{ss} , % W12 x 170 / 10.33 W12 x 120 / 7.29 W12 x 72 / 4.36 W10 x 112 / 6.80 W10 x 68 / 4.13 W8 x 67 / 4.07	6
ℓ/h	10; 15; 20; 25; 30	5
e/h	0.05; 0.1; 0.2; 0.3; 0.4; 0.5 0.6; 0.7; 0.8; 0.9; 1.0	11

* Total number of columns equals (4 x 3 x 3 x 6 x 5 x 11 =) 11880 with each column having a different combination of specified properties shown above. All columns had a cross section size of 22 x 22 in. with lateral ties conforming to ACI 318-89 Clause 10.14.8.

Note: 1.0 in. = 25.4 mm; 1000 psi = 6.895 MPa.

STEEL SECTION					LONGITUDINAL REINFORCING									
								Corner Rebars			Add'l Rebars		Total Area of Rebars	
Designation	A_{ss} (in.^{2})	b_f (in.)	d_{ss} (in.)	ρ_{ss} (%)	Y (in.)	Max. bar dia. for Z=1.0 in.	Max. bar dia. for lap	Bar Dia. (in.)	No. Req.	Clear Dist. Z (in.)	Bar Dia. (in.)	No. Req.	(in.^{2})	ρ_{rs} (%)
W12 x 170	50.0	14.03	12.57	10.33	1.99	1.90	1.72	1.693	4	1.342	1.000	8	15.32	3.17
(W310 x 253)								1.000	4	2.167	1.000	8	9.48	1.96
								0.750	4	2.465	0.750	8	5.28	1.09
W12 x 120	35.3	13.12	12.32	7.29	2.44	2.20	1.84	1.693	4	1.706	1.000	8	15.32	3.17
(W310 x 179)								1.000	4	2.540	1.000	8	9.48	1.96
								0.750	4	2.841	0.750	8	5.28	1.09
W12 x 72	21.1	12.25	12.04	4.36	2.88	2.60	1.98	1.693	4	2.097	1.000	8	15.32	3.17
(W310 x 107)								1.000	4	2.934	1.000	8	9.48	1.96
								0.750	4	3.236	0.750	8	5.28	1.09
W10 x 112	32.9	11.36	10.41	6.80	3.32	3.30	2.80	1.693	4	3.002	1.000	8	15.32	3.17
(W250 x 167)								1.000	4	11.521	1.000	8	9.48	1.96
								0.750	4	11.823	0.750	8	5.28	1.09
W10 x 68	20.0	10.40	10.13	4.13	3.80	3.70	2.94	1.693	4	3.427	1.000	8	15.32	3.17
(W250 x 101)								1.000	4	4.263	1.000	8	9.48	1.96
								0.750	4	4.565	0.750	8	5.28	1.09
W8 x 67	19.7	9.00	8.28	4.07	4.50	4.60	3.86	1.693	4	4.581	1.000	8	15.32	3.17
(W200 x 100)								1.000	4	5.417	1.000	8	9.48	1.96
								0.750	4	5.719	0.750	8	5.28	1.09

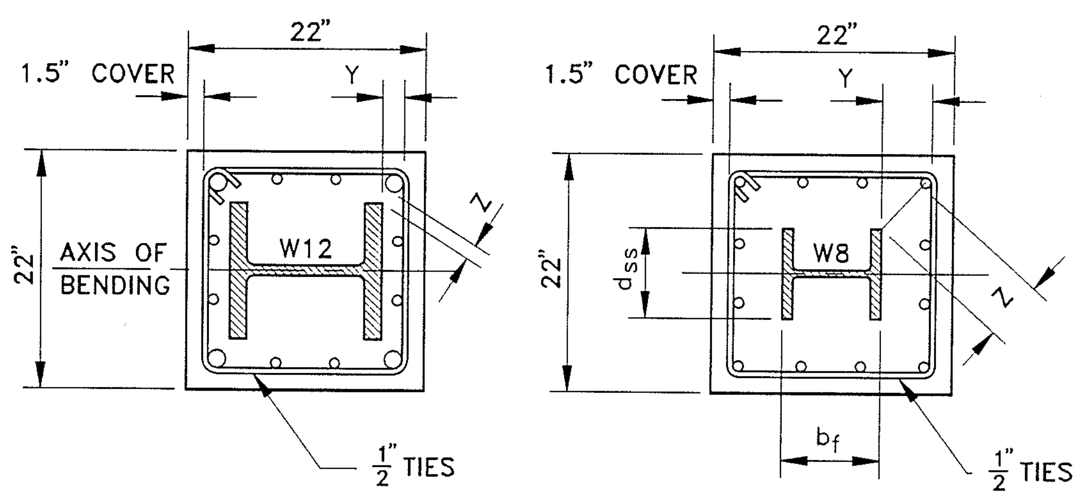

Figure 6.1 - Details of composite column cross-section for columns subject to bending about the minor axis.

structural steel core. Difficulty in lap splicing the reinforcing bars reduces the maximum limit of ρ_{rs} to about 3 to 4 percent when a relatively large structural steel core is encased. The reinforcing steel ratio is, therefore, usually expected to range from 1 to 3 percent. Even three percent reinforcing steel will restrict ρ_{ss} to a maximum of about 10 percent, giving a range of ρ_{ss} about 4 to 10 percent. The AISC Code (Chapter I, Section I2) specifies that f'_c be restricted to range from 3000 psi to 8000 psi and that the maximum yield strength for structural steel and reinforcing bars shall not exceed 55,000 psi in calculating the strength of the column. The ACI Building Code, on the other hand, specifies that f'_c shall not be less than 2500 psi (Clause 10.14.8.1) and that the design yield strength of the structural steel shall not exceed 50,000 psi (Clause 10.14.8.2), but no restriction is placed on the design yield strength of the reinforcing steel. With these requirements in mind, the strengths for concrete and structural steel shown in Table 6.1 were selected. The yield strength of the reinforcing bars was taken as 60 ksi for all of the cross section arrangements, because this represents the standard strength of reinforcing bars used in the construction industry. Figure 6.1 shows the cross section arrangements that were used in this study.

Utilizing six different sizes of structural steel shapes (Figure 6.1) provided the means to study the effect of concrete cover over the structural steel section. The ratio of the depth of the structural steel shape to the depth of the concrete cross-section d_{ss}/h was used as an index for concrete cover over structural steel.

Table 6.1 shows that eleven end eccentricity ratios e/h ranging from 0.05 to 1.0 were used. This is consistent with the findings of Mirza and MacGregor (1982) that, for reinforced concrete buildings, e/h usually varies from 0.1 to 0.65. Five slenderness ratios ℓ/h were chosen to represent the range of ℓ/h for columns in braced frames designed in accordance with ACI 318-89 Clause 10.11.

As the purpose of this study is to simulate the actual stiffness EI of beam-columns described by nominal cross-sectional properties, the specified nominal values for material strength and cross-sectional properties will not provide an accurate estimation of EI. Mean values established by Skrabek and Mirza (1990) corresponding to the nominal specified properties were, therefore, used to compute the theoretical stiffness for each column. Table 6.2 lists the mean values corresponding to the specified nominal values.

The short-term theoretical effective flexural stiffness EI for each of the 11,880 columns studied was computed using Equation 2.7, the cross-section and slender column interaction diagrams described in Section 2.2, and the mean values of the variables specified in Table 6.2. The simulated column stiffness data were then statistically analyzed for examining the current ACI column stiffness, the equivalent AISC column

Table 6.2 - Mean Values of Variables Used for Computing Theoretical Strength and Stiffness.

(a) Concrete

Nominal Strength f'_c (psi)	Mean Values		
	Compressive Strength f_c (psi)	Modulus of Rupture f_r (psi)	Elastic Modulus E_c (ksi)
4,000	3,388	445	3,260
5,000	4,013	485	3,537
6,000	4,641	523	3,795
8,000	5,904	591	4,263

(b) Structural Steel Strength*

Nominal Strength f_y (psi)	Mean Values	
	Static Yield Strength	
	Web f_{ysw} (psi)	Flange f_{ysf}
36,000	39,240	0.95 f_{ysw}
44,000	47,960	0.95 f_{ysw}
50,000	54,500	0.95 f_{ysw}

(c) Residual Stresses in Structural Steel

Steel Shape	Flange Tip (psi)	Flange - web Juncture (psi)
W12 x 170 (W310 x 253)	-18,367	11,792
W12 x 120 (W310 x 179)	-17,983	11,267
W12 x 72 (W310 x 107)	-17,896	11,152
W10 x 112 (W250 x 167)	-18,576	12,089
W10 x 68 (W250 x 101)	-18,384	11,816
W8 x 67 (W200 x 100)	-18,465	11,931

* Note: Modulus of Elasticity for Structural Steel, E_s = 29,000 ksi

Table 5.2 - continued

(d) Structural Steel Dimensions

	Section Depth d	Flange Width b	Flange Thickness t	Web Thickness w
Ratio of Actual to Specified Dimensions	1.000	1.005	0.976	1.017

(e) Reinforcing Steel

Nominal Strength f_y (psi)	Static Yield Strength f_{ys} (psi)	Elastic Modulus E_s (ksi)
60,000	66,800	29,000

(f) Deviation of Overall Beam-Column Dimensions from Nominal Specified Dimensions

Length (in.)	0.0
Cross-Section Depth (in.)	+0.06
Cross-Section Width (in.)	+0.06
Concrete Cover to Lateral Ties (in.)	+0.33
Spacing of Lateral Ties (in.)	0.0

stiffness, and for developing the proposed design equations for *EI*.

Note that the specified nominal values listed in Table 6.1 and the mean values for material properties and cross section descriptions listed in Table 6.2 are the same as those given in Chapter 5. The only difference between the columns described in Chapters 5 and 6 is the 90 degree rotation of the axis of bending.

6.2 EXAMINATION OF ACI AND AISC STIFFNESSES

The ACI Building Code and the comparable AISC Code equivalent flexural stiffnesses (Equation 4.1 and 4.30 described in Chapter 4) were compared with the theoretical *EI* data generated for all of the 11,880 composite columns subjected to bending about the minor axis of the steel section. The nominal values of variables shown in Table 6.1 and Figure 6.1 were used for computing the ACI and AISC *EI* values. Note the theoretical *EI* values were computed using the mean values of variables shown in Table 6.2.

The histograms in Figure 6.2 show the ratios of theoretical *EI* to design *EI* (EI_{th}/EI_{des}). The results shown in Figure 6.2 (a) were computed based on EI_{des} taken equal to the ACI *EI* equation (Equation 4.1) and those shown in Figure 6.2(b) were based on EI_{des} set equal to AISC *EI* expression (Equation 4.30). Figure 6.2 that includes data for all ρ_{rs} values (1.09, 1.96, 3.17 percent) indicates that relatively

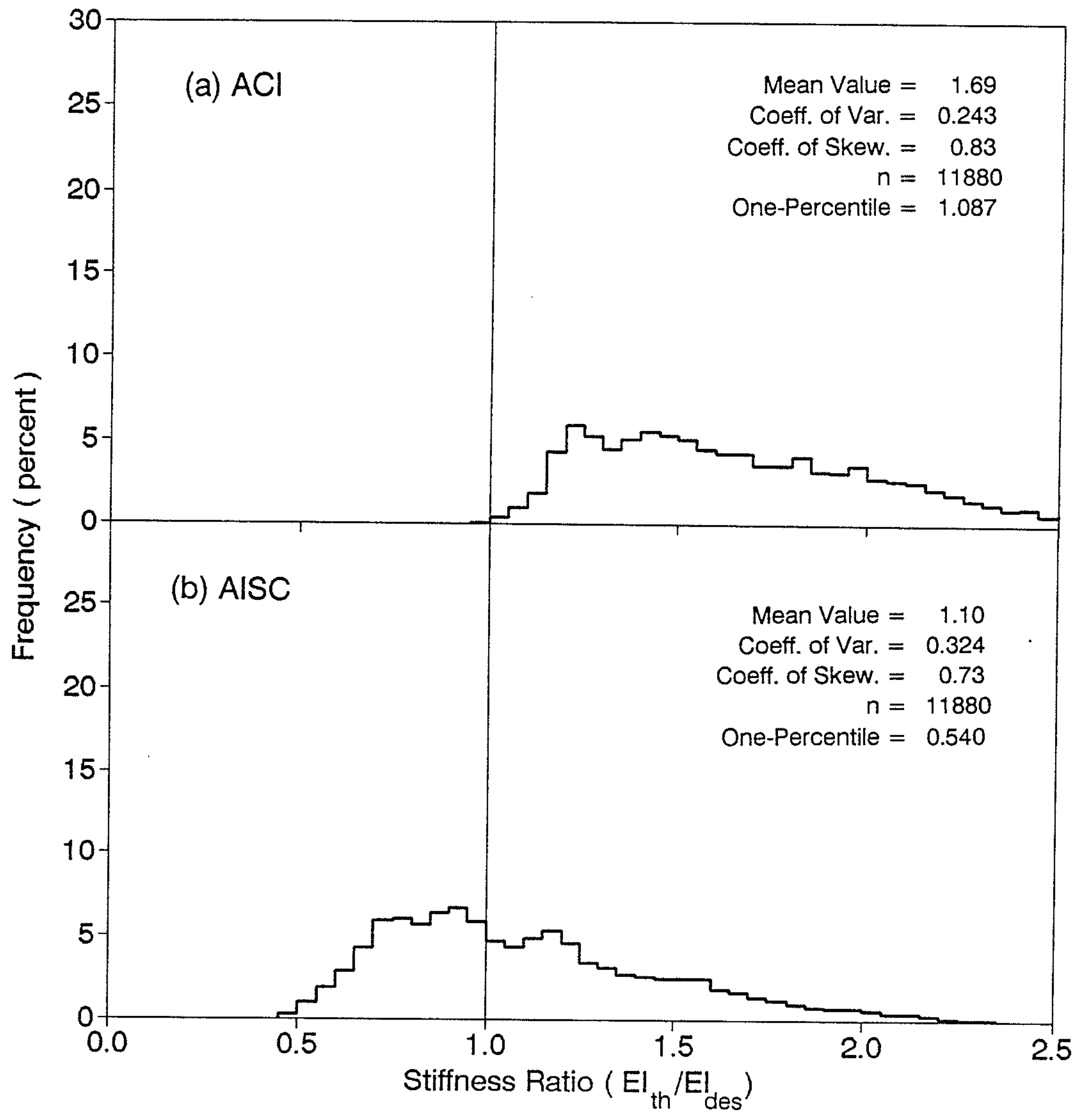

Figure 6.2 - Frequency histogram comparing ACI and AISC stiffness equations with theoretical results for all columns bending about minor axis.

high mean stiffness ratios and coefficients of variation (*CV*) are obtained from the ACI equation (mean value = 1.69, *CV* = 24.3 percent for Equation 4.1). This means that the ACI equation on the average predicts conservative *EI* values, which are about 70 percent lower than the theoretically computed values, but the ACI *EI* values deviate substantially from the corresponding theoretically computed values for a significant number of columns studied. The AISC expression, on the other hand, gives a mean value that is much closer to 1.0 than the ACI, but also gives a large coefficient of variation and extremely low one-percentile value (mean value = 1.10; *CV* = 32.4 percent; and one-percentile = 0.540 for Equation 4.30).

A second comparison showing only the data where ρ_{rs} = 1 percent was plotted in Figure 6.3 for both the ACI and AISC stiffnesses. Mean values of 1.42 and 0.91 were obtained for ACI and AISC, respectively, along with coefficients of variation similar to those in Figure 6.2. This significant change in mean value indicates that the ACI and AISC design equations were most likely calibrated for the minimum required reinforcing steel ratio. This also appears to confirm the general belief that ACI equation is, in most cases, on the safe side. For the AISC, however, a mean stiffness ratio less than 1.0 in Figure 6.3(b) and extremely low one percentile values (0.540 and 0.507) in Figures 6.2(b) and 6.3(b) indicate that the AISC design expression gives non-conservative results for a large number of cases. Mirza (1990) pointed out that

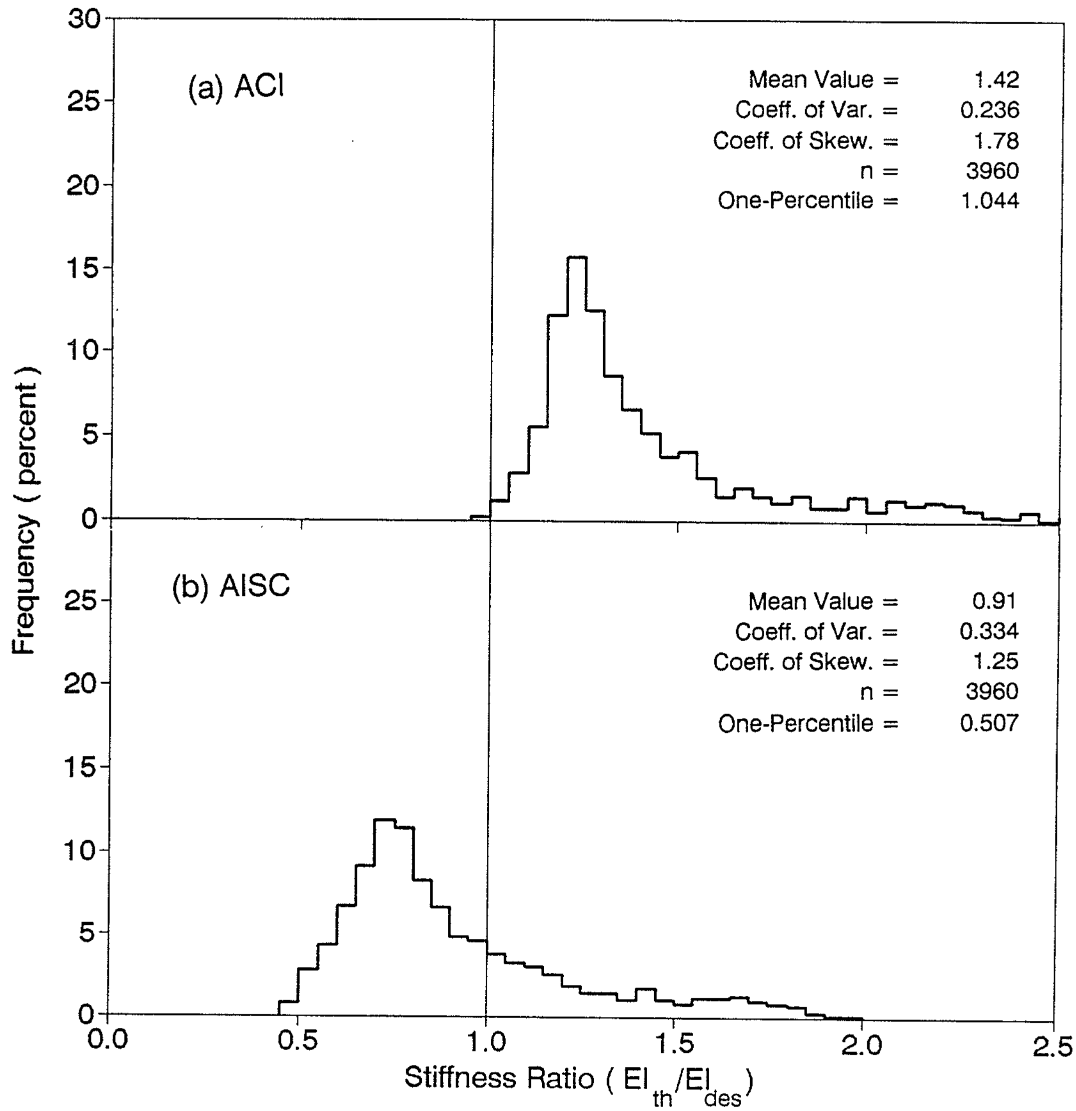

Figure 6.3 - Frequency histogram comparing ACI and AISC stiffness equations with theoretical results for columns bending about minor axis where ρ_{rs} = 1.09 percent.

for establishing safety into design equations the one-percentile value is more important than the mean value.

Note the ACI and AISC design equations do not include all the parameters that affect the stiffness of slender columns. The ACI equation does not account for the longitudinal reinforcing steel whereas the AISC design equations modify the properties of a composite column to that of an "equivalent steel" column in which cracking of the concrete is not considered.

It is evident from Figures 6.2 and 6.3 and the related discussions that there appears to be a need for modification in the existing ACI stiffness equation and AISC strength interaction equations used for the design of composite beam-columns.

6.3 DEVELOPMENT OF PROPOSED DESIGN EQUATIONS FOR SHORT-TERM EI

Mirza (1990) among others pointed out that the effective flexural stiffness of a slender reinforced concrete column is significantly affected by cracking along its length and inelastic actions in the concrete and reinforcing steel. This is also expected for a composite column although to a lesser degree, because the structural steel core is expected to stiffen the concrete cross-section. However, the inelastic actions within the encased structural steel shape affect the overall stiffness of a composite column. *EI* is then represented by a complex function of a number of variables that cannot be readily transformed into a unique and simple analytical solution. The objective in this study is to develop simple equations for *the EI* of composite columns subjected to bending about the minor axis of the steel section. These equations are similar to the ones that were produced in Chapter 5 and those developed by Mirza (1990) for reinforced concrete columns. Multiple linear regression analysis was chosen to evaluate *EI* from the generated theoretical stiffness data.

6.3.1 Variables Used for Regression Analysis

The variables used in this study were divided into two major groups: (A) variables that affect the contribution of concrete to the overall effective stiffness; and (B) variables that influence the contribution of structural and reinforcing steel to the overall effective stiffness of a composite beam-column.

Group A consists of five subgroups, similar to those described by Mirza(1990): (1) end eccentricity ratio e/h or P_u/P_o (subgroup X_1), in which P_u is the factored axial load acting on the slender column and P_o is the pure axial load capacity of the cross-section; (2) slenderness ratio ℓ/h or ℓ/r (subgroup X_2), where r is the radius of gyration calculated according to the ACI Building Code Equation (10-13) reproduced here as Equation 6.1; (3) steel index ρ_{ss}, or ρ_{rs}, or $\rho_g = (\rho_{ss} + \rho_{rs})$, or ρ_{rs}/ρ_{ss}, or $\rho_{ss}f_{yss}/f'_c$, or $\rho_{rs}f_{yrs}/f'_c$, or $(\rho_{ss}f_{yss} + \rho_{rs}f_{yrs})/f'_c$ (subgroup X_3), where ρ_g is the total steel ratio and f_{yrs} is the specified yield strength of the reinforcing steel; (4) stiffness index I_{rs}/I_{ss}, or I_{ss}/I_g, or I_{rs}/I_g, or $(I_{ss} + I_{rs})/I_g$ (subgroup X_4) where I_g = the moment of inertia of the gross concrete cross-section neglecting structural and reinforcing steel; and (5) concrete cover index d_{ss}/h (subgroup X_5) where d_{ss}, the depth of the structural steel section, is divided by the overall depth of the composite cross-section perpendicular to the axis of bending being considered.

$$r = \sqrt{\frac{(E_c I_g/5) + E_s I_{ss}}{(E_c A_g/5) + E_s A_{ss}}} \qquad (6.1)$$

In Equation 6.1, A_g equals the area of the gross concrete cross-section neglecting structural and reinforcing steel and A_{ss} equals the gross cross-sectional area of the structural steel section. The Group A variables are listed in Table 6.3.

Group B, on the other hand, consists of two variables, E_sI_{ss} and E_sI_{rs}, that were considered to have a significant affect on the overall effective stiffness of a composite column.

Mirza and MacGregor (1989) found that for reinforced concrete slender columns the variables in the first and second

Table 6.3 - Variable combinations used for regression analysis - Minor Axis Bending

Variable Combination Number	Group "A" Variables: X_1 End Eccentricity Ratio		X_2 Slenderness Ratio		X_3 Steel Index							X_4 Stiffness Index				X_5 Concrete Cover Index	Standard Error	Multiple Correlation Coefficient
	e/h	P_u/P_o	ℓ/h	ℓ/r	ρ_{ss}	ρ_{rs}	ρ_g	$\frac{\rho_{rs}}{\rho_{ss}}$	$\frac{\rho_{ss} f_{yss}}{f'_c}$	$\frac{\rho_{rs} f_{yrs}}{f'_c}$	(11)+(12)	$\frac{I_{rs}}{I_{ss}}$	$\frac{I_{ss}}{I_g}$	$\frac{I_{rs}}{I_g}$	$\frac{I_{rs}+I_{ss}}{I_g}$	d_{ss}/h	S_e^*	R_c
(1)	(2)	(3)	(4)	(5)	(6)	(7)	(8)	(10)	(11)	(12)	(13)	(14)	(15)	(16)	(17)	(18)	(19)	(20)
1	X		X					X						X		X	0.047	0.912
2	X		X					X						X			0.047	0.911
3	X		X					X				X					0.048	0.909
4	X		X					X					X				0.047	0.912
5	X		X					X							X		0.047	0.912
6	X		X					X									0.048	0.908
7	X		X		X												0.048	0.910
8	X		X			X											0.047	0.911
9	X		X				X										0.047	0.911
10	X		X						X								0.048	0.910
11	X		X							X							0.047	0.911
12	X		X								X						0.048	0.911
13	X		X														0.048	0.908
14	X			X													0.048	0.908
15		X	X														0.049	0.903
16		X		X													0.049	0.903
17	X																0.050	0.901
18		X															0.061	0.847
19			X														0.079	0.724
20				X													0.079	0.724
21						X											0.080	0.719
22								X									0.080	0.715
23													X				0.080	0.720
24														X			0.080	0.719
25																X	0.080	0.716

* S_e was computed for the constant α_k.

subgroup of group A are important in the study of the strength and behaviour of slender columns. Mirza (1990) verified this in his analysis of the flexural stiffness of rectangular reinforced concrete columns. The third subgroup variables of Group A took into consideration the influence of the quantity of steel in proportion to the area of concrete cross-section. The fourth subgroup was intended to examine the effects of relative stiffnesses of steel and concrete. The fifth and final subgroup of Group A was included to investigate the effect of concrete cover to the structural steel shape on column stiffness.

The variables within an individual subgroup of Group A were considered as dependent variables, while variables between the subgroups were taken as independent variables. For example, e/h was considered dependent on P_u/P_o but was taken independent of variables related to slenderness ratio, steel index, stiffness index, and concrete cover index. The variables of Group B were always considered independent variables. A maximum of one variable from any of the chosen subgroups of Group A was, therefore, used for a particular regression analysis of the theoretical stiffness data. When one variable from each subgroup of Group A and both variables from Group B are included into the regression analysis, Equation 2.2 becomes:

$$EI = (\alpha_k + \alpha_1 X_1 + \alpha_2 X_2 + \alpha_3 X_3 + \alpha_4 X_4 + \alpha_5 X_5) E_c (I_g - I_{ss}) + \alpha_{ss} E_s I_{ss} + \alpha_{rs} E_s I_{rs} \quad (6.2a)$$

in which α_k is a constant (equivalent to the intercept of a simple linear equation). The remaining α values are dimensionless reduction factors corresponding to independent variables X_1, X_2, X_3, X_4, X_5, E_sI_{ss} and E_sI_{rs}. X_1 through X_5 represent one variable chosen from each of the subgroups (i.e. end eccentricity ratio, slenderness ratio, steel index, stiffness index, and concrete cover index) in Group A.

The combination of Group A variables used for different regression analyses are given in Table 6.3. Group B variables were included in all regression analyses shown in Table 6.3.

The prediction accuracy for a particular regression equation was based on the standard error S_e, a measure of sampling variability, and the multiple correlation coefficient R_c, an index of relative strength of the relationship. The smaller the value of S_e the smaller the sampling variability of the regression equation. An R_c value equal to zero signifies no correlation, and $R_c = \pm 1.0$ indicates 100 percent correlation. R_c values greater than +1.0 and less than -1.0 are not possible. The calculated values of S_e and R_c for each regression analysis are also given in Table 6.3. To reduce the relative magnitude of the standard error S_e, both sides of Equation 6.2a were divided by $E_c(I_g - I_{ss})$ to "normalize" the Equation. This also allowed the S_e obtained in this study to be compared to the S_e obtained by Mirza (1990) for reinforced concrete columns. The normalized version of Equation 6.2a is shown in Equation 6.2b.

$$\frac{EI}{E_c(I_g - I_{ss})} = \alpha_k + \alpha_1 X_1 + \alpha_2 X_2 + \alpha_3 X_3 + \alpha_4 X_4 + \alpha_5 X_5 + \alpha_{ss}\frac{E_s I_{ss}}{E_c(I_g - I_{ss})} + \alpha_{rs}\frac{E_s I_{rs}}{E_c(I_g - I_{ss})} \tag{6.2b}$$

Note that S_e in this study was computed for α_k.

6.3.2 Regression Analysis

Table 6.3 shows the S_e and R_c values calculated for 25 regression equations. The insignificant changes in S_e and R_c for the first thirteen variable combinations indicate that variables other than those used in combination 13 (e/h and ℓ/h) do not significantly influence the EI of slender composite columns. A correlation analysis confirmed that this was due to the fact that the variables in subgroups X_3 and X_4 were included explicitly or implicitly in the format of the regression equations, Equations 6.2a and 6.2b.

Variable combinations 13 to 16 involving e/h, P_u/P_o, ℓ/h, and ℓ/r proved that e/h and ℓ/h (or ℓ/r) are the most significant pair of variables from Group A influencing EI. The ratios ℓ/h and ℓ/r are obviously correlated, however, ℓ/h is much simpler to compute. A correlation analysis of the variables used in combinations 13 to 16, including the Group B variables, confirmed Mirza's observation indicating that: (a) no correlation exists between e/h and ℓ/h (or ℓ/r) ratios; (b) there is some correlation between P_u/P_o and ℓ/h (or ℓ/r) ratios; and (c) a strong correlation exists between P_u/P_o and e/h ratios. This means that e/h and ℓ/h (or ℓ/r) are independent variables and P_u/P_o is dependent on e/h.

Finally, combinations 17 through 25 show that when only one of the variables in Group A was combined with the two variables in Group B, e/h is the most significant variable from Group A.

In summary, the lowest S_e and highest R_c values among the regression equations concerning two variables and one variable from Group A, combined with the two variables from Group B, were obtained for variable combinations 13 and 17, respectively. The resulting regression equations are:

$$EI = (0.334 + 0.00185\ \ell/h - 0.204\ e/h)\ E_c(I_g - I_{ss}) + 0.808 E_s I_{ss} + 0.732 E_s I_{rs} \qquad (6.3)$$

$$EI = (0.371 - 0.204\ e/h)\ E_c(I_g - I_{ss}) + 0.808 E_s I_{ss} + 0.732 E_s I_{rs} \qquad (6.4)$$

Equations 6.3 and 6.4 are similar in format to regression Equations 5.3 and 5.4 developed for beam-columns subjected to major axis bending (Chapter 5) and Equations 6.5 and 6.6 developed by Mirza (1990) for reinforced concrete columns.

$$EI = (0.294 + 0.00323\ \ell/h - 0.299\ e/h)\ E_c I_g + E_s I_{rs} \qquad (6.5)$$

$$EI = (0.358 - 0.299\ e/h)\ E_c I_g + E_s I_{rs} \qquad (6.6)$$

Equations 6.3 to 6.6 show that with an increase in e/h ratio there is a corresponding decrease in EI for a column. This is because an increase in e/h means a corresponding increase in bending moment and tension stresses at the outer fibre, resulting in more cracking of the column. The coefficient of

0.204 associated with e/h in Equations 6.3 and 6.4 for composite columns is about 2/3 of that in Equations 6.5 and 6.6 for reinforced concrete columns. This is due to the structural steel shape in composite columns interrupting the continuity of the cracks that remain unarrested in reinforced concrete columns. Equations 6.3 and 6.5 indicate that for an increase in ℓ/h ratio there is an increase in EI. Mirza (1990) suggests that this is because in a longer column the cracks are likely to be more widely spaced with more concrete in between the cracks contributing to the EI of the column. The coefficients of 0.808 and 0.732 related to E_sI_{ss} and E_sI_{rs}, respectively, in Equations 6.3 and 6.4 compare to the values of corresponding coefficients obtained for Equations 5.3 and 5.4 (Chapter 5 for columns subjected to major axis bending). These coefficients indicate "softening" of structural and reinforcing steel. This is the result of elastic-plastic nature of the stresses developed in the structural steel and the reinforcing steel at ultimate load.

For composite columns S_e = 0.048 and R_c = 0.908 were obtained for Equation 6.3. This compares to an S_e = 0.050 and R_c = 0.964 obtained for Equation 5.3 for columns subjected to major axis bending and S_e = 0.058 and R_c = 0.86 reported by Mirza (1990) for Equation 6.5. For the second composite column equation (Equation 6.4) S_e equals 0.050 and R_c equals 0.901. The corresponding values for Equation 5.4 were 0.056 and 0.955 and those reported by Mirza (1990) for Equation 6.6

were 0.061 and 0.84.

A scatter diagram (Figure 6.4) shows the values of *EI* computed from Equations 6.3 and 6.4 plotted against the corresponding theoretical *EI*. Regression *EI* from Equation 6.3 is shown in Figure 6.4 (a), and Figure 6.4 (b) is for Equation 6.4. Both equations exhibit reasonable correlation with the theoretical *EI* values when compared to the line of unity labelled as 45° line. Equation 6.3 produced somewhat, but not very significantly, better results.

The histograms and related statistical data for the ratio of theoretical *EI* to regression *EI* (EI_{th}/EI_{reg}) developed from all the columns studied (n = 11,880) are virtually identical for Equations 6.3 and 6.4, as shown in Figure 6.5. EI_{reg} in Figure 6.5(a) was taken from Equation 6.3 and that in Figure 6.5(b) from Equation 6.4. Both equations give mean values of 1.00. The coefficient of variation (*CV*) for Equation 6.3 is 0.095 and 0.097 for Equation 6.4. This represents a very significant improvement when compared to mean values of 1.69 and 1.10 and *CV* of 0.243 and 0.324 shown in Figure 6.2 obtained for ACI and AISC equations, respectively.

The histograms and statistical data for the columns where the longitudinal reinforcement ratio (ρ_{rs}) is one percent (n=3960), shown in Figure 6.6, again indicates that the two equations give almost the same results. Both equations give mean values of 0.99. The *CV* for Equation 6.3 is 0.114 and 0.117 for Equation 6.4. This still represents a very

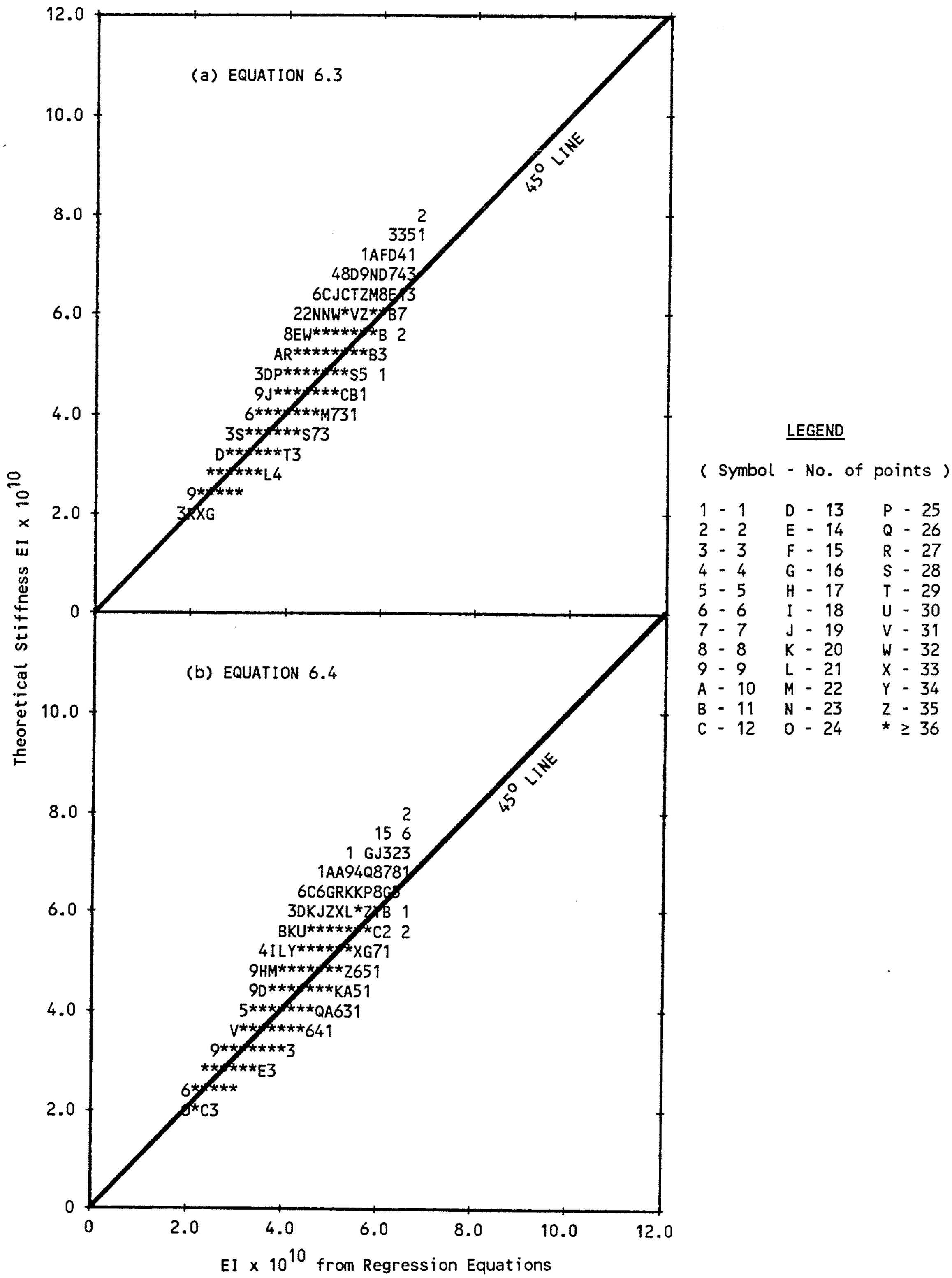

Figure 6.4 - Comparison of selected regression equations with theoretical data for all columns bending about minor axis.

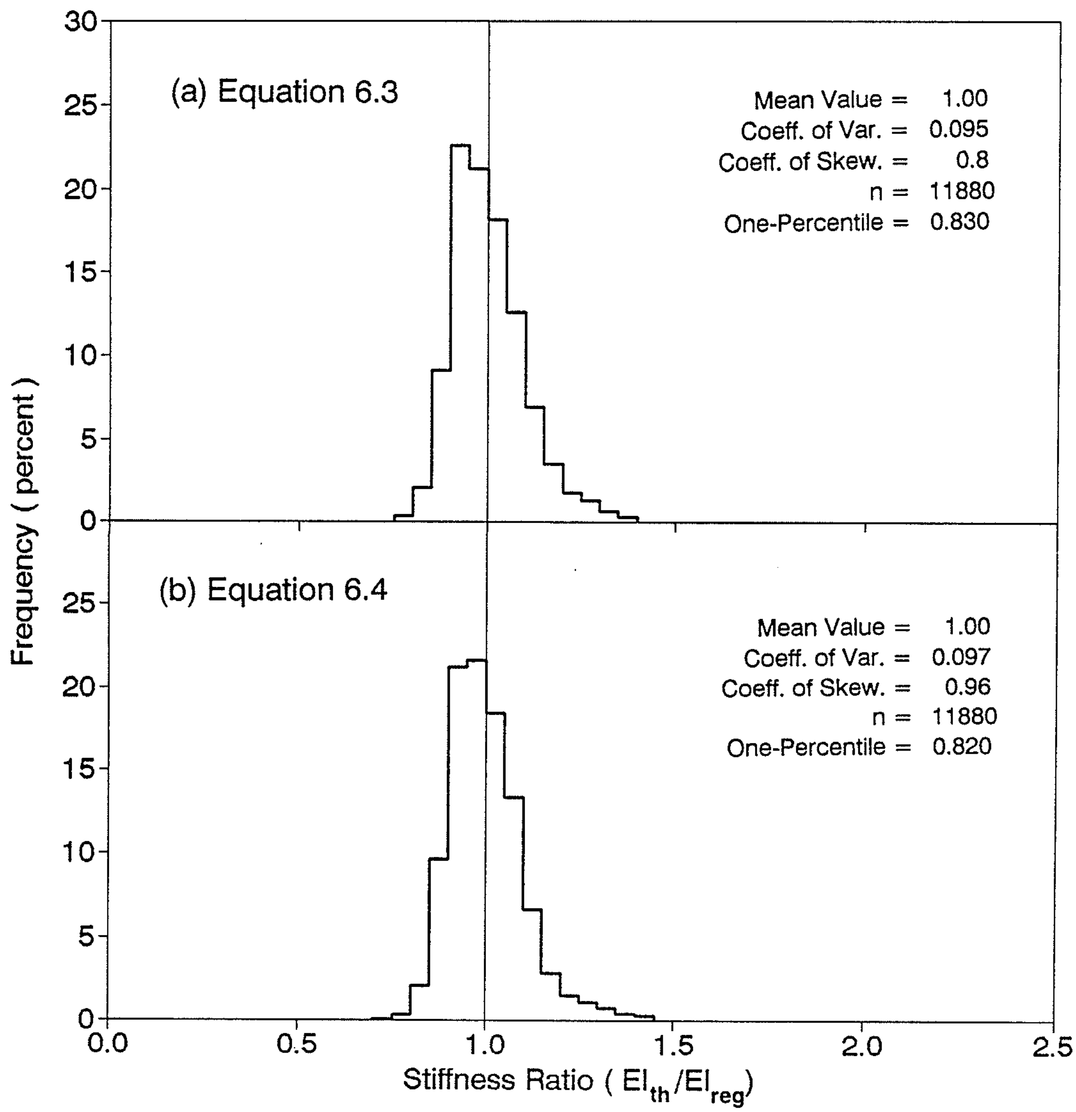

Figure 6.5 - Frequency histograms comparing selected regression equations with theoretical data for all columns bending about minor axis.

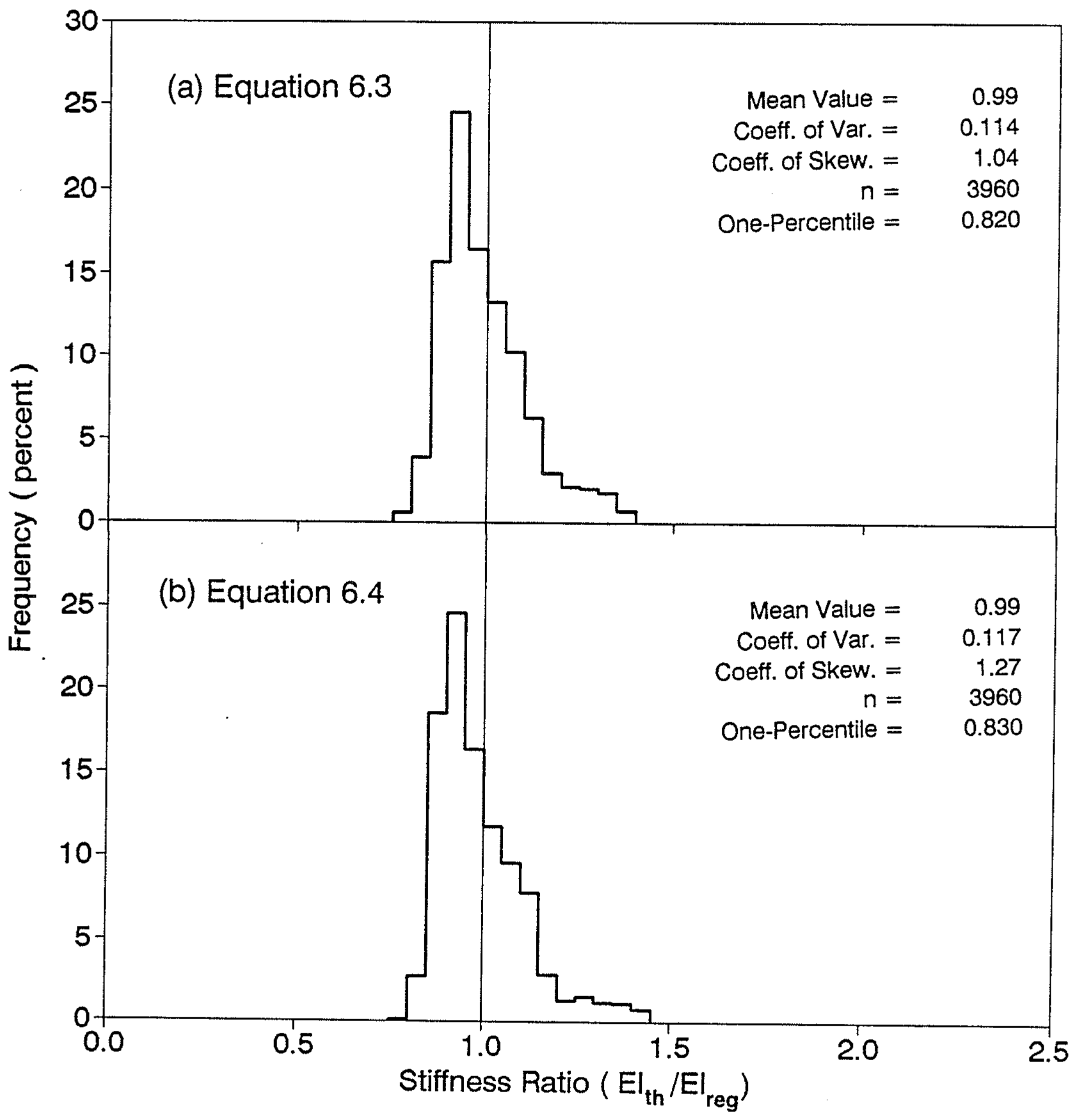

Figure 6.6 - Frequency histograms comparing selected regression equations with theoretical data for columns bending about minor axis where ρ_{rs} = 1.09 percent.

significant improvement over the mean values of 1.42 and 0.91, and the coefficients of variation of 0.236 and 0.334 obtained from the ACI and AISC stiffness equations shown in Figure 6.3.

6.3.3 Proposed Design Equations

Equations 6.7 and 6.8, proposed for design use, were simplified from Equation 6.3 and 6.4 and were chosen to be identical to Equation 5.7 and 5.8 (Chapter 5) proposed for composite beam-columns subjected to bending about the major axis.

$$EI = [(0.27 + 0.003\,\ell/h - 0.2\,e/h)\,E_c(I_g - I_{ss}) + 0.8E_s(I_{ss} + I_{rs})] \geq E_sI_{ss} \tag{6.7}$$

$$EI = [(0.3 - 0.2\,e/h)\,E_c(I_g - I_{ss}) + 0.8\,E_s(I_{ss} + I_{rs})] \geq E_sI_{ss} \tag{6.8}$$

These compare to Equations 6.9 and 6.10 suggested by Mirza (1990) for reinforced concrete columns.

$$EI = [(0.27 + 0.003\,\ell/h - 0.3\,e/h)\,E_cI_g + E_sI_{rs}] \geq E_sI_{rs} \tag{6.9}$$

$$EI = [(0.3 - 0.3\,e/h)\,E_cI_g + E_sI_{rs}] \geq E_sI_{rs} \tag{6.10}$$

At ℓ/h of 10, Equations 6.7 and 6.8 yield the same results. For values of $\ell/h > 10$, Equation 6.8 is more conservative than Equation 6.7. However, Equation 6.8 is less conservative than Equation 6.7 for $\ell/h < 10$. For very large e/h ratios ($e/h >$ 1.5 in Equation 6.8), a lower limit of E_sI_{ss} is used for both equations to insure that the effective stiffness of the composite column is at least equal to that of the encased structural steel shape.

Histograms and statistical data were prepared using the proposed design equations for all the columns studied (n=11880). The histograms for the ratios of theoretical EI to design EI (EI_{th}/EI_{des}) are plotted in Figure 6.7. EI_{des} in Figure 6.7(a) was taken from Equation 6.7 and that in Figure 6.7(b) from Equation 6.8. As expected, Figure 6.7 indicates that the stiffness ratios (EI_{th}/EI_{des}) for Equation 6.8 (Figure 6.7 (b)) are more conservative than those for Equation 6.7 (Figure 6.7(a)).

The histograms and statistical data prepared for the columns having one percent reinforcing steel (n=3960), using the proposed design equations, are shown in Figure 6.8. The results are similar to those obtained for the data plotted in Figure 6.7.

6.4 ANALYSIS OF STIFFNESS DATA

6.4.1 Overview of Stiffness Ratio Statistics

An overview of the stiffness ratio (EI_{th}/EI_{des}) statistics computed for different design equations are given in Table 6.4 for all data and in Table 6.5 for beam-columns having a reinforcing steel ratio of one percent. To calculate the stiffness ratio of a column, EI_{th} was taken as the computed theoretical stiffness and EI_{des} was calculated from Equation 6.7, 6.8, 4.1 and 4.30. Equations 6.7 and 6.8 are the proposed design equations, Equation 4.1 is the ACI design

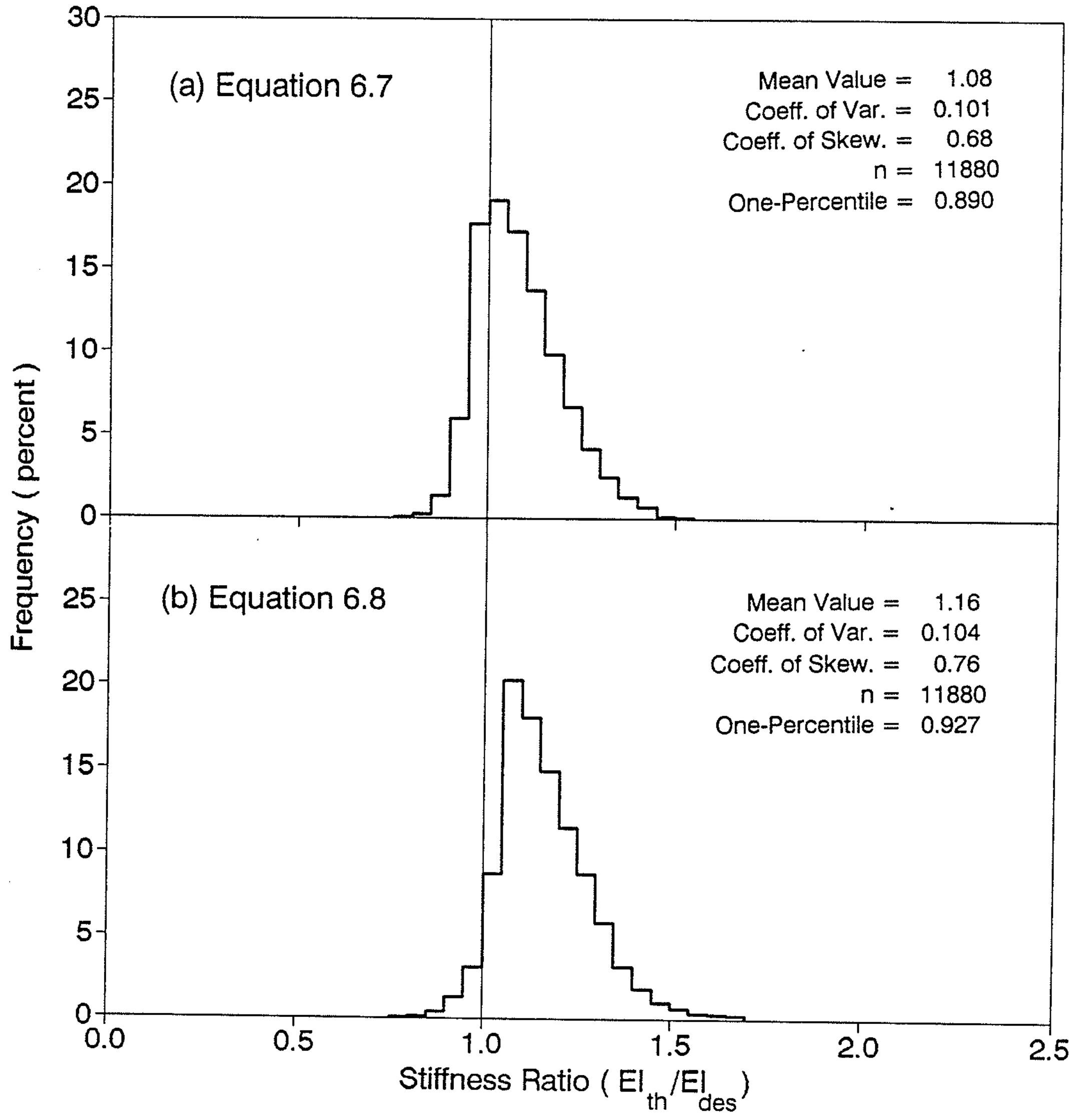

Figure 6.7 - Frequency histograms comparing proposed design equations with theoretical data for all columns bending about minor axis.

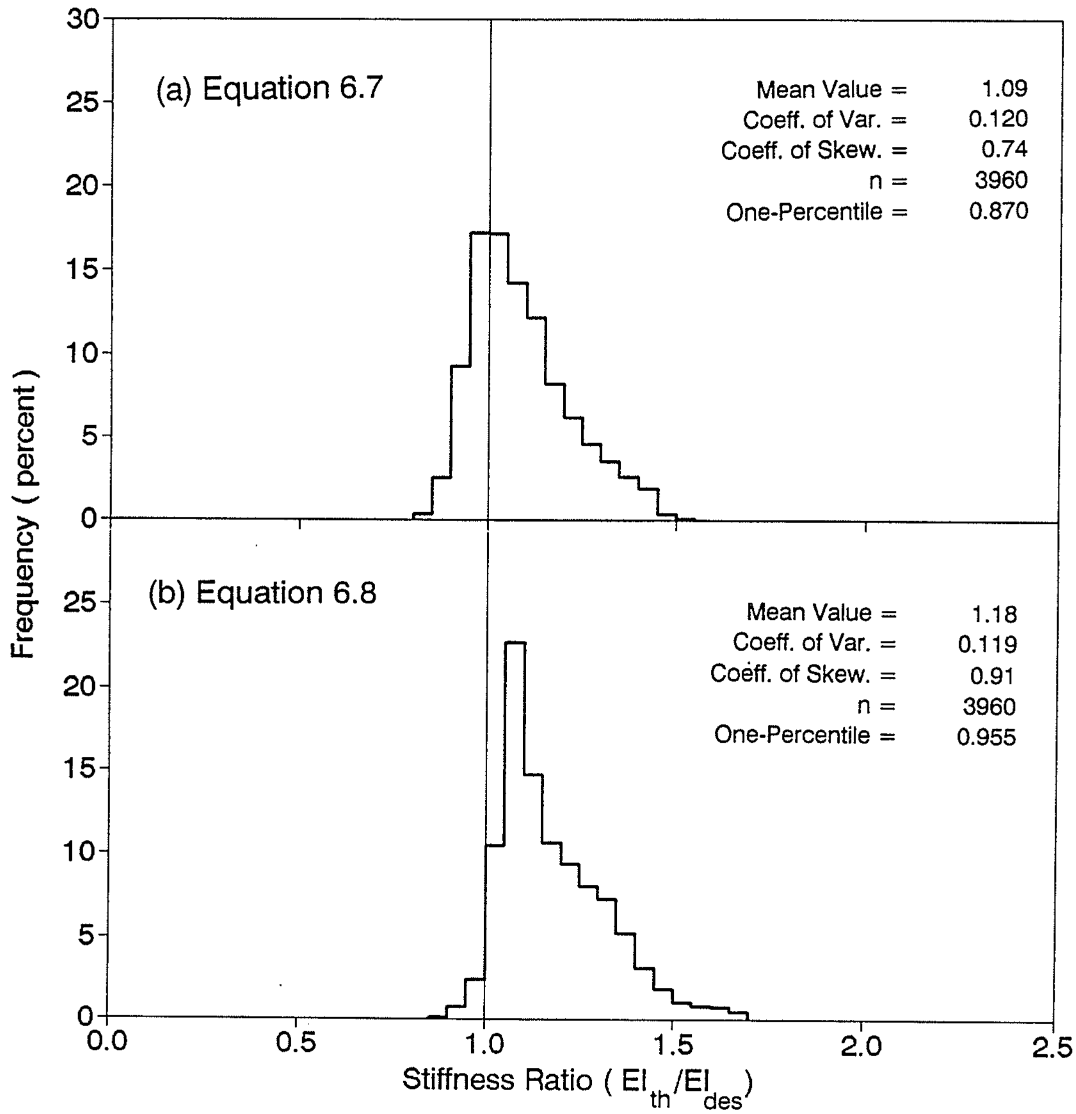

Figure 6.8 - Frequency histograms comparing proposed design equations with theoretical data for columns bending about minor axis where ρ_{rs} = 1.09 percent.

Table 6.4 - Stiffness Ratio Statistics for Different Design Equations for all Beam-Columns Subjected to Minor Axis Bending

Group Number (1)	Slenderness Ratio ℓ/h (2)	Eccentricity Ratio e/h (3)	Proposed Equations Eq. 6.7 (4)	Proposed Equations Eq. 6.8 (5)	ACI Eq. 4.1 (6)	AISC Eq. 4.30 (7)	Number of Columns (8)
			(a) Coefficient of Variation				
A1	10	0.05 - 1.0	0.107	0.107	0.223	0.365	2376
A2	15		0.085	0.089	0.237	0.349	2376
A3	20		0.088	0.093	0.243	0.320	2376
A4	25		0.098	0.102	0.247	0.299	2376
A5	30		0.109	0.111	0.252	0.281	2376
A6	10 - 30		0.101	0.104	0.243	0.324	11880
B1	10	0.1 - 0.7	0.090	0.090	0.220	0.334	1512
B2	15		0.075	0.076	0.221	0.310	1512
B3	20		0.059	0.059	0.210	0.276	1512
B4	25		0.055	0.052	0.203	0.255	1512
B5	30		0.057	0.053	0.199	0.242	1512
B6	10 - 30		0.079	0.069	0.211	0.286	7560
			(b) Mean Stiffness Ratio				
A1	10	0.05 - 1.0	1.110	1.110	1.606	1.086	2376
A2	15		1.115	1.158	1.684	1.098	2376
A3	20		1.092	1.175	1.709	1.088	2376
A4	25		1.062	1.183	1.721	1.100	2376
A5	30		1.036	1.192	1.734	1.140	2376
A6	10 - 30		1.083	1.164	1.691	1.103	11880
B1	10	0.1 - 0.7	1.081	1.081	1.659	1.140	1512
B2	15		1.073	1.111	1.708	1.139	1512
B3	20		1.041	1.115	1.711	1.121	1512
B4	25		1.007	1.114	1.708	1.122	1512
B5	30		0.978	1.116	1.710	1.147	1512
B6	10 - 30		1.036	1.107	1.699	1.134	7560

Table 6.4 - continued

Group Number (1)	Slenderness Ratio ℓ/h (2)	Eccentricity Ratio e/h (3)	Proposed Equations Eq. 6.7 (4)	Proposed Equations Eq. 6.8 (5)	ACI Eq. 4.1 (6)	AISC Eq. 4.30 (7)	Number of Columns (8)
			(c) Five-Percentile				
A1	10	0.05 - 1.0	0.927	0.927	1.121	0.585	2376
A2	15		0.977	1.005	1.159	0.606	2376
A3	20		0.971	1.037	1.186	0.636	2376
A4	25		0.941	1.046	1.198	0.671	2376
A5	30		0.904	1.049	1.212	0.715	2376
A6	10 - 30		0.937	1.002	1.174	0.636	11880
B1	10	0.1 - 0.7	0.932	0.932	1.156	0.643	1512
B2	15		0.966	0.992	1.212	0.669	1512
B3	20		0.965	1.031	1.234	0.698	1512
B4	25		0.931	1.040	1.243	0.725	1512
B5	30		0.893	1.043	1.252	0.758	1512
B6	10 - 30		0.927	0.990	1.221	0.699	7560
			(d) One-Percentile				
A1	10	0.05 - 1.0	0.863	0.863	1.039	0.505	2376
A2	15		0.941	0.966	1.066	0.523	2376
A3	20		0.952	1.012	1.110	0.552	2376
A4	25		0.914	1.027	1.140	0.586	2376
A5	30		0.865	1.020	1.155	0.632	2376
A6	10 - 30		0.890	0.927	1.087	0.541	11880
B1	10	0.1 - 0.7	0.884	0.884	1.047	0.545	1512
B2	15		0.932	0.956	1.102	0.576	1512
B3	20		0.948	1.007	1.146	0.608	1512
B4	25		0.903	1.022	1.181	0.647	1512
B5	30		0.853	1.012	1.197	0.683	1512
B6	10 - 30		0.885	0.932	1.122	0.597	7560

Table 6.5 - Stiffness Ratio Statistics for Different Design Equations for Beam-Columns Subjected to Minor Axis Bending for which ρ_{rs} = 1.09 percent.

Group Number (1)	Slenderness Ratio ℓ/h (2)	Eccentricity Ratio e/h (3)	Proposed Equations Eq. 6.7 (4)	Proposed Equations Eq. 6.8 (5)	ACI Eq. 4.1 (6)	AISC Eq. 4.30 (7)	Number of Columns (8)
(a) Coefficient of Variation							
A1	10	0.05 - 1.0	0.105	0.105	0.198	0.371	792
A2	15		0.097	0.100	0.222	0.363	792
A3	20		0.110	0.112	0.237	0.334	792
A4	25		0.124	0.125	0.248	0.309	792
A5	30		0.138	0.136	0.258	0.287	792
A6	10 - 30		0.120	0.119	0.236	0.334	3960
B1	10	0.1 - 0.7	0.091	0.091	0.197	0.336	504
B2	15		0.084	0.084	0.190	0.305	504
B3	20		0.074	0.071	0.173	0.260	504
B4	25		0.070	0.066	0.161	0.224	504
B5	30		0.075	0.069	0.157	0.203	504
B6	10 - 30		0.094	0.077	0.176	0.270	2520
(b) Mean Stiffness Ratio							
A1	10	0.05 - 1.0	1.130	1.130	1.355	0.899	792
A2	15		1.122	1.173	1.413	0.910	792
A3	20		1.092	1.190	1.435	0.903	792
A4	25		1.059	1.202	1.449	0.910	792
A5	30		1.029	1.214	1.463	0.945	792
A6	10 - 30		1.086	1.182	1.423	0.913	3960
B1	10	0.1 - 0.7	1.098	1.098	1.414	0.944	504
B2	15		1.072	1.116	1.436	0.936	504
B3	20		1.030	1.115	1.432	0.919	504
B4	25		0.991	1.114	1.429	0.922	504
B5	30		0.959	1.117	1.431	0.949	504
B6	10 - 30		1.030	1.112	1.428	0.934	2520

Table 6.5 - continued

Group Number (1)	Slenderness Ratio ℓ/h (2)	Eccentricity Ratio e/h (3)	Proposed Equations Eq. 6.7 (4)	Proposed Equations Eq. 6.8 (5)	ACI Eq. 4.1 (6)	AISC Eq. 4.30 (7)	Number of Columns (8)
(c) Five-Percentile							
A1	10	0.05 - 1.0	0.958	0.958	1.050	0.521	792
A2	15		0.982	1.019	1.092	0.546	792
A3	20		0.959	1.037	1.126	0.576	792
A4	25		0.922	1.041	1.154	0.605	792
A5	30		0.876	1.035	1.171	0.655	792
A6	10 - 30		0.918	1.016	1.112	0.570	3960
B1	10	0.1 - 0.7	0.949	0.949	1.073	0.574	504
B2	15		0.972	1.006	1.124	0.600	504
B3	20		0.954	1.032	1.173	0.638	504
B4	25		0.916	1.035	1.197	0.675	504
B5	30		0.866	1.022	1.210	0.700	504
B6	10 - 30		0.903	1.005	1.152	0.627	2520
(d) One-Percentile							
A1	10	0.05 - 1.0	0.908	0.908	1.003	0.476	792
A2	15		0.948	0.978	1.041	0.493	792
A3	20		0.942	1.016	1.077	0.515	792
A4	25		0.887	1.018	1.108	0.545	792
A5	30		0.840	1.000	1.132	0.598	792
A6	10 - 30		0.873	0.955	1.044	0.507	3960
B1	10	0.1 - 0.7	0.901	0.901	1.020	0.506	504
B2	15		0.934	0.963	1.066	0.528	504
B3	20		0.940	1.007	1.120	0.576	504
B4	25		0.880	1.011	1.152	0.622	504
B5	30		0.834	0.996	1.179	0.649	504
B6	10 - 30		0.866	0.948	1.061	0.549	2520

equation, and Equation 4.30 is the stiffness expression developed from the AISC strength interaction curves.

Tables 6.4 and 6.5 give the coefficient of variation, mean, five-percentile and one-percentile values for each of the different design equations. For statistical analysis, the beam-columns studied are divided into two groups: Group A includes all columns and Group B includes only the columns with usual e/h values ($0.1 \leq e/h \leq 0.7$). The statistics provided within each of these groups are based on subgroups that were taken according to ℓ/h ratio but also include the statistics for the overall sample.

After reviewing Tables 6.4 and 6.5 the following observations are made:

(1) The coefficients of variation for the proposed design equations are considerably lower and remain relatively constant compared to those for the ACI or AISC equations.

(2) The mean stiffness ratios for the ACI equation tend to be significantly more conservative than those for the proposed design equations and for the AISC expression.

3) The AISC expression mean stiffness ratio for columns with 1 percent reinforcing steel is less than 1.0 for all subgroups of ℓ/h in both groups of e/h.

(4) A comparison of Table 6.4 (for all data) and Table 6.5 (for beam-columns having one percent reinforcing steel) shows that the mean, five-percentile and one-percentile stiffness ratios for the ACI and AISC equations are

subjected to greater variations due to ρ_{rs} than are those for the proposed design equations.

5) The proposed design equations and the ACI equation gave five-percentile and one-percentile values that in all cases exceeded 0.86 and 0.8, respectively. The AISC expression, on the other hand, resulted in five-percentile and one-percentile values that were in all cases significantly less than 0.86 and 0.8, respectively.

Figure 6.9 shows the cumulative frequency distribution of stiffness ratios (EI_{th}/EI_{des}) for the different design equations plotted on normal probability paper and represents the data for all 11,880 columns studied. The curves for Equations 6.7 and 6.8 follow one another. The ACI equation (Equation 4.1) produces more conservative results than the proposed design equations, whereas the AISC expression (Equation 4.30) is less conservative than the proposed design equations for 50 percent of the columns studied. In fact, the AISC expression produces very low stiffness ratios for a significant number of beam-columns studied, as indicated by Figure 6.9.

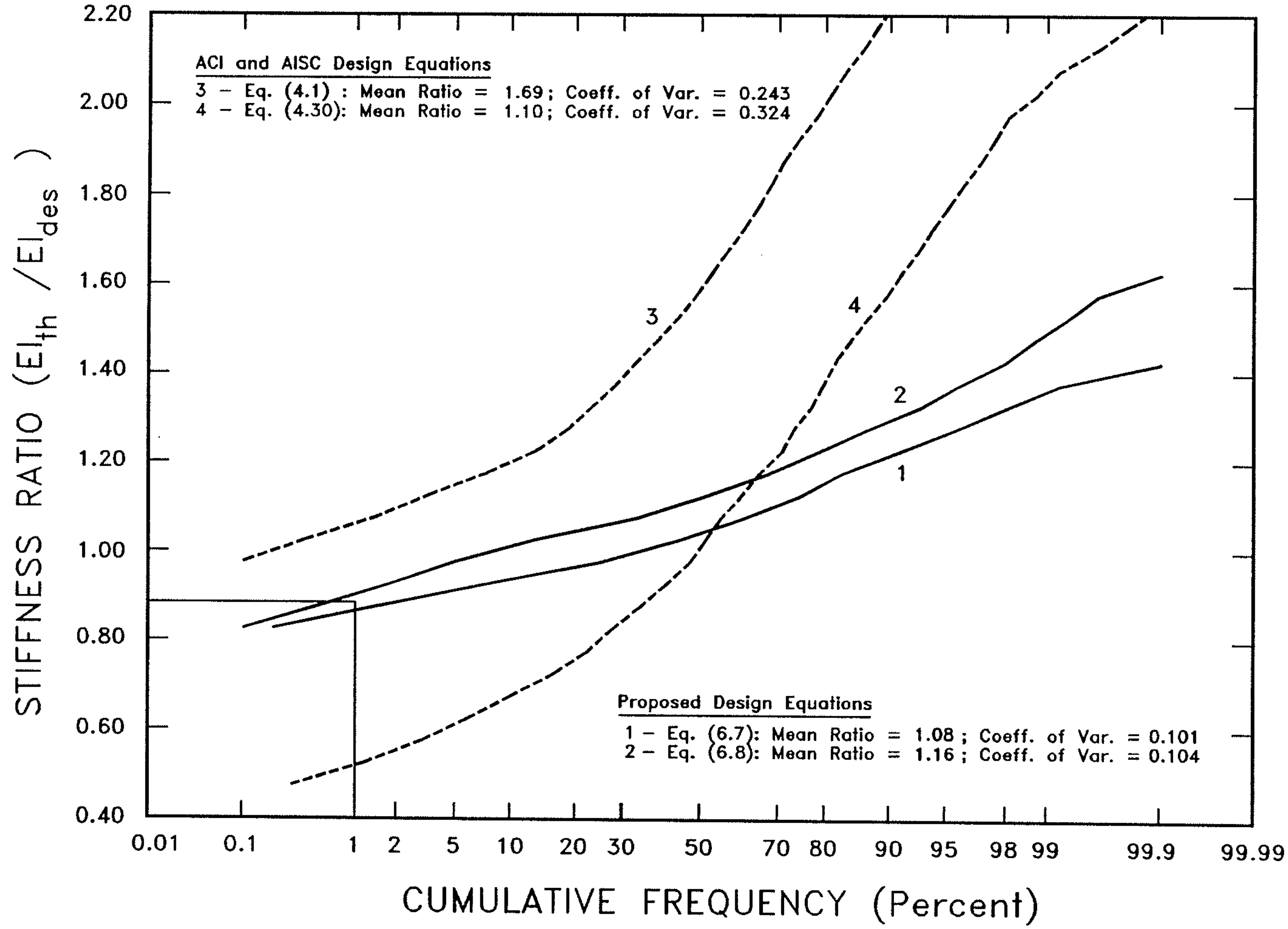

Figure 6.9 - Probability distribution of stiffness ratios computed from data for all columns bending about minor axis (n = 11880).

6.4.2 Effect of Variables on Stiffness Ratios

The effects that each of the variables listed in Table 6.3 has on the mean, five-percentile, and one-percentile values of stiffness ratios (EI_{th}/EI_{des}) obtained from the proposed design equations (Equations 6.7 and 6.8), ACI equation (Equation 4.1) and AISC equation (Equation 4.30) were examined in detail.

Figures 6.10, 6.11 and 6.12 examine the effect of e/h on mean, five-percentile, and one-percentile (minimum in case of Figure 6.12) stiffness ratios. Figure 6.10 is plotted for all data (n = 11,880), Figure 6.11 includes beam-columns having ρ_{rs} = 1 percent (n = 3960), and Figure 6.12 considers beam-columns with ρ_{rs} = 1 percent and ℓ/h = 10 (n = 792). Minimum values in place of one-percentile values are used for Figure 6.12 because each e/h ratio represents only 72 beam-columns. An examination of these figures indicates that proposed design equations (Equations 6.7 and 6.8) produce mean, five-percentile and one-percentile values that are relatively constant for the entire range of e/h studied. The ACI and AISC expressions produce stiffness ratios that varied with e/h. This is because neither equation uses e/h as a variable. The mean, five-percentile and one-percentile stiffness ratios for the ACI equation appear to be overly conservative at low e/h ratios when compared to the stiffness ratios produced by the proposed stiffness equations. Mirza (1990) pointed out that, for establishing safety in design equations, the five-

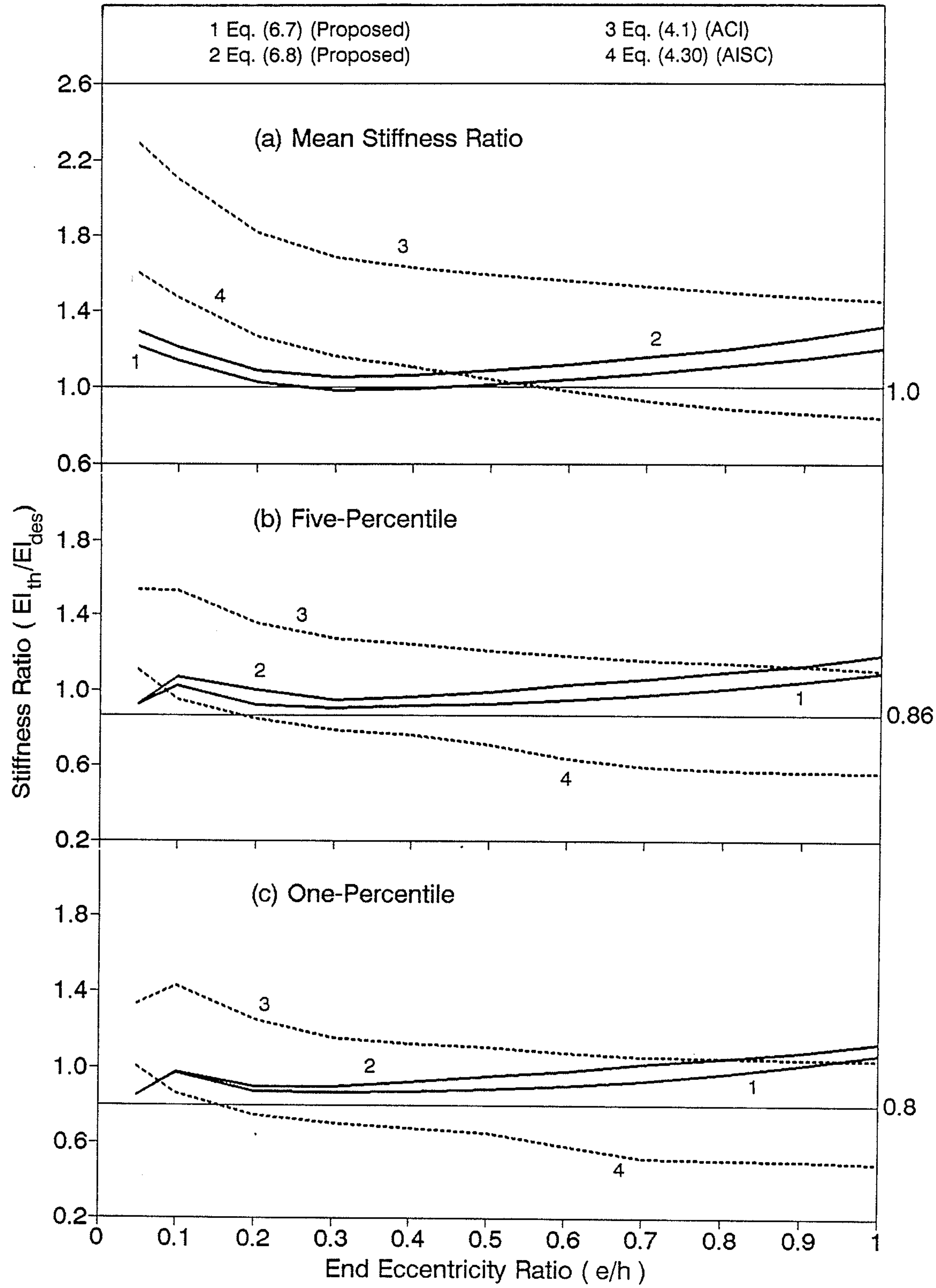

Figure 6.10 - Effect of end eccentricity ratio on stiffness ratio for different design equations for all columns bending about minor axis (n = 1080 for each e/h ratio equal to 0.05, 0.1, 0.2, 0.3, 0.4, 0.5, 0.6, 0.7, 0.8, 0.9 and 1.0).

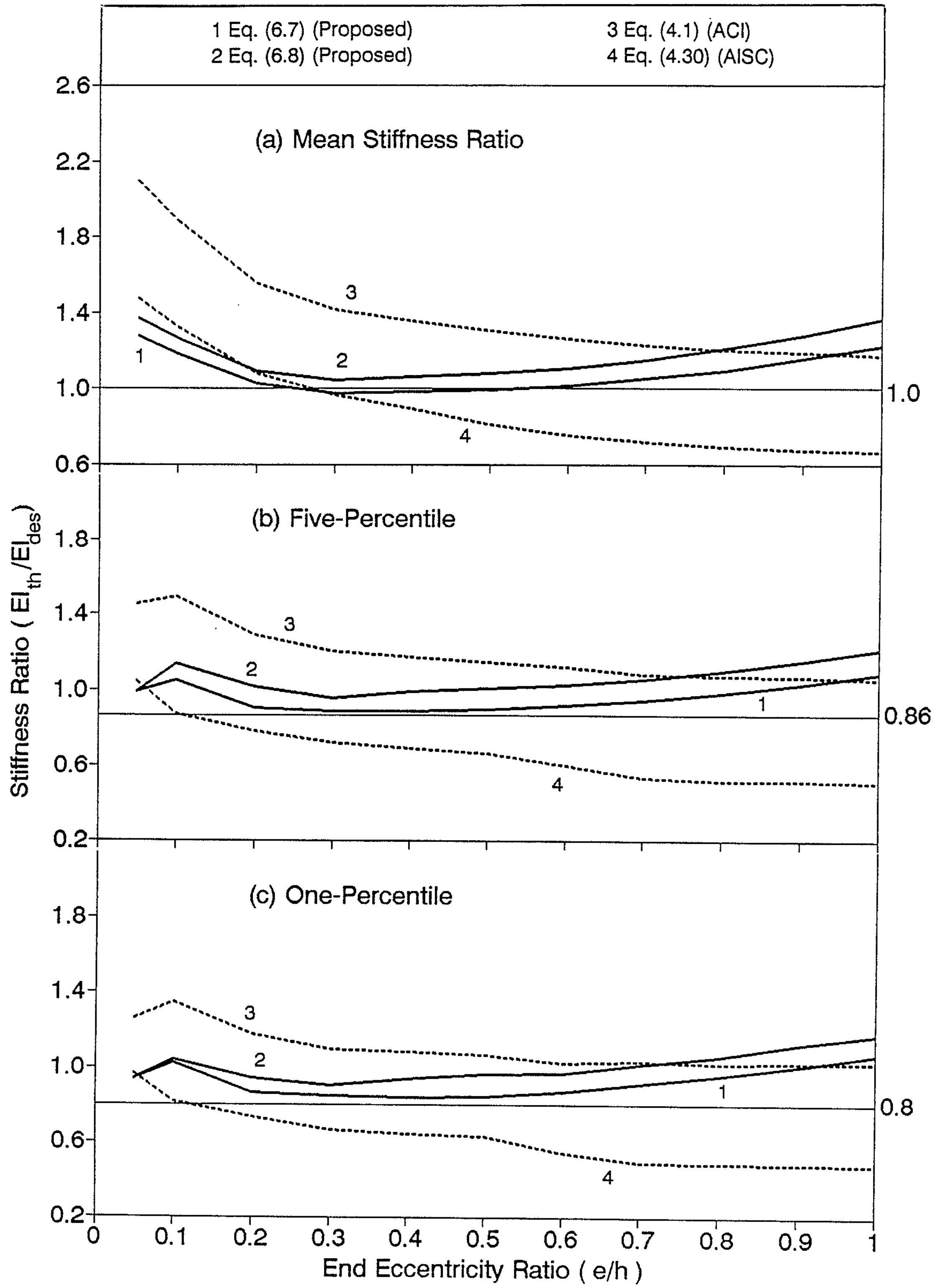

Figure 6.11 - Effect of end eccentricity ratio on stiffness ratio for different design equations for columns bending about minor axis where ρ_{rs} = 1.09 percent (n = 360 for each e/h ratio equal to 0.05, 0.1, 0.2, 0.3, 0.4, 0.5, 0.6, 0.7, 0.8, 0.9 and 1.0).

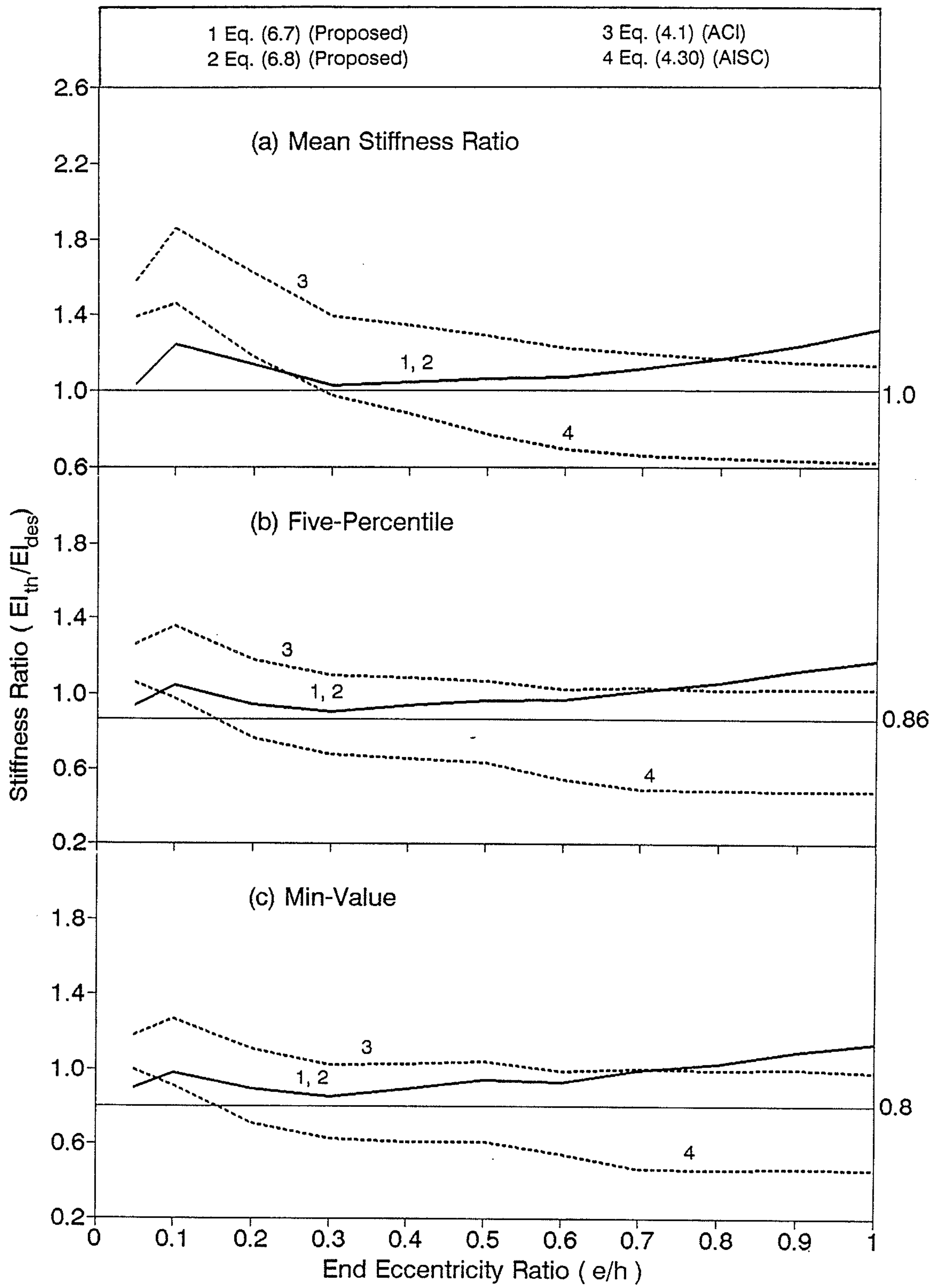

Figure 6.12 - Effect of end eccentricity ratio on stiffness ratio for different design equations for columns bending about minor axis where ρ_{rs} = 1.09 percent and ℓ/h = 10 (n = 72 for each e/h ratio equal to 0.05, 0.1, 0.2, 0.3, 0.4, 0.5, 0.6, 0.7, 0.8, 0.9 and 1.0).

percentile and one-percentile values are more important than the mean value. The proposed design equations and the ACI equation gave mean, five-percentile and one-percentile (or minimum in case of Figure 6.12) values that exceeded 1.0, 0.86 and 0.80,respectively, for most e/h ratios shown in Figures 6.10, 6.11 and 6.12. The AISC expression (Equation 4.30), on the other hand, is less conservative than the other equations for the five-percentile and one-percentile values at almost all *values of* e/h and these values are less than 0.86 and 0.80 for $e/h \geq 0.2$.

Figure 6.13 illustrates the effect of the axial load ratio (P_u/P_o) on the stiffness ratios resulting from different design equations. The axial load ratio was not a controlled variable in this study, i.e. there are as many different axial load ratios as the number of beam-columns studied. This required grouping of stiffness ratios into a number of ranges of P_u/P_o values. The statistics for stiffness ratios in each range of P_u/P_o values were then determined. Grouping the stiffness ratios according to axial load ratio resulted in having a significantly different number of columns in each of the ranges of P_u/P_o. For example, less columns were grouped in the range of 0.7 to 0.9 P_u/P_o (n = 212) than in the range of 0.2 to 0.25 P_u/P_o (n = 1128). The ranges of P_u/P_o ratios were set at 0.05-0.1, 0.1-0.15, 0.15-0.2, 0.2-0.25, 0.25-0.3, 0.3-0.35, 0.35-0.4, 0.4-0.5, 0.5-0.6, 0.6-0.7, 0.7-0.9. The mean P_u/P_o ratio for each range is plotted against the mean,

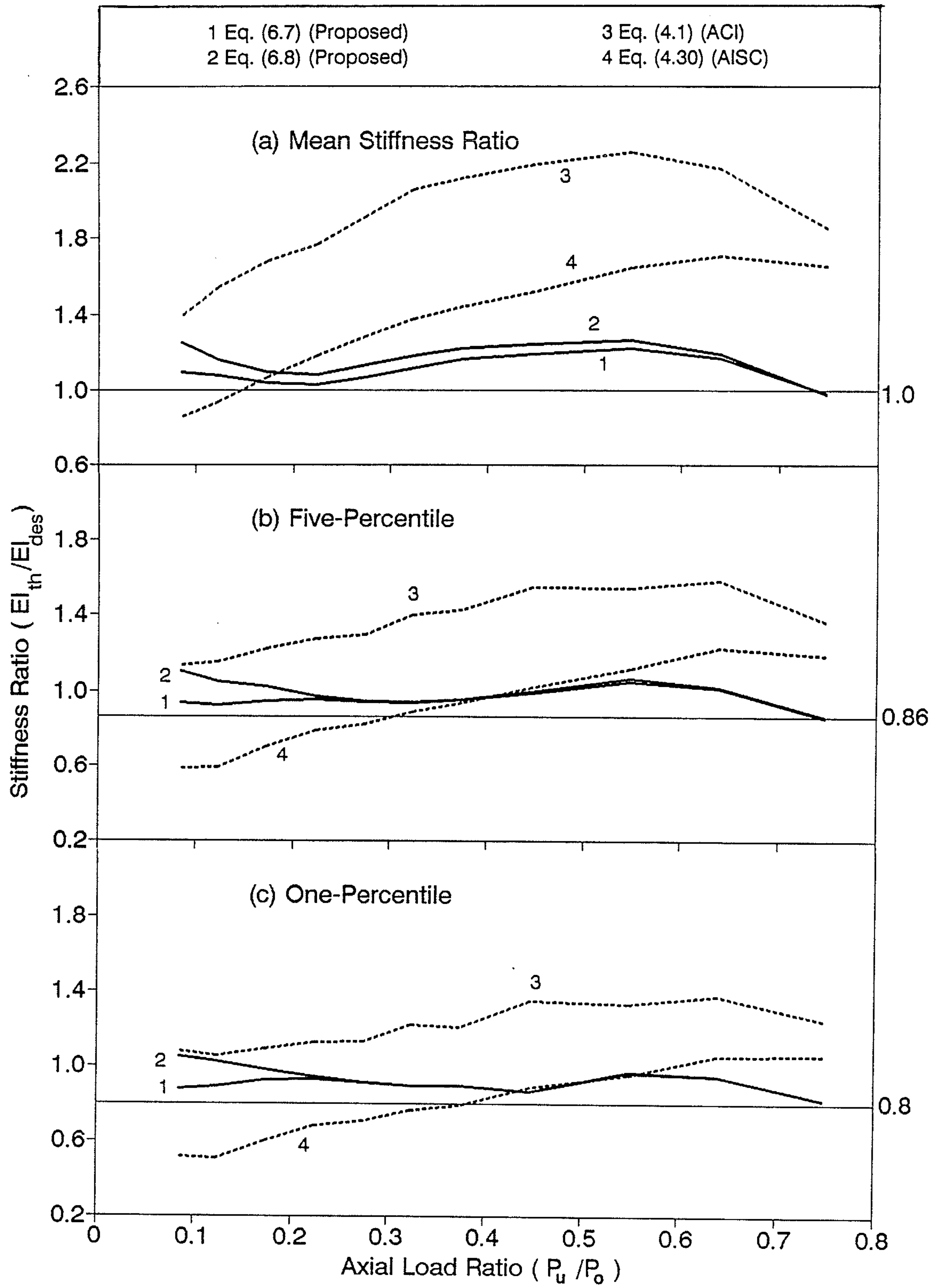

Figure 6.13 - Effect of axial load ratio on stiffness ratio for different design equations for all columns bending about minor axis (n varies for each P_u/P_o ratio; total n = 11,880).

five-percentile and one-percentile stiffness ratios for each corresponding range. Figure 6.13 shows that the mean, five-percentile and one-percentile stiffness ratios for the ACI equation continue to be more conservative than those for the proposed design equations. The AISC stiffness values for five-percentile and one-percentile are less than 0.86 and 0.80, respectively, for $P_u/P_o < 0.4$. This is expected since there is a strong correlation between P_u/P_o and e/h. Figure 6.14 and 6.15 show that by excluding the values of P_u/P_o for beam-columns where either e/h equals 0.05 or ℓ/h equals 10 eliminates the values of P_u/P_o greater than 0.7. This is expected because high P_u/P_o occurs at very low e/h or ℓ/h ratios.

An examination of Figure 6.16 concerning slenderness in terms of ℓ/h ratio shows relatively constant but different values of mean, five-percentile and one-percentile stiffness ratios obtained for all four design equations, even though only Equation 6.7 includes ℓ/h as a variable. This suggests that ℓ/h is not as significant as initially considered. The AISC expression, however, yields the lowest five-percentile and one-percentile for all values of ℓ/h. The mean, five-percentile and one-percentile stiffness ratios for the ACI stiffness expression are again more conservative than the proposed design equations.

Figure 6.17 shows the effect of slenderness using ℓ/r ratio. The ACI expression for radius of gyration (Equation

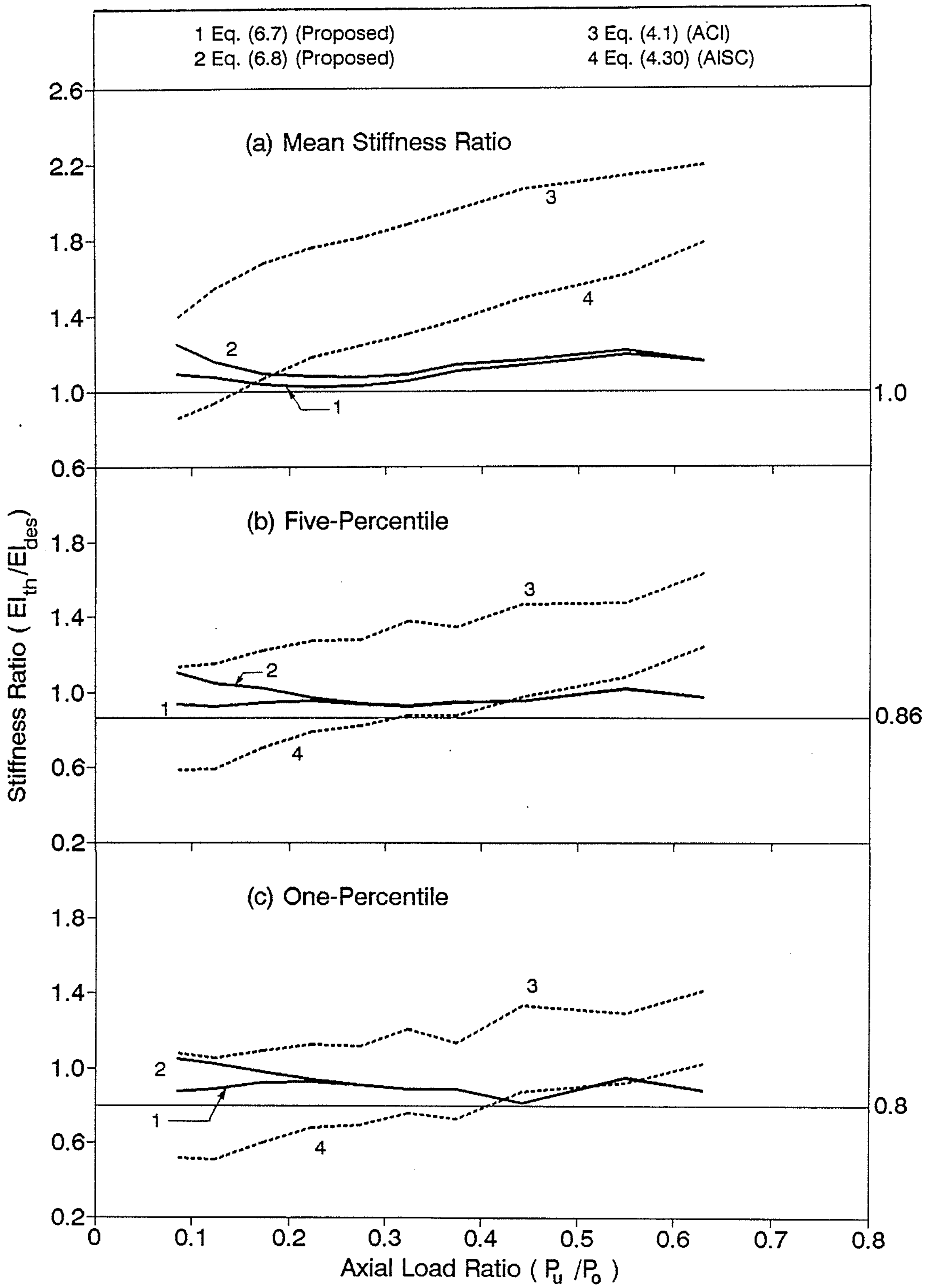

Figure 6.14 - Effect of axial load ratio on stiffness ratio for different design equations in which columns bending about minor axis with e/h = 0.05 not included (n varies for each P_u/P_o ratio; total n = 10,800).

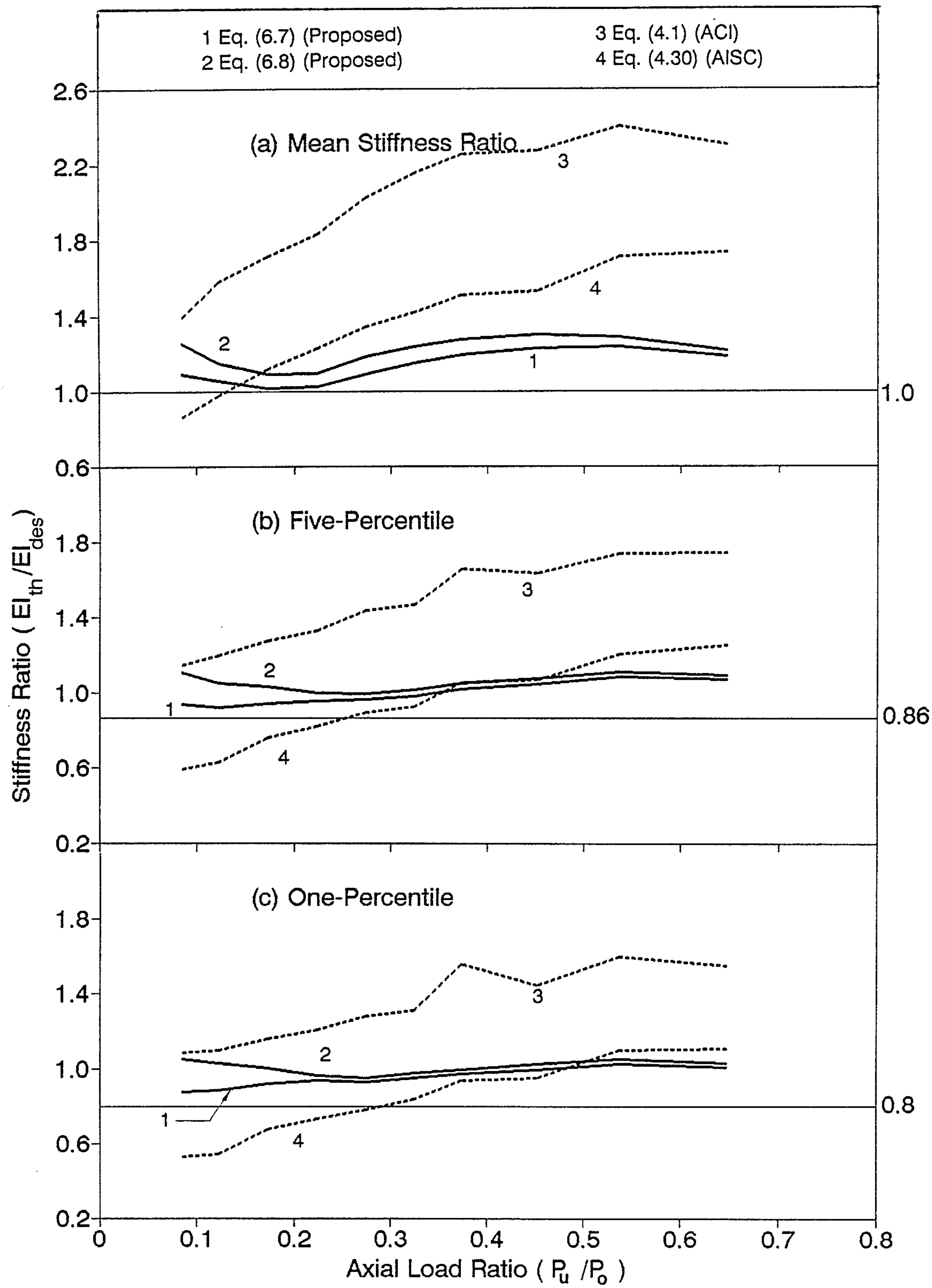

Figure 6.15 - Effect of axial load ratio on stiffness ratio for different design equations in which columns bending about minor axis with ℓ/h = 10 not included (n varies for each P_u/P_o ratio; total n = 9,504).

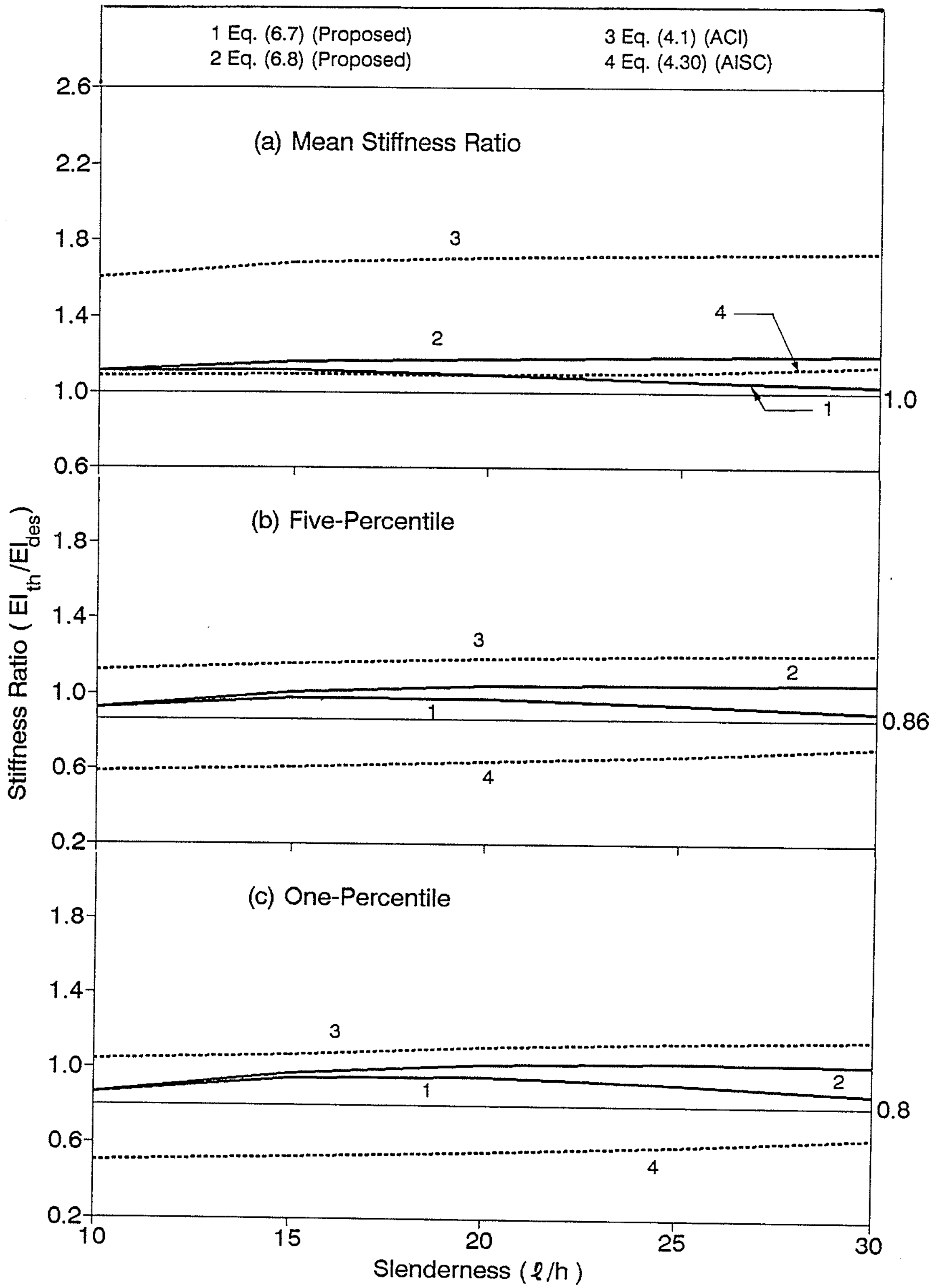

Figure 6.16 - Effect of slenderness ratio (ℓ/h) on stiffness ratio for different design equations for all columns bending about minor axis (n = 2376 for each ℓ/h ratio equal to 0.05, 0.1, 0.2, 0.3, 0.4, 0.5, 0.6, 0.7, 0.8, 0.9 and 1.0).

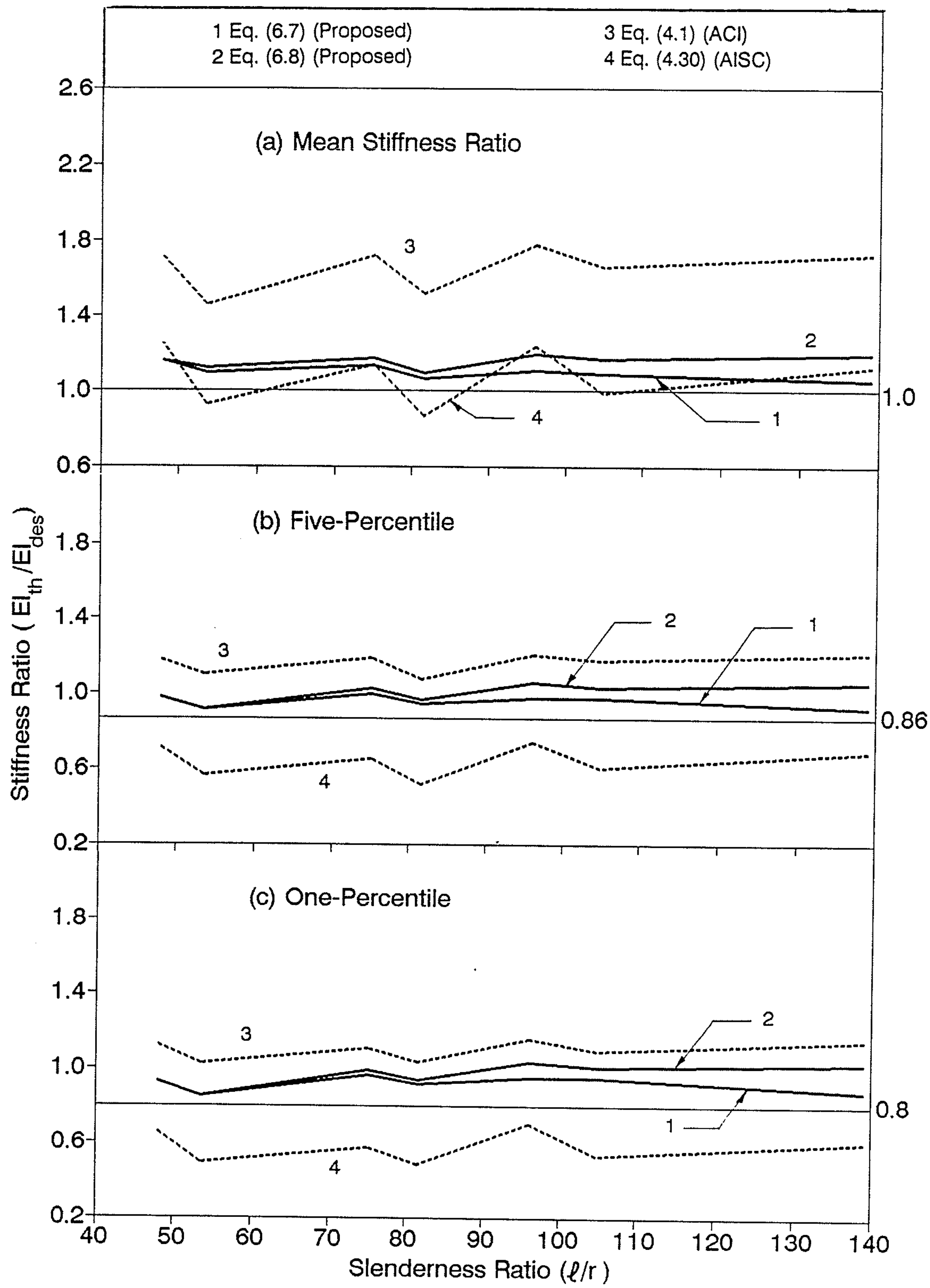

Figure 6.17 - Effect of slenderness ratio (ℓ/r) on stiffness ratio for different design equations for all columns bending about minor axis (n varies for each range of ℓ/r ratio; total n = 11,880).

6.1) was used to determine r. One hundred and twenty different values of ℓ/r for 11,880 beam-columns studied necessitated the grouping of ℓ/r into ranges. The ranges of ℓ/r ratio were set at 40-50, 50-60, 60-70, 70-80, 80-90, 90-100, 100-110, 110-140. The mean ℓ/r ratio for each range is plotted against the mean, five-percentile and one-percentile stiffness ratios for each corresponding range, similar to what was done to study the effect of P_u/P_o. The apparent zig-zag nature of the plots in Figure 6.17 for the ACI equation is, probably, caused by grouping of ℓ/r and due to the fact that the contribution of reinforcing steel to beam-column stiffness is not included in Equation 4.1. For the AISC expression, even though the area of the reinforcing steel is included in computing the equivalent cross-section properties, the full effect of the reinforcing steel is not accounted for in determining the nominal axial load capacity of a beam-column. The mean, five-percentile and one-percentile stiffness ratios appear to follow the trends stated previously for ℓ/h ratio.

The effect of longitudinal reinforcing steel in terms of ρ_{rs} is shown in Figure 6.18. The stiffness ratios for the ACI and AISC expressions increase proportionally with the reinforcing steel ratio. This is because the ACI expression (Equation 4.1) does not account for the effect of reinforcing steel. This also suggests that the AISC expression does not properly account for the effect of reinforcing steel.

Figure 6.19 shows the effect of structural steel in terms

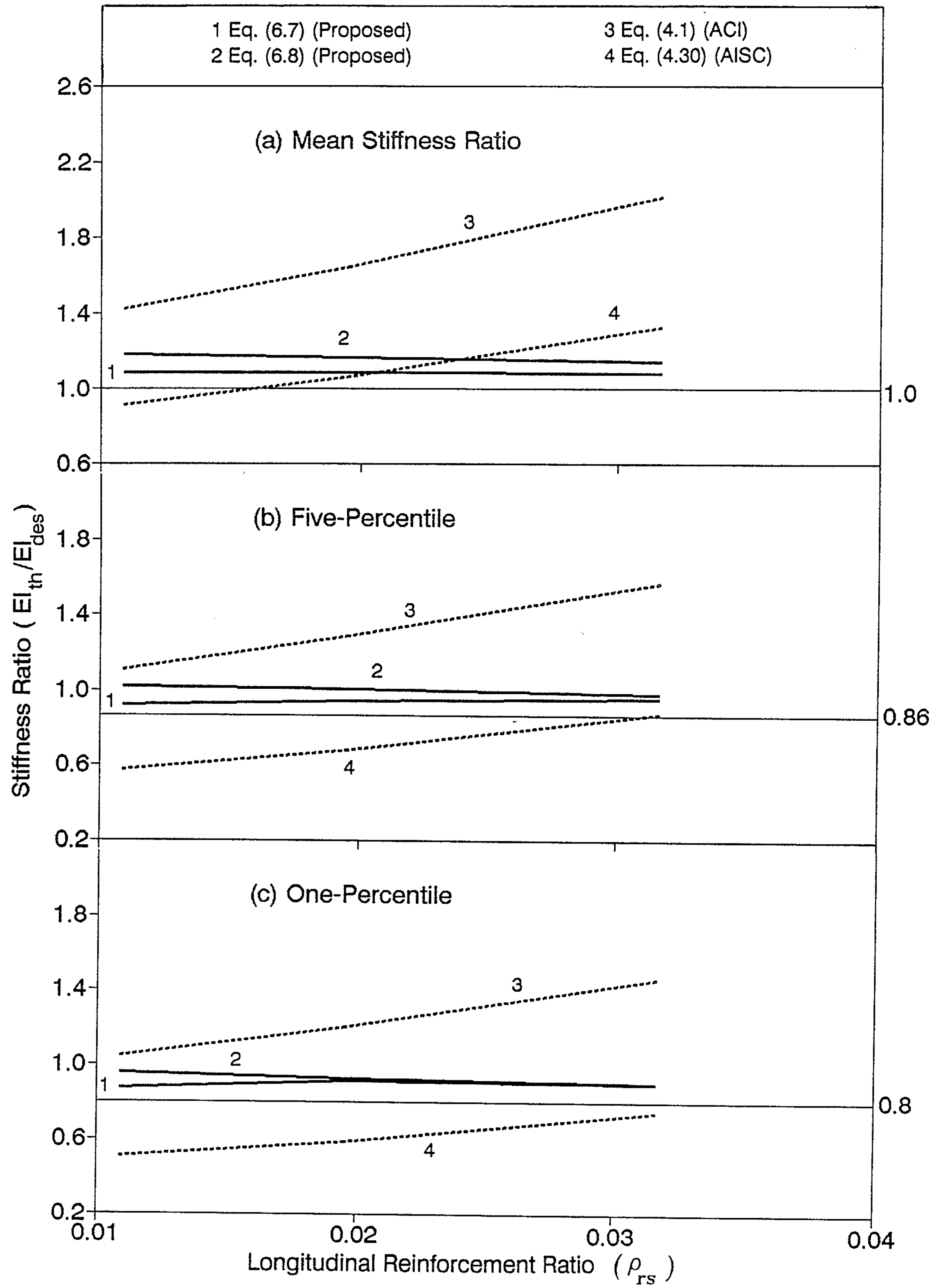

Figure 6.18 - Effect of longitudinal reinforcement ratio on stiffness ratio for different design equations for all columns bending about minor axis (n = 3960 for each ρ_{rs} ratio equal to 1.09, 1.96 and 3.17 percent).

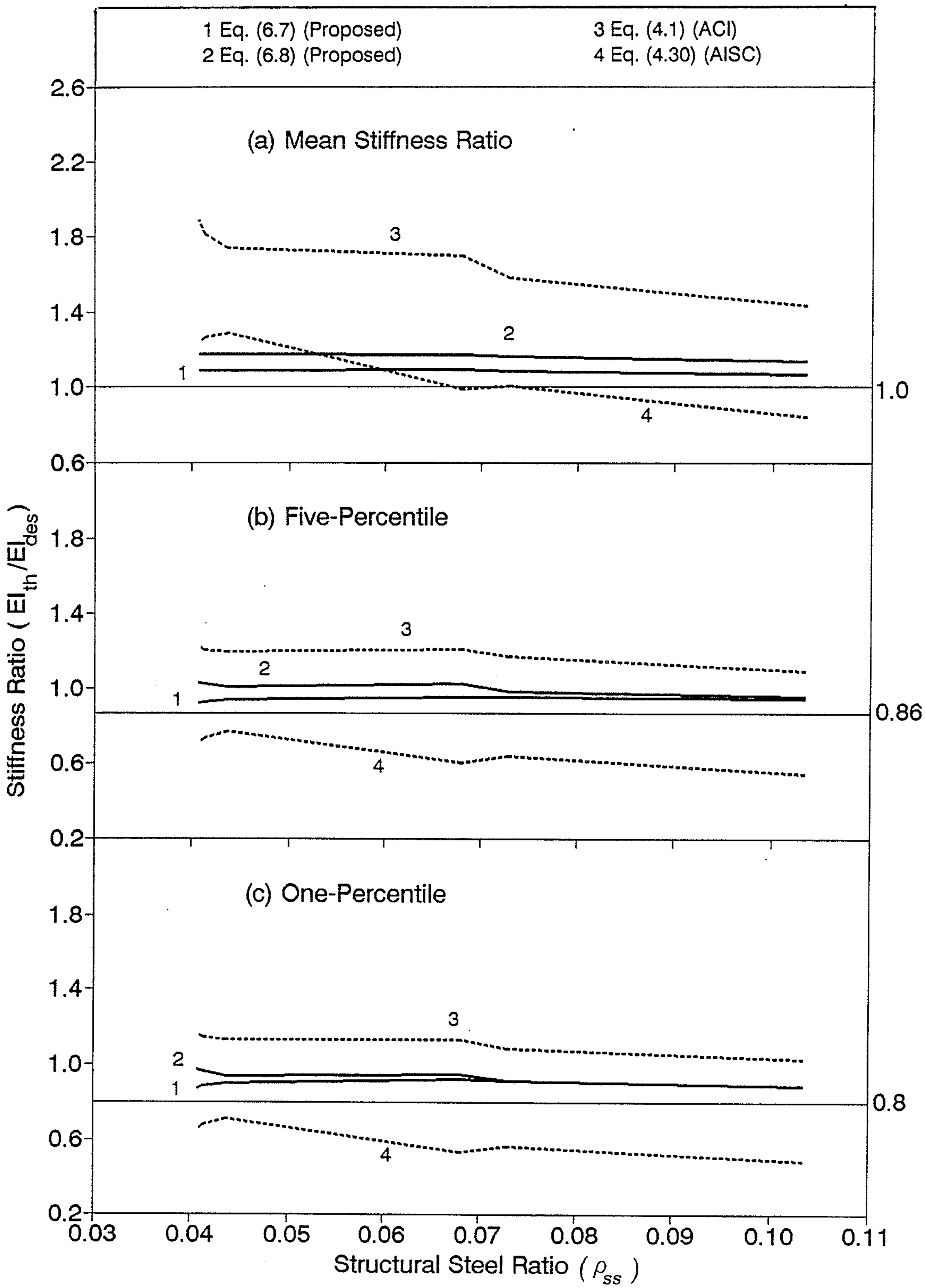

Figure 6.19 - Effect of structural steel ratio on stiffness ratio for different design equations for all columns bending about minor axis (n = 1980 for each ρ_{ss} ratio equal to 4.07, 4.13, 4.36, 6.80, 7.29 and 10.33 percent).

of ρ_{ss} on the stiffness ratios. Figure 6.20 shows the effect of ρ_{ss} on stiffness ratios of beam-columns having reinforcing steel of only one percent. Both figures indicate that the ACI and AISC expressions are more susceptible to the effect of ρ_{ss} than the proposed equations. This influence is due to the proportion of stiffness the reinforcing steel contributes to the overall stiffness in relation to the stiffness contributed by the structural steel section. For example, three steel shapes with significantly different moments of inertia were used to give a structural steel ratio of approximately 4 percent (actual values 4.07, 4.13 and 4.36 percent). This means when the ACI equation is used, a composite column containing a steel section with a relatively small moment of inertia gives a more conservative result than a column with a stiffer steel section. Figures 6.19 and 6.20 also indicate that the ACI equation is more conservative and the AISC equation is less conservative than the proposed equations over the entire range of ρ_{ss} at mean, five-percentile and one-percentile levels.

Figure 6.21 concerning the effect of gross steel ratio ρ_g confirms the inconsistency of the ACI and AISC expressions for determining *EI*. Fluctuations appearing in the stiffness ratios for the proposed design equations are quite minor compared to the irregularities resulting from the ACI and AISC equations. This observation is also true for the effect of ρ_{rs}/ρ_{ss} (ratio of reinforcing steel to structural steel) as

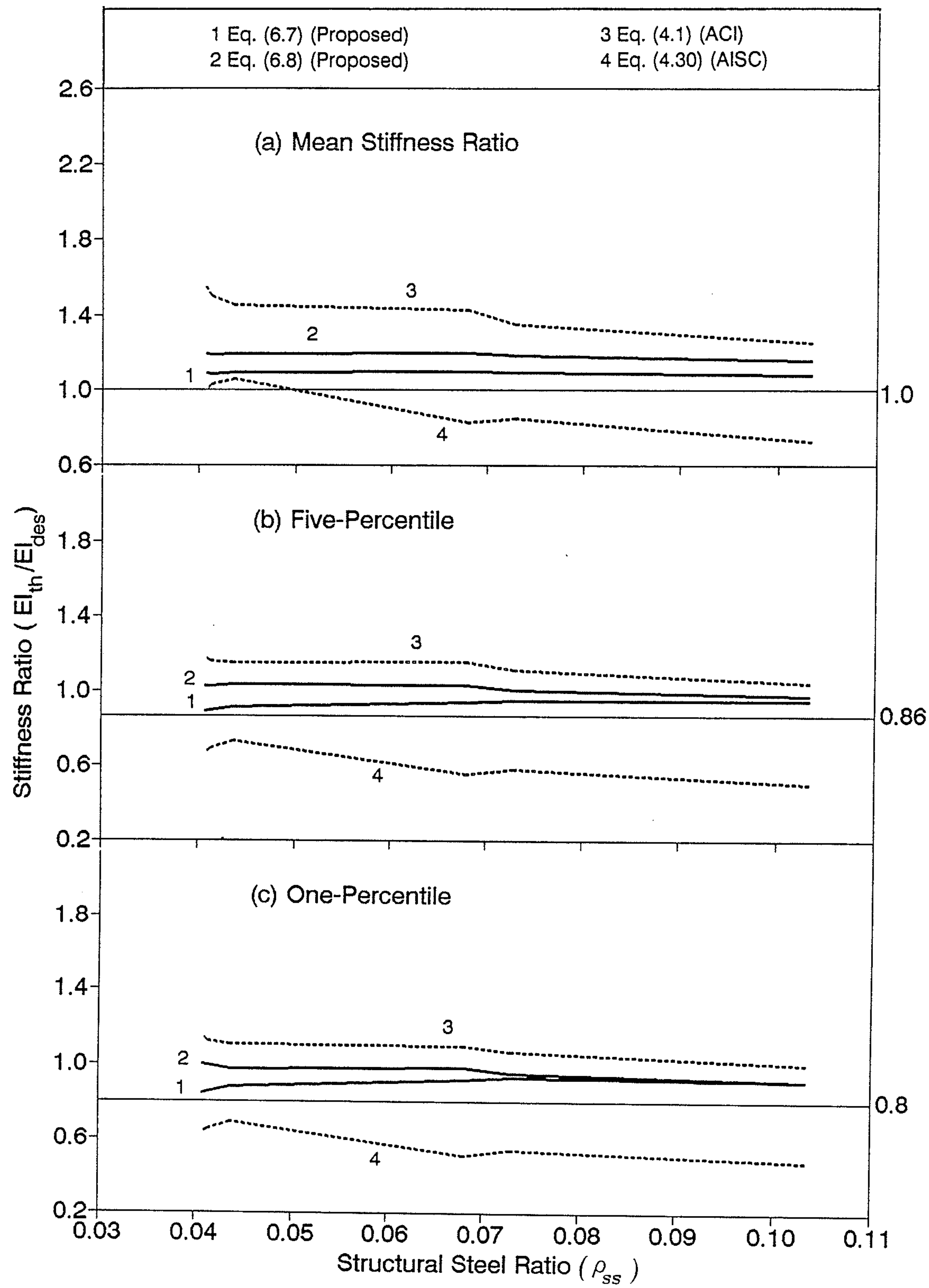

Figure 6.20 - Effect of structural steel ratio on stiffness ratio for different design equations for columns bending about minor axis where ρ_{rs} = 1.09 percent (n = 660 for each ρ_{ss} ratio equal to 4.07, 4.13, 4.36, 6.80, 7.29 and 10.33 percent).

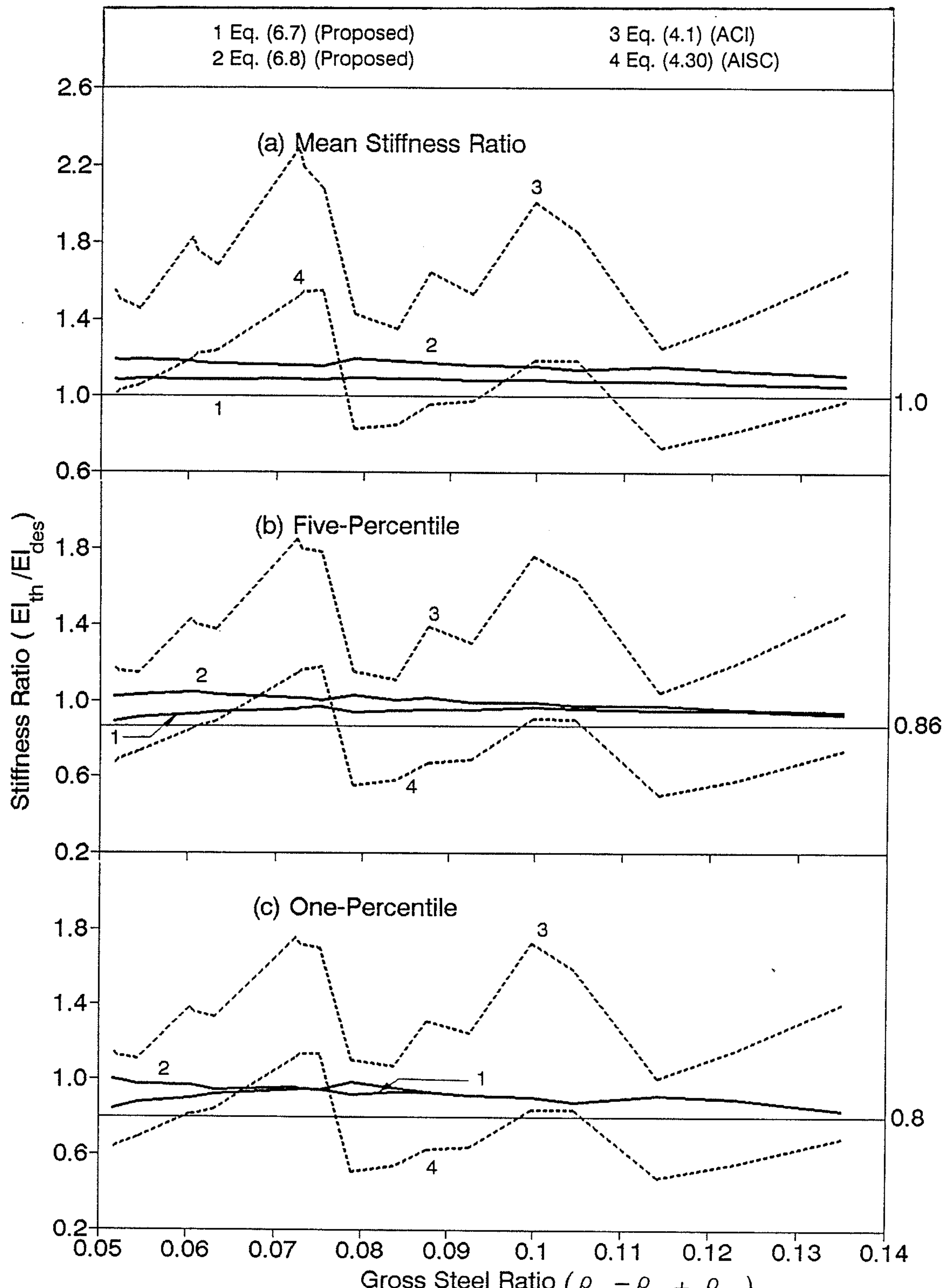

Figure 6.21 - Effect of gross steel ratio on stiffness ratio for different design equations for all columns bending about minor axis (n = 660 for each $\rho_g=(\rho_{rs}+\rho_{ss})$ ratio equal to 5.16, 5.22, 5.45, 6.03, 6.09, 6.32, 7.24, 7.30, 7.53, 7.89, 8.38, 8.76, 9.25, 9.97, 10.46, 11.42, 12.29 and 13.50 percent).

indicated by Figure 6.22. In both figures, the ACI and proposed design equations produced mean, five-percentile and one-percentile stiffness ratios that exceeded 1.0, 0.86, 0.80, respectively. The AISC expression followed the usual trend of being non-conservative in most cases.

Figures 6.23, 6.24 and 6.25 examine the effects of the structural steel index $\rho_{ss}f_{yss}/f'_c$, the reinforcing steel index $\rho_{rs}f_{yrs}/f'_c$ and the gross steel index $(\rho_{ss}f_{yss}+\rho_{rs}f_{yrs})/f'_c$. Figures 6.23, 6.24, and 6.25, respectively, represent 72, 12, and 216 possible combinations of the related steel index. This resulted in stiffness ratios in Figures 6.23 and 6.25 being plotted for ranges of $\rho_{ss}f_{yss}/f'_c$ and $(\rho_{ss}f_{yss}+\rho_{rs}f_{yrs})/f'_c$, each range with a different number of stiffness ratios for statistical calculations. The ranges for $\rho_{ss}f_{yss}/f'_c$ plotted in Figure 6.23 were set at 0.20-0.25, 0.25-0.35, 0.35-0.45, 0.45-0.55, 0.55-0.65, 0.65-0.75, 0.75-0.85, 0.85-0.95, 0.95-1.05, 1.05-1.15, 1.15-1.25, 1.25-1.35; and those for $(\rho_{ss}f_{yss}+\rho_{rs}f_{yrs})/f'_c$ plotted in Figure 6.25 were set at 0.2-0.3, 0.3-0.4, 0.4-0.5, 0.5-0.6, 0.6-0.7, 0.7-0.8, 0.8-0.9, 0.9-1.00, 1.00-1.10, 1.10-1.20, 1.20-1.30, 1.30-1.40, 1.40-1.50, 1.50-1.60, 1.60-1.80. The mean steel index for each range is plotted against the mean, five-percentile and one-percentile stiffness ratios for each corresponding range. These figures show that the fluctuations in stiffness ratios for the proposed design equations are subtle compared to the fluctuations occurring for the ACI and AISC expressions.

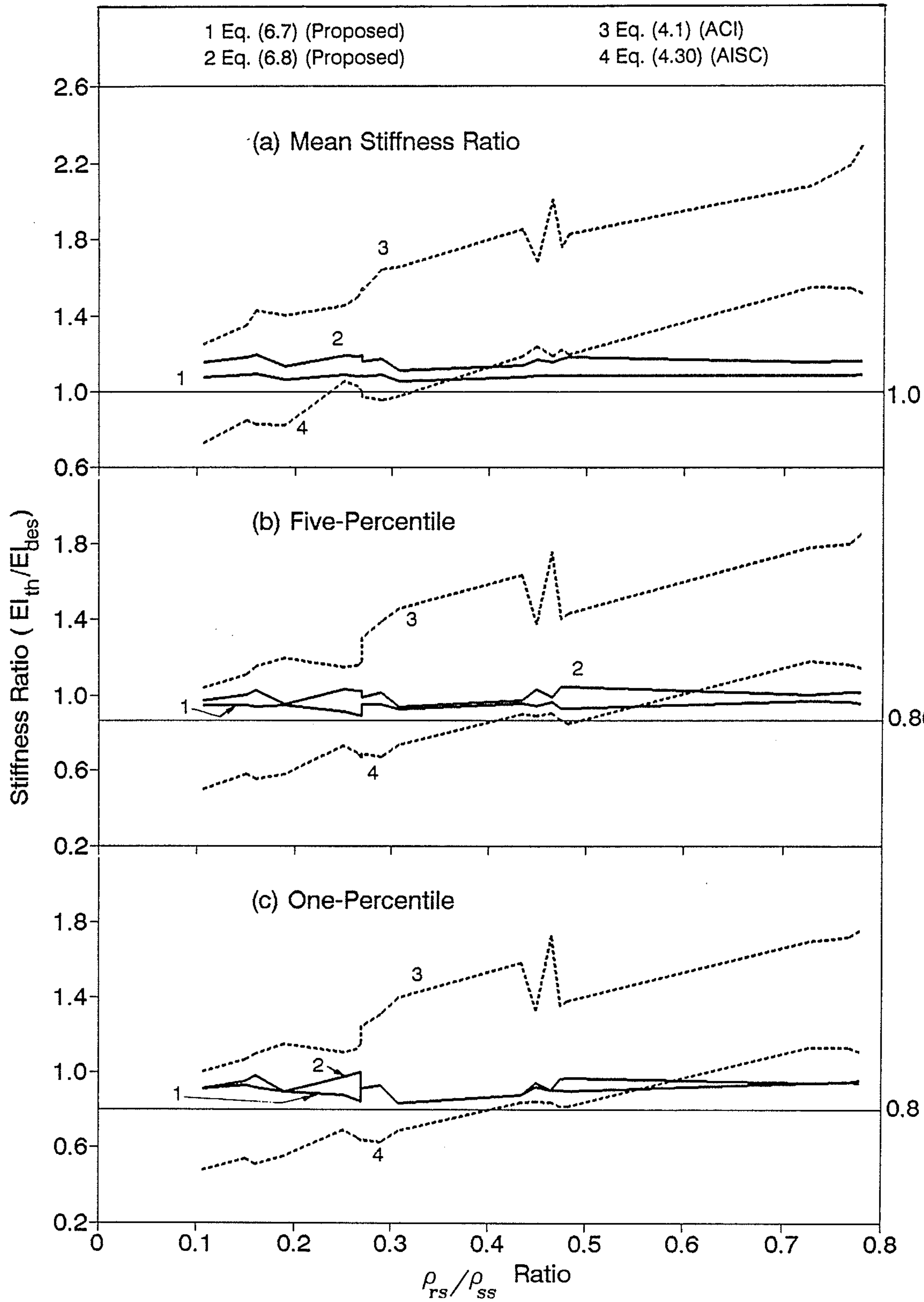

Figure 6.22 - Effect of ρ_{rs}/ρ_{ss} ratio on stiffness ratio for different design equations for all columns bending about minor axis (n = 660 for each ρ_{rs}/ρ_{ss} ratio equal to 0.106, 0.150, 0.160, 0.190, 0.250, 0.264, 0.268, 0.269, 0.288, 0.306, 0.434, 0.449, 0.466, 0.474, 0.481, 0.726, 0.766 and 0.788).

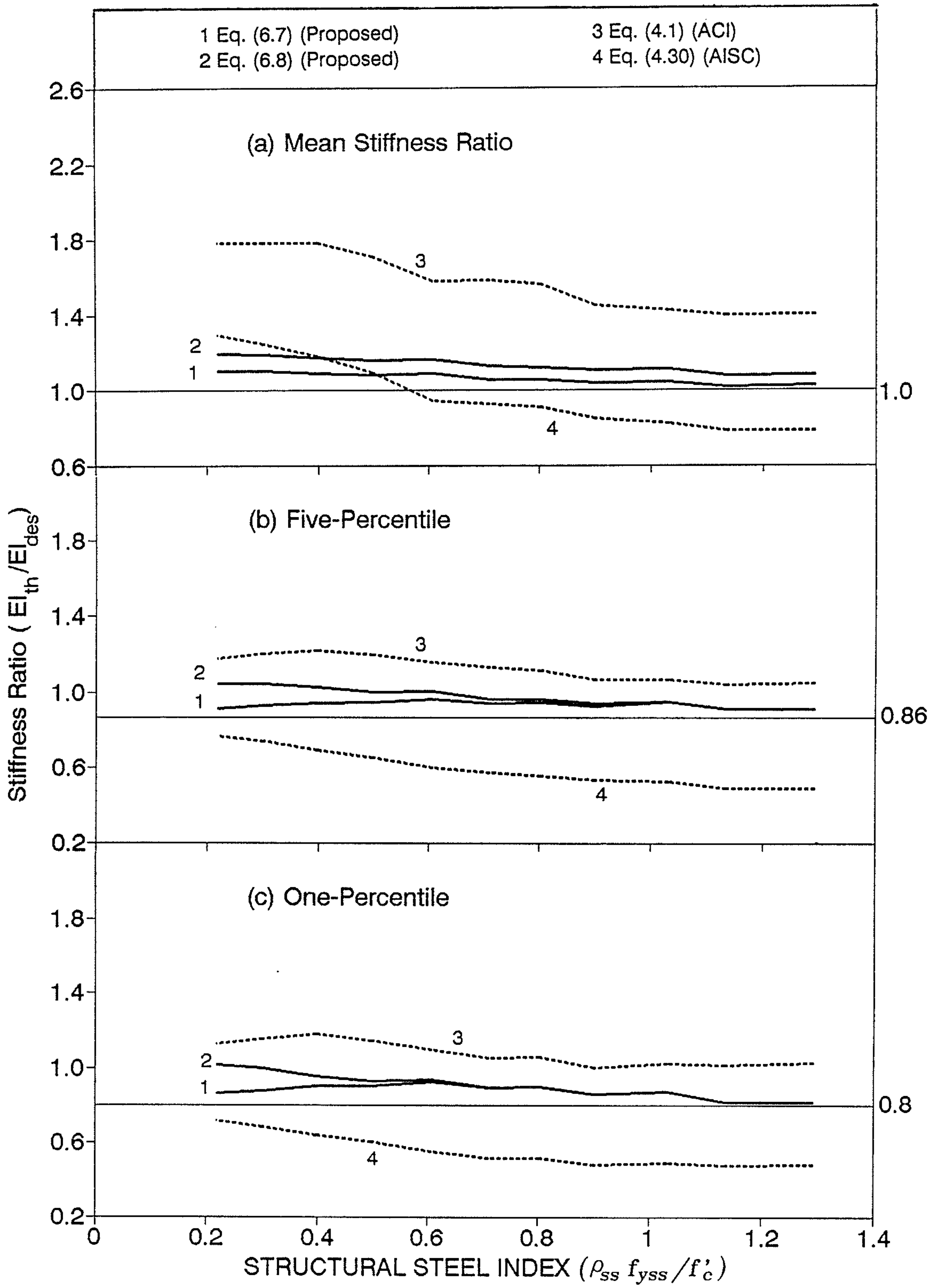

Figure 6.23 - Effect of structural steel index on stiffness ratio for different design equations for all columns bending about minor axis (n varies for each $\rho_{ss}f_{yss}/f'_c$ range; total n = 11,880).

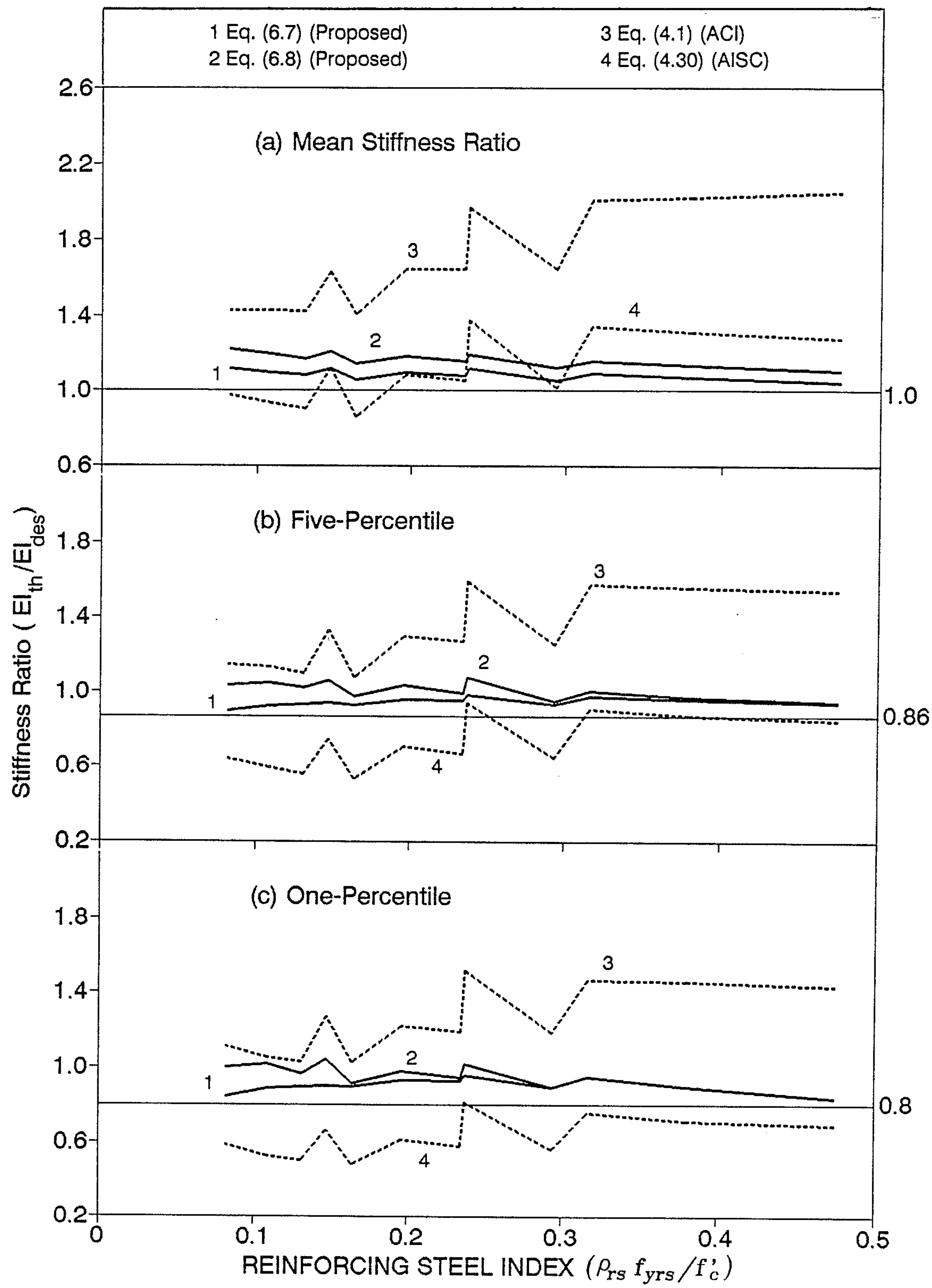

Figure 6.24 - Effect of reinforcing steel index on stiffness ratio for different design equations for all columns bending about minor axis (n=990 for each $\rho_{rs}f_{yrs}/f'_c$ equal to 0.082, 0.109, 0.131, 0.147, 0.164, 0.196, 0.235, 0.237, 0.294, 0.317, 0.380 and 0.475).

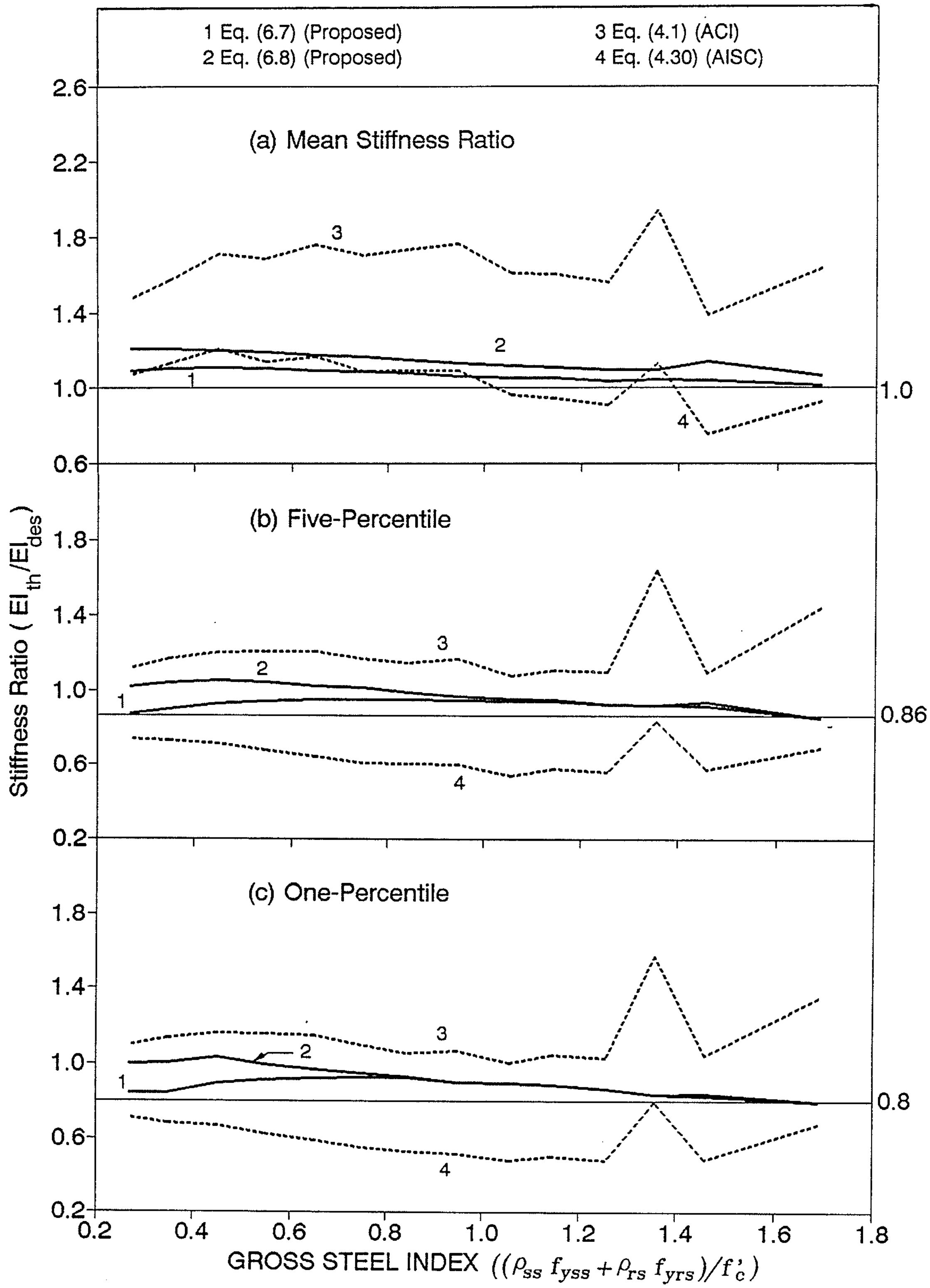

Figure 6.25 - Effect of gross steel index on stiffness ratio for different design equations for all columns bending about minor axis (n varies for each $(\rho_{ss}f_{yss}+\rho_{rs}f_{yrs})/f'_c$ range; total n = 11,880).

The effects of I_{rs}/I_{ss}, I_{ss}/I_g, I_{rs}/I_g and $(I_{ss} + I_{rs})/I_g$ on stiffness ratios (EI_{th}/EI_{des}) are respectively shown in Figures 6.26, 6.27, 6.28, and 6.29. The trends shown in these figures are similar to those discussed for Figures 6.18 to 6.25 related to the steel indices. This is particularly true when Figure 6.21 is compared to Figures 6.26 and 6.29, and Figure 6.18 to Figure 6.28. As expected, Figures 6.27 and 6.28 indicate that the ACI equation is more conservative when the moment of inertia of the steel section is relatively small or when the moment of inertia of the reinforcing steel is relatively large compared to the moment of inertia of the gross cross-section.

Figure 6.30 examines the effect of d_{ss}/h (ratio of depth of structural steel section to the overall depth of the composite cross section) on stiffness ratios. As expected, the results are somewhat similar to those obtain from Figure 6.27 plotted for the effect of I_{ss}/I_g. The proposed design equations produce practically constant values of mean, five-percentile and one-percentile stiffness ratios over the entire range of d_{ss}/h plotted, while the ACI and AISC equations are somewhat subjected to variations for different values of d_{ss}/h.

The following can be summarized from the data plotted in Figures 6.10 to 6.30 and the related discussions:

(1) The proposed design equations (Equations 6.7 and 6.8) were not significantly affected by any of the variables

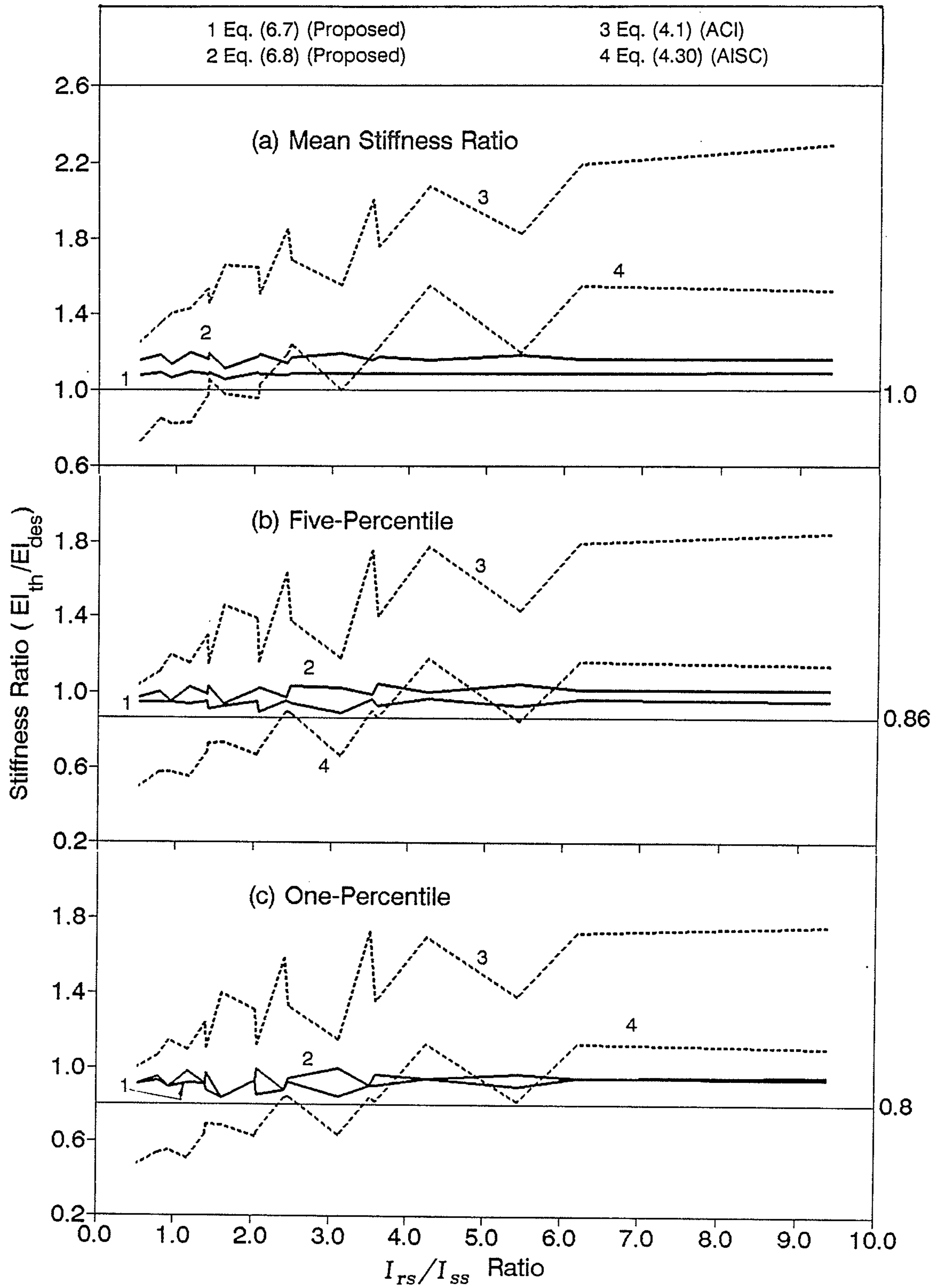

Figure 6.26 - Effect of I_{rs}/I_{ss} ratio on stiffness ratio for different design equations for all columns bending about minor axis (n=660 for each I_{rs}/I_{ss} ratio equal to 0.53, 0.80, 0.93, 1.17, 1.40, 1.42, 1.61, 2.04, 2.06, 2.41, 2.47, 3.11, 3.52, 3.59, 4.26, 5.44, 6.21 and 9.39).

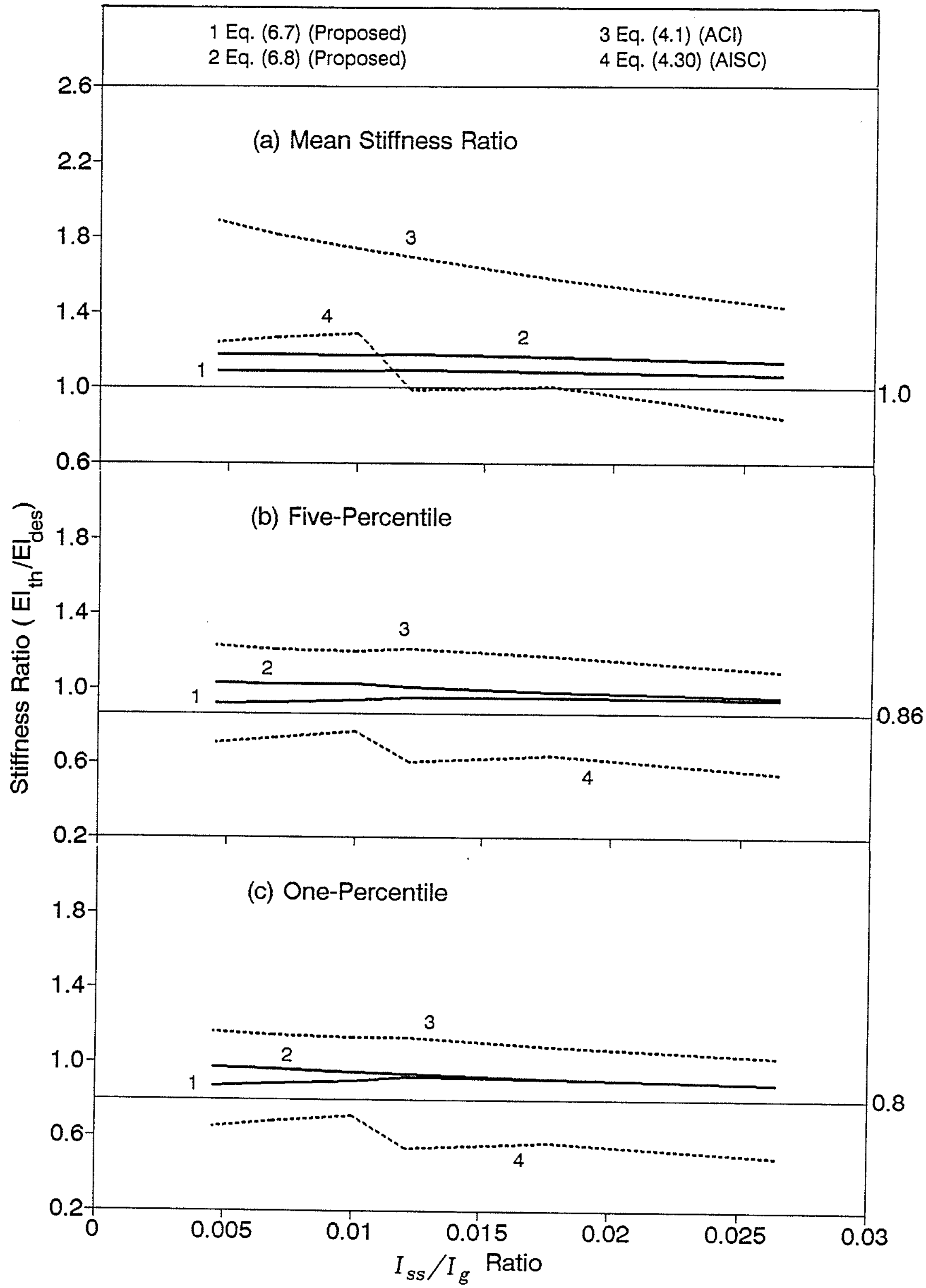

Figure 6.27 - Effect of I_{ss}/I_g ratio on stiffness ratio for different design equations for all columns bending about minor axis (n=1980 for each I_{ss}/I_g ratio equal to 0.005, 0.007, 0.010, 0.012, 0.018 and 0.026).

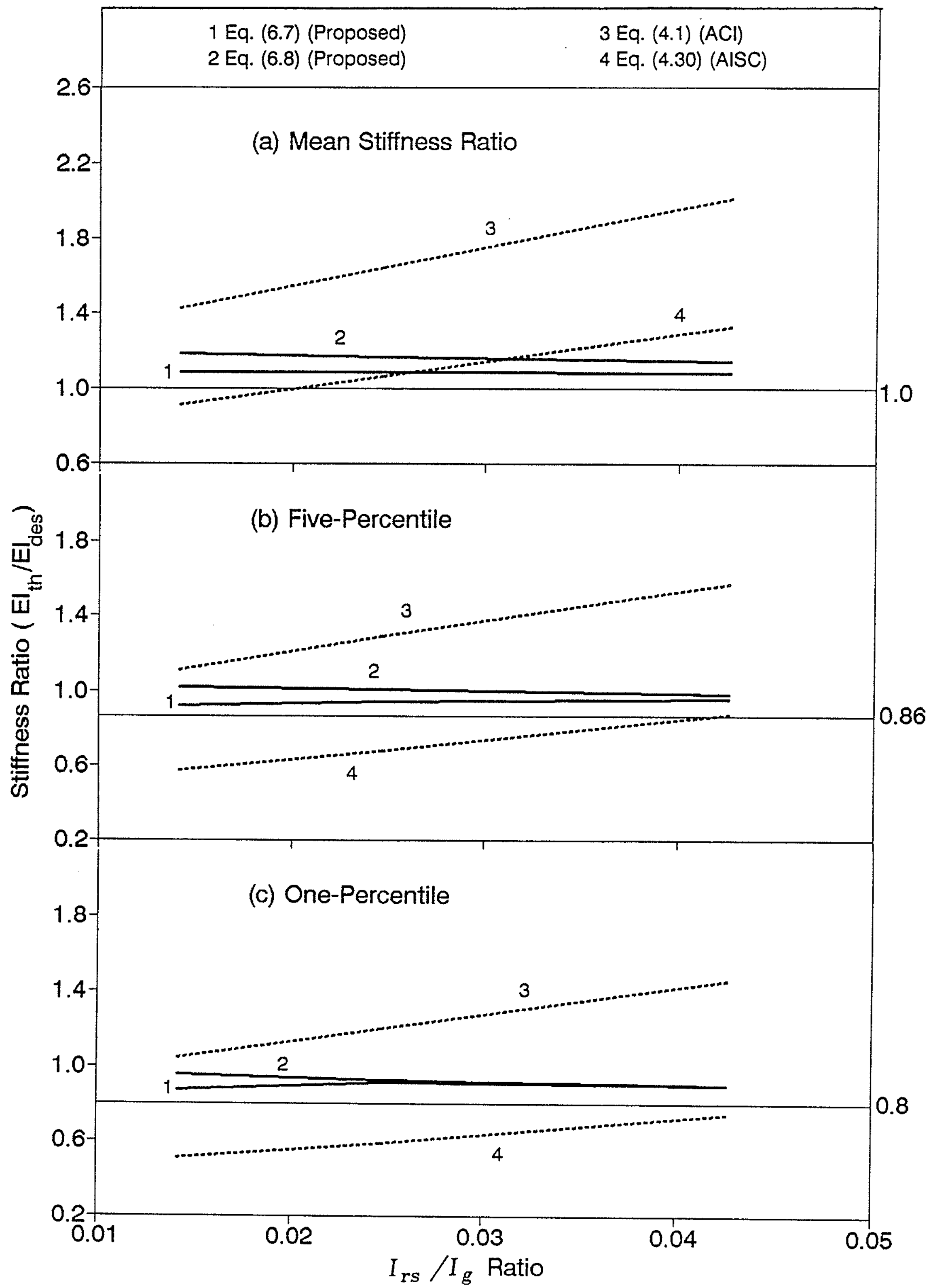

Figure 6.28 - Effect of I_{rs}/I_g ratio on stiffness ratio for different design equations for all columns bending about minor axis (n=3960 for each I_{rs}/I_g ratio equal to 0.014, 0.025, 0.043).

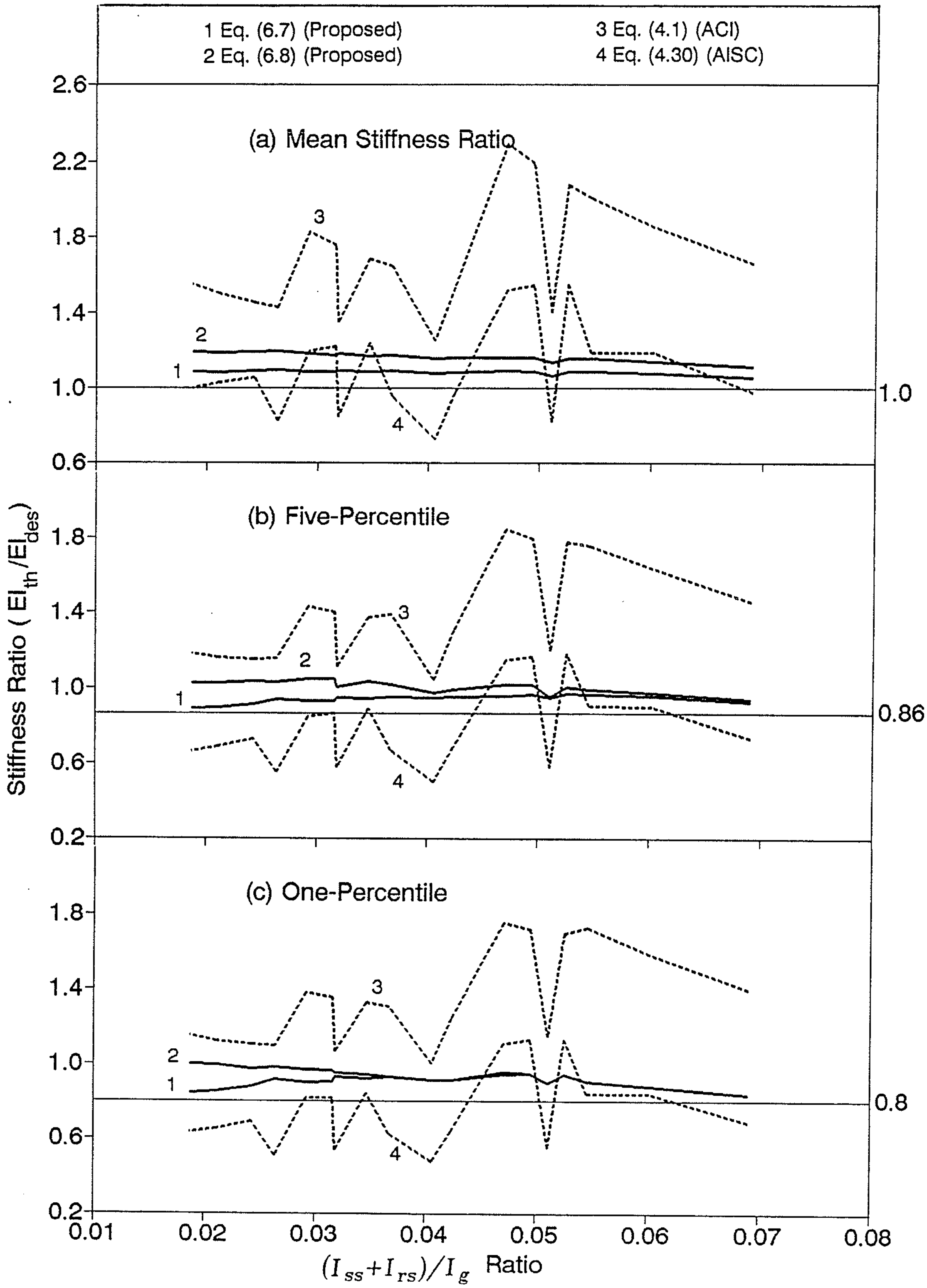

Figure 6.29 - Effect of $(I_{ss}+I_{rs})/I_g$ ratio on stiffness ratio for different design equations for all columns bending about minor axis (n=660 for each $(I_{ss}+I_{rs})/I_g$ ratio equal to 0.019, 0.021, 0.024, 0.026, 0.029, 0.0318, 0.0319, 0.035, 0.037, 0.041, 0.042, 0.047, 0.049, 0.051, 0.053, 0.055, 0.061 and 0.069).

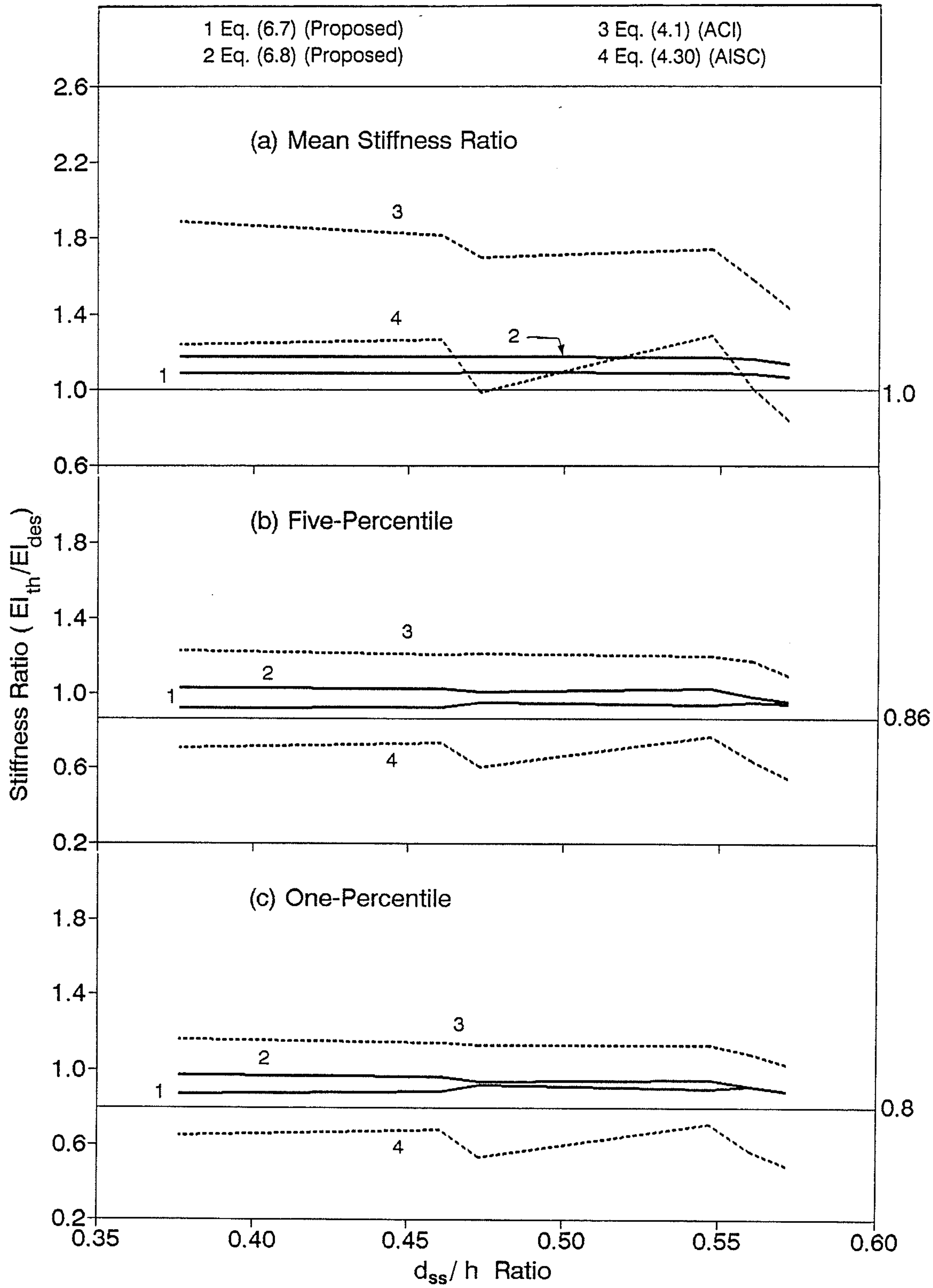

Figure 6.30 - Effect of d_{ss}/h ratio on stiffness ratio for different design equations for all columns bending about minor axis (n=1980 for each d_{ss}/h ratio equal to 0.38, 0.46, 0.47, 0.55, 0.56 and 0.57).

(Equations 4.1 and 4.30) were significantly affected by most of these same variables.

(2) The ACI design equation produced results that are consistently more conservative than the results of the proposed design equations for the mean, five-percentile and one-percentile stiffness ratios plotted against all of the variables.

3) The AISC equation gives stiffness ratios that are in many cases less conservative than those obtained for the proposed and ACI design equations. This is particularly valid for five-percentile and one-percentile values.

4) A comparison of plots for columns subjected to minor axis bending to the plots for columns subjected to major axis bending (Chapter 5) shows that the shape of the plotted curves for each of the four design equations remained essentially the same. It appears that the stiffness ratios obtained for the ACI equation became more conservative and the values obtained for the AISC expression became less conservative when columns were subjected to bending about the minor axis of the steel section.

6.4.3 Stiffness Ratios Produced by Proposed Design Equations for Usual Columns

For composite beam-columns, neither the ACI Code nor the AISC Code sets an upper limit on the amount of structural steel. However, the AISC Code states that to qualify as a composite column the structural steel ratio (ρ_{ss}) must be greater than or equal to 4 percent. The ACI Building code requires that a minimum of 1 percent to a maximum of 8 percent of longitudinal reinforcing (ρ_{rs}) be included with the structural steel core. Difficulty in lap splicing the reinforcing bars reduces the maximum limit of ρ_{rs} to about 3 percent when a relatively large structural steel core is encased. The reinforcing steel ratio is, therefore, usually expected to range from 1 to 3 percent. Even three percent reinforcing steel will restrict ρ_{ss} to a maximum of about 10 percent, giving the ρ_{ss} range of about 4 to 10 percent. Mirza and MacGregor (1982) determined that the end eccentricity ratio for columns in reinforced concrete buildings usually ranged from 0.1 to 0.65. Therefore, the usual columns in this study were defined as those for which e/h = 0.1, 0.2, 0.3, 0.4, 0.5, 0.6, or 0.7, and ρ_{ss} = 4.2 (actual values = 4.07, 4.13, 4.36), 7.0 (actual values of 6.80, 7.29), or 10.3 (actual value = 10.33) percent, and ρ_{rs} equal to 1.09, 1.96, or 3.17 percent.

Figures 6.31 (a) to (e) examine the variations in mean and minium values of the stiffness ratios with respect to e/h

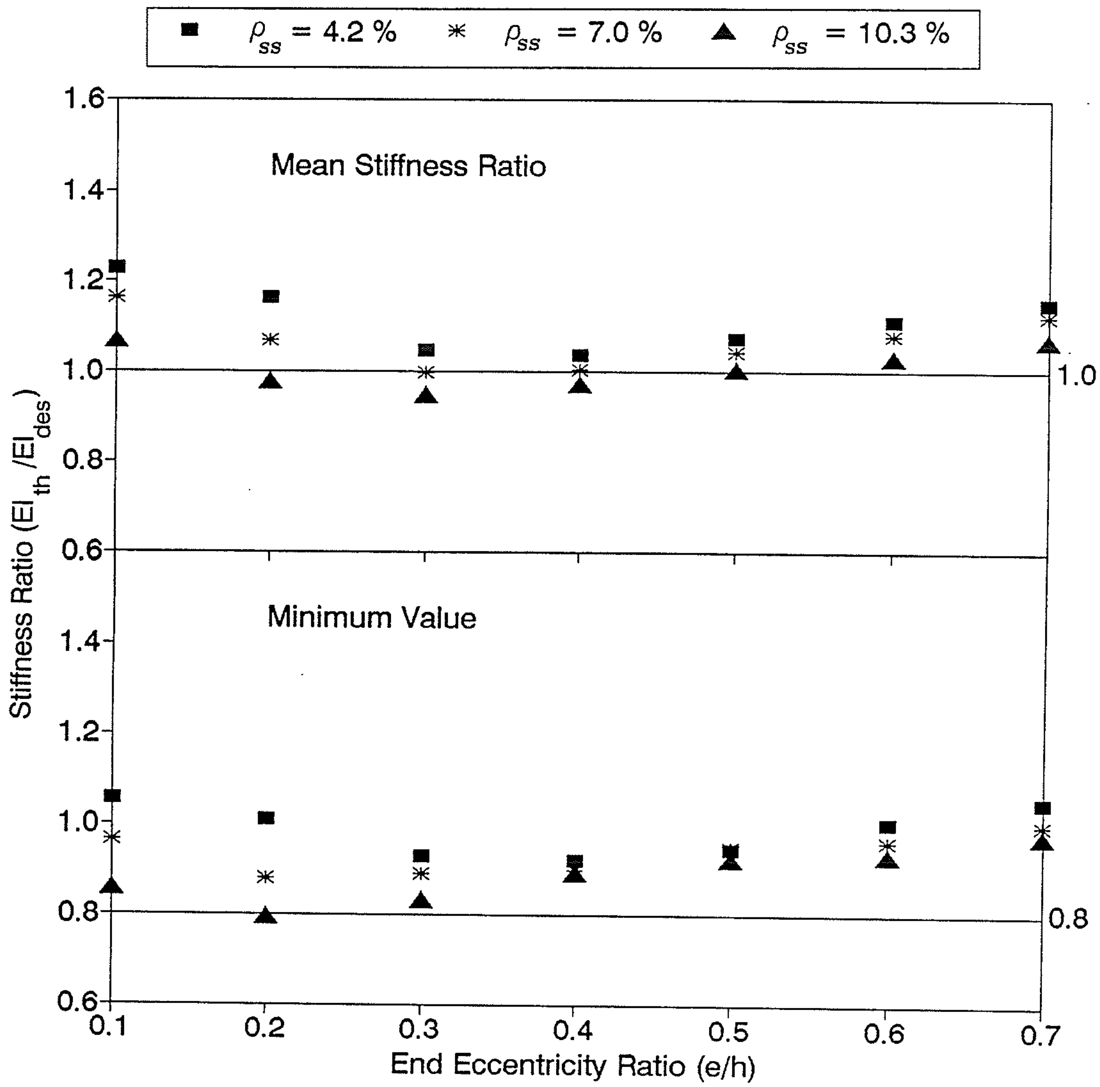

Figure 6.31(a) - Stiffness ratios obtained from proposed design equations, Eq. (6.7) or (6.8), for usual columns bending about minor axis with ℓ/h = 10 (for each combination of e/h and ρ_{ss} ratios plotted n=108 for ρ_{ss}=4.2 percent, n=72 when ρ_{ss}=7.0 percent and n=36 when ρ_{ss}=10.3 percent).

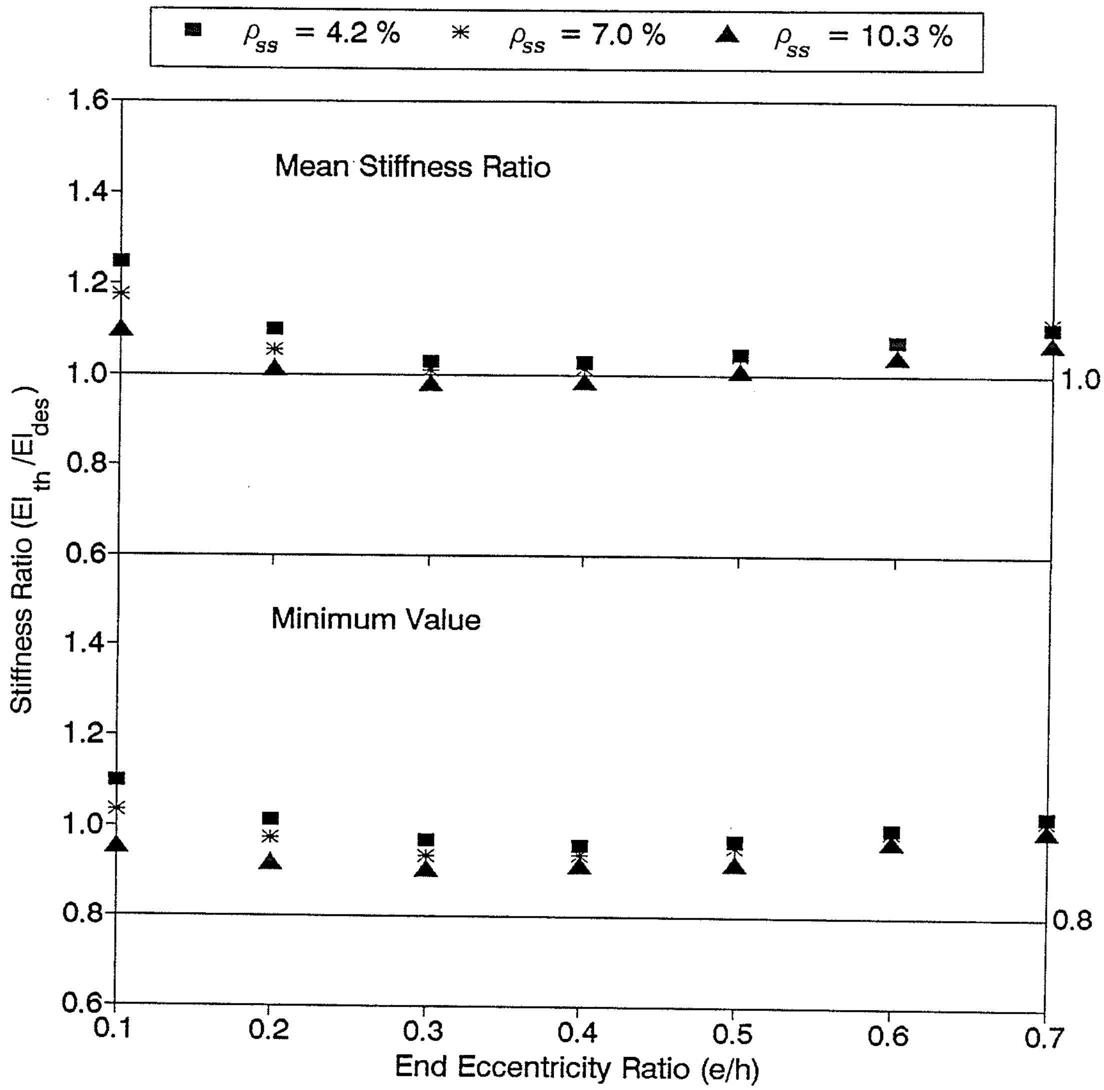

Figure 6.31(b) - Stiffness ratios obtained from proposed design Equation (6.7) for usual columns bending about minor axis with ℓ/h = 15 (for each combination of e/h and ρ_{ss} ratios plotted n = 108 for ρ_{ss}=4.2 percent, n=72 when ρ_{ss}=7.0 percent and n=36 when ρ_{ss}=10.3 percent).

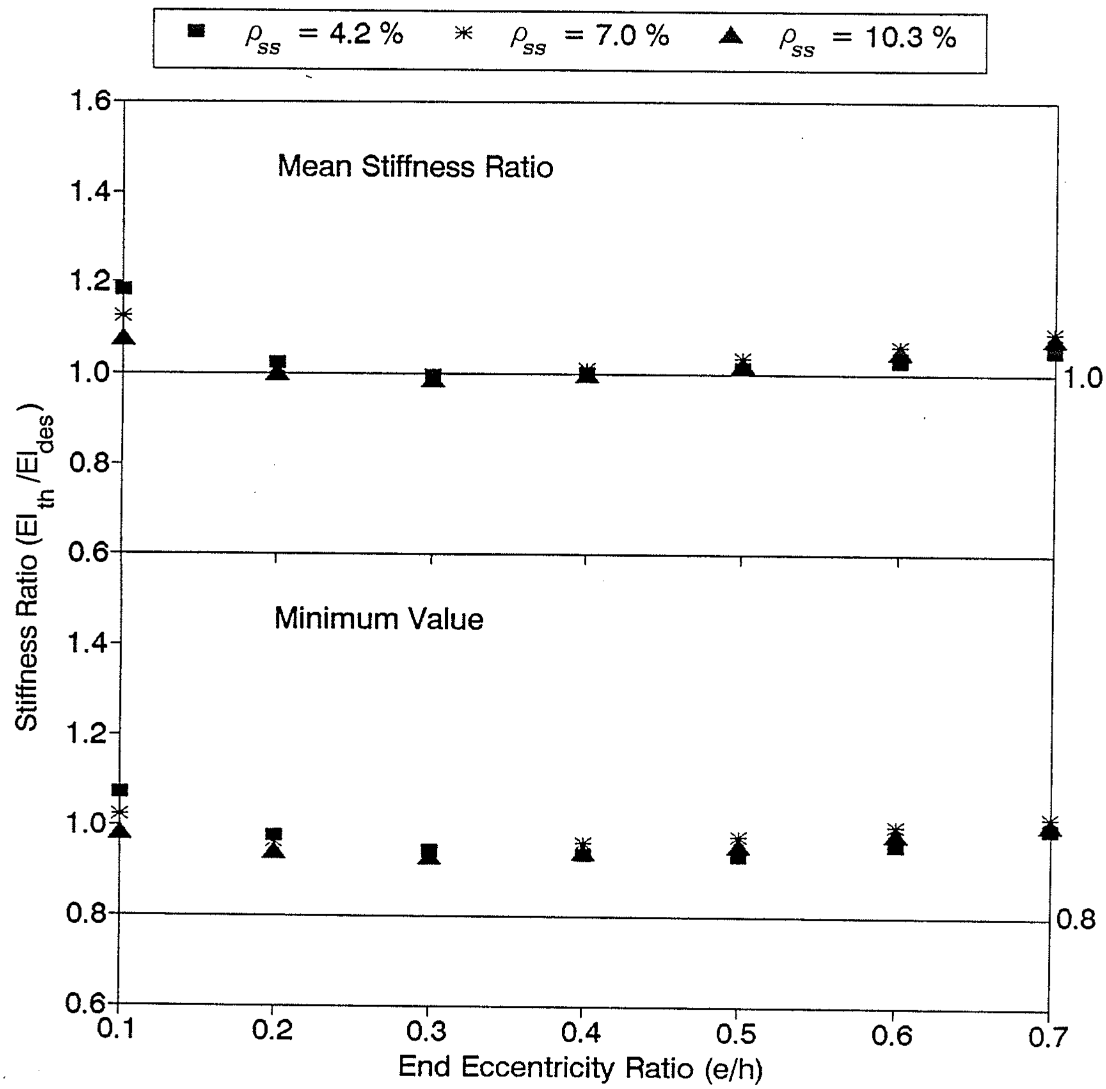

Figure 6.31(c) - Stiffness ratios obtained from proposed design Equation (6.7) for usual columns bending about minor axis with ℓ/h = 20 (for each combination of e/h and ρ_{ss} ratios plotted n = 108 for ρ_{ss}=4.2 percent, n=72 when ρ_{ss}=7.0 percent and n=36 when ρ_{ss}=10.3 percent).

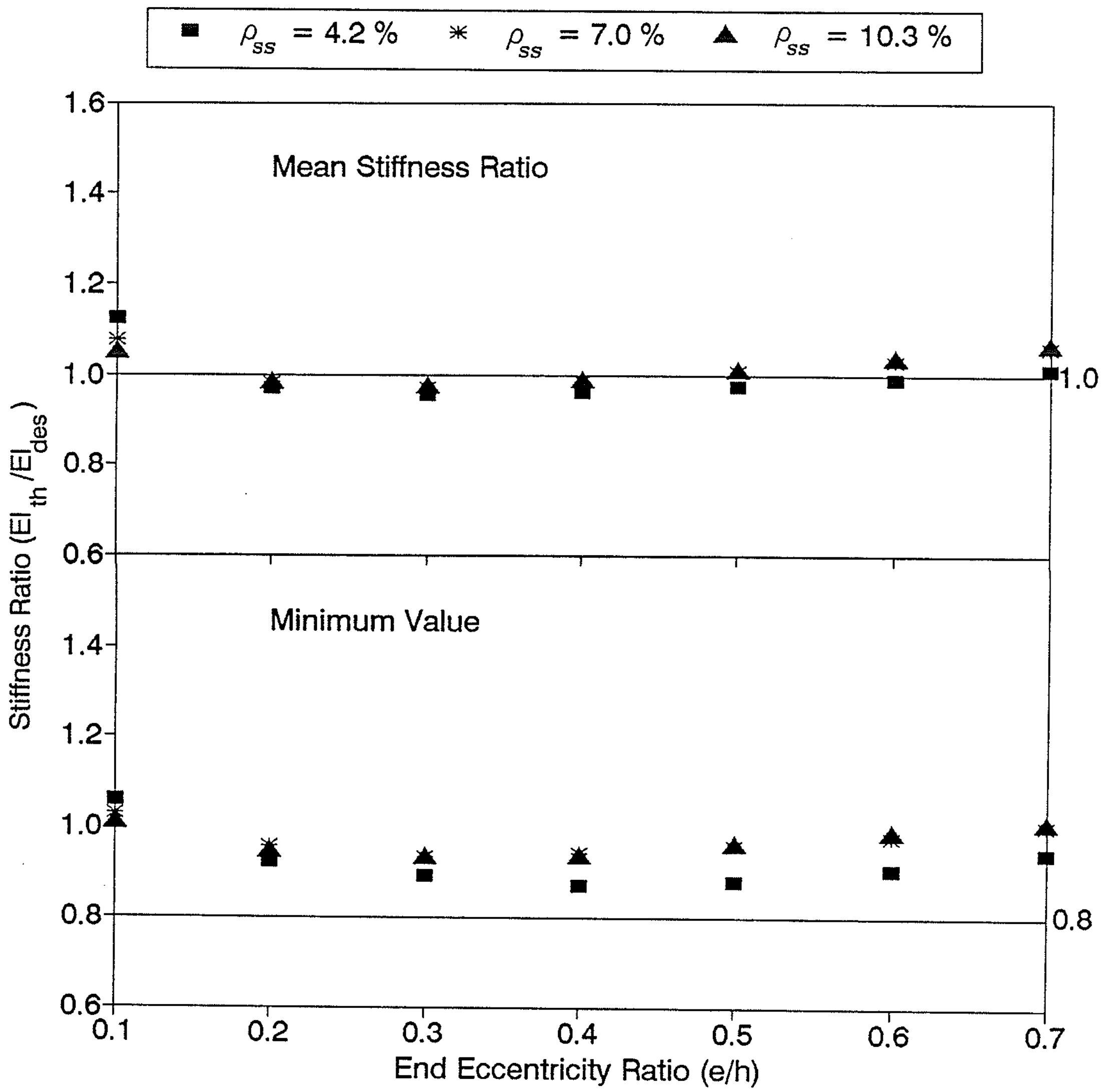

Figure 6.31(d) - Stiffness ratios obtained from proposed design Equation (6.7) for usual columns bending about minor axis with ℓ/h = 25 (for each combination of e/h and ρ_{ss} ratios plotted n = 108 for ρ_{ss}=4.2 percent, n=72 when ρ_{ss}=7.0 percent and n=36 when ρ_{ss}=10.3 percent).

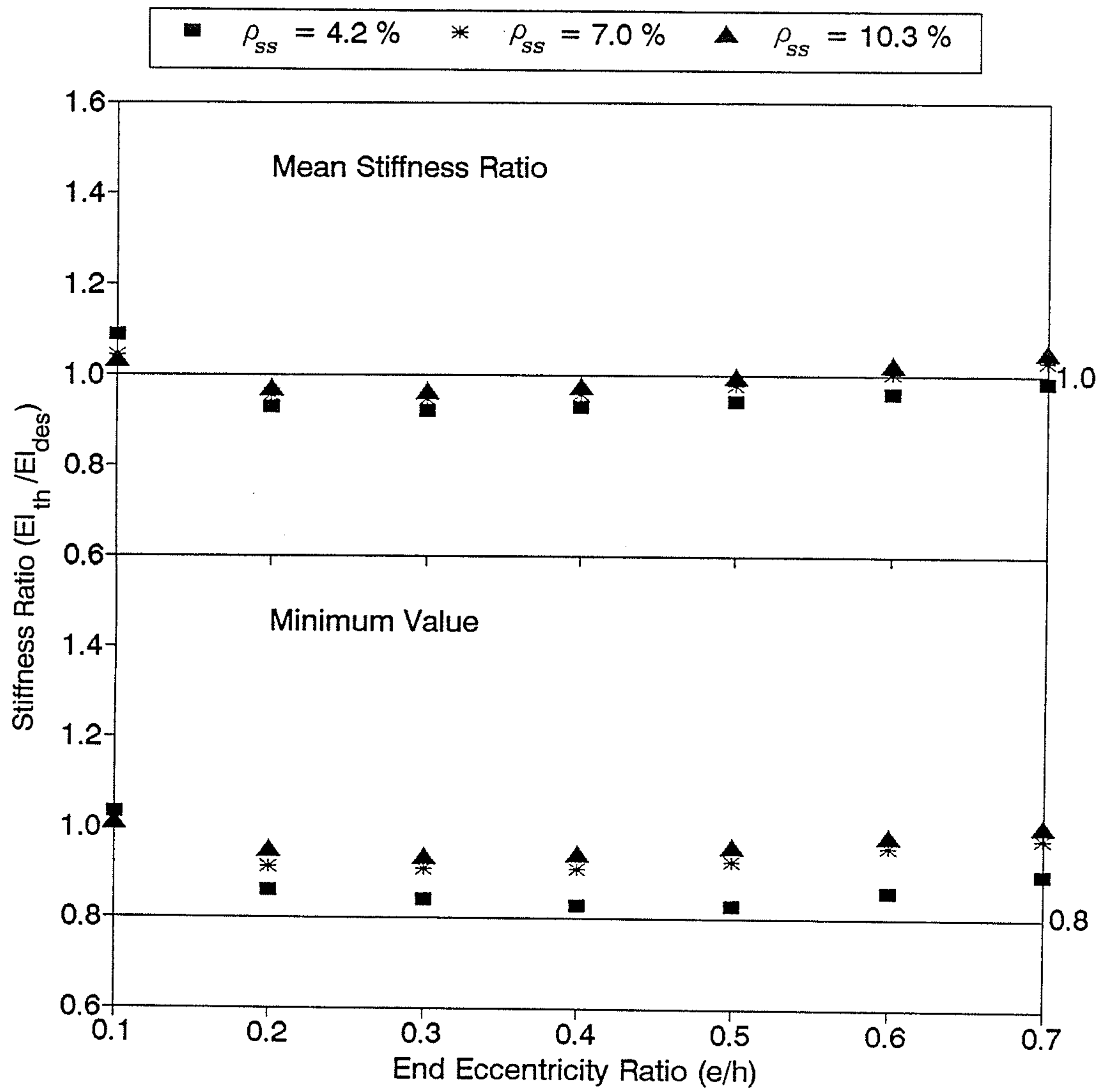

Figure 6.31(e) - Stiffness ratios obtained from proposed design Equation (6.7) for usual columns bending about minor axis with ℓ/h = 30 (for each combination of e/h and ρ_{ss} ratios plotted n = 108 for ρ_{ss}=4.2 percent, n=72 when ρ_{ss}=7.0 percent and n=36 when ρ_{ss}=10.3 percent).

computed from Equation 6.7 and plotted for ℓ/h = 10, 15, 20, 25 and 30, respectively. The number of values available for plotting each point were 36, 72 and 108 for ρ_{ss} = 10.3, 7.0 and 4.2 percent, respectively. The one-percentile values were not plotted in these figures because the minimum values represented 2.8, 1.4 and 0.93 percentiles. The mean stiffness ratios exceeded 1.0 for most of the columns for all ℓ/h, while the minimum values exceeded 0.8 in all cases. Only for ρ_{ss} equal to 10.3 percent and e/h equal to 0.2 to 0.4 were the mean stiffness ratios consistently less than 1.0. This indicated by Figures 6.31(a) to (e).

Equation 6.8 is identical to Equation 6.7 for ℓ/h = 10, and becomes more conservative as ℓ/h increases. This becomes evident by Figures 6.31(f), (g), (h), and (i) plotted for Equation 6.8.

The following conclusions appear to be valid for columns with e/h = 0.1 to 0.7, ρ_{ss} = 4.2 to 10.3 percent, ρ_{rs} = 1.1 to 3.2 percent, and ℓ/h = 10 to 30:

(1) The mean and minimum stiffness ratios for Equation 6.7 or 6.8 may be taken as 1.0 and 0.8, respectively;

(2) The proposed design equations (Equations 6.7 and 6.8) are not subject to significant variation due to e/h, ρ_{ss} or ℓ/h ratios.

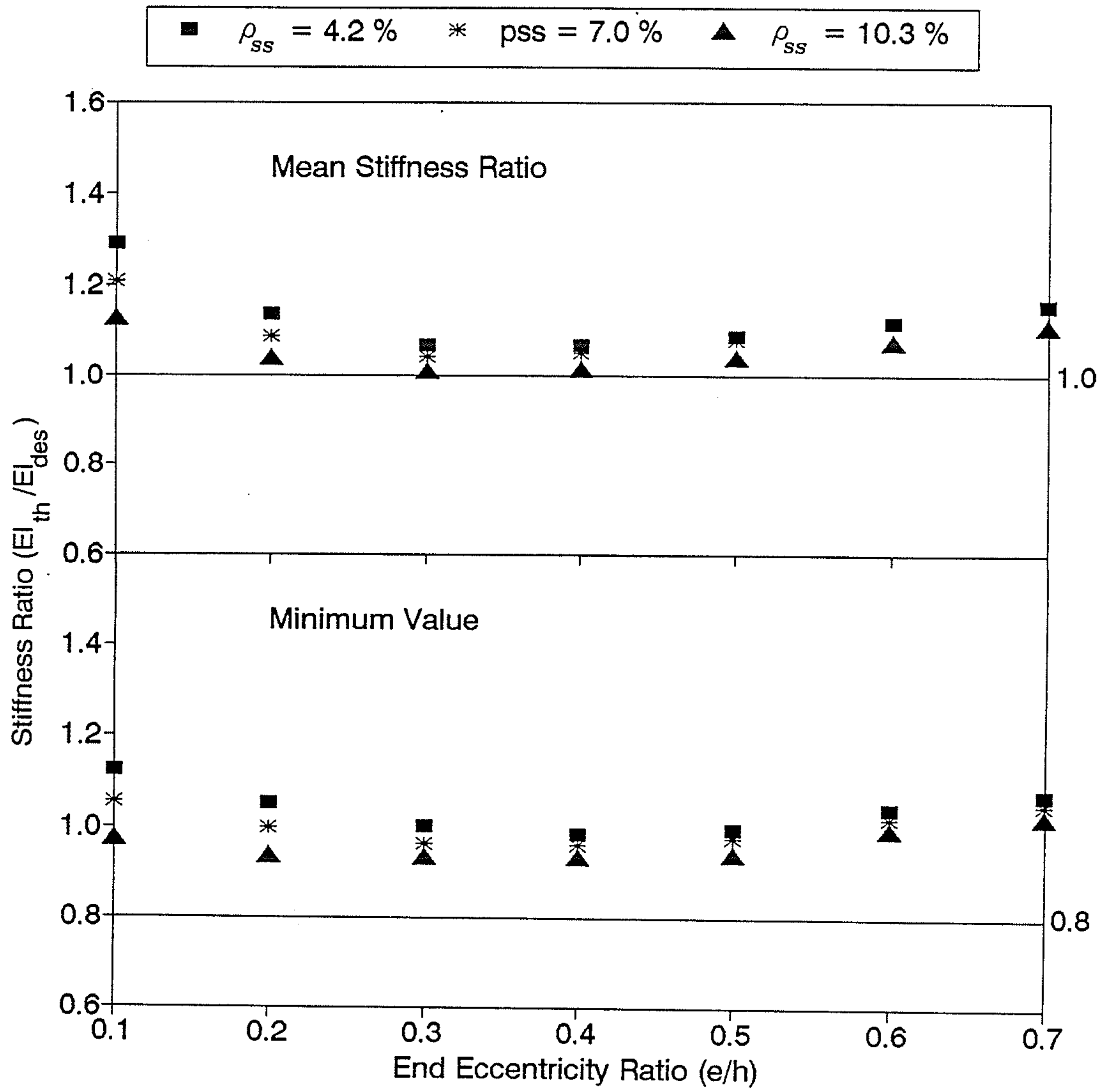

Figure 6.31(f) - Stiffness ratios obtained from proposed design Equation (6.8) for usual columns bending about minor axis with ℓ/h = 15 (for each combination of e/h and ρ_{ss} ratios plotted n = 108 for ρ_{ss}=4.2 percent, n=72 when ρ_{ss}=7.0 percent and n=36 when ρ_{ss}=10.3 percent).

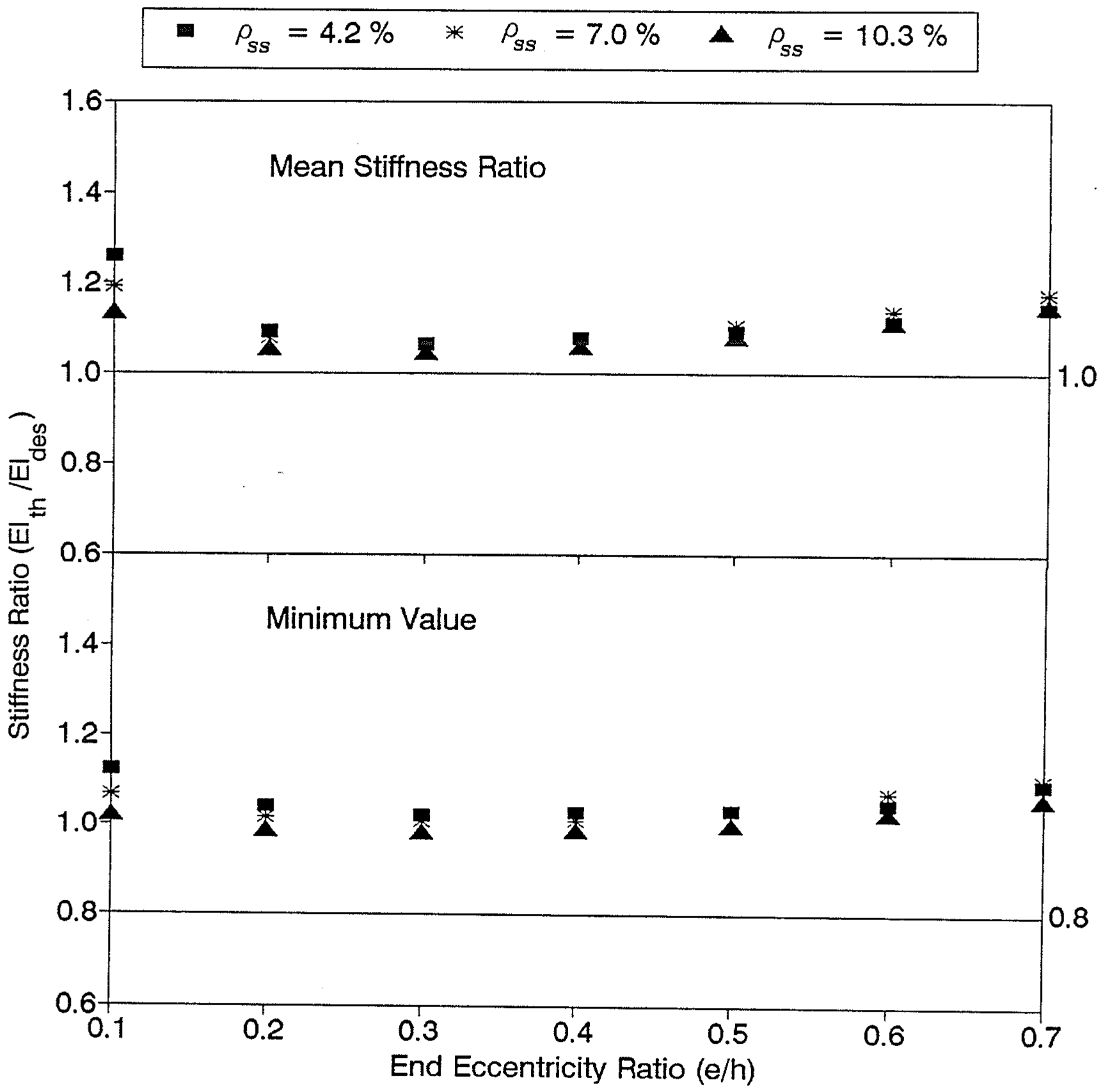

Figure 6.31(g) - Stiffness ratios obtained from proposed design Equation (6.8) for usual columns bending about minor axis with ℓ/h = 20 (for each combination of e/h and ρ_{ss} ratios plotted n = 108 for ρ_{ss}=4.2 percent, n=72 when ρ_{ss}=7.0 percent and n=36 when ρ_{ss}=10.3 percent).

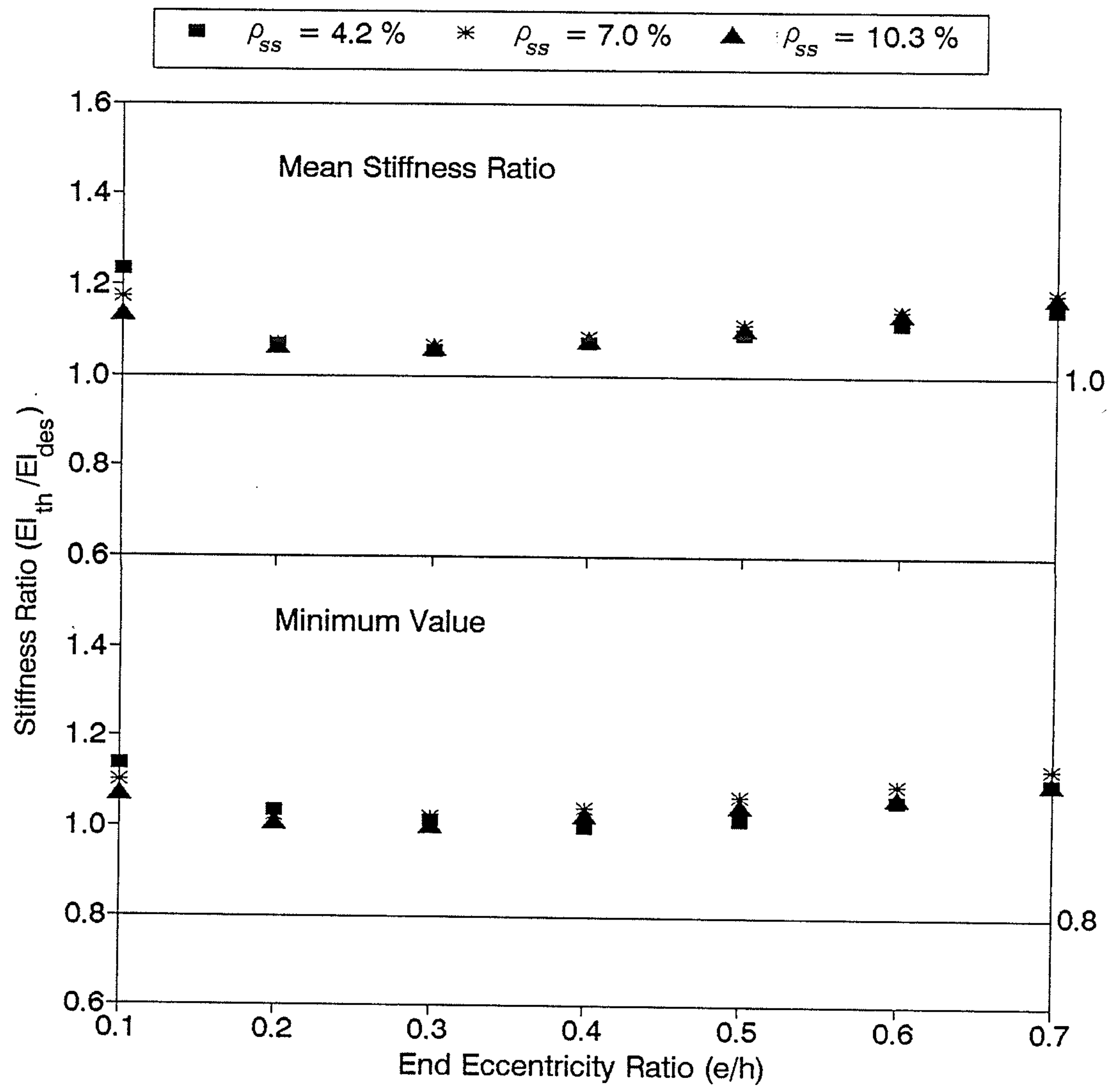

Figure 6.31(h) - Stiffness ratios obtained from proposed design Equation (6.8) for usual columns bending about minor axis with ℓ/h = 25 (for each combination of e/h and ρ_{ss} ratios plotted n = 108 for ρ_{ss}=4.2 percent, n=72 when ρ_{ss}=7.0 percent and n=36 when ρ_{ss}=10.3 percent).

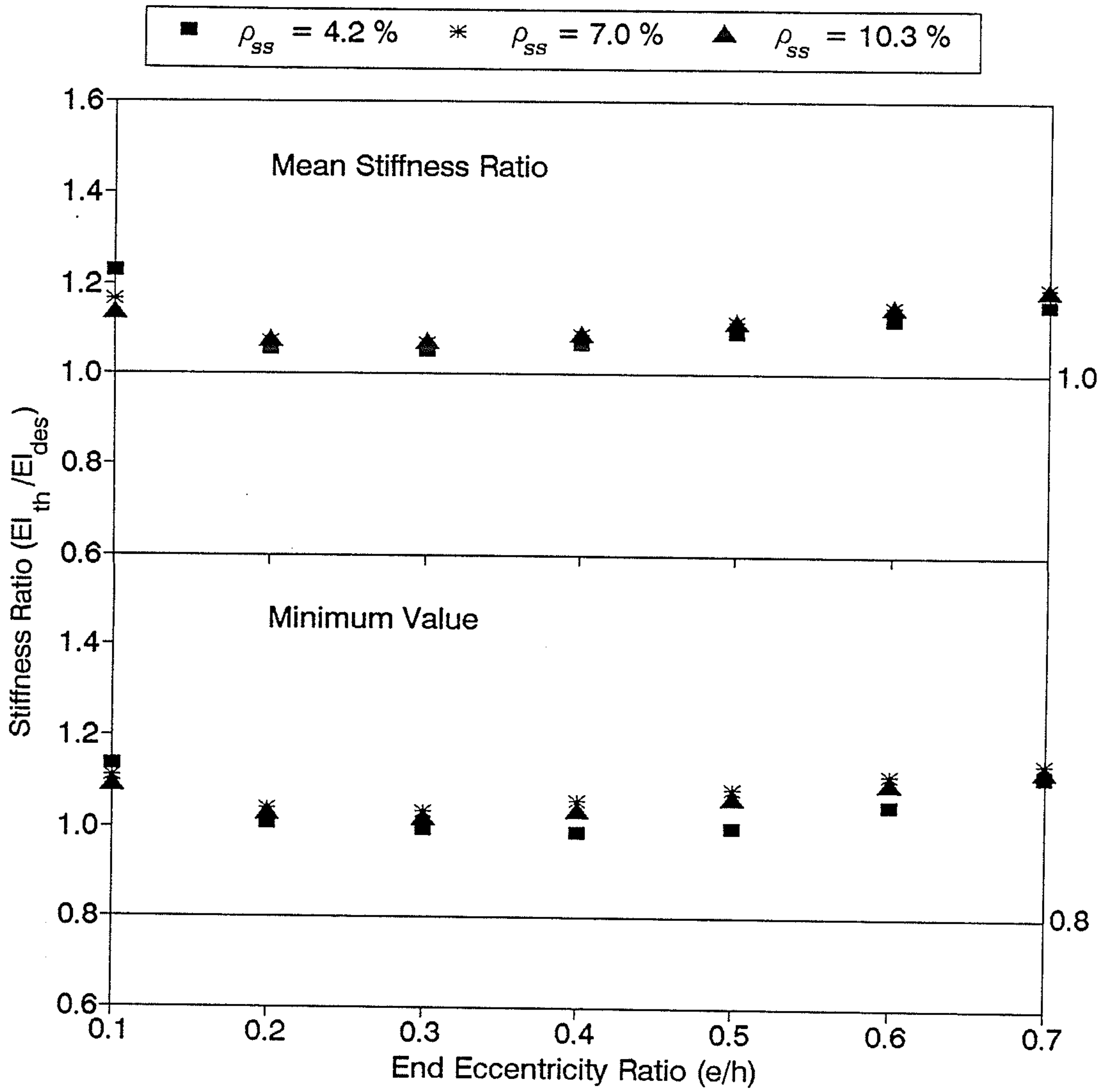

Figure 6.31(i) - Stiffness ratios obtained from proposed design Equation (6.8) for usual columns bending about minor axis with ℓ/h = 30 (for each combination of e/h and ρ_{ss} ratios plotted n = 108 for ρ_{ss}=4.2 percent, n=72 when ρ_{ss}=7.0 percent and n=36 when ρ_{ss}=10.3 percent).

6.5 THEORETICALLY CALCULATED CRITICAL BUCKLING LOAD

The ratio of axial load acting on the column to critical buckling load, given as P_u/P_{cr}, is used by ACI (Equation 4.26) and AISC (Equation 4.11) to evaluate the second order effects of slenderness.

The frequency histogram and statistics shown in Figure 6.32 and Table 6.6 represent the critical load ratio $P_{u(th)}/P_{cr(th)}$ for 10800 columns with e/h ranging from 0.1 to 1.0. $P_{u(th)}$ is the computed theoretical axial load capacity and $P_{cr(th)}$ is calculated by substituting the computed theoretical effective flexural stiffness EI_{th} in Equation 2.4, yielding:

$$P_{cr(th)} = \frac{\pi^2 EI_{th}}{\ell^2} \tag{6.11}$$

Table 6.6 lists the mean value of 0.335, standard deviation of 0.179 and coefficient of variation of 0.535 for the range of critical load ratios shown in Figure 6.32. The critical load ratios of 0.4, 0.5, 0.6, 0.7 and 0.8 represent the 66th, 82nd, 89th, 96th, and 99.7th percentiles, respectively, as indicated in Figure 6.32.

For design purposes, it is proposed that the mean value plus one standard deviation, 0.5, be used as the upper limit for P_u/P_{cr}. This means that 82 percent of the beam-columns used for plotting Figure 6.32 would be considered practical columns. This compares to the value obtained for the columns subjected to major axis bending (Chapter 5). The suggested

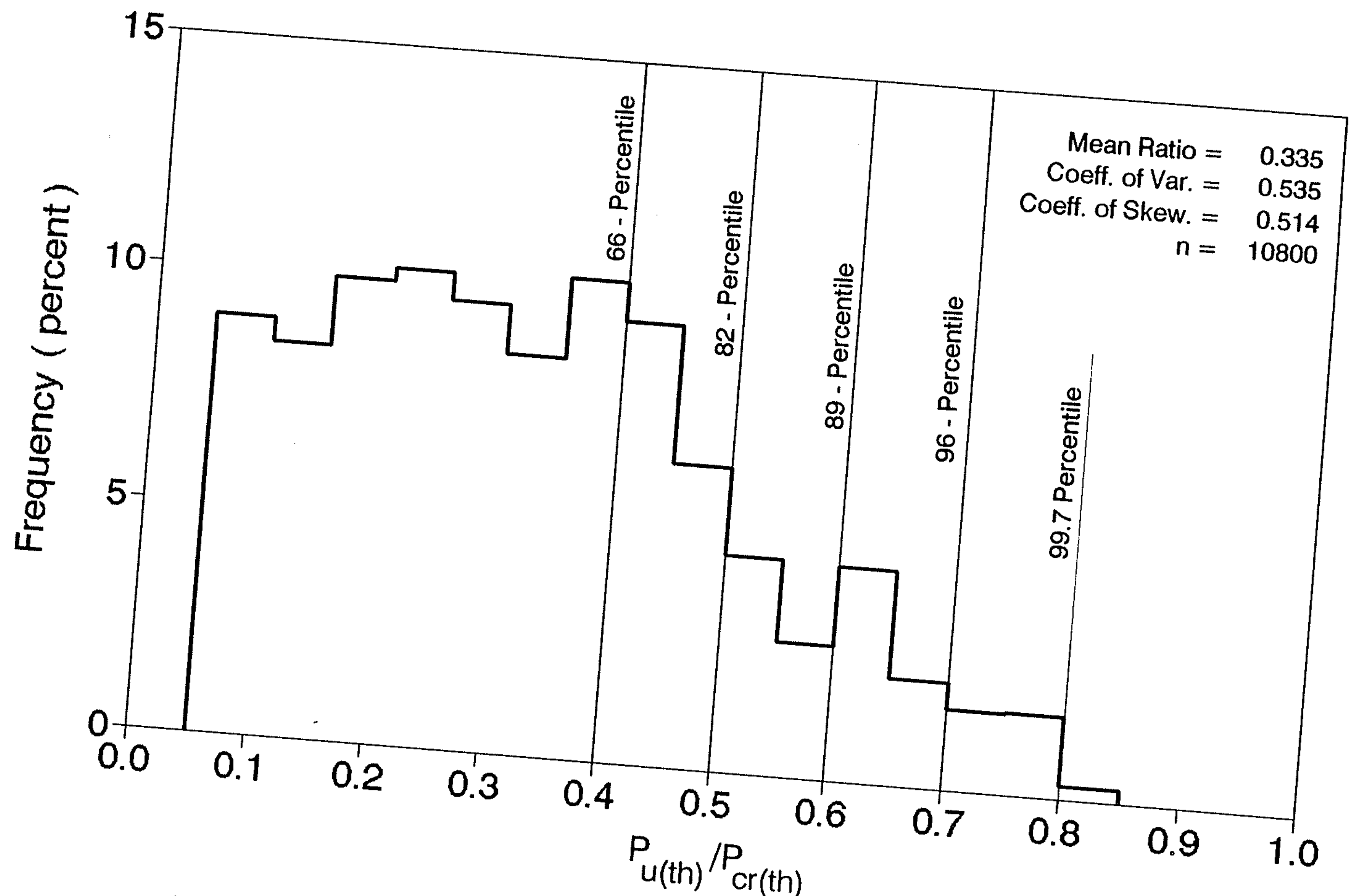

Figure 6.32 - Frequency histogram for critical load ratio for all columns bending about minor axis other than those for which $e/h = 0.05$.

Table 6.6 - Statistics for critical load ratio $P_{u(th)}/P_{cr(th)}$

NUMBER OF COLUMNS STUDIED = 10800

COLUMNS WITH e/h = 0.05 NOT INCLUDED

STATISTICAL EVALUATION

MEAN-VALUE	STND-DEV.	COEF.VAR	COEF. SKEW.	KURTOSIS
0.33464	0.17912	0.53527	0.51358	2.57418

MIN-VALUE	MAX-VALUE	MEDIAN
0.06114	0.80794	0.31864

ONE-PERCENTILE	FIVE-PERCENTILE
0.06800	0.08069

MOMENTS ABOUT THE MEAN

2ND-MOMENT	3RD-MOMENT	4TH-MOMENT
0.3208220E-01	0.2951641E-02	0.2650016E-02

CUMULATIVE FREQUENCY TABLE

CLASS-NO.	LOWER-LIMIT	UPPER-LIMIT	%CUM-FREQ.	GROSS-NO.	%FREQ.	No.
1	0.00000	0.04999	0.00000	0	0.00000	0
2	0.05000	0.09999	8.97222	969	8.97222	969
3	0.10000	0.14999	17.42593	1882	8.45370	913
4	0.15000	0.19999	27.34259	2953	9.91667	1071
5	0.20000	0.24999	37.50926	4051	10.16667	1098
6	0.25000	0.29999	47.10185	5087	9.59259	1036
7	0.30000	0.34999	55.62963	6008	8.52778	921
8	0.35000	0.39999	65.88889	7116	10.25926	1108
9	0.40000	0.44999	75.33334	8136	9.44444	1020
10	0.45000	0.49999	81.87037	8842	6.53704	706
11	0.50000	0.54999	86.53704	9346	4.66667	504
12	0.55000	0.59999	89.40741	9656	2.87037	310
13	0.60000	0.64999	94.00000	10152	4.59259	496
14	0.65000	0.69999	96.28704	10399	2.28704	247
15	0.70000	0.74999	98.00000	10584	1.71296	185
16	0.75000	0.79999	99.74074	10772	1.74074	188
17	0.80000	0.84999	100.00000	10800	0.25926	28
18	0.85000	0.89999	100.00000	10800	0.00000	0

upper limit of 0.5 for P_u/P_{cr} is plotted in Figures 6.33(a) and 6.33(b) to examine the effects of e/h and ℓ/h on $P_{u(th)}/P_{cr(th)}$. Figures 6.33(a) and 6.33(b) indicate that some columns with low e/h, high ℓ/h, or both have $P_{u(th)}/P_{cr(th)}$ ratio greater than the suggested upper limit. This means that the suggested upper limit would control the design of very slender columns in lower storeys of high-rise buildings.

6.6 ANOTHER LOOK AT THE AISC EFFECTIVE STIFFNESS

The somewhat low stiffness ratios (EI_{th}/EI_{des}) obtained in some cases for the AISC expression (Equation 4.30) raised some concerns. This prompted a further examination of the AISC interaction equations.

A comparison of the ratios of the theoretical ultimate strength $P_{u(th)}$ to the AISC ultimate strength $P_{u(AISC)}$ was undertaken to assess the accuracy of the AISC interaction equations (Equation 4.16 and 4.17) used for predicting the beam-column strength. Figure 6.34(a) plotted from the data for all beam-columns studied shows that the probability distribution of the strength ratios yield a mean value of 1.23, coefficient of variation of 0.19, and one-percentile value of 0.803. This is clearly an improvement over the probability distribution properties of the stiffness ratios (mean value = 1.10, coefficient of variation of 0.32, and one-percentile value = 0.540) obtained from the same beam-column data and shown in Figure 6.2(b).

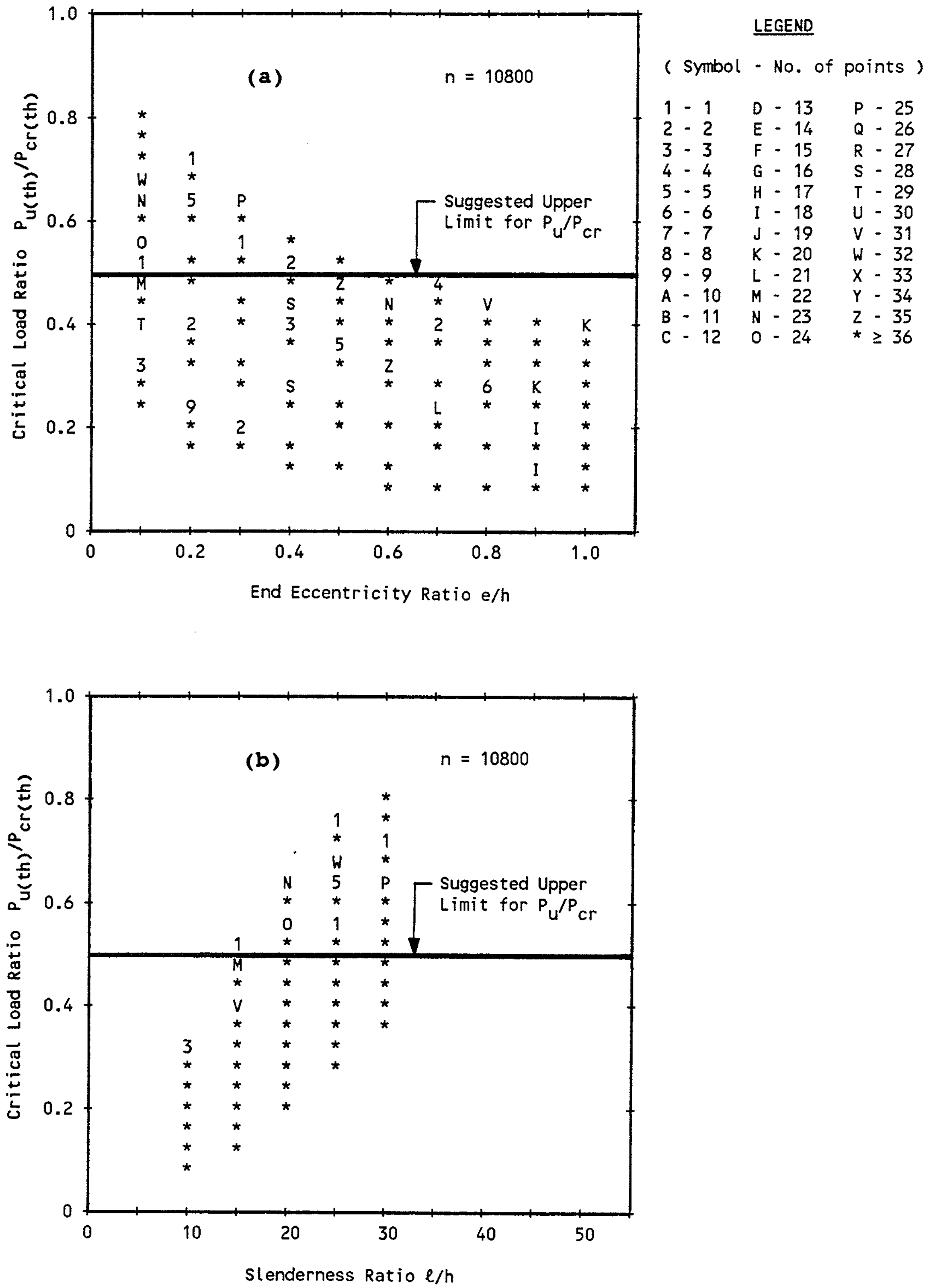

Figure 6.33 - Effect of (a) end eccentricity ratio and (b) slenderness ratio on critical load for all columns bending about the minor axis other than those for which e/h = 0.05.

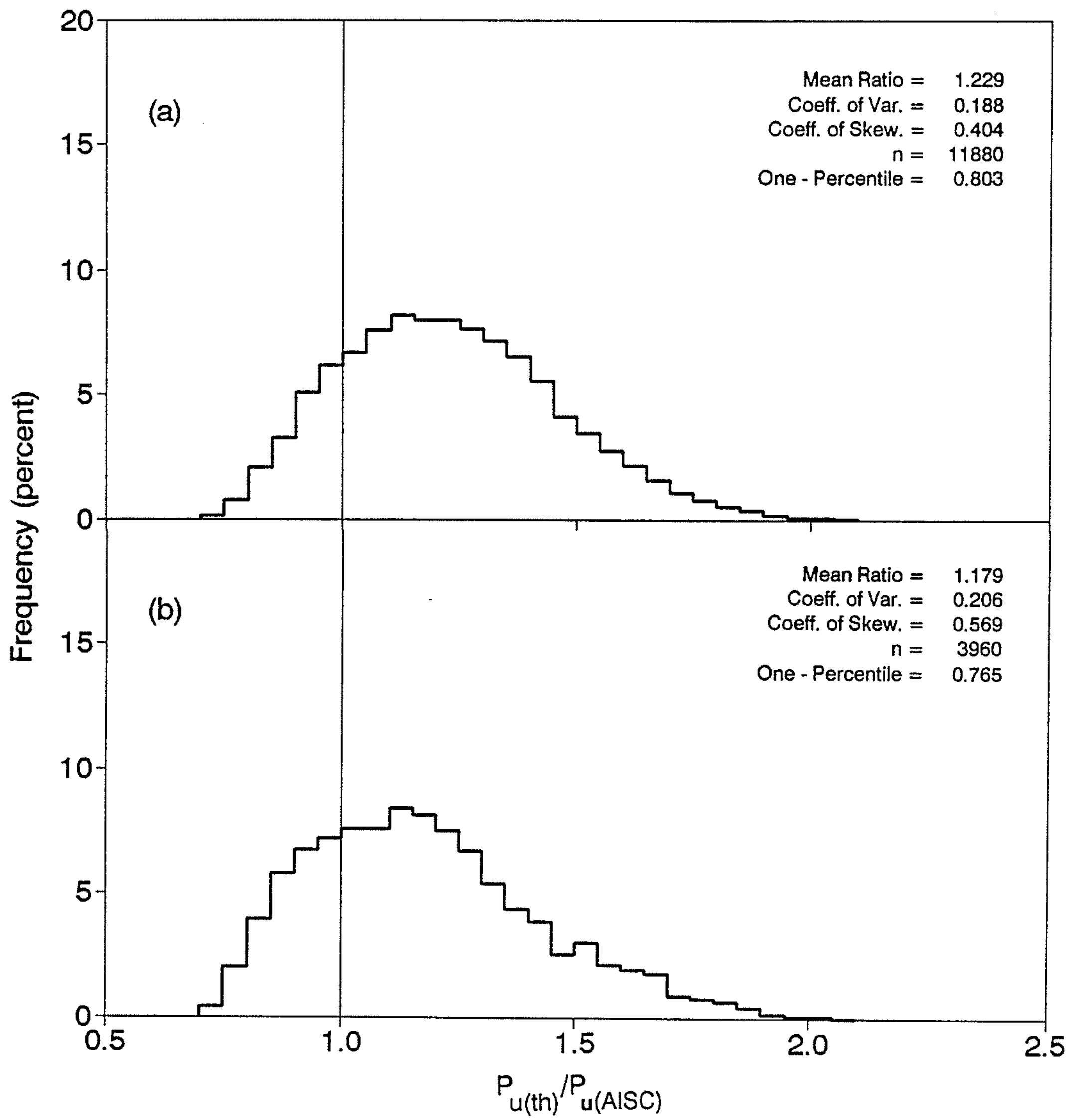

Figure 6.34 - Frequency histogram for ratio of theoretical ultimate strength to AISC ultimate strength for columns bending about the minor axis: (a) ρ_{rs} = 1.09, 1.96 and 3.17 percent; and (b) ρ_{rs} = 1.09 percent.

For the strength ratio data shown in Figure 6.34(b) for beam-columns having only 1 percent of reinforcing steel, the mean value of 1.18, coefficient of variation of 0.21, and one-percentile value of 0.765 were obtained. Again, this is a considerable improvement over the comparable values (0.91, 0.33, and 0.507) shown in Figure 6.3(b) for stiffness ratios.

The above-noted differences in strength ratios and stiffness ratios are expected since the stiffness of a composite beam-column is more susceptible to concrete cracking and material nonlinearities than its strength.

Figures 6.35 and 6.36 show the strength ratios plotted against e/h for all the data and for data from beam-columns having ρ_{rs} of 1 percent. Figure 6.35 shows mean, five-percentile and one-percentile greater than or equal to 1.0, 0.86, and 0.80, respectively. However, Figure 6.36 shows the five-percentile and one-percentile values to be somewhat less than 0.86 and 0.80, respectively, when $e/h > 0.2$. The data plotted in Figures 6.35 and 6.36 do not include the effect of resistance factors for compression and bending (ϕ_c, ϕ_b) specified by the AISC Code. Introduction of ϕ_c and ϕ_b factors will partially offset the understrength indicated by five-percentile and one-percentile values in Figure 6.36. However, it is unlikely that ϕ_c and ϕ_b will fully offset this understrength.

From the data plotted in Figure 6.34, 6.35, and 6.36 and the related discussion, it is concluded that the AISC method

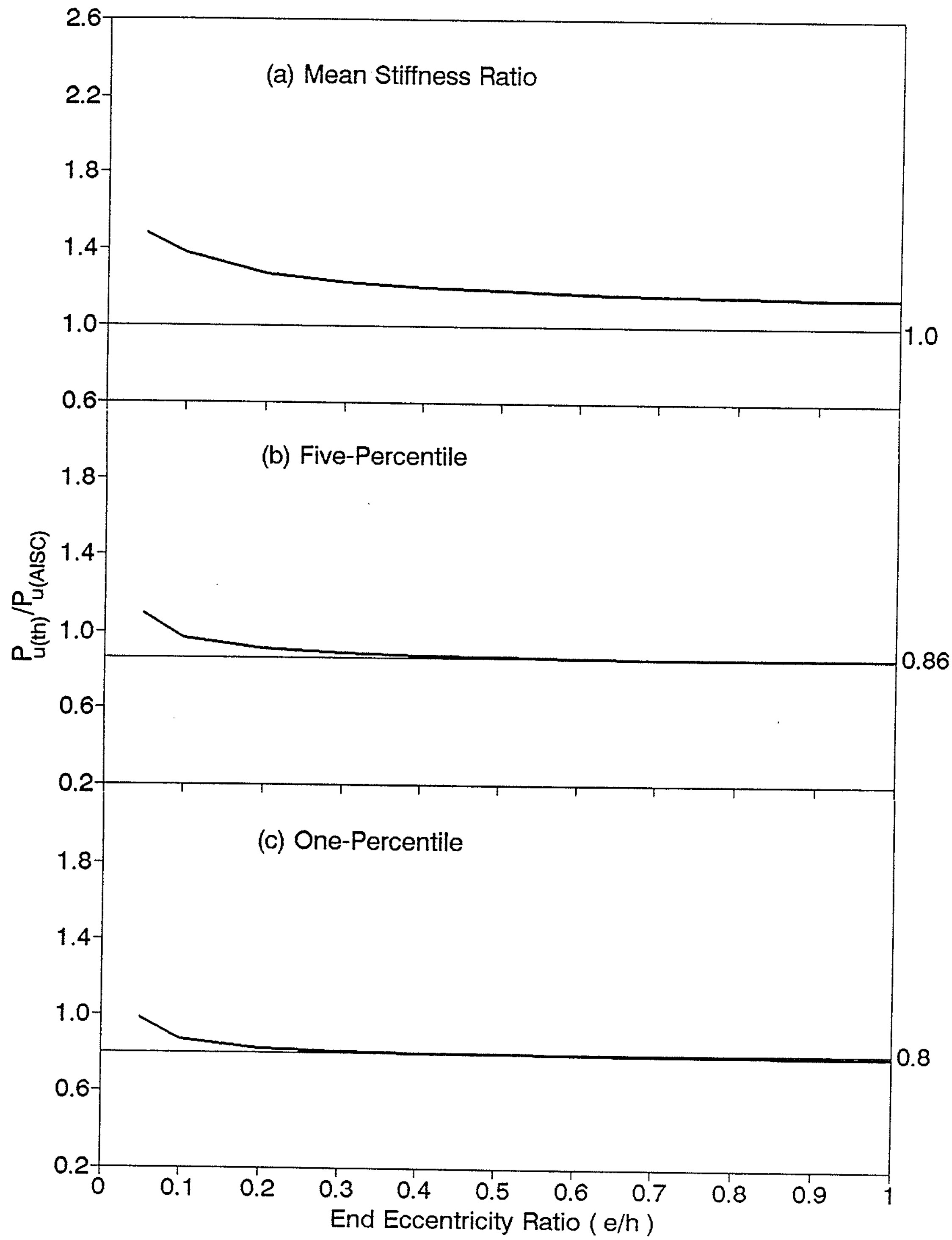

Figure 6.35 - Effect of end eccentricity ratio on ratio of theoretical ultimate strength to AISC ultimate strength for columns bending about the minor axis (n = 1080 for each *e/h* ratio equal to 0.05, 0.1, 0.2, 0.3, 0.4, 0.5, 0.6, 0.7, 0.8, 0.9 and 1.0).

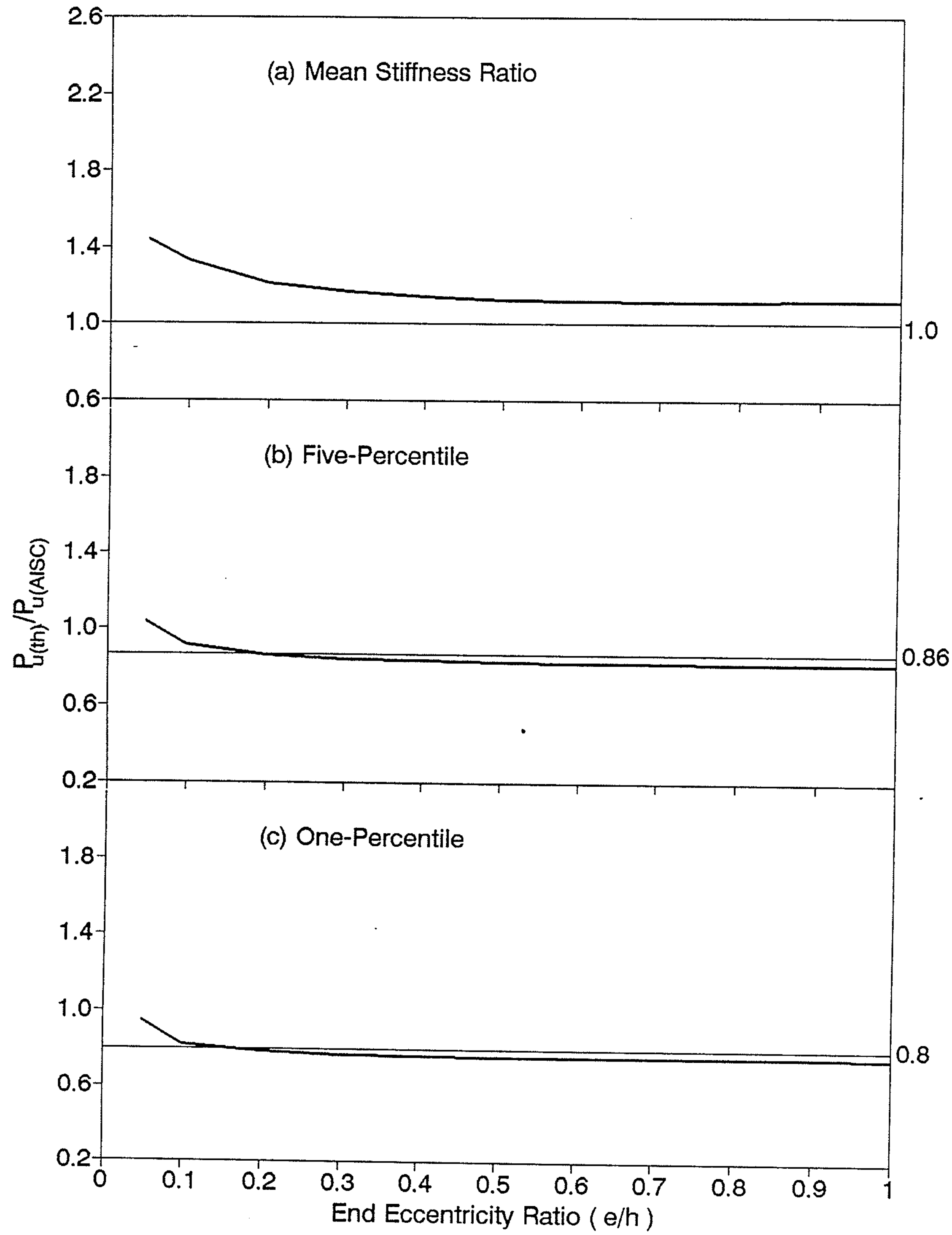

Figure 6.36 - Effect of end eccentricity ratio on ratio of theoretical ultimate strength to AISC ultimate strength for columns bending about the minor axis where ρ_{rs} = 1.09 percent (n = 360 for each e/h ratio equal to 0.05, 0.1, 0.2, 0.3, 0.4, 0.5, 0.6, 0.7, 0.8, 0.9 and 1.0).

produces a safe design for most of the composite beam-columns subjected to bending about the minor axis of the steel section. The matter of concern are the AISC beam-columns in which ρ_{rs} is 1 percent.

7 - SUMMARY, CONCLUSIONS AND RECOMMENDATIONS

7.1 SUMMARY

This study presents a statistical evaluation of the parameters that affect flexural stiffness *EI* of slender composite beam-columns (structural steel shapes encased in concrete) subjected to short-term loading. The columns studied were pin-ended with equal load eccentricities acting at both ends. To study the full range of variables, 11880 composite beam-columns were used to evaluate the flexural stiffness of beam-columns bending about the major axis of the encased structural steel shape and 11880 composite beam-columns were used to evaluate the flexural stiffness of beam-columns bending about the minor axis of the encased structural steel shape.

Various combinations of the specified concrete strength, the longitudinal steel ratio, the specified structural steel strength, the structural steel ratio, the slenderness ratio, and the end eccentricity ratio were used to study the effects of these variables on *EI* of composite beam-columns.

Based on the statistical evaluations of the parameters affecting *EI,* the most dominant variables were selected and placed into equation form (Equation 5.7, 5.8, 6.7 and 6.8). Note that Equations 5.7 and 5.8 for beam-columns bending about the major axis in Chapter 5 are identical to Equations 6.7 and 6.8 for beam-columns subjected to minor axis bending described in Chapter 6. The ACI *EI* expression (ACI 318-89 Eq. 10-14) and a computed AISC *EI* equation (Equation 4.30) were compared to the theoretically computed *EI* and to the proposed design equations (Equation 5.7 and 5.8 or 6.7 and 6.8).

7.2 CONCLUSIONS RELATED TO COMPOSITE BEAM-COLUMNS BENDING ABOUT THE MAJOR AXIS

From the discussions, tables and plots given in Chapter 5 for beam-columns subjected to bending about the major axis, the following conclusions seem to be valid:

(1) The mean, five-percentile and one-percentile stiffness ratios for the ACI and AISC equations are subject to greater variations due to ρ_{rs} than are those for the proposed design equations.

(2) The proposed design equations (Equations 5.7 and 5.8) were not significantly affected by any of the variables investigated, while the ACI and AISC expressions (Equation 4.1 and 4.30) were significantly affected by most of these same variables. The overall coefficients of variations related to the proposed stiffness equations were about one-third of those for the ACI and AISC stiffness expressions.

(3) The ACI design equation produced results that are similar to the results of the proposed design equations for the five-percentile and one-percentile stiffness ratios for many of the variables.

(4) The AISC equation, in many cases, gives the most

conservative results for mean stiffness ratios and the least conservative values for the five-percentile and one-percentile stiffness ratios.

(5) The mean and minimum stiffness ratios for Equation 5.7 or 5.8 may be taken as 1.0 and 0.8, respectively, for columns with e/h = 0.1 to 0.7, ρ_{ss} = 4.2 to 10.3 percent, ρ_{rs} = 1.1 to 3.2 percent, and ℓ/h = 10 to 30.

(6) There is no significant difference between the results of Equations 5.7 and 5.8.

(7) For the critical load ratio P_u/P_{cr}, this study shows that 83 percent of the columns studied with e/h ranging from 0.1 to 1.0 fall below the value of 0.5.

(8) Even though the stiffness ratios EI_{th}/EI_{AISC} raised some concerns with respect to the AISC expression for stiffness, the strength ratios $P_{u(th)}/P_{u(AISC)}$ seem to show that the AISC method produces safe design for composite beam-columns subjected to bending about the major axis.

7.3 CONCLUSIONS RELATED TO COMPOSITE BEAM-COLUMNS BENDING ABOUT THE MINOR AXIS

From the discussions, tables and plots given in Chapter 6 for beam-columns subjected to bending about the minor axis, the following conclusions seem to be valid:

(1) The mean, five-percentile and one-percentile stiffness ratios for the ACI and AISC equations are subject to greater variations due to ρ_{rs} than are those for the

proposed design equations.

(2) The proposed design equations (Equations 6.7 and 6.8) were not significantly affected by any of the variables investigated, while the ACI and AISC expressions (Equation 4.1 and 4.30) were significantly affected by most of these same variables. The overall coefficients of variation for the proposed stiffness expression were in the order of 30-40 percent of those related to the ACI and AISC stiffness equations.

(3) The ACI design equation produced results that are consistently more conservative than the results of the proposed design equations for the mean, five-percentile and one-percentile stiffness ratios for all of the variables investigated.

(4) The mean and minimum stiffness ratios for Equation 5.7 or 5.8 may be taken as 1.0 and 0.8, respectively, for columns with e/h = 0.1 to 0.7, ρ_{ss} = 4.2 to 10.3 percent, ρ_{rs} = 1.1 to 3.2 percent, and ℓ/h = 10 to 30.

(5) There is no significant difference between the results of Equations 6.7 and 6.8.

(6) For the critical load ratio P_u/P_{cr}, this study shows that 82 percent of the columns studied with e/h ranging from 0.1 to 1.0 fall below the value of 0.5.

(7) Even though the AISC stiffness ratios EI_{th}/EI_{AISC} were consistently non-conservative, the strength ratios $P_{u(th)}/P_{u(AISC)}$ seem to show that the AISC method should

produce safe design for most of the composite beam-columns subjected to bending about the minor axis. However, there is a concern regarding the AISC approach with respect such columns when ρ_{rs} = 1 percent.

7.4 RECOMMENDATIONS

For design purposes Equation 5.8 or 6.8 is recommended in determining the flexural stiffness of composite beam-columns for final (more accurate) designs. The ACI expression (Equation 4.1) may be used as a substitute, particularly for initial sizing of members. A critical load ratio P_u/P_{cr} equal to 0.5 is suggested as upper limit to control the design of slender columns. This value will be useful in the initial sizing of the members.

The AISC expression (Equation 4.30) and the strength ratio $P_{u(th)}/P_{u(AISC)}$ seem to show problems with regard to some composite beam-columns bending about the minor axis of the encased structural steel section. Further analysis of the AISC interaction equations is recommended.

LIST OF SYMBOLS

b	flange width of structural steel section.
b_f	width of structural steel section taken parallel to the axis of bending.
d	depth of structural steel section.
d_{ss}	depth of structural steel section taken perpendicular to the axis of bending.
d_{vert}	distance from the web to vertex of the parabola taken at the mid-height of the steel section.
e	end eccentricity of axial load at column ends.
e/h	end eccentricity ratio.
Δ_m	deflection of slender column at mid-height.
e_t	total eccentricity of axial load at mid-height of slender column.
f'_c	specified strength of concrete.
f_r	modulus of rupture of concrete.
f_{yss}	specified yield strength of structural steel.
f_{cr}	critical buckling stress.
f_{yr}	static yield strength of reinforcing steel.
f_{ys}	static yield strength of structural steel.
f_{us}	static ultimate strength of structural steel.
f_{ur}	static ultimate strength of reinforcing steel.
h	overall depth of composite section taken perpendicular to the axis of bending.
k	effective column length factor (equal to 1.0 in this study).
ℓ	column length.
r	radius of gyration.
r_m	modified radius of gyration (AISC).

t	flange thickness of structural steel section.
t_1	thickness of flange tip of structural steel section.
t_2	thickness of flange at web-flange juncture of structural steel section.
w	web thickness of structural steel section.
A_c	area of concrete.
A_r	area of longitudinal reinforcing steel (AISC).
A_f	area of one flange of structural shape (bt).
A_w	area of web of structural steel shape (w(d-2t)).
A_g	gross area of cross-section.
A_{ss}	area of structural steel section.
C_m	factor related to actual bending moment diagram to an equivalent uniform bending moment diagram (taken equal to 1.0 in this study).
DNA	perpendicular distance from plastic centroid of column to neutral axis (see Figure 2.8).
EI	effective flexural stiffness of slender composite column.
E	modulus of elasticity of structural steel (AISC).
E_c	initial tangent modulus of elasticity of concrete.
E_m	modified modulus of elasticity of structural steel section (AISC).
E_s	modulus of elasticity of structural steel.
E_t	tangent modulus of elasticity of element.
E_{rstrn}	initial tangent modulus of strain-hardening curve of reinforcing bars.
E_{sstrn}	initial tangent modulus of strain-hardening curve of structural steel.
E_r	modulus of elasticity of reinforcing steel.
F_y	yield stress for structural steel section (AISC).

F_{my} modified yield stress for structural steel section (AISC).

I moment of inertia.

I_g gross moment of inertia of cross-section.

I_{rs} moment of inertia of reinforcing steel taken about the centroidal axis of the composite cross-section.

I_{ss} moment of inertia of structural steel section taken about the centroidal axis of the composite cross-section.

M bending moment.

M_{col} overall column bending moment capacity.

M_{cs} cross-section bending moment capacity.

$M_{\ell t}$ required flexural strength for member due to lateral translation.

M_m bending moment at mid-height of slender column.

M_n nominal flexural strength.

M_{nt} required flexural strength assuming no lateral translation.

M_u ultimate flexural strength.

M-ϕ-P moment, curvature, axial load relationship.

P axial load.

P_n nominal compressive strength.

P_u ultimate compressive strength.

Z plastic section modulus of structural steel section.

α_c effective stiffness factor for concrete.

α_{rs} effective stiffness factor for longitudinal reinforcing steel.

α_{ss} effective stiffness factor for structural steel section.

β_d	absolute value of the ratio of maximum factored dead load moment t the maximum factored total load moment (taken equal to 0.0 in this study).
δ_b	moment magnification factor for second-order length effects.
δ_s	moment magnifier for lateral loads (taken equal to 0.0 in this study).
ϵ_c	strain in concrete.
ϵ_o	strain in unconfined concrete at peak compressive stress.
ϵ_{sstrn}	strain at start of strain-hardening curve of structural steel.
ϵ_{rstrn}	strain at start of strain-hardening curve of reinforcing bars.
ϵ_{ur}	ultimate strain in longitudinal reinforcing bars.
ϕ	curvature (inclination of strain gradient) or design code resistance factor.
ϕ_c	resistance factor for compression.
ϕ_b	resistance factor for bending.
ϕ_m	curvature at mid-height of slender column.
ϕ_e	curvature at column ends.
ρ_{rs}	ratio of area of longitudinal reinforcing bars to gross cross-section area.
ρ_{ss}	ratio of area of structural steel to gross cross-section area.
σ_{rw}	residual stress at centroid of structural steel section.
σ_{rft}	residual stress at flange tip of structural steel section.
σ_{rfw}	residual stress at juncture of flange and web of structural steel section.

LIST OF REFERENCES

ACI 318-89. 1989. Building code requirements for reinforced concrete. American Concrete Institute, Detroit, MI.

AISC (1986). "Load and Resistance Factor Design Specification for Structural Steel Buildings." American Institute of Steel Construction, Chicago, Illinois.

Basu, A.K. (1967). "Computation of failure loads of composite columns." Procedures Institution of Civil Engineers (London), 36 (March): 557-578.

Beedle, L.S., and Tall, L. (1960). "Basic column strength." Journal of the Structural Division ASCE, 86 (ST7): 139-173.

Bolotin, V.V. (1969). "Statistical methods in structural mechanics," translated by Samuel Aroni. Holden-Day Inc. San Francisco, California.

Bondale, S. (1966a). "Column theory with special reference to composite columns." The Consulting Engineer, July: 72-77.

Bondale, S. (1966b). "Column theory with special reference to composite columns." The Consulting Engineer, August: 43-48.

Bondale, S. (1966c). "Column theory with special reference to composite columns." The Consulting Engineer, September: 68-70.

CSA. (1984). Design of concrete structures for buildings - a national standard of Canada. CAN3-A23.3-M84, Canada Standards Association, Ottawa, Ont.

Evans, R.H. (1943). "The Plastic Theories for the ultimate strength of reinforced concrete beams." Journal of the Institution of Civil Engineers, London, Vol. 21: 98-121.

Furlong, R.W. (1976). "AISC column logic makes sense for composite columns, too." Engineering Journal, American Institute of Steel Construction, First Quarter, 13(1): 1-7.

Galambos, T.V. (1963). "Inelastic lateral buckling of beams." Journal of the Structural Division ASCE, 89 (ST5): p. 217-242.

Galambos, T.V., and Ravindra, M.K. 1978. "Properties of steel for use in LRFD." Journal of the Structural Division ASCE, 104 (ST9): 1459-1468.

Janss, J., and Anslijn, R. (1974). "Le calcul des charges ultimes des colonnes métalliques enrobés de béton." Rapport C.R.I.F., MT 89, Bruxelles.

Janss, J., and Piraprez, E. (1974). "Le calcul des charges ultimes des colonnes métalliques enrobés de béton leger." Rapport C.R.I.F., MT 100, Bruxelles.

Kennedy, D.L.J., and Gad Aly, M. (1980). "Limit states design of steel structures - performance factors." Canadian Journal of Civil Engineering, 7: 45-77.

Kent, D.C., and Park, R. (1971). "Flexural members with confined concrete." Journal of the Structural Division ASCE, 97 (ST7): 1968-1990.

Kikuchi, D.K., Mirza, S.A., and MacGregor, J.G. (1978). "Strength Variability of Bonded Prestressed Concrete Beams." Structural Engineering Report no. 68, University of Alberta, Edmonton, Alberta.

LaChance, L., and Hays, C.O. (1980). "Accuracy of Composite Section Nonlinear Solutions." Journal of the Structural Division ASCE, 106(ST11): 2203-2219.

L'Hermite, R. (1955). "Idées actualles sur la technologie du béton." Documentation Technique du Bâtiment et des Travaux Publics, Paris.

Llewellyn, S. (1986). "Parametric study of the strength of composite columns." B.Eng. thesis, School of Engineering, Lakehead University, Thunder Bay, Ontario.

May, I.M., and Johnson, R.P. (1978). "Tests on restrained composite columns." The Structural Engineer, 56B(2): 21-27.

Mirza, S.A., Hatzinikolas, M., and MacGregor, J.G. (1979c). "Statistical descriptions of strength of concrete." Journal of the Structural Division ASCE 105(ST6): 10221-1037.

Mirza, S.A., and MacGregor, J.G. (1982). "Probabilistic study of strength of reinforced concrete members." Canadian Journal of Civil Engineering, 9(3): 431-448.

Mirza, S.A., and MacGregor, J.G. (1989). "Slenderness and strength reliability of reinforced concrete columns." American Concrete Institute Structural Journal, 86(4): 428-438.

Mirza, S.A. (1989). "Parametric study of composite column strength variability." Journal Constructional Steel Research, 14: 121-137.

Mirza, S.A. (1990). "Flexural stiffness of rectangular reinforced concrete columns." American Concrete Institute Structural Journal, 87(4): 425-435.

Morino, S., Matsui, C., and Watanabe, H. (1984). "Strength of biaxially loaded SRC columns." Composite and Mixed Construction, American Society of Civil Engineers: 241-253.

Neville, A.M. (1973). "Properties of Concrete." 2nd Edition, John - Wiley and Sons Inc., New York: p. 686.

Park, R., Priestly, M.J.N., and Gill, W.D. (1982). "Ductility of square-confined concrete columns." Journal of the Structural Division ASCE, 108(ST4): 929-950.

Park, R., and Pauley, T. (1975). "Reinforced concrete structures." John Wiley and Sons.

Procter, A.N. (1967). "Full size tests facilitate derivation of reliable design methods." The Consulting Engineer, 31(8): 54-60.

Quast, U. (1970). "Geeignete vereinfachungen fur die losung des traglastproblems der ausmittig gedruckten prismatischen stahbetonstutze mit rechtekcquerschnitt." Dr.-Ing. Dissertation, Fakultat fur Bauwesen at Technischen Universität Carlo-Wilhelmina, Braunschweig, FRG.

Roderick, J.W., and Loke, Y.O. (1974). "Pin-ended composite columns bent about the minor axis." Sydney University, Australia, Civil Engineering Labs, Report No. R-254: p. 35.

Roderick, J.W., and Rogers, D.F. (1969). "Load carrying capacity of simple composite columns." Journal of the Structural Division, Proceedings of the ASCE, 95(ST2): 209-228.

Roik, K., and Bergmann, R. (1989). "Harmonisation of the European Construction Codes - Report on Eurocode 4." Report EC4/6/89, Ruhr-Universität Bochum, Germany.

Roik, K., and Mangerig, I. (1987). "Experimentelle Untersuchungen der Tragfähigkeit von einbetonierten Stahlprofilstützen unter desonderer Berücksichtigung des Langzeitverhaltens von Beton." Bericht zu P102, Studiengesellschaft für Anwendungstechnik von Eisen und Stahl e.V., Düsseldorf.

Roik, K.H., and Schwalbenhofer, K. (1988). "Experimentelle Untersuchungen zum plastischen Verhalten van Verbundstützen." Bericht zu P125, Studiengesellschaft für Anwendungstechnik von Eisen und Stahl e.V., Düsseldorf.

Sheikh, S.A., and Uzumeri, S.M. (1982). "Analytical model for concrete confinement in tied columns." Journal of the Structural Division ASCE, 108(ST12): 2703-2721.

Sheikh, S.A., and Yeh, C.C. (1986). "Flexural behaviour of confined concrete columns." American Concrete Institute Journal, 83(3): 389-404.

Skrabek, B.W., and Mirza, S.A. (1990). "Strength reliability of short and slender composite steel-concrete columns." Civil Engineering Report Series. No. CE-90-1, Lakehead University, Thunder Bay, Ontario.

Stevens, R.F. (1965). "The strength of encased stanchions." National Building Studies, Research Paper 38, Ministry of Technology Building Station, London.

Suzuki, T., Takiguchi, K., Ichinose, T., and Okamoto, T. (1983). "Effects of hoop reinforcement in steel and reinforced concrete composite sections." Third South Pacific Regional Conference on Earthquake Engineering. Wellington, New Zealand.

Timoshenko, S.P., and Gere, J.M. (1961). "Theory of elastic stability." 2nd Edition, McGraw - Hill Book Co., New York: p. 541.

Virdi, K.S., and Dowling, P.J. (1973). "The ultimate strength of composite columns in biaxial bending." Procedures Institution of Civil Engineers (London), 56(May): 251-272.

Virdi, K.S., and Dowling, P.J. (1982). "Composite columns in biaxial loading." Axially Compressed Structures, Stability and Strength, edited by R. Narayanan. Applied Science Publishers, London: 129-147.

Wakabayashi, M. (1976). "A proposal for design formulas of composite columns and beam-columns." Second International Colloquium on Stability of Structures, Tokyo: 65-87.

Young, B.W. (1971). "Residual stresses in hot rolled sections." Report CUED/C-Struct/TR.8. Dept. of Engineering, University of Cambridge.

APPENDIX A

Table A1 - Specimen Configuration for Columns Bending About the Major Axis

Author	Col. Desig.	h in.	b in.	Steel Profile	Long. Reinf.	A_{ss} in.^{2}	A_c in.^{2}	A_{rs} in.^{2}	* Vol'met' Ratio
Bondale (1966)	RS 60.3	6.00	3.75	4"x1.75"@5#	4-0.21"	1.47	20.89	0.14	0.00644
	RS 80.2	6.00	3.75	4"x1.75"@5#	4-0.21"	1.47	20.89	0.14	0.00644
	RS 100.1	6.00	3.75	4"x1.75"@5#	4-0.21"	1.47	20.89	0.14	0.00644
	RS 120.0	6.00	3.75	4"x1.75"@5#	4-0.21"	1.47	20.89	0.14	0.00644
May & Johnson (1978)	RC1	7.87	7.87	152X152 UC23	4-Y6	4.62	57.21	0.18	0.00190
	RC3	7.87	7.87	152X152 UC23	4-Y6	4.62	57.21	0.18	0.00190
	RC4	7.87	7.87	152X152 UC23	4-Y6	4.62	57.21	0.18	0.00190
Morino et al. (1984)	A4-90	6.30	6.30	H100x100x6x8	4-6mm	3.45	36.08	0.14	0.00258
	B4-90	6.30	6.30	H100x100x6x8	4-6mm	3.45	36.08	0.14	0.00258
	C4-90	6.30	6.30	H100x100x6x8	4-6mm	3.45	36.08	0.14	0.00258
	D4-90	6.30	6.30	H100x100x6x8	4-6mm	3.45	36.08	0.14	0.00258
	A8-90	6.30	6.30	H100x100x6x8	4-6mm	3.45	36.08	0.14	0.00258
	B8-90	6.30	6.30	H100x100x6x8	4-6mm	3.45	36.08	0.14	0.00258
	C8-90	6.30	6.30	H100x100x6x8	4-6mm	3.45	36.08	0.14	0.00258
	D8-90	6.30	6.30	H100x100x6x8	4-6mm	3.45	36.08	0.14	0.00258
Procter (1967)	S1	11.00	8.00	7"x4"@14.5#		4.26	83.74		
	S2	11.00	8.00	7"x4"@14.5#		4.26	83.74		
	S3	12.00	8.00	8"x4"@17#		5.00	91.00		
	S4	12.00	8.00	8"x4"@17#		5.00	91.00		
	1	11.25	8.00	7"x4"@14.5#		4.26	85.74		
	2	11.25	8.00	7"x4"@14.5#		4.26	85.74		
	3	11.25	8.00	7"x4"@14.5#		4.26	85.74		
	4	11.25	8.00	7"x4"@14.5#		4.26	85.74		
	5	11.25	8.00	7"x4"@14.5#		4.26	85.74		
	6	12.00	8.00	8"x4"@17#		5.00	91.00		
	7	12.00	8.00	8"x4"@17#		5.00	91.00		
	8	12.00	8.00	8"x4"@17#		5.00	91.00		
	9	11.25	8.00	7"x4"@14.5#		4.26	85.74		
	10	11.25	8.00	7"x4"@14.5#		4.26	85.74		
	11	12.00	8.00	8"x4"@17#		5.00	91.00		
	12	12.00	8.00	8"x4"@17#		5.00	91.00		
Suzuki et al. (1983)	LH-000-C	8.27	8.27	H150x100x3.2x4.5	4-6mm	1.98	66.23	0.14	0.00000
	LH-020-C	8.27	8.27	H150x100x3.2x4.5	4-6mm	1.98	66.23	0.14	0.00232
	LH-040-C	8.27	8.27	H150x100x3.2x4.5	4-6mm	1.98	66.23	0.14	0.00116
	LH-100-C	8.27	8.27	H150x100x3.2x4.5	4-6mm	1.98	66.23	0.14	0.00046
	RH-000-C	8.27	8.27	H150x100x6x9	4-6mm	3.74	64.48	0.14	0.00000
	RH-020-C	8.27	8.27	H150x100x6x9	4-6mm	3.74	64.48	0.14	0.00232
	RH-040-C	8.27	8.27	H150x100x6x9	4-6mm	3.74	64.48	0.14	0.00116
	RH-100-C	8.27	8.27	H150x100x6x9	4-6mm	3.74	64.48	0.14	0.00046
	HT60-000-C	8.27	8.27	H150x100x8x8	4-6mm	4.10	64.11	0.14	0.00000
	HT60-020-C	8.27	8.27	H150x100x8x8	4-6mm	4.10	64.11	0.14	0.00232
	HT60-040-C	8.27	8.27	H150x100x8x8	4-6mm	4.10	64.11	0.14	0.00116
	HT60-100-C	8.27	8.27	H150x100x8x8	4-6mm	4.10	64.11	0.14	0.00046
	HT80-000-C	8.27	8.27	H150x100x8x8	4-6mm	4.32	63.89	0.14	0.00000
	HT80-020-C	8.27	8.27	H150x100x8x8	4-6mm	4.32	63.89	0.14	0.00232
	HT80-040-C	8.27	8.27	H150x100x8x8	4-6mm	4.32	63.89	0.14	0.00116
	HT80-100-C	8.27	8.27	H150x100x8x8	4-6mm	4.32	63.89	0.14	0.00046

Table A1 - Specimen Configuration for Columns Bending About the Major Axis

continued

Author	Col. Desig.	I_{ss} in.^{4}	I_c in.^{4}	I_{rs} in.^{4}	Fy web	Fy flange	f'c psi	Fy Reinf.	ρ_{ss}	ρ_{rs}
Bondale	RS 60.3	3.66	63.05	0.79	44800	44800	4506	60000	0.0653	0.0062
(1966)	RS 80.2	3.66	63.05	0.79	44800	44800	4382	60000	0.0653	0.0062
	RS 100.1	3.66	63.05	0.79	44800	44800	4260	60000	0.0653	0.0062
	RS 120.0	3.66	63.05	0.79	44800	44800	4700	60000	0.0653	0.0062
May &	RC1	30.34	289.12	0.87	42050	41630	4308	60000	0.0745	0.0028
Johnson	RC3	30.34	289.12	0.87	42050	41630	3390	60000	0.0745	0.0028
(1978)	RC4	30.34	289.12	0.87	42050	41630	5191	60000	0.0745	0.0028
Morino	A4-90	9.30	121.08	0.83	52055	42485	3060	56115	0.0870	0.0036
et al.	B4-90	9.30	121.08	0.83	50750	41615	3393	56115	0.0870	0.0036
(1984)	C4-90	9.30	121.08	0.83	45675	44660	3379	56115	0.0870	0.0036
	D4-90	9.30	121.08	0.83	52055	42485	3074	56115	0.0870	0.0036
	A8-90	9.30	121.08	0.83	53360	43935	4872	56115	0.0870	0.0036
	B8-90	9.30	121.08	0.83	53070	45095	4829	56115	0.0870	0.0036
	C8-90	9.30	121.08	0.83	53505	44225	3567	56115	0.0870	0.0036
	D8-90	9.30	121.08	0.83	53360	43790	3321	56115	0.0870	0.0036
Procter	S1	37.48	849.85		42112	42112	4722		0.0484	0.0000
(1967)	S2	37.48	849.85		42112	42112	4722		0.0484	0.0000
	S3	53.62	1098.38		42560	42560	5407		0.0520	0.0000
	S4	53.62	1098.38		42560	42560	5407		0.0520	0.0000
	1	37.48	911.74		42112	42112	4722		0.0473	0.0000
	2	37.48	911.74		42112	42112	4722		0.0473	0.0000
	3	37.48	911.74		42112	42112	4722		0.0473	0.0000
	4	37.48	911.74		42112	42112	4722		0.0473	0.0000
	5	37.48	911.74		42112	42112	5407		0.0473	0.0000
	6	53.62	1098.38		42560	42560	5407		0.0520	0.0000
	7	53.62	1098.38		42560	42560	5407		0.0520	0.0000
	8	53.62	1098.38		42560	42560	5407		0.0520	0.0000
	9	37.48	911.74		42112	42112	6007		0.0473	0.0000
	10	37.48	911.74		42112	42112	6007		0.0473	0.0000
	11	53.62	1098.38		42560	42560	6007		0.0520	0.0000
	12	53.62	1098.38		42560	42560	6007		0.0520	0.0000
Suzuki	LH-000-C	12.55	375.09	1.73	45240	45661	4785	48430	0.0290	0.0021
et al.	LH-020-C	12.55	375.09	1.73	45240	45661	4785	48430	0.0290	0.0021
(1983)	LH-040-C	12.55	375.09	1.73	45240	45661	4785	48430	0.0290	0.0021
	LH-100-C	12.55	375.09	1.73	45240	45661	4785	48430	0.0290	0.0021
	RH-000-C	22.68	364.96	1.73	55477	48503	4858	48430	0.0546	0.0021
	RH-020-C	22.68	364.96	1.73	55477	48503	4858	48430	0.0546	0.0021
	RH-040-C	22.68	364.96	1.73	55477	48503	4858	48430	0.0546	0.0021
	RH-100-C	22.68	364.96	1.73	55477	48503	4858	48430	0.0546	0.0021
	HT60-000-C	23.06	364.58	1.73	83781	83781	4858	48430	0.0600	0.0021
	HT60-020-C	23.06	364.58	1.73	83781	83781	4858	48430	0.0600	0.0021
	HT60-040-C	23.06	364.58	1.73	83781	83781	4858	48430	0.0600	0.0021
	HT60-100-C	23.06	364.58	1.73	83781	83781	4858	48430	0.0600	0.0021
	HT80-000-C	24.17	363.48	1.73	113651	113651	4858	48430	0.0633	0.0021
	HT80-020-C	24.17	363.48	1.73	113651	113651	4858	48430	0.0633	0.0021
	HT80-040-C	24.17	363.48	1.73	113651	113651	4858	48430	0.0633	0.0021
	HT80-100-C	24.17	363.48	1.73	113651	113651	4858	48430	0.0633	0.0021

Table A1 - Specimen Configuration for Columns Bending About the Major Axis

continued

Author	Col. Desig.	$\frac{\rho_{ss} f_{yss}}{f'_c}$	ℓ in.	ℓ/h	e in.	e/h	Tested Strength	Theor. Strength	Strength Ratio
Bondale (1966)	RS 60.3	0.649	60.0	10.0	3.00	0.500	55.8	47.0	1.1880
	RS 80.2	0.667	80.0	13.3	2.00	0.333	70.1	55.8	1.2572
	RS 100.1	0.687	100.0	16.7	1.00	0.167	92.3	72.9	1.2653
	RS 120.0	0.622	120.0	20.0	0.00	0.000	107.1	115.3	0.9286
May & Johnson (1978)	RC1	0.727	63.5	8.1	0.88	0.112	301.2	282.2	1.0674
	RC3	0.924	63.5	8.1	1.07	0.136	305.7	239.1	1.2787
	RC4	0.603	116.7	14.8	1.55	0.197	191.1	217.9	0.8771
Morino et al. (1984)	A4-90	1.481	36.4	5.8	1.57	0.250	166.5	121.4	1.3719
	B4-90	1.302	90.9	14.4	1.57	0.250	114.6	104.0	1.1020
	C4-90	1.177	136.4	21.7	1.57	0.250	93.9	83.0	1.1313
	D4-90	1.474	181.9	28.9	1.57	0.250	64.7	63.5	1.0189
	A8-90	0.953	36.4	5.8	2.95	0.469	118.1	98.6	1.1968
	B8-90	0.957	90.9	14.4	2.95	0.469	94.0	84.3	1.1144
	C8-90	1.305	136.4	21.7	2.95	0.469	68.0	62.5	1.0889
	D8-90	1.399	181.9	28.9	2.95	0.469	50.1	49.2	1.0196
Procter (1967)	S1	0.432	24.0	2.2	0	0.000	470.4	522.9	0.8997
	S2	0.432	24.0	2.2	0	0.000	481.6	522.9	0.9211
	S3	0.410	24.0	2.0	0	0.000	698.9	642.1	1.0885
	S4	0.410	24.0	2.0	0	0.000	703.4	642.1	1.0955
	1	0.422	132.0	11.7	6	0.533	132.2	127.7	1.0347
	2	0.422	132.0	11.7	9	0.800	87.4	87.4	0.9997
	3	0.422	132.0	11.7	0	0.000	470.4	508.0	0.9259
	4	0.422	132.0	11.7	6	0.533	143.4	127.7	1.1224
	5	0.369	132.0	11.7	9	0.800	91.8	90.5	1.0154
	6	0.410	132.0	11.0	9	0.750	129.9	114.1	1.1383
	7	0.410	132.0	11.0	6	0.500	199.4	168.6	1.1827
	8	0.410	132.0	11.0	0	0.000	560.0	613.6	0.9126
	9	0.332	132.0	11.7	3	0.267	268.8	243.5	1.1039
	10	0.332	132.0	11.7	3	0.267	250.9	243.5	1.0303
	11	0.369	132.0	11.0	0	0.000	533.1	658.5	0.8096
	12	0.369	132.0	11.0	3	0.250	315.8	290.9	1.0859
Suzuki et al. (1983)	LH-000-C	0.274	23.6	2.9	0.00	0.000	380.0	366.4	1.0373
	LH-020-C	0.274	23.6	2.9	0.00	0.000	374.3	429.4	0.8716
	LH-040-C	0.274	23.6	2.9	0.00	0.000	374.3	398.0	0.9403
	LH-100-C	0.274	23.6	2.9	0.00	0.000	385.8	379.2	1.0173
	RH-000-C	0.624	23.6	2.9	0.00	0.000	547.0	462.7	1.1823
	RH-020-C	0.624	23.6	2.9	0.00	0.000	561.4	523.7	1.0720
	RH-040-C	0.624	23.6	2.9	0.00	0.000	521.1	493.4	1.0563
	RH-100-C	0.624	23.6	2.9	0.00	0.000	521.1	475.2	1.0967
	HT60-000-C	1.035	23.6	2.9	0.00	0.000	598.8	562.8	1.0640
	HT60-020-C	1.035	23.6	2.9	0.00	0.000	656.4	674.0	0.9739
	HT60-040-C	1.035	23.6	2.9	0.00	0.000	662.2	639.2	1.0359
	HT60-100-C	1.035	23.6	2.9	0.00	0.000	627.6	611.8	1.0259
	HT80-000-C	1.480	23.6	2.9	0.00	0.000	716.9	626.3	1.1447
	HT80-020-C	1.480	23.6	2.9	0.00	0.000	734.2	797.3	0.9208
	HT80-040-C	1.480	23.6	2.9	0.00	0.000	728.4	759.4	0.9592
	HT80-100-C	1.480	23.6	2.9	0.00	0.000	711.1	721.0	0.9863

Table A1 - Specimen Configuration for Columns Bending About the Major Axis

continued

Author	Col. Desig.	h in.	b in.	Steel Profile	Long. Reinf.	A_{ss} in.^{2}	A_c in.^{2}	A_{rs} in.^{2}	* Vol'met' Ratio
Suzuki	HT80-000-CB	8.27	8.27	H150x100x5x5	4-6mm	2.89	65.32	0.14	0.00000
et al.	HT80-020-CB	8.27	8.27	H150x100x5x5	4-6mm	2.89	65.32	0.14	0.00232
(1983)	LH-000-B	8.27	8.27	H150x100x3.2x4.5	4-6mm	1.98	66.23	0.14	0.00000
	LH-020-B	8.27	8.27	H150x100x3.2x4.5	4-6mm	1.98	66.23	0.14	0.00232
	LH-040-B	8.27	8.27	H150x100x3.2x4.5	4-6mm	1.98	66.23	0.14	0.00116
	LH-100-B	8.27	8.27	H150x100x3.2x4.5	4-6mm	1.98	66.23	0.14	0.00046
	RH-000-B	8.27	8.27	H150x100x6x9	4-6mm	3.74	64.48	0.14	0.00000
	RH-020-B	8.27	8.27	H150x100x6x9	4-6mm	3.74	64.48	0.14	0.00232
	RH-040-B	8.27	8.27	H150x100x6x9	4-6mm	3.74	64.48	0.14	0.00116
	RH-100-B	8.27	8.27	H150x100x6x9	4-6mm	3.74	64.48	0.14	0.00046
	HT60-000-B	8.27	8.27	H150x100x8x8	4-6mm	4.10	64.11	0.14	0.00000
	HT60-020-B	8.27	8.27	H150x100x8x8	4-6mm	4.10	64.11	0.14	0.00232
	HT60-040-B	8.27	8.27	H150x100x8x8	4-6mm	4.10	64.11	0.14	0.00116
	HT60-100-B	8.27	8.27	H150x100x8x8	4-6mm	4.10	64.11	0.14	0.00046
	HT80-000-B	8.27	8.27	H150x100x8x8	4-6mm	4.32	63.89	0.14	0.00000
	HT80-020-B	8.27	8.27	H150x100x8x8	4-6mm	4.32	63.89	0.14	0.00232
	HT80-040-B	8.27	8.27	H150x100x8x8	4-6mm	4.32	63.89	0.14	0.00116
	HT80-100-B	8.27	8.27	H150x100x8x8	4-6mm	4.32	63.89	0.14	0.00046
Roik	23	11.81	11.81	HE200B	4-12mm	12.11	126.69	0.70	0.00293
Mangerig	24	11.81	11.81	HE200B	4-12mm	12.11	126.69	0.70	0.00293
(1987)	25	11.81	11.81	HE200B	4-12mm	12.11	126.69	0.70	0.00293
	26	11.81	11.81	HE200B	4-12mm	12.11	126.69	0.70	0.00293
Roik	V11	11.02	11.02	HE120B	4-14mm	5.27	115.30	0.95	0.00283
Schwal'r	V12	11.02	11.02	HE120B	4-14mm	5.27	115.30	0.95	0.00283
(1988)	V13	11.02	11.02	HE120B	4-14mm	5.27	115.30	0.95	0.00283
	V21	11.02	11.02	HE160A	4-14mm	6.01	114.55	0.95	0.00283
	V22	11.02	11.02	HE160A	4-14mm	6.01	114.55	0.95	0.00283
	V23	11.02	11.02	HE160A	4-14mm	6.01	114.55	0.95	0.00283
	V31	11.02	11.02	HE200B	4-14mm	12.11	108.46	0.95	0.00283
	V32	11.02	11.02	HE200B	4-14mm	12.11	108.46	0.95	0.00283
	V33	11.02	11.02	HE200B	4-14mm	12.11	108.46	0.95	0.00283
	V41	11.02	11.02	HE180M	4-14mm	17.52	103.05	0.95	0.00283
	V42	11.02	11.02	HE180M	4-14mm	17.52	103.05	0.95	0.00283
	V43	11.02	11.02	HE180M	4-14mm	17.52	103.05	0.95	0.00283

* - Volumetric Ratio for transverse reinforcement

$$p'' = \frac{2(b'' + d'')A}{b''d''s};$$

b" - outside width of transverse reinforcing
d" - outside depth of transverse reinforcing
A - area of bar
s - spacing of reinforcing

Table A1 - Specimen Configuration for Columns Bending About the Major Axis

continued

Author	Col. Desig.	I_{ss} in.^{4}	I_c in.^{4}	I_{rs} in.^{4}	Fy web	Fy flange	f'c psi	Fy Reinf.	ρ_{ss}	ρ_{rs}
Suzuki	HT80-000-CB	16.77	370.87	1.73	110809	110809	4423	48430	0.0423	0.0021
et al.	HT80-020-CB	16.77	370.87	1.73	110809	110809	4423	48430	0.0423	0.0021
(1983)	LH-000-B	12.55	375.09	1.73	45240	45661	4292	48430	0.0290	0.0021
	LH-020-B	12.55	375.09	1.73	45240	45661	4597	48430	0.0290	0.0021
	LH-040-B	12.55	375.09	1.73	45240	45661	4524	48430	0.0290	0.0021
	LH-100-B	12.55	375.09	1.73	45240	45661	4365	48430	0.0290	0.0021
	RH-000-B	22.68	364.96	1.73	55477	48503	4858	48430	0.0546	0.0021
	RH-020-B	22.68	364.96	1.73	55477	48503	4858	48430	0.0546	0.0021
	RH-040-B	22.68	364.96	1.73	55477	48503	4858	48430	0.0546	0.0021
	RH-100-B	22.68	364.96	1.73	55477	48503	4858	48430	0.0546	0.0021
	HT60-000-B	23.06	364.58	1.73	83781	83781	4814	48430	0.0600	0.0021
	HT60-020-B	23.06	364.58	1.73	83781	83781	4814	48430	0.0600	0.0021
	HT60-040-B	23.06	364.58	1.73	83781	83781	4814	48430	0.0600	0.0021
	HT60-100-B	23.06	364.58	1.73	83781	83781	4814	48430	0.0600	0.0021
	HT80-000-B	24.17	363.48	1.73	113651	113651	4771	48430	0.0633	0.0021
	HT80-020-B	24.17	363.48	1.73	113651	113651	4771	48430	0.0633	0.0021
	HT80-040-B	24.17	363.48	1.73	113651	113651	4771	48430	0.0633	0.0021
	HT80-100-B	24.17	363.48	1.73	113651	113651	4771	48430	0.0633	0.0021
Roik	23	136.94	1467.77	16.99	39150	39150	6570	60900	0.0868	0.0050
Mangerig	24	136.94	1467.77	16.99	39150	39150	6570	60900	0.0868	0.0050
(1987)	25	136.94	1467.77	16.99	39150	39150	6570	60900	0.0868	0.0050
	26	136.94	1467.77	16.99	39150	39150	6570	60900	0.0868	0.0050
Roik	V11	20.76	1191.28	18.55	33655	33655	6351	60900	0.0434	0.0079
Schwal'r	V12	20.76	1191.28	18.55	33655	33655	6351	60900	0.0434	0.0079
(1988)	V13	20.76	1191.28	18.55	33655	33655	6786	60900	0.0434	0.0079
	V21	40.12	1171.92	18.55	45675	45675	6786	60900	0.0495	0.0079
	V22	40.12	1171.92	18.55	45675	45675	5365	60900	0.0495	0.0079
	V23	40.12	1171.92	18.55	45675	45675	5365	60900	0.0495	0.0079
	V31	136.94	1075.10	18.55	32886	32886	5902	60900	0.0996	0.0079
	V32	136.94	1075.10	18.55	32886	32886	5902	60900	0.0996	0.0079
	V33	136.94	1075.10	18.55	32886	32886	5699	60900	0.0996	0.0079
	V41	179.71	1032.33	18.55	31465	31465	5699	60900	0.1441	0.0079
	V42	179.71	1032.33	18.55	39295	39295	6119	60900	0.1441	0.0079
	V43	179.71	1032.33	18.55	42239	42239	6119	60900	0.1441	0.0079

Table A1 - Specimen Configuration for Columns Bending About the Major Axis

continued

Author	Col. Desig.	$\frac{\rho_{ss} f_{yss}}{f'_c}$	ℓ in.	ℓ/h	e in.	e/h	Tested Strength	Theor. Strength	Strength Ratio
Suzuki	HT80-000-CB	1.060	23.6	2.9	7.22	0.874	110.4	104.0	1.0612
et al.	HT80-020-CB	1.060	23.6	2.9	8.78	1.062	110.4	108.7	1.0156
(1983)	LH-000-B	0.306	23.6	2.9	inf.	inf.	27.4	27.8	0.9877
	LH-020-B	0.286	23.6	2.9	inf.	inf.	29.4	32.1	0.9162
	LH-040-B	0.290	23.6	2.9	inf.	inf.	28.2	30.1	0.9386
	LH-100-B	0.301	23.6	2.9	inf.	inf.	28.2	28.0	1.0083
	RH-000-B	0.624	23.6	2.9	inf.	inf.	48.9	52.1	0.9397
	RH-020-B	0.624	23.6	2.9	inf.	inf.	54.5	56.9	0.9578
	RH-040-B	0.624	23.6	2.9	inf.	inf.	53.3	45.5	1.1710
	RH-100-B	0.624	23.6	2.9	inf.	inf.	50.9	52.3	0.9736
	HT60-000-B	1.045	23.6	2.9	inf.	inf.	68.8	73.4	0.9372
	HT60-020-B	1.045	23.6	2.9	inf.	inf.	79.2	79.7	0.9934
	HT60-040-B	1.045	23.6	2.9	inf.	inf.	77.2	76.2	1.0127
	HT60-100-B	1.045	23.6	2.9	inf.	inf.	72.0	75.9	0.9488
	HT80-000-B	1.507	23.6	2.9	inf.	inf.	93.5	98.8	0.9459
	HT80-020-B	1.507	23.6	2.9	inf.	inf.	104.2	105.3	0.9895
	HT80-040-B	1.507	23.6	2.9	inf.	inf.	101.0	102.8	0.9830
	HT80-100-B	1.507	23.6	2.9	inf.	inf.	97.9	99.6	0.9826
Roik	23	0.804	196.9	16.7	3.54	0.300	526.3	442.3	1.1900
Mangerig	24	0.804	196.9	16.7	5.91	0.500	368.3	324.8	1.1340
(1987)	25	0.804	315.0	26.7	3.54	0.300	377.8	314.4	1.2017
	26	0.804	315.0	26.7	5.91	0.500	200.9	238.6	0.8420
Roik	V11	0.416	136.2	12.4	6.30	0.571	171.7	169.6	1.0124
Schwal'r	V12	0.416	136.2	12.4	2.36	0.214	366.3	373.3	0.9812
(1988)	V13	0.389	136.2	12.4	3.94	0.357	322.9	272.7	1.1842
	V21	0.444	136.2	12.4	3.94	0.357	338.2	321.8	1.0509
	V22	0.562	136.2	12.4	6.30	0.571	213.8	201.7	1.0599
	V23	0.562	136.2	12.4	2.36	0.214	437.2	388.9	1.1243
	V31	1.028	136.2	12.4	3.94	0.357	384.1	383.3	1.0020
	V32	1.028	136.2	12.4	2.36	0.214	506.9	501.2	1.0114
	V33	1.065	136.2	12.4	6.30	0.571	294.3	280.8	1.0481
	V41	1.540	136.2	12.4	3.94	0.357	477.7	422.9	1.1295
	V42	1.434	136.2	12.4	6.30	0.571	344.9	359.6	0.9592
	V43	1.434	136.2	12.4	2.36	0.214	614.9	650.6	0.9451

NOTE : For e/h = inf., strength is given in kip-ft (1 kip-ft = 1.356 kN-m).

For all other values of e/h, the strength is shown in kips (1 kip = 4.448 kN).

b = width of the concrete cross-section parrallel to the axis of bending;

h = depth of the concrete cross-section perpendicular to the axis of bending.

The term f_{yss} was taken as the web yield strength for computing the $\rho_{ss} f_{yss}/f'_c$ ratio.

The strain-hardening of both steels was included in the analysis.

Table A2 - Specimen Configuration for Major Axis Bending
Ratio of Test to Calculated Ultimate Strength - STRAIN HARDENING NOT INCLUDED

Author	Col. Desig.	h in.	b in.	f'c psi	ρ_{ss}	ρ_{rs}	$\frac{\rho_{ss} f_{yss}}{f'_c}$	ℓ/h	e/h	Tested Strength	Theor. Strength	Strength Ratio
Bondale	RS 60.3	6.00	3.75	4506	0.0653	0.0062	0.649	10.0	0.500	55.8	47.0	1.1880
(1966)	RS 80.2	6.00	3.75	4382	0.0653	0.0062	0.667	13.3	0.333	70.1	55.8	1.2572
	RS 100.1	6.00	3.75	4260	0.0653	0.0062	0.687	16.7	0.167	92.3	72.9	1.2653
	RS 120.0	6.00	3.75	4700	0.0653	0.0062	0.622	20.0	0.000	107.1	115.3	0.9286
May &	RC1	7.87	7.87	4308	0.0745	0.0028	0.727	8.1	0.112	301.2	282.2	1.0674
Johnson	RC3	7.87	7.87	3390	0.0745	0.0028	0.924	8.1	0.136	305.7	239.1	1.2787
(1978)	RC4	7.87	7.87	5191	0.0745	0.0028	0.603	14.8	0.197	191.1	217.9	0.8771
Morino	A4-90	6.30	6.30	3060	0.0870	0.0036	1.481	5.8	0.250	166.5	121.4	1.3719
et al.	B4-90	6.30	6.30	3393	0.0870	0.0036	1.302	14.4	0.250	114.6	104.0	1.1020
(1984)	C4-90	6.30	6.30	3379	0.0870	0.0036	1.177	21.7	0.250	93.9	83.0	1.1313
	D4-90	6.30	6.30	3074	0.0870	0.0036	1.474	28.9	0.250	64.7	63.5	1.0189
	A8-90	6.30	6.30	4872	0.0870	0.0036	0.953	5.8	0.469	118.1	98.6	1.1968
	B8-90	6.30	6.30	4829	0.0870	0.0036	0.957	14.4	0.469	94.0	84.3	1.1144
	C8-90	6.30	6.30	3567	0.0870	0.0036	1.305	21.7	0.469	68.0	62.5	1.0889
	D8-90	6.30	6.30	3321	0.0870	0.0036	1.399	28.9	0.469	50.1	49.2	1.0196
Procter	S1	11.00	8.00	4722	0.0484	0.0000	0.432	2.2	0.000	470.4	522.9	0.8997
(1967)	S2	11.00	8.00	4722	0.0484	0.0000	0.432	2.2	0.000	481.6	522.9	0.9211
	S3	12.00	8.00	5407	0.0520	0.0000	0.410	2.0	0.000	698.9	642.1	1.0885
	S4	12.00	8.00	5407	0.0520	0.0000	0.410	2.0	0.000	703.4	642.1	1.0955
	1	11.25	8.00	4722	0.0473	0.0000	0.422	11.7	0.533	132.2	127.7	1.0347
	2	11.25	8.00	4722	0.0473	0.0000	0.422	11.7	0.800	87.4	87.4	0.9997
	3	11.25	8.00	4722	0.0473	0.0000	0.422	11.7	0.000	470.4	508.0	0.9259
	4	11.25	8.00	4722	0.0473	0.0000	0.422	11.7	0.533	143.4	127.7	1.1224
	5	11.25	8.00	5407	0.0473	0.0000	0.369	11.7	0.800	91.8	90.5	1.0154
	6	12.00	8.00	5407	0.0520	0.0000	0.410	11.0	0.750	129.9	114.1	1.1383
	7	12.00	8.00	5407	0.0520	0.0000	0.410	11.0	0.500	199.4	168.6	1.1827
	8	12.00	8.00	5407	0.0520	0.0000	0.410	11.0	0.000	560.0	613.6	0.9126
	9	11.25	8.00	6007	0.0473	0.0000	0.332	11.7	0.267	268.8	243.5	1.1039
	10	11.25	8.00	6007	0.0473	0.0000	0.332	11.7	0.267	250.9	243.5	1.0303
	11	12.00	8.00	6007	0.0520	0.0000	0.369	11.0	0.000	533.1	658.5	0.8096
	12	12.00	8.00	6007	0.0520	0.0000	0.369	11.0	0.250	315.8	290.9	1.0859
Suzuki	LH-000-C	8.27	8.27	4785	0.0290	0.0021	0.274	2.9	0.000	380.0	366.4	1.0373
et al.	LH-020-C	8.27	8.27	4785	0.0290	0.0021	0.274	2.9	0.000	374.3	429.4	0.8716
(1983)	LH-040-C	8.27	8.27	4785	0.0290	0.0021	0.274	2.9	0.000	374.3	398.0	0.9403
	LH-100-C	8.27	8.27	4785	0.0290	0.0021	0.274	2.9	0.000	385.8	379.2	1.0173
	RH-000-C	8.27	8.27	4858	0.0546	0.0021	0.624	2.9	0.000	547.0	462.7	1.1823
	RH-020-C	8.27	8.27	4858	0.0546	0.0021	0.624	2.9	0.000	561.4	523.7	1.0720
	RH-040-C	8.27	8.27	4858	0.0546	0.0021	0.624	2.9	0.000	521.1	493.4	1.0563
	RH-100-C	8.27	8.27	4858	0.0546	0.0021	0.624	2.9	0.000	521.1	475.2	1.0967
	HT60-000-C	8.27	8.27	4858	0.0600	0.0021	1.035	2.9	0.000	598.8	562.8	1.0640
	HT60-020-C	8.27	8.27	4858	0.0600	0.0021	1.035	2.9	0.000	656.4	674.0	0.9739
	HT60-040-C	8.27	8.27	4858	0.0600	0.0021	1.035	2.9	0.000	662.2	639.2	1.0359
	HT60-100-C	8.27	8.27	4858	0.0600	0.0021	1.035	2.9	0.000	627.6	611.8	1.0259
	HT80-000-C	8.27	8.27	4858	0.0633	0.0021	1.480	2.9	0.000	716.9	626.3	1.1447
	HT80-020-C	8.27	8.27	4858	0.0633	0.0021	1.480	2.9	0.000	734.2	797.3	0.9208
	HT80-040-C	8.27	8.27	4858	0.0633	0.0021	1.480	2.9	0.000	728.4	759.4	0.9592
	HT80-100-C	8.27	8.27	4858	0.0633	0.0021	1.480	2.9	0.000	711.1	721.0	0.9863

Table Continued

Author	Col. Desig.	h in.	b in.	f'c psi	ρ_{ss}	ρ_{rs}	$\frac{\rho_{ss} f_{yss}}{f'_c}$	ℓ/h	e/h	Tested Strength	Theor. Strength	Strength Ratio
Suzuki	HT80-000-CB	8.27	8.27	4423	0.0423	0.0021	1.060	2.9	0.874	110.4	102.1	1.0809
et al.	HT80-020-CB	8.27	8.27	4423	0.0423	0.0021	1.060	2.9	1.062	110.4	104.8	1.0528
(1983)	LH-000-B	8.27	8.27	4292	0.0290	0.0021	0.306	2.9	inf.	27.4	23.3	1.1760
	LH-020-B	8.27	8.27	4597	0.0290	0.0021	0.286	2.9	inf.	29.4	23.9	1.2317
	LH-040-B	8.27	8.27	4524	0.0290	0.0021	0.290	2.9	inf.	28.2	23.7	1.1932
	LH-100-B	8.27	8.27	4365	0.0290	0.0021	0.301	2.9	inf.	28.2	23.4	1.2080
	RH-000-B	8.27	8.27	4858	0.0546	0.0021	0.624	2.9	inf.	48.9	44.8	1.0931
	RH-020-B	8.27	8.27	4858	0.0546	0.0021	0.624	2.9	inf.	54.5	45.9	1.1873
	RH-040-B	8.27	8.27	4858	0.0546	0.0021	0.624	2.9	inf.	53.3	45.5	1.1710
	RH-100-B	8.27	8.27	4858	0.0546	0.0021	0.624	2.9	inf.	50.9	45.2	1.1265
	HT60-000-B	8.27	8.27	4814	0.0600	0.0021	1.045	2.9	inf.	68.8	69.8	0.9865
	HT60-020-B	8.27	8.27	4814	0.0600	0.0021	1.045	2.9	inf.	79.2	73.1	1.0823
	HT60-040-B	8.27	8.27	4814	0.0600	0.0021	1.045	2.9	inf.	77.2	72.3	1.0677
	HT60-100-B	8.27	8.27	4814	0.0600	0.0021	1.045	2.9	inf.	72.0	71.5	1.0069
	HT80-000-B	8.27	8.27	4771	0.0633	0.0021	1.507	2.9	inf.	93.5	83.3	1.1224
	HT80-020-B	8.27	8.27	4771	0.0633	0.0021	1.507	2.9	inf.	104.2	91.1	1.1437
	HT80-040-B	8.27	8.27	4771	0.0633	0.0021	1.507	2.9	inf.	101.0	89.3	1.1312
	HT80-100-B	8.27	8.27	4771	0.0633	0.0021	1.507	2.9	inf.	97.9	87.2	1.1217
Roik	23	11.81	11.81	6570	0.0868	0.0050	0.517	16.7	0.300	526.3	442.3	1.1900
Mangeri	24	11.81	11.81	6570	0.0868	0.0050	0.517	16.7	0.500	368.3	324.8	1.1340
(1987)	25	11.81	11.81	6570	0.0868	0.0050	0.517	26.7	0.300	377.8	314.4	1.2017
	26	11.81	11.81	6570	0.0868	0.0050	0.517	26.7	0.500	200.9	238.6	0.8420
Roik	V11	11.02	11.02	6351	0.0434	0.0079	0.230	12.4	0.571	171.7	169.6	1.0124
Schwal'r	V12	11.02	11.02	6351	0.0434	0.0079	0.230	12.4	0.214	366.3	373.3	0.9812
(1988)	V13	11.02	11.02	6786	0.0434	0.0079	0.215	12.4	0.357	322.9	272.7	1.1842
	V21	11.02	11.02	6786	0.0495	0.0079	0.333	12.4	0.357	338.2	321.8	1.0509
	V22	11.02	11.02	5365	0.0495	0.0079	0.421	12.4	0.571	213.8	201.7	1.0599
	V23	11.02	11.02	5365	0.0495	0.0079	0.421	12.4	0.214	437.2	388.9	1.1243
	V31	11.02	11.02	5902	0.0996	0.0079	0.555	12.4	0.357	384.1	383.3	1.0020
	V32	11.02	11.02	5902	0.0996	0.0079	0.555	12.4	0.214	506.9	501.2	1.0114
	V33	11.02	11.02	5699	0.0996	0.0079	0.575	12.4	0.571	294.3	280.8	1.0481
	V41	11.02	11.02	5699	0.1441	0.0079	0.796	12.4	0.357	477.7	422.9	1.1295
	V42	11.02	11.02	6119	0.1441	0.0079	0.926	12.4	0.571	344.9	359.6	0.9592
	V43	11.02	11.02	6119	0.1441	0.0079	0.995	12.4	0.214	614.9	650.6	0.9451

NOTE : For e/h = inf., strength is given in kip-ft (1 kip-ft = 1.356 kN-m).

For all other values of e/h, the strength is shown in kips (1 kip = 4.448 kN).

b = width of the concrete cross-section parrallel to the axis of bending;

h = depth of the concrete cross-section perpendicular to the axis of bending.

The term f_{yss} was taken as the web yield strength for computing the $\rho_{ss} f_{yss}/f'_c$ ratio.

Table A3 - Specimen Configuration for Columns Bending About the Minor Axis

Author	Col. Desig.	b in.	h in.	Steel Profile	Long. Reinf.	A_{ss} in.^{2}	A_c in.^{2}	A_{rs} in.^{2}	Vol'met' Ratio*
Stevens (1965)	CV2	7.00	6.50	5"x4.5"@20#		5.87	39.63		
	CV3	7.00	6.50	5"x4.5"@20#		5.87	39.63		
	CV4	7.00	6.50	5"x4.5"@20#		5.87	39.63		
	CV5	7.00	6.50	5"x4.5"@20#		5.87	39.63		
	CV6	7.00	6.50	5"x4.5"@20#		5.87	39.63		
	AE1	7.00	6.50	5"x4.5"@20#		5.87	39.63		
	AE2	7.00	6.50	5"x4.5"@20#		5.87	39.63		
	AE3	7.00	6.50	5"x4.5"@20#		5.87	39.63		
	AE4	7.00	6.50	5"x4.5"@20#		5.87	39.63		
	AE5	7.00	6.50	5"x4.5"@20#		5.87	39.63		
	AE6	7.00	6.50	5"x4.5"@20#		5.87	39.63		
	AE7	7.00	6.50	5"x4.5"@20#		5.87	39.63		
	AE8	7.00	6.50	5"x4.5"@20#		5.87	39.63		
	AE9	7.00	6.50	5"x4.5"@20#		5.87	39.63		
	AE10	7.00	6.50	5"x4.5"@20#		5.87	39.63		
	AE11	7.00	6.50	5"x4.5"@20#		5.87	39.63		
	FE1	16.00	12.00	12"x8"@65#	4-0.5"	19.13	172.09	0.79	0.0028
	FE2	16.00	12.00	12"x8"@65#	4-0.5"	19.13	172.09	0.79	0.0028
	FE3	16.00	12.00	12"x8"@65#	4-0.5"	19.13	172.09	0.79	0.0028
	FE4	16.00	12.00	12"x8"@65#	4-0.5"	19.13	172.09	0.79	0.0028
	FE5	16.00	12.00	12"x8"@65#	4-0.5"	19.13	172.09	0.79	0.0028
	FE6	16.00	12.00	12"x8"@65#	4-0.5"	19.13	172.09	0.79	0.0028
	FE7	16.00	12.00	12"x8"@65#	4-0.5"	19.13	172.09	0.79	0.0028
	FE8	16.00	12.00	12"x8"@65#	4-0.5"	19.13	172.09	0.79	0.0028
	FE9	16.00	12.00	12"x8"@65#	4-0.5"	19.13	172.09	0.79	0.0028
	FE10	16.00	12.00	12"x8"@65#	4-0.5"	19.13	172.09	0.79	0.0028
	FE11	16.00	12.00	12"x8"@65#	4-0.5"	19.13	172.09	0.79	0.0028
	FE12	16.00	12.00	12"x8"@65#	4-0.5"	19.13	172.09	0.79	0.0028
	B1	5.00	3.50	3"x1.5"@4#		1.18	16.32		
	B2	5.00	3.50	3"x1.5"@4#		1.18	16.32		
	B3	5.00	3.50	3"x1.5"@4#		1.18	16.32		
	B4	5.00	3.50	3"x1.5"@4#		1.18	16.32		
	B5	5.00	3.50	3"x1.5"@4#		1.18	16.32		
	B6	5.00	3.50	3"x1.5"@4#		1.18	16.32		
	B7	5.00	3.50	3"x1.5"@4#		1.18	16.32		
	A1	7.00	6.50	5"x4.5"@20#		5.87	39.63		
	A2	7.00	6.50	5"x4.5"@20#		5.87	39.63		
	A3	7.00	6.50	5"x4.5"@20#		5.87	39.63		
	A4	7.00	6.50	5"x4.5"@20#		5.87	39.63		
	A5	7.00	6.50	5"x4.5"@20#		5.87	39.63		
	A6	7.00	6.50	5"x4.5"@20#		5.87	39.63		
	RE1a	7.00	6.50	5"x4.5"@20#		5.87	39.63		
	RE1b	7.00	6.50	5"x4.5"@20#		5.87	39.63		
	RE2a	7.00	6.50	5"x4.5"@20#		5.87	39.63		0.0057
	RE2b	7.00	6.50	5"x4.5"@20#		5.87	39.63		0.0057
	RE3a	7.00	6.50	5"x4.5"@20#	4 - 1/4"	5.87	39.43	0.20	0.0057
	RE3b	7.00	6.50	5"x4.5"@20#	4 - 1/4"	5.87	39.43	0.20	0.0057
	RE4a	7.00	6.50	5"x4.5"@20#		5.87	39.63		
	RE4b	7.00	6.50	5"x4.5"@20#		5.87	39.63		

Table A3 - Specimen Configuration for Columns Bending About the Minor Axis

continued

Author	Col. Desig.	I_{ss} in.^{4}	I_c in.^{4}	I_{rs} in.^{4}	Fy web	Fy flange	f'c Col. Stored **	f'c Water Stored	Fy Reinf.	ρ_{ss}	ρ_{rs}
Stevens (1965)	CV2	6.58	153.62		36060	36060	1115	1012		0.1291	0.0000
	CV3	6.58	153.62		36060	36060	1900	2083		0.1291	0.0000
	CV4	6.58	153.62		36060	36060	2491	2982		0.1291	0.0000
	CV5	6.58	153.62		36060	36060	3058	3983		0.1291	0.0000
	CV6	6.58	153.62		36060	36060	3672	4414		0.1291	0.0000
	AE1	6.58	153.62		36060	36060	2046	2379		0.1291	0.0000
	AE2	6.58	153.62		36060	36060	2679	2792		0.1291	0.0000
	AE3	6.58	153.62		36060	36060	2566	2830		0.1291	0.0000
	AE4	6.58	153.62		36060	36060	2906	3020		0.1291	0.0000
	AE5	6.58	153.62		36060	36060	2305	2491		0.1291	0.0000
	AE6	6.58	153.62		36060	36060	2010	2379		0.1291	0.0000
	AE7	6.58	153.62		36060	36060	2083	2379		0.1291	0.0000
	AE8	6.58	153.62		36060	36060	2157	2342		0.1291	0.0000
	AE9	6.58	153.62		36060	36060	1467	1682		0.1291	0.0000
	AE10	6.58	153.62		36060	36060	1900	2120		0.1291	0.0000
	AE11	6.58	153.62		36060	36060	2305	2305		0.1291	0.0000
	FE1	65.18	2219.20	15.92	33031	33031	2083	2641	60000	0.0996	0.0041
	FE2	65.18	2219.20	15.92	33031	33031	2268	3020	60000	0.0996	0.0041
	FE3	65.18	2219.20	15.92	33031	33031	2083	2717	60000	0.0996	0.0041
	FE4	65.18	2219.20	15.92	33031	33031	1936	2231	60000	0.0996	0.0041
	FE5	65.18	2219.20	15.92	33031	33031	2454	2792	60000	0.0996	0.0041
	FE6	65.18	2219.20	15.92	33031	33031	2231	2641	60000	0.0996	0.0041
	FE7	65.18	2219.20	15.92	33031	33031	2231	2529	60000	0.0996	0.0041
	FE8	65.18	2219.20	15.92	33031	33031	2342	2792	60000	0.0996	0.0041
	FE9	65.18	2219.20	15.92	33031	33031	2268	2566	60000	0.0996	0.0041
	FE10	65.18	2219.20	15.92	33031	33031	2604	2830	60000	0.0996	0.0041
	FE11	65.18	2219.20	15.92	33031	33031	2529	2754	60000	0.0996	0.0041
	FE12	65.18	2219.20	15.92	33031	33031	2529	2830	60000	0.0996	0.0041
	B1	0.13	17.73		41200	41200	2120	2417		0.0674	0.0000
	B2	0.13	17.73		41200	41200	1467	1538		0.0674	0.0000
	B3	0.13	17.73		41200	41200	1827	2454		0.0674	0.0000
	B4	0.13	17.73		41200	41200	1610	1574		0.0674	0.0000
	B5	0.13	17.73		41200	41200	2083	2083		0.0674	0.0000
	B6	0.13	17.73		41200	41200	1791	1610		0.0674	0.0000
	B7	0.13	17.73		41200	41200	2305	2046		0.0674	0.0000
	A1	6.58	153.62		42100	42100	1900	2046		0.1291	0.0000
	A2	6.58	153.62		42100	42100	1682	1973		0.1291	0.0000
	A3	6.58	153.62		42100	42100	1900	2417		0.1291	0.0000
	A4	6.58	153.62		42100	42100	2046	2231		0.1291	0.0000
	A5	6.58	153.62		42100	42100	1864	2120		0.1291	0.0000
	A6	6.58	153.62		42100	42100	2216	2342		0.1291	0.0000
	RE1a	6.58	153.62		43800	43800	2010			0.1291	0.0000
	RE1b	6.58	153.62		43800	43800	1791			0.1291	0.0000
	RE2a	6.58	153.62		43800	43800	1900			0.1291	0.0000
	RE2b	6.58	153.62		43800	43800	2305			0.1291	0.0000
	RE3a	6.58	152.52	1.1	43800	43800	2231		60000	0.1291	0.0043
	RE3b	6.58	152.52	1.1	43800	43800	1900		60000	0.1291	0.0043
	RE4a	6.58	153.62		43800	43800	1973		60000	0.1291	0.0000
	RE4b	6.58	153.62		43800	43800	1827		60000	0.1291	0.0000

** Two sets of concrete tests reported by Steven's. Concrete specimens stored with columns were used in this study.

Table A3 - Specimen Configuration for Columns Bending About the Minor Axis

continued

Author	Col. Desig.	$\frac{\rho_{ss} f_{yss}}{f'_c}$	ℓ in.	ℓ/h	e in.	e/h	Tested Strength	Theor. Strength	Strength Ratio
Stevens (1965)	CV2	4.175	82.0	12.6	0.75	0.115	134.4	98.0	1.3714
	CV3	2.450	82.0	12.6	0.75	0.115	161.3	110.6	1.4586
	CV4	1.869	82.0	12.6	0.75	0.115	179.2	122.4	1.4636
	CV5	1.523	82.0	12.6	0.75	0.115	201.6	134.5	1.4989
	CV6	1.268	82.0	12.6	0.80	0.123	228.5	142.6	1.6025
	AE1	2.275	28.0	4.3	1.00	0.154	165.8	137.4	1.2065
	AE2	1.738	46.0	7.1	1.00	0.154	163.5	135.6	1.2056
	AE3	1.814	82.0	12.6	1.00	0.154	141.1	105.9	1.3321
	AE4	1.602	118.0	18.2	1.00	0.154	118.7	88.5	1.3409
	AE5	2.020	154.0	23.7	1.00	0.154	98.6	63.2	1.5588
	AE6	2.317	46.0	7.1	0.00	0.000	291.2	257.0	1.1333
	AE7	2.235	46.0	7.1	0.50	0.077	224.0	176.8	1.2673
	AE8	2.158	118.0	18.2	0.50	0.077	161.3	108.5	1.4860
	AE9	3.174	154.0	23.7	1.50	0.231	78.4	44.6	1.7563
	AE10	2.450	154.0	23.7	2.00	0.308	72.8	42.2	1.7263
	AE11	2.020	108.0	16.6	inf.	inf.	20.9	19.4	1.0760
	FE1	1.580	180.0	15.0	0.00	0.000	985.6	814.6	1.2099
	FE2	1.451	180.0	15.0	0.00	0.000	1055.0	846.1	1.2470
	FE3	1.580	180.0	15.0	1.00	0.083	672.0	479.5	1.4016
	FE4	1.699	180.0	15.0	2.00	0.167	486.1	331.9	1.4645
	FE5	1.341	180.0	15.0	2.00	0.167	515.2	365.7	1.4089
	FE6	1.475	180.0	15.0	3.00	0.250	360.6	278.6	1.2943
	FE7	1.475	180.0	15.0	4.00	0.333	295.7	234.9	1.2587
	FE8	1.405	180.0	15.0	5.00	0.417	262.1	206.1	1.2717
	FE9	1.451	180.0	15.0	6.00	0.500	230.7	178.9	1.2897
	FE10	1.264	180.0	15.0	7.00	0.583	199.4	168.4	1.1836
	FE11	1.301	180.0	15.0	8.00	0.667	168.0	149.9	1.1211
	FE12	1.301	120.0	10.0	inf.	inf.	131.4	128.6	1.0219
	B1	1.310	46	13.1	0.00	0.00	82.9	64.7	1.2802
	B2	1.894	64	18.3	0.00	0.00	61.2	42.6	1.4352
	B3	1.520	82	23.4	0.00	0.00	64.1	38.0	1.6881
	B4	1.725	100	28.6	0.00	0.00	44.4	27.6	1.6070
	B5	1.334	118	33.7	0.00	0.00	51.5	25.0	2.0649
	B6	1.551	136	38.9	0.00	0.00	36.7	18.4	1.9922
	B7	1.205	154	44.0	0.00	0.00	34.5	17.0	2.0244
	A1	2.861	9	1.4	0.00	0.00	358.4	304.0	1.1791
	A2	3.231	46	7.1	0.00	0.00	313.6	259.2	1.2099
	A3	2.861	82	12.6	0.00	0.00	322.6	239.7	1.3456
	A4	2.656	82	12.6	0.00	0.00	302.4	246.2	1.2282
	A5	2.917	118	18.2	0.00	0.00	293.4	200.7	1.4623
	A6	2.453	154	23.7	0.00	0.00	235.2	164.3	1.4314
	RE1a	2.814	118	18.2	0.00	0.00	300.2	214.7	1.3978
	RE1b	3.158	118	18.2	0.00	0.00	280.0	206.5	1.3558
	RE2a	2.976	118	18.2	0.00	0.00	275.5	217.4	1.2676
	RE2b	2.453	118	18.2	0.00	0.00	268.8	230.9	1.1640
	RE3a	2.535	118	18.2	0.00	0.00	313.6	271.9	1.1535
	RE3b	2.976	118	18.2	0.00	0.00	277.8	260.2	1.0674
	RE4a	2.866	118	18.2	0.00	0.00	271.0	209.5	1.2937
	RE4b	3.095	118	18.2	0.00	0.00	284.5	204.1	1.3936

Table A3 - Specimen Configuration for Columns Bending About the Minor Axis

continued

Author	Col. Desig.	b in.	h in.	Steel Profile	Long. Reinf.	A_{ss} in.^{2}	A_c in.^{2}	A_{rs} in.^{2}	Vol'met'* Ratio
Stevens (1965)	FA1	16.00	12.00	12"x8"@65#		19.13	172.87		
	FA2	16.00	12.00	12"x8"@65#		19.13	172.87		
	FA3	16.00	12.00	12"x8"@65#		19.13	172.87		
	FA4	16.00	12.00	12"x8"@65#		19.13	172.87		
	FA5	16.00	12.00	12"x8"@65#		19.13	172.87		
Bondale (1966)	RW 60.3	6.00	3.75	4"x1.75"@5#	4-0.21"	1.47	20.89	0.14	0.00644
	RW 80.2	6.00	3.75	4"x1.75"@5#	4-0.21"	1.47	20.89	0.14	0.00644
	RW 100.1	6.00	3.75	4"x1.75"@5#	4-0.21"	1.47	20.89	0.14	0.00644
	RW 120.0	6.00	3.75	4"x1.75"@5#	4-0.21"	1.47	20.89	0.14	0.00644
May (1978)	RC5	7.87	7.87	152X152 UC23	4-Y6	4.62	57.18	0.20	0.0018
Janss Anslijn (1974)	1.1	9.45	9.45	HE140B	4-12mm	6.67	81.91	0.70	0.00205
	1.2	9.45	9.45	HE140B	4-12mm	6.67	81.91	0.70	0.00205
	1.3	9.45	9.45	HE140B	4-12mm	6.67	81.91	0.70	0.00205
	2.1	9.45	9.45	HE140B	4-12mm	6.67	81.91	0.70	0.00205
	2.2	9.45	9.45	HE140B	4-12mm	6.67	81.91	0.70	0.00205
	2.3	9.45	9.45	HE140B	4-12mm	6.67	81.91	0.70	0.00205
	3.1	9.45	9.45	HE140B	4-12mm	6.67	81.91	0.70	0.00205
	3.2	9.45	9.45	HE140B	4-12mm	6.67	81.91	0.70	0.00205
	3.3	9.45	9.45	HE140B	4-12mm	6.67	81.91	0.70	0.00205
	4.1	9.45	9.45	HE140B	4-12mm	6.67	81.91	0.70	0.00205
	4.2	9.45	9.45	HE140B	4-12mm	6.67	81.91	0.70	0.00205
	4.3	9.45	9.45	HE140B	4-12mm	6.67	81.91	0.70	0.00205
	5.1	9.45	9.45	HE140B	4-12mm	6.67	81.91	0.70	0.00205
	5.2	9.45	9.45	HE140B	4-12mm	6.67	81.91	0.70	0.00205
	5.3	9.45	9.45	HE140B	4-12mm	6.67	81.91	0.70	0.00205
	6.1	9.45	9.45	HE140B	4-12mm	6.67	81.91	0.70	0.00205
	6.2	9.45	9.45	HE140B	4-12mm	6.67	81.91	0.70	0.00205
	6.3	9.45	9.45	HE140B	4-12mm	6.67	81.91	0.70	0.00205
	7.1	9.45	9.45	HE140B	4-12mm	6.67	81.91	0.70	0.00205
	7.2	9.45	9.45	HE140B	4-12mm	6.67	81.91	0.70	0.00205
	7.3	9.45	9.45	HE140B	4-12mm	6.67	81.91	0.70	0.00205
	8.1	9.45	9.45	HE140B	4-12mm	6.67	81.91	0.70	0.00205
	8.2	9.45	9.45	HE140B	4-12mm	6.67	81.91	0.70	0.00205
	8.3	9.45	9.45	HE140B	4-12mm	6.67	81.91	0.70	0.00205
	9.1	12.60	8.27	IPE220	4-12mm	5.18	98.28	0.70	0.00192
	9.2	12.60	8.27	IPE220	4-12mm	5.18	98.28	0.70	0.00192
	9.3	12.60	8.27	IPE220	4-12mm	5.18	98.28	0.70	0.00192
	10.1	12.60	8.27	IPE220	4-12mm	5.18	98.28	0.70	0.00192
	10.2	12.60	8.27	IPE220	4-12mm	5.18	98.28	0.70	0.00192
	10.3	12.60	8.27	IPE220	4-12mm	5.18	98.28	0.70	0.00192
	11.1	9.45	9.45	HE140B	4-12mm	6.67	81.91	0.70	0.00205
	11.2	9.45	9.45	HE140B	4-12mm	6.67	81.91	0.70	0.00205
	11.3	9.45	9.45	HE140B	4-12mm	6.67	81.91	0.70	0.00205
	12.1	9.45	9.45	HE140B	4-12mm	6.67	81.91	0.70	0.00205
	12.2	9.45	9.45	HE140B	4-12mm	6.67	81.91	0.70	0.00205
	12.3	9.45	9.45	HE140B	4-12mm	6.67	81.91	0.70	0.00205

Table A3 - Specimen Configuration for Columns Bending About the Minor Axis

continued

Author	Col. Desig.	I_{ss} in.^{4}	I_c in.^{4}	I_{rs} in.^{4}	Fy web	Fy flange	f'c Col. Stored **	f'c Water Stored	Fy Reinf.	ρ_{ss}	ρ_{rs}
Stevens	FA1	65.18	2238.82		32900	32900	1864	2231		0.0996	0.0000
(1965)	FA2	65.18	2238.82		32900	32900	2010	2342		0.0996	0.0000
	FA3	65.18	2238.82		32900	32900	1755	2417		0.0996	0.0000
	FA4	65.18	2238.82		32900	32900	1973	2604		0.0996	0.0000
	FA5	65.18	2238.82		32900	32900	1973	2454		0.0996	0.0000
Bondale	RW 60.3	0.19	67.09	0.22	44800	44800	4665			0.0653	0.0099
(1966)	RW 80.2	0.19	67.09	0.22	44800	44800	5557			0.0653	0.0099
	RW 100.1	0.19	67.09	0.22	44800	44800	4488			0.0653	0.0099
	RW 120.0	0.19	67.09	0.22	44800	44800	3927			0.0653	0.0099
May (1978)	RC5	30.34	288.17	1.82	42050	41615	5278		60000	0.0745	0.0294
Janss	1.1	13.21	641.23	9.80	41383	41383	6014		31900	0.0747	0.0079
Anslijn	1.2	13.21	641.23	9.80	41383	41383	5517		31900	0.0747	0.0079
(1974)	1.3	13.21	641.23	9.80	39672	39672	5263		31900	0.0747	0.0079
	2.1	13.21	641.23	9.80	42514	42514	5263		31900	0.0747	0.0079
	2.2	13.21	641.23	9.80	42514	42514	4507		31900	0.0747	0.0079
	2.3	13.21	641.23	9.80	42514	42514	5517		31900	0.0747	0.0079
	3.1	13.21	641.23	9.80	40035	40035	5957		31900	0.0747	0.0079
	3.2	13.21	641.23	9.80	40035	40035	6014		31900	0.0747	0.0079
	3.3	13.21	641.23	9.80	40035	40035	5263		31900	0.0747	0.0079
	4.1	13.21	641.23	9.80	40035	40035	5263		31900	0.0747	0.0079
	4.2	13.21	641.23	9.80	40035	40035	4507		31900	0.0747	0.0079
	4.3	13.21	641.23	9.80	40035	40035	5574		31900	0.0747	0.0079
	5.1	13.21	641.23	9.80	55028	55028	4870		31900	0.0747	0.0079
	5.2	13.21	641.23	9.80	55028	55028	5277		31900	0.0747	0.0079
	5.3	13.21	641.23	9.80	55028	55028	4982		31900	0.0747	0.0079
	6.1	13.21	641.23	9.80	72805	72805	4870		31900	0.0747	0.0079
	6.2	13.21	641.23	9.80	72805	72805	5277		31900	0.0747	0.0079
	6.3	13.21	641.23	9.80	72805	72805	4996		31900	0.0747	0.0079
	7.1	13.21	641.23	9.80	70818	70818	4968		31900	0.0747	0.0079
	7.2	13.21	641.23	9.80	70818	70818	5291		31900	0.0747	0.0079
	7.3	13.21	641.23	9.80	70818	70818	4996		31900	0.0747	0.0079
	8.1	13.21	641.23	9.80	72515	72515	5263		31900	0.0747	0.0079
	8.2	13.21	641.23	9.80	72515	72515	6014		31900	0.0747	0.0079
	8.3	13.21	641.23	9.80	72515	72515	5957		31900	0.0747	0.0079
	9.1	4.93	581.46	6.97	39527	39527	4507		31900	0.0497	0.0067
	9.2	4.93	581.46	6.97	39527	39527	5957		31900	0.0497	0.0067
	9.3	4.93	581.46	6.97	39527	39527	5291		31900	0.0497	0.0067
	10.1	4.93	581.46	6.97	70818	70818	5263		31900	0.0497	0.0067
	10.2	4.93	581.46	6.97	70818	70818	4968		31900	0.0497	0.0067
	10.3	4.93	581.46	6.97	70818	70818	4982		31900	0.0497	0.0067
	11.1	13.21	641.23	9.80	41528	41528	5390		31900	0.0747	0.0079
	11.2	13.21	641.23	9.80	41528	41528	5574		31900	0.0747	0.0079
	11.3	13.21	641.23	9.80	41528	41528	4772		31900	0.0747	0.0079
	12.1	13.21	641.23	9.80	70673	70673	5390		31900	0.0747	0.0079
	12.2	13.21	641.23	9.80	70673	70673	5207		31900	0.0747	0.0079
	12.3	13.21	641.23	9.80	70673	70673	4772		31900	0.0747	0.0079

Table A3 - Specimen Configuration for Columns Bending About the Minor Axis

continued

Author	Col. Desig.	$\frac{\rho_{ss} f_{yss}}{f'_c}$	ℓ in.	ℓ/h	e in.	e/h	Tested Strength	Theor. Strength	Strength Ratio
Stevens	FA1	1.759	36	3.0	0.00	0.00	1070.7	899.4	1.1905
(1965)	FA2	1.631	72	6.0	0.00	0.00	1008.0	912.8	1.1044
	FA3	1.868	108	9.0	0.00	0.00	943.0	817.3	1.1539
	FA4	1.661	144	12.0	0.00	0.00	954.2	807.0	1.1825
	FA5	1.661	180	15.0	0.00	0.00	949.8	738.5	1.2861
Bondale	RW 60.3	0.627	60.0	16.0	3.00	0.800	17.9	14.9	1.2019
(1966)	RW 80.2	0.526	80.0	21.3	2.00	0.533	21.7	19.1	1.1370
	RW 100.1	0.652	100.0	26.7	1.00	0.267	20.8	20.8	1.0030
	RW 120.0	0.745	120.0	32.0	0.00	0.000	52.9	53.0	0.9969
May (1978)	RC5	0.594	112.6	14.3	0.79	0.100	185.5	231.2	0.8021
Janss	1.1	0.514	168.5	17.8	0.00	0.000	483.3	528.9	0.9139
Anslijn	1.2	0.560	168.5	17.8	0.00	0.000	489.8	506.8	0.9665
(1974)	1.3	0.563	168.3	17.8	0.00	0.000	470.0	491.5	0.9563
	2.1	0.603	137.2	14.5	0.00	0.000	527.4	564.9	0.9336
	2.2	0.704	136.7	14.5	0.00	0.000	489.8	517.9	0.9458
	2.3	0.575	136.9	14.5	0.00	0.000	580.3	581.6	0.9978
	3.1	0.502	98.0	10.4	0.00	0.000	591.3	680.8	0.8685
	3.2	0.497	97.5	10.3	0.00	0.000	503.1	685.2	0.7342
	3.3	0.568	98.0	10.4	0.00	0.000	527.4	634.0	0.8318
	4.1	0.568	50.7	5.4	0.00	0.000	573.8	658.3	0.8715
	4.2	0.663	50.5	5.3	0.00	0.000	556.0	604.2	0.9201
	4.3	0.536	49.3	5.2	0.00	0.000	617.9	618.0	0.9997
	5.1	0.844	137.4	14.5	0.00	0.000	529.7	585.6	0.9045
	5.2	0.778	137.1	14.5	0.00	0.000	591.3	611.3	0.9673
	5.3	0.825	137.2	14.5	0.00	0.000	556.0	592.9	0.9378
	6.1	1.116	168.3	17.8	0.00	0.000	529.7	517.0	1.0244
	6.2	1.030	168.3	17.8	0.00	0.000	485.3	541.0	0.8971
	6.3	1.088	168.3	17.8	0.00	0.000	558.2	524.6	1.0642
	7.1	1.064	137.4	14.5	0.00	0.000	556.0	624.1	0.8908
	7.2	0.999	137.4	14.5	0.00	0.000	589.1	648.3	0.9086
	7.3	1.058	137.3	14.5	0.00	0.000	578.0	626.6	0.9225
	8.1	1.029	97.8	10.4	0.00	0.000	547.2	759.3	0.7207
	8.2	0.900	98.2	10.4	0.00	0.000	531.7	816.8	0.6509
	8.3	0.909	98.0	10.4	0.00	0.000	573.8	812.9	0.7058
	9.1	0.436	137.3	16.6	0.00	0.000	514.1	497.1	1.0342
	9.2	0.330	137.3	16.6	0.00	0.000	569.3	592.9	0.9601
	9.3	0.371	137.2	16.6	0.00	0.000	463.3	549.6	0.8430
	10.1	0.669	137.2	16.6	0.00	0.000	518.6	579.1	0.8956
	10.2	0.709	137.2	16.6	0.00	0.000	609.1	557.6	1.0923
	10.3	0.707	137.1	16.6	0.00	0.000	531.7	559.2	0.9508
	11.1	0.575	135.9	14.4	1.57	0.167	251.6	257.9	0.9755
	11.2	0.556	135.9	14.4	1.57	0.167	264.8	262.9	1.0072
	11.3	0.650	135.9	14.4	1.57	0.167	240.5	240.1	1.0018
	12.1	0.979	135.7	14.4	1.57	0.167	264.8	271.9	0.9739
	12.2	1.013	135.7	14.4	1.57	0.167	251.6	243.7	1.0321
	12.3	1.106	136.0	14.4	1.57	0.167	222.8	253.3	0.8796

Table A3 - Specimen Configuration for Columns Bending About the Minor Axis

continued

Author	Col. Desig.	b in.	h in.	Steel Profile	Long. Reinf.	A_{ss} in.^{2}	A_c in.^{2}	A_{rs} in.^{2}	* Vol'met' Ratio
Janss	13.1	12.60	8.27	IPE220	4-12mm	5.18	98.28	0.70	0.00192
Anslijn	13.2	12.60	8.27	IPE220	4-12mm	5.18	98.28	0.70	0.00192
(1974)	13.3	12.60	8.27	IPE220	4-12mm	5.18	98.28	0.70	0.00192
Janss	1	12.60	8.27	IPE220	4-12mm	5.18	98.28	0.70	0.00192
Piraprez	3	12.60	8.27	IPE220	4-12mm	5.18	98.28	0.70	0.00192
(1974)	5	12.60	8.27	IPE220	4-12mm	5.18	98.28	0.70	0.00192
	7	12.60	8.27	IPE220	4-12mm	5.18	98.28	0.70	0.00192
	9	12.60	8.27	IPE220	4-12mm	5.18	98.28	0.70	0.00192
	11	12.60	8.27	IPE220	4-12mm	5.18	98.28	0.70	0.00192
	13	12.60	8.27	IPE220	4-12mm	5.18	98.28	0.70	0.00192
	15	12.60	8.27	IPE220	4-12mm	5.18	98.28	0.70	0.00192
	17	12.60	8.27	IPE220	4-12mm	5.18	98.28	0.70	0.00192
	19	12.60	8.27	IPE220	4-12mm	5.18	98.28	0.70	0.00192
	23	12.60	8.27	IPE220	4-12mm	5.18	98.28	0.70	0.00192
	27	12.60	8.27	IPE220	4-12mm	5.18	98.28	0.70	0.00192
	2	9.45	9.45	HE140B	4-12mm	6.67	81.91	0.70	0.00205
	4	9.45	9.45	HE140B	4-12mm	6.67	81.91	0.70	0.00205
	6	9.45	9.45	HE140B	4-12mm	6.67	81.91	0.70	0.00205
	8	9.45	9.45	HE140B	4-12mm	6.67	81.91	0.70	0.00205
	10	9.45	9.45	HE140B	4-12mm	6.67	81.91	0.70	0.00205
	12	9.45	9.45	HE140B	4-12mm	6.67	81.91	0.70	0.00205
	14	9.45	9.45	HE140B	4-12mm	6.67	81.91	0.70	0.00205
	16	9.45	9.45	HE140B	4-12mm	6.67	81.91	0.70	0.00205
	18	9.45	9.45	HE140B	4-12mm	6.67	81.91	0.70	0.00205
	21	9.45	9.45	HE140B	4-12mm	6.67	81.91	0.70	0.00205
	25	9.45	9.45	HE140B	4-12mm	6.67	81.91	0.70	0.00205
	29	9.45	9.45	HE140B	4-12mm	6.67	81.91	0.70	0.00205
	20	12.60	8.27	IPE220	4-12mm	5.18	98.28	0.70	0.00192
	24	12.60	8.27	IPE220	4-12mm	5.18	98.28	0.70	0.00192
	28	12.60	8.27	IPE220	4-12mm	5.18	98.28	0.70	0.00192
	22	9.45	9.45	HE140B	4-12mm	6.67	81.91	0.70	0.00205
	26	9.45	9.45	HE140B	4-12mm	6.67	81.91	0.70	0.00205
	30	9.45	9.45	HE140B	4-12mm	6.67	81.91	0.70	0.00205
Roderick	SE 1	8.00	7.00	4"x3"@10#		2.94	53.06		
Loke	SE 2	8.00	7.00	4"x3"@10#		2.94	53.06		
(1974)	SE 3	8.00	7.00	4"x3"@10#		2.94	53.06		
Australia	SE 4	8.00	7.00	4"x3"@10#		2.94	53.06		
	SE 5	8.00	7.00	4"x3"@10#		2.94	53.06		
	SE 6	8.00	7.00	4"x3"@10#		2.94	53.06		
	SE 7	8.00	7.00	4"x3"@10#		2.94	53.06		
	SE 8	8.00	7.00	4"x3"@10#		2.94	53.06		
	SE 9	8.00	7.00	4"x3"@10#		2.94	53.06		
	SE10	8.00	7.00	4"x3"@10#		2.94	53.06		
	SE11	8.00	7.00	4"x3"@10#		2.94	53.06		
	SE12	8.00	7.00	4"x3"@10#		2.94	53.06		
	SE13	8.00	7.00	4"x1.75"@5#		1.47	54.53		
	SE14	8.00	7.00	4"x1.75"@5#		1.47	54.53		
	SE15	8.00	7.00	4"x1.75"@5#		1.47	54.53		

Table A3 - Specimen Configuration for Columns Bending About the Minor Axis

continued

Author	Col. Desig.	I_{ss} in.^{4}	I_c in.^{4}	I_{rs} in.^{4}	Fy web	Fy flange	f'c Col. Stored **	f'c Water Stored	Fy Reinf.	ρ_{ss}	ρ_{rs}
Janss	13.1	4.93	581.46	6.97	39527	39527	5574		31900	0.0497	0.0067
Anslijn	13.2	4.93	581.46	6.97	39527	39527	5207		31900	0.0497	0.0067
(1974)	13.3	4.93	581.46	6.97	39527	39527	5094		31900	0.0497	0.0067
Janss	1	4.93	581.46	6.97	40528	40528	4721		31900	0.0497	0.0067
Piraprez	3	4.93	581.46	6.97	40528	40528	4721		31900	0.0497	0.0067
(1974)	5	4.93	581.46	6.97	40528	40528	5158		31900	0.0497	0.0067
	7	4.93	581.46	6.97	40528	40528	5158		31900	0.0497	0.0067
	9	4.93	581.46	6.97	40528	40528	5531		31900	0.0497	0.0067
	11	4.93	581.46	6.97	40528	40528	5531		31900	0.0497	0.0067
	13	4.93	581.46	6.97	40528	40528	4990		31900	0.0497	0.0067
	15	4.93	581.46	6.97	40528	40528	5108		31900	0.0497	0.0067
	17	4.93	581.46	6.97	40528	40528	5040		31900	0.0497	0.0067
	19	4.93	581.46	6.97	40528	40528	4738		31900	0.0497	0.0067
	23	4.93	581.46	6.97	40528	40528	4571		31900	0.0497	0.0067
	27	4.93	581.46	6.97	40528	40528	4105		31900	0.0497	0.0067
	2	13.21	641.23	9.80	39382	39382	4721		31900	0.0747	0.0079
	4	13.21	641.23	9.80	39382	39382	4721		31900	0.0747	0.0079
	6	13.21	641.23	9.80	39382	39382	5158		31900	0.0747	0.0079
	8	13.21	641.23	9.80	39382	39382	5158		31900	0.0747	0.0079
	10	13.21	641.23	9.80	39382	39382	5531		31900	0.0747	0.0079
	12	13.21	641.23	9.80	39382	39382	5531		31900	0.0747	0.0079
	14	13.21	641.23	9.80	39382	39382	4990		31900	0.0747	0.0079
	16	13.21	641.23	9.80	39382	39382	5108		31900	0.0747	0.0079
	18	13.21	641.23	9.80	39382	39382	5040		31900	0.0747	0.0079
	21	13.21	641.23	9.80	39382	39382	4738		31900	0.0747	0.0079
	25	13.21	641.23	9.80	39382	39382	4571		31900	0.0747	0.0079
	29	13.21	641.23	9.80	39382	39382	4105		31900	0.0747	0.0079
	20	4.93	581.46	6.97	40528	40528	4738		31900	0.0497	0.0067
	24	4.93	581.46	6.97	40528	40528	4571		31900	0.0497	0.0067
	28	4.93	581.46	6.97	40528	40528	4105		31900	0.0497	0.0067
	22	13.21	641.23	9.80	39382	39382	4738		31900	0.0747	0.0079
	26	13.21	641.23	9.80	39382	39382	4571		31900	0.0747	0.0079
	30	13.21	641.23	9.80	39382	39382	4105		31900	0.0747	0.0079
Roderick	SE 1	1.32	227.35		42400	42400	3690			0.0525	0.0000
Loke	SE 2	1.32	227.35		42400	42400	4280			0.0525	0.0000
(1974)	SE 3	1.32	227.35		42400	42400	3910			0.0525	0.0000
Australia	SE 4	1.32	227.35		40700	40700	3880			0.0525	0.0000
	SE 5	1.32	227.35		40700	40700	3710			0.0525	0.0000
	SE 6	1.32	227.35		45600	45600	3280			0.0525	0.0000
	SE 7	1.32	227.35		39300	39300	4200			0.0525	0.0000
	SE 8	1.32	227.35		39400	39400	4140			0.0525	0.0000
	SE 9	1.32	227.35		39500	39500	4580			0.0525	0.0000
	SE10	1.32	227.35		39400	39400	4310			0.0525	0.0000
	SE11	1.32	227.35		42700	42700	3250			0.0525	0.0000
	SE12	1.32	227.35		39500	39500	4280			0.0525	0.0000
	SE13	0.32	228.34		43000	43000	3070			0.0263	0.0000
	SE14	0.32	228.34		43000	43000	2890			0.0263	0.0000
	SE15	0.32	228.34		43000	43000	3810			0.0263	0.0000

Table A3 - Specimen Configuration for Columns Bending About the Minor Axis

continued

Author	Col. Desig.	$\frac{\rho_{ss} f_{yss}}{f'_c}$	ℓ in.	ℓ/h	e in.	e/h	Tested Strength	Theor. Strength	Strength Ratio
Janss	13.1	0.352	96.3	11.6	1.57	0.190	269.1	277.3	0.9703
Anslijn	13.2	0.377	96.6	11.7	1.57	0.190	234.0	264.6	0.8845
(1974)	13.3	0.386	96.3	11.7	1.57	0.190	229.5	259.5	0.8846
Janss	1	0.427	136.9	16.6	0.00	0.000	606.8	515.2	1.1779
Piraprez	3	0.427	50.2	6.1	0.00	0.000	591.3	628.1	0.9414
(1974)	5	0.391	136.9	16.6	0.00	0.000	617.9	544.3	1.1352
	7	0.391	50.2	6.1	0.00	0.000	646.4	665.6	0.9713
	9	0.364	136.9	16.6	0.00	0.000	428.0	568.8	0.7524
	11	0.364	50.2	6.1	0.00	0.000	461.3	697.6	0.6612
	13	0.404	168.3	20.4	0.00	0.000	419.2	478.9	0.8753
	15	0.394	168.3	20.4	0.00	0.000	441.2	484.5	0.9107
	17	0.400	168.3	20.4	0.00	0.000	437.0	481.4	0.9077
	19	0.425	97.5	11.8	0.00	0.000	575.8	599.4	0.9606
	23	0.441	97.5	11.8	0.00	0.000	600.1	586.3	1.0236
	27	0.491	97.5	11.8	0.00	0.000	551.7	549.4	1.0042
	2	0.623	136.9	14.5	0.00	0.000	518.6	521.3	0.9949
	4	0.623	50.2	5.3	0.00	0.000	522.9	615.4	0.8496
	6	0.570	136.9	14.5	0.00	0.000	538.4	549.2	0.9805
	8	0.570	50.2	5.3	0.00	0.000	545.0	646.8	0.8426
	10	0.532	136.9	14.5	0.00	0.000	481.1	572.6	0.8401
	12	0.532	50.2	5.3	0.00	0.000	503.1	660.6	0.7616
	14	0.589	168.3	17.8	0.00	0.000	403.9	479.1	0.8431
	16	0.576	168.3	17.8	0.00	0.000	533.9	484.1	1.1029
	18	0.583	168.3	17.8	0.00	0.000	472.3	481.3	0.9812
	21	0.621	97.5	10.3	0.00	0.000	573.8	593.5	0.9667
	25	0.643	97.5	10.3	0.00	0.000	547.2	580.9	0.9420
	29	0.716	97.5	10.3	0.00	0.000	448.0	545.2	0.8217
	20	0.425	96.8	11.7	1.57	0.190	269.1	248.0	1.0852
	24	0.441	96.8	11.7	1.57	0.190	231.8	241.5	0.9598
	28	0.491	96.8	11.7	1.57	0.190	236.0	224.3	1.0521
	22	0.621	96.8	10.2	1.57	0.167	264.8	275.5	0.9614
	26	0.643	96.8	10.2	1.57	0.167	218.5	269.5	0.8106
	30	0.716	96.8	10.2	1.57	0.167	280.1	251.4	1.1143
Roderick	SE 1	0.603	84	12.0	0.000	0.000	273.0	268.1	1.0184
Loke	SE 2	0.520	84	12.0	0.400	0.057	211.0	211.2	0.9993
(1974)	SE 3	0.569	84	12.0	0.800	0.114	129.0	139.7	0.9235
Australia	SE 4	0.551	84	12.0	0.000	0.000	264.0	275.3	0.9591
	SE 5	0.576	84	12.0	0.400	0.057	195.0	188.4	1.0349
	SE 6	0.730	84	12.0	0.800	0.114	108.0	122.1	0.8844
	SE 7	0.491	84	12.0	1.500	0.214	88.0	88.3	0.9967
	SE 8	0.500	84	12.0	0.000	0.000	290.0	285.8	1.0148
	SE 9	0.453	120	17.1	0.200	0.029	201.0	213.6	0.9409
	SE10	0.480	120	17.1	0.400	0.057	135.0	168.1	0.8031
	SE11	0.690	120	17.1	0.800	0.114	88.0	92.2	0.9547
	SE12	0.485	120	17.1	1.500	0.214	67.0	70.2	0.9543
	SE13	0.368	84	12.0	0.000	0.000	180.0	192.9	0.9333
	SE14	0.391	84	12.0	0.400	0.057	116.0	134.0	0.8659
	SE15	0.296	84	12.0	0.800	0.114	108.0	126.3	0.8551

Table A3 - Specimen Configuration for Columns Bending About the Minor Axis

continued

Author	Col. Desig.	b in.	h in.	Steel Profile	Long. Reinf.	A_{ss} in.^{2}	A_c in.^{2}	A_{rs} in.^{2}	Vol'met' Ratio *
Morino et al. (1984)	A4-90	6.30	6.30	H100x100x6x8	4-6mm	3.45	36.08	0.14	0.00258
	B4-90	6.30	6.30	H100x100x6x8	4-6mm	3.45	36.08	0.14	0.00258
	C4-90	6.30	6.30	H100x100x6x8	4-6mm	3.45	36.08	0.14	0.00258
	D4-90	6.30	6.30	H100x100x6x8	4-6mm	3.45	36.08	0.14	0.00258
	A8-90	6.30	6.30	H100x100x6x8	4-6mm	3.45	36.08	0.14	0.00258
	B8-90	6.30	6.30	H100x100x6x8	4-6mm	3.45	36.08	0.14	0.00258
	C8-90	6.30	6.30	H100x100x6x8	4-6mm	3.45	36.08	0.14	0.00258
	D8-90	6.30	6.30	H100x100x6x8	4-6mm	3.45	36.08	0.14	0.00258
Roik Mangerig (1987)	7	11.81	11.81	HE200B	4-12mm	12.11	126.69	0.70	0.00293
	8	11.81	11.81	HE200B	4-12mm	12.11	126.69	0.70	0.00293
	9	11.81	11.81	HE200B	4-12mm	12.11	126.69	0.70	0.00293
	10	11.81	11.81	HE200B	4-12mm	12.11	126.69	0.70	0.00293
	11	11.81	11.81	HE200B	4-12mm	12.11	126.69	0.70	0.00293
	12	11.81	11.81	HE200B	4-12mm	12.11	126.69	0.70	0.00293
Roik Schwal'r (1988)	V102	11.02	11.02	HE160A	4-14mm	6.01	114.55	0.95	0.00283
	V111	11.02	11.02	HE160A	4-28mm	6.01	111.69	3.82	0.00283
	V112	11.02	11.02	HE160A	4-28mm	6.01	111.69	3.82	0.00283
	V113	11.02	11.02	HE160A	4-28mm	6.01	111.69	3.82	0.00283
	V121	11.02	11.02	HE120B	4-28mm	5.27	112.43	3.82	0.00283
	V122	11.02	11.02	HE120B	4-28mm	5.27	112.43	3.82	0.00283
	V123	11.02	11.02	HE120B	4-28mm	5.27	112.43	3.82	0.00283

* - Volumetric ratio for transverse reinforcement

$$p'' = \frac{2(b'' + d'')\,A}{b''\,d''\,s};$$

b" - outside width of transverse reinforcement
d" - outside depth of transverse reinforcement
A - area of bar
s - spacing of reinforcing

Table A3 - Specimen Configuration for Columns Bending About the Minor Axis

continued

Author	Col. Desig.	I_{ss} in.^{4}	I_c in.^{4}	I_{rs} in.^{4}	Fy web	Fy flange	f'c Col. Stored **	f'c Water Stored	Fy Reinf.	ρ_{ss}	ρ_{rs}
Morino	A4-90	3.22	127.16	0.83	52055	42485	3060		56115	0.0870	0.0036
et al.	B4-90	3.22	127.16	0.83	50750	41615	3393		56115	0.0870	0.0036
(1984)	C4-90	3.22	127.16	0.83	45675	44660	3379		56115	0.0870	0.0036
	D4-90	3.22	127.16	0.83	52055	42485	3074		56115	0.0870	0.0036
	A8-90	3.22	127.16	0.83	53360	43935	4872		56115	0.0870	0.0036
	B8-90	3.22	127.16	0.83	53070	45095	4829		56115	0.0870	0.0036
	C8-90	3.22	127.16	0.83	53505	44225	3567		56115	0.0870	0.0036
	D8-90	3.22	127.16	0.83	53360	43790	3321		56115	0.0870	0.0036
Roik	7	48.05	1556.66	16.99	39150	39150	6570		60900	0.0868	0.0050
Mangerig	8	48.05	1556.66	16.99	39150	39150	6570		60900	0.0868	0.0050
(1987)	9	48.05	1556.66	16.99	39150	39150	6570		60900	0.0868	0.0050
	10	48.05	1556.66	16.99	39150	39150	6570		60900	0.0868	0.0050
	11	48.05	1556.66	16.99	39150	39150	6570		60900	0.0868	0.0050
	12	48.05	1556.66	16.99	39150	39150	6570		60900	0.0868	0.0050
Roik	V102	14.80	1197.25	18.55	44515	44515	5956		60900	0.0495	0.0079
Schwal'r	V111	14.80	1150.57	65.23	43529	43529	6015		60900	0.0495	0.0314
(1988)	V112	14.80	1150.57	65.23	43529	43529	6015		60900	0.0495	0.0314
	V113	14.80	1150.57	65.23	43529	43529	6015		60900	0.0495	0.0314
	V121	7.64	1157.73	65.23	34757	34757	6015		60900	0.0434	0.0314
	V122	7.64	1157.73	65.23	34757	34757	6015		60900	0.0434	0.0314
	V123	7.64	1157.73	65.23	34757	34757	6015		60900	0.0434	0.0314

Table A3 - Specimen Configuration for Columns Bending About the Minor Axis

continued

Author	Col. Desig.	$\frac{\rho_{ss} f_{yss}}{f'_c}$	ℓ in.	ℓ/h	e in.	e/h	Tested Strength	Theor. Strength	Strength Ratio
Morino	A4-90	1.481	36.4	5.8	1.575	0.250	113.0	88.4	1.2791
et al.	B4-90	1.302	90.9	14.4	1.575	0.250	83.6	69.1	1.2090
(1984)	C4-90	1.177	136.4	21.7	1.575	0.250	61.7	52.4	1.1773
	D4-90	1.474	181.9	28.9	1.575	0.250	46.4	37.1	1.2502
	A8-90	0.953	36.4	5.8	2.953	0.469	77.4	66.7	1.1608
	B8-90	0.957	90.9	14.4	2.953	0.469	59.5	53.7	1.1068
	C8-90	1.305	136.4	21.7	2.953	0.469	39.7	36.8	1.0779
	D8-90	1.399	181.9	28.9	2.953	0.469	30.3	28.2	1.0759
								218.5	269.5
Roik	7	0.517	118.1	10.0	1.181	0.100	1023.1	789.0	1.2967
Mangerig	8	0.517	118.1	10.0	3.543	0.300	502.0	406.4	1.2352
(1987)	9	0.517	196.9	16.7	1.181	0.100	824.6	587.6	1.4034
	10	0.517	196.9	16.7	3.543	0.300	410.9	316.3	1.2989
	11	0.517	315.0	26.7	1.181	0.100	455.0	334.8	1.3588
	12	0.517	315.0	26.7	3.543	0.300	223.9	206.8	1.0827
Roik	V102	0.370	139.2	12.6	3.937	0.357	252.2	236.3	1.0674
Schwal'r	V111	0.358	139.2	12.6	3.937	0.357	394.9	347.9	1.1351
(1988)	V112	0.358	139.2	12.6	2.362	0.214	565.9	478.7	1.1822
	V113	0.358	139.2	12.6	0.000	0.000	1032.8	1069.1	0.9660
	V121	0.251	139.2	12.6	6.299	0.571	256.1	237.7	1.0772
	V122	0.251	139.2	12.6	7.874	0.714	182.9	196.6	0.9305
	V123	0.251	139.2	12.6	3.937	0.357	345.4	333.2	1.0367

NOTE : For e/h = inf., strength is given in kip-ft (1 kip-ft = 1.356 kN-m).

For all other values of e/h, the strength is shown in kips (1 kip = 4.448 kN).

b = width of the concrete cross-section parrallel to the axis of bending;

h = depth of the concrete cross-section perpendicular to the axis of bending.

The term f_{yss} was taken as the web yield strength for computing the $\rho_{ss} f_{yss}/f'_c$ ratio. The strain-hardening of both steels was included in the analysis.